School of Mechanical, Materials and Manufacturing Engineering

The University of Nottingham

THE DEVELOPMENT OF A MANUFACTURABILITY ANALYSIS SYSTEM FOR MICRO-MILLING

by

SYAIMAK ABDUL SHUKOR

2010

Thesis submitted to the University of Nottingham for the degree of Doctor of Philosophy

CONTENTS

Abstract

Manufacturability analysis systems (MASs) have been developed to enable the evaluation of manufacturability aspects during the design stage. MASs have been shown to be useful for macro-manufacturing processes but less attention or effort has been put for their development in the scope of micro-manufacturing. This thesis describes the development of a MAS for a micro-machining domain (MicroMAS) with a custom-made 4-axis Miniature Machine Tool (MMT) being the scope of implementation.

There are three important components in this study which are; MAS, Uncertainty Evaluation Model (UEM) and micro-milling experiments. The integration between the results from the UEM analysis and micro-machining experiments were being incorporated into the MicroMAS to provide the system with the real condition of the MMT.

In MicroMAS, Primitive Feature Analysis (PFA) is introduced as a new technique in gathering information from a CAD model and analysing its manufacturability. The results from the manufacturability assessment in MicroMAS are successfully achieved through the manufacturability index which indicates the relative ease of machining the CAD model and list of related suggestions.

UEM is developed to analyse the influence of the errors stemmed from the MMT construction on the geometrical accuracy of the machined micro-parts. The model has allowed a methodology for the errors in a custom-made machine tool to be predicted and to further understand the origin of the errors on the machined micro-part (either from the machine or the process itself). The abilities of the MMT are evaluated through various types of experiments where the surface quality and geometrical accuracy can be concluded to be at an acceptable range.

From the experience gained from the research, the development of MicroMAS for micro-milling has been found to be practical in assisting a user to generate micro-parts using the MMT.

Acknowledgements

First of all, I would like to express my deepest gratitude to my main supervisor Dr Axinte for providing me the opportunity to pursue a research degree at University of Nottingham. His valuable knowledge and guidance at each stage of the project ensured that I was able to achieve my objectives successfully.

I would like to acknowledge the support of Universiti Kebangsaan Malaysia and Kementerian Pengajian Tinggi for providing the opportunity, assistance and scholarship for my study.

My sincere thanks go to Mark Daine and to all other technicians in the Manufacturing Lab for their suggestions, helpful insights and exchanging experience in design and manufacture issues. Special thanks go to Mr. Steven Weston from Sandvik Coromant UK for his continuous support in providing tools for experiments. I also wish to thank my colleagues from MCM research group who helped me keep my motivation alive and assisting me with all the related research works.

None of this would have been possible if it had not been for the confidence, support, love and sacrifices of my husband, *Ady Aswany* and my son, *Thaqif*. I also would like to thank my parents (*Abdul Shukor* and *Ramah*), my parents-in-law (*Ahmad* and *Shabinar*), my sisters (*Syahirah*, *Syadiyah* and *Syadwa*) and the rest of the family for their support and inspiration. Hence, this thesis is directly dedicated to them.

Finally, thanks to the others I have overlooked here for their contribution and encouragement in every way…

Syaimak Abdul Shukor
Nottingham, February 2010

Publications

This research work in this thesis has contributed in part or full to the following publications:

Shukor, S.A., Axinte, D.A., *Manufacturability analysis system: issues and future trends.* International Journal of Production Research, 2009, **47**(5): p.1369-1390.

Shukor, S.A., Axinte, D.A., *An approach of using primitive feature analysis in manufacturability analysis system for micro-milling/drilling.* International Journal of Computer Integrated Manufacturing, 2009, **22**(8): p.727-744.

Axinte, D.A., Shukor, S.A., Bozdana, A.T., *An analysis of the functional capability of an in-house developed miniature 4-axis machine tool.* International Journal of Machine Tools and Manufacture, 2009, Accepted and in Press

Two more journal papers/conference papers are in draft form for work carried out in Chapter 6 and the overall system development.

Nomenclature

$\Delta x_1, \Delta y_1, \Delta z_1$	Errors due to x, y and z planes deviation(mm)
$\Delta x_2, \Delta y_2, \Delta z_2$	Errors related to the evaluation of workpiece reference point for x, y and z axes (mm)
$\Delta x_3, \Delta y_3, \Delta z_3$	Errors related to the temperature variations for x, y and z axes (mm)
$\Delta x_4, \Delta y_4, \Delta z_4$	Errors originating from the positioning inaccuracies of x, y and z linear stages(mm)
Δt	Incremental value of the cutting time (s)
Δy_0	Linear deviation on y axis (mm)
a_e	Radial depth of cut (mm)
a_p	Axial depth of cut (mm)
A_{Ra}	Surface profiling area
f_z	Feed per tooth (mm)
k	Coverage factor
n	Spindle speed(min^{-1})
θ	Side angle
Ø	Diameter
r	Radius (mm)
R_a	Average surface roughness
R_{St}	Stiffness ratio
R_z	Average maximum height of the analysed profile
t	Cutting time (s)
U	Expanded uncertainty
$u(x_i)$	Standard uncertainty
$u_c(y)$	Combined standard uncertainty
UX, UY, UZ	Expanded uncertainty of positioning errors of cutting tool on x, y and z axes (mm)
V/V_c	Cutting speed (m/min)
V_f	Feed speed (m/min)
V_z	Feed speed of the tool along z axis (mm/min)
x, y, z	Theoretical position of the cutting tool (mm)
X, Y, Z	Real position of the cutter affected by uncertainties (mm)
Y	Measurand
Z	Number of teeth of the milling cutter
α	Angle between tool (z axis) and side of U table (degree)
α_1, α_2	Angles at the base of thin wall
α_o	Extension angle of the cylindrical surface
β	Surface angle = Angle made from the surface to the centre point
γ	Angle between tool (z axis) and top of U table (degree)
σ	Standard deviation
ω	Angular speed (rad/s)

Abbreviation

ABS	Agent-based system
AHP	Analytical hierarchy process
AI	Artificial intelligence
CAD	Computer aided design
CAM	Computer aided manufacturing
CBR	Case-based reasoning
CE	Concurrent engineering
CFA	Coupled feature analysis
CMM	Coordinate measuring machine
D	Diameter
DFM	Design for Manufacture
DH	Diameter-to-height ratio
ECM	Electro Chemical Machining
EDM	Electro Discharge Machining
ES	Expert system
FI	Fixturability index
FL	Fuzzy logic
GUM	Guide to the expression of uncertainty in measurement
H	Height
HA	Hybrid approach
IA	Initial assessment
IE	Inference engine
ISO	International standard organization
ITG	International tolerance grade
KB	Knowledge-based
K_i	Weighting factor
K_{RD}	Pre-defined coefficient for relative distance
L	Length
LH	Length-to-height ratio
MAS	Manufacturability analysis system
MD	Minimum acceptable distance
MEMS	Micro-Electro Mechanical Systems
MET	Micro-Engineering Technologies
MI	Manufacturability index
MI_{CFA}	Manufacturability index for coupled feature analysis phase
MI_{DIM}	Manufacturability index for dimension
MI_{MAT}	Manufacturability index for material
$MI_{OVERALL}$	Manufacturability index for overall component
MI_{PF}	Manufacturability index for primitive feature
MI_{Ra}	Manufacturability index for surface roughness
MI_{SFA}	Manufacturability index for single feature analysis phase
MI_{TOL}	Manufacturability index for tolerance
MI_{UEM}	Manufacturability index for uncertainty impact in machining PF
MMT	Miniature machine tool
MST	Micro-System Technologies
NIST	National Institute of Standards and Technology
NN	Neural network
OOT	Object oriented technique

PF	Primitive feature
PFA	Primitive feature analysis
PMT	Precision Machine Tool
RBS	Rule-based system
RD	Relative distance
R_{St}	Stiffness ratio
SFA	Single feature analysis
UEM	Uncertainty evaluation model
VB	Visual basic.NET
VIM	International Vocabulary of Basic and General Terms in Metrology
W	Width

CHAPTER 1: INTRODUCTION

1.1. Introduction

This chapter presents the aims and objectives of this study. The background information and the problem definition are discussed briefly as well as the structure of the thesis. To illustrate the significance of this thesis to the academic field, key research highlights and findings will also be described at the end of this chapter.

1.2. Background information

Traditionally, the translation of a conceptual design into a final product has been accomplished by repetitive iterations between design and manufacturing stages of the product development life cycle. The concepts generated at the design stage are passed to the manufacturing stage for the engineers to check on any manufacturing-related problems. If manufacturing engineers encounter significant machining difficulties, the designs are passed back to the design department for appropriate modifications. Designers might be unaware of specific manufacturing details or rules, which sometimes result in 'non-manufacturable' designs or require unreasonable increase of machining costs. This is the main reason of the time-consuming iterations occurring between the designs and manufacturing stages.

According to Gupta *et al.* [1], in order to expedite or minimise the number of these iterations, **manufacturability analysis systems (MASs)** were developed to allow manufacturability aspects to be analysed during the design stage and

thus to enable a 'smooth' transition between the design and manufacturing stages. When the number of the iterations are lessen, the time taken to bring the product to the market is shortened and consequently that enables the reduction of manufacturing costs of the designs [2-3].

MASs implementation can cover a wide range of applications, either the systems were generally developed to cater various types of manufacturing process or for a 'specific' application. MASs have been proved to work for various manufacturing processes such as milling [4-6], drilling [5, 7-8], turning [9-11], grinding [7, 12], die/sand casting [13-14], injection moulding [4, 15-16], forging [5] and blanking/piercing [17-18].

Among the examples of MASs 'specific' applications are for shipbuilding projects, where MAS supports automated virtual assembly of parts/sub-assemblies [19], designing an improved version of golf club heads [20], assist product designers, process planners and die designers working in small and medium sheet metalworking industries for assessing manufacturability of presswork parts [21], the fabrication of printed circuit board (PCB) [22] and assisting users in selecting a set of process parameters and a powder material that would meet the strength requirement of the part in powder metallurgy process for mould fabrication [23-24]. Within the broader context of modern design and manufacturing digitisation, the steps made towards the unification of concepts (design and manufacturing) into intelligent and industrially usable, MASs is regarded as a strategic step towards next fully integrated production systems.

As product development technology becomes more advanced, the size of devices produced decreases and this is where micro-products came into view. Micro-engineering deals with the development and manufacture of products, whose functional features or at least one dimension are at micro-metric level [25]. The use of micro-products and micro-components has been strongly increased through the past decade and the product development and design on new micro-products is likely to become the core competence of the specialist companies [25]. The increasing demands of micro-products in various industries have geared up the development of specific micro-manufacturing processes and technologies. Thus, all the constitutive elements of micro-manufacturing systems have to be optimised to enable cost and time efficient mass generation of ever-growing micro-engineered products. The needs to bring micro-products faster to the market caused the development and the design phases to become more challenging tasks. One of the main issues in designing micro-products is the methods used to design them with the required quality specifications which can be manufactured 'easily'.

MASs have been successfully developed for various manufacturing processes but they are mainly applicable for macro-manufacturing domain such as milling, drilling, forming and casting. In the present study, MASs have proved to work for macro-manufacturing processes but there are less attention or effort has been shown for its development in the scope of micro-manufacturing.

1.3. Problem definition

Micro-products with high accuracy such as sensors, lenses, surgery devices, gears, and actuators have become demanded products in industries such as Information Technology (IT), aerospace, medical and biomedical, automotive, telecommunication and electronic industries [25-32]. With the demands for micro-products, there is an interesting opportunity in the related research field to provide a mechanism or method in assisting the production of micro-parts/components. In order to design competitive micro-products, which ideally fulfil the required product functions, the designers need to develop products that relate to the fast-developing manufacturing details and rules [33]. Thus, a systematic approach in designing quality micro-products allows the designs to be easily manufactured and compatible with the production needs.

Currently, the applicability of MASs is also limited to the macro-manufacturing domain and less attention is given to the new emerging processes such as micro-manufacturing technique. Even though micro-machining (e.g. micro-milling/drilling/turning) are becoming more popular for generating small and high accuracy parts [25, 34-35], there is no clear indication that systems to assist with manufacturability assessment of these micro-parts have been developed.

Owing to demands of micro-products in the market, the applicability of MAS in this field has a big research potential that needs to be explored as it assists in machining high quality micro-products and also provides opportunity for manufacturing issues to be incorporated during design stage. This means that

the designer is able to check the micro-manufacturability aspects in their designs before submitting them for machining.

Furthermore, there is a strong need of MASs in micro-machining domain as these processes (e.g. micro-milling/drilling/turning) have been reported to have their own specifics characteristic compared to the macro-manufacturing area [25, 27, 36-38]. The fundamental difference between micro-machining and conventional process arises due to scale of the operation, while they are kinematically the same. According to Bissacco *et al.* [39], blind use of the geometrical downscaling approach for this process based on the knowledge available for the conventional size process would lead to errors such as excessive tool deflections and high risk of tool breakage. Among the differences due to the downscaled of the process which change the whole material removal geometry as compared to the conventional size machining process are:

- Tool runout greatly affect the accuracy of the machined micro-part compared in macro-machining [40].
- Minimum chip thickness phenomena occurred where no chip is formed during the machining of the micro-processes, which is due to the small value of the ratio between the depth of cut and the tool edge radius [41].
- As the diameter decreases, the rigidity of the tool also decreases which leads to tool deflections that greatly affect the chip formation and accuracy of the desired surface [42].

- The assumption used in conventional process that the tool is sharp, completely cuts the surface and generated chip is not valid in micro-machining [43].

An implication of this is the possibility of developing an efficient MASs to check micro-manufacturability aspects such as materials used, manufacturing processes involved, acceptable and suitable tolerances and also dimensions of micro-products that can be manufactured by a specific setup/process. Further research on implementing MAS in designing and launching micro-products is believed to enhance the rapid development of micro-manufacturing techniques. Therefore, there is and will be a clear need for analysing the micro-manufacturability aspects during the design stage products in order to produce accurate and cost-effective micro-products

In-house developed multi-axis Miniature Machine Tools (MMTs) are now becoming more popular with the demand for reduced energy consumption and workshop floor when machining small/medium batch size micro-components. As an example in watch manufacturing, due to the size of the miniature machines used, the amount of energy consumption may be reduced to approximately 30% of the conventional factory by the half-miniaturization of the production systems [44]. According to Hansen *et al.* [45], among the advantages of machine tools' miniaturization are the decrease of heat deformation of machine tools with subsequent reduction of their sizes, decrease of material consumption for machine tool construction (more expensive material with better properties can be used), decrease of vibration amplitudes, and decrease in space and energy consumption. In-line with the above

advantages, the development of an in-house 4-axis MMT by the MCM Research Group at the University of Nottingham triggers a requirement for a system that can assist the user in generating micro-component using this custom-made machine. Based on this ground, it is a meaningful effort to develop MAS with the MMT as its domain of application for the manufacturability aspects of the micro-parts to be evaluated.

Moreover, as there are no guidelines, standards or manuals to refer to in operating the MMT, the need to evaluate its functional characteristics such as uncertainties related to the MMT construction is imperative. In this context, there is a clear need to understand the influence of the errors stemming from the MMT construction on the geometrical accuracy of the machined micro-part. Furthermore, as a custom-made machine, there is also an advantage for this study to evaluate and assess the capability and performance of the MMT, as it can provide the real environment for the MAS.

1.4. Aims and objectives

The aim of this study is directed towards the possibility of developing a manufacturability analysis system for micro-machining domain (MicroMAS). Additionally, it is intended to address the need of the 4-axis Miniature Machine Tool (MMT) that require such a system (i.e. MicroMAS) to assist the user in generating micro-component through manufacturability evaluation of the proposed CAD models that will be machined using this custom-made machine.

To accomplish this, the following objectives are to be achieved:

- *To introduce and demonstrate the application of the Primitive Feature Analysis (PFA) technique as a key element in the developed MicroMAS.* The PFA customised and implemented for micro-machining so that it assists in defining and gathering essential data from the proposed CAD models of the analysed micro-components. Furthermore, this technique is being executed throughout the entire system (MicroMAS) intentionally for assessing the manufacturability aspects of the analysed CAD models.
- *To develop a new method that is capable to indicate the level of manufacturability for each PF and overall part through a novel sequential aggregate indexes scheme.* Manufacturability Indexes (MIs) reflect the relative ease of machining of the micro-component based on associated ratings of various aspects such as PF characteristics (e.g. type of PF, orientation, shape, end-corner specification), quality measures (e.g. surface roughness, tolerances), machinability of selected materials, tool dimensions and interactions between PFs. These indexes are represented by a rating convention that is divided into three levels: *Hard to manufacture*, *Medium to manufacture* and *Easy to manufacture*.
- *To investigate the variables that affect the geometrical accuracy of the generated micro-part stemmed from the construction of the MMT.* It is important to analyse the functional characteristic of the custom-made MMT in order to understand the origin of the errors on the machined micro-part (either from the machine or the process itself).
- *To analyse the identified errors that affect the geometrical accuracy of the generated micro-parts by employing the Uncertainty Evaluation*

Model (UEM). This analysis calculates the value of uncertainty and indicates the main source of errors stemming from the MMT construction.

- *To propose a methodology to evaluate uncertainties of any similar in-house developed machine tools.* This is through the generated UEM model which can identify/predict the main sources of errors that affect the quality of the machined part.
- *To evaluate the limitations and capabilities of the custom-made MMT through various types of experiments and observations.* Among the proposed experiments were machining an "adapted standard" of micro-testpiece, producing micro-component and finally generating micro-slots and thin walls. From here, the surface quality and geometrical accuracy of the machined workpieces on the MMT are evaluated and analysed.
- *To integrate results from the UEM and micro-machining experiments into the MicroMAS.* In order to provide the system with the real condition of the MMT, the results from the UEM analysis on the effects of uncertainty on micro-machining of the PFs were incorporated. While the results from the micro-machining experiments were used to populate relevant data for the MicroMAS such as the generated surface quality and geometrical accuracy.

1.5. Structure of the thesis

Chapter 2 presents general information and an extensive literature review of all aspects on manufacturability analysis system (MAS) such as its development's methodology, outputs, applicability, advantages and trends. Furthermore, a comprehensive review was also made on micro-machining,

uncertainty evaluation models and their significance towards this study. Besides that, at the end of the chapter a summary will be provided to illustrate the main knowledge gaps in this field of research.

Chapter 3 describes in detail the research approach (e.g. procedures, objectives, approaches, software, tools, techniques) taken in this study. The development of this study is basically divided into 4 major phases, which are: *(i) the development of MicroMAS; (ii) UEM analysis; (iii) micro-machining experiments; (iv) the integration between UEM, micro-machining experiments and MicroMAS.*

The Primitive Feature Analysis technique was introduced and explained in details in **Chapter 4**. The principles and mechanism of this technique will be discussed extensively in this chapter. Based on this technique, a simulation was thoroughly illustrated using a CAD model of a micro-component; this is to prove that this technique is applicable in defining and gathering data from the CAD model. It also explained on how PFA technique is implemented in MicroMAS.

Chapter 5 describes the development of Uncertainty Evaluation Model that analysed the variables that affect the geometrical accuracy of the machined micro-parts stemming from the construction of the MMT. It also presents the analysis of the model in GUM Workbench (an available commercial software to estimate the measurement of uncertainty). The inputs, analysis and results obtained for this study are also reported in this chapter.

The micro-machining experiments implemented to assess the capability of the MMT and on the same time to populate relevant data for the MicroMAS are described in details in **Chapter 6**. For each experiment, the objectives, machining procedures and parameters and finally the results and discussion are being presented. The limitations and advantages of the MMT are also discussed in this chapter. In the end of the chapter, the integration of the results from the experiments into the MicroMAS is illustrated and explained.

Following this chapter, the implementation of MicroMAS is described in **Chapter 7**. The development of the system is explained in this chapter which covers the implemented Rule-based system, the usage of database and Visual Basic.NET. A simulation of the MicroMAS's application by utilizing the micro-component is also illustrated step-by-step in this chapter.

Finally, **Chapter 8** includes the discussion and conclusion of this study. The results obtained from micro-machining experiments, UEM analysis are discussed and summarised. The possible future studies are reported in the final section.

1.6. Highlights of significant contribution of the thesis

This thesis consists of many key findings in the field of developing MAS for micro-machining domain and explicitly in catering the need of the custom-made MMT. In the following section, the major contributions of the thesis are listed and a brief description is provided as appropriate.

- This study reports for the first time on an approach to develop a Manufacturability Analysis System exclusively for micro-machining application. At the same time, it provides assistance to the user in using the custom-made Miniature Machine Tool by analysing the manufacturability aspects of the analysed CAD model of the micro-parts.
- A new technique (Primitive Feature Analysis) has been developed and implemented in the MicroMAS for gathering essential data from the proposed CAD model of the analysed micro-component that enables the assessment of its manufacturability aspects. This has allowed a novel and simple way to 'translate' the CAD data into the system, instead of using laborious methods of data extraction as implemented in previous MAS.
- A newly proposed framework on developing the MicroMAS was introduced which involved the implementation of PFA technique, combination of *user-system interaction* and *a priori database* for input and also the integration between the system, UEM analysis and micro-machining experiments.
- For the first time, in-depth analysis of indicating the errors that affect the geometrical accuracy of the machined micro-part stemming from the construction of the MMT has been developed. This can be considered as a guideline for academics/industrialists that intend to develop and assess the associated errors of their own customised miniature machine tools.
- Uncertainty Evaluation Model has been developed for the first time to account for the construction errors that affect the geometrical accuracy of the machined micro-part stemming from the construction of the MMT.

This model also provides opportunity in predicting errors of an in-house/custom-made machine tool.

- Various and unique (performed on a proposed "adapted standard" testpiece) micro-machining experiments have been developed to assess the capability of the MMT; these can become a first step into developing a new testing procedure of the performances of the machine tools when performing micro-machining. The results from these experiments enabled the understanding of the MMT performance in machining micro-components based on optimised machining parameters suggested by the tool manufacturer.

CHAPTER 2: LITERATURE REVIEW

2.1. Introduction

In Chapter 2, a comprehensive literature review on manufacturability analysis system (MAS) with particular focus on topics such as its development, methodology, generated outputs, applicability, advantages, limitations and trends are presented. Details on MAS development methodology will discuss the input mechanisms and also the method used for assessing the manufacturability aspects. Following this, a section on Uncertainty Evaluation Modelling (UEM) will be included to provide an overview on its development, application and also its relationship in the direction of MAS development for micro-machining operations and MMTs utilisation. In addition, relevant to the scope of the research on micro-machining field with attention given into micro-milling process is also conducted; discussion on the challenges of the process and also its utilization in the manufacturing industry are presented. Furthermore, a summary that described the in-house miniature-machine tool is also provided under the micro-machining sub-topic. Finally at the end of this chapter, the knowledge gaps in this field of research will be summarised and concluded.

2.2. Manufacturability analysis system

Manufacturability is defined as the ability to reproduce a given part with minimal waste, such that it satisfies the requirements in intended use while meeting the business goal [46]. With the development of Computer Aided Design/Manufacturing (CAD/M) and the introduction of the concurrent

engineering (CE) concept in product development life cycle, manufacturability has become a key element that has to be assessed and analysed at the design stage. In order to do so, the designer needs to have access to knowledge and information about the manufacturing environment which facilitates the decision making activities.

Manufacturability Analysis Systems (MASs) have been developed to enable the evaluation of easy to manufacture parts during the design stage, enabling the reduction of costs and time to market of the designed products. Gupta *et al.* [1] highlighted that MASs are one of the tools that have been developed to meet the purpose of the concept *design right at the first time* by allowing the manufacturability aspects to be analysed during the design stage that enable a 'smooth' transition between the design and manufacturing phase.

The main objective of the current efforts' in this field is to develop a tool for computer-aided design for manufacture (DFM) that can be used during early design stages to improve product quality from the manufacturing point of view [47-48]. It is envisaged that a MAS will enable the analysis of both manufacturability and functionality aspects such as tolerances, surface finish, dimension, machining strategies related to material properties and part geometrical specifications, all considered at the early stages of product development with direct implications on the reduction of lead times taken of the product to the market.

Figure 2.1 shows the stages involved in product development life cycle as illustrated by Pugh [49]. MAS was proposed to be implemented at the *detailed design* stage to reduce the iterations between the design and manufacturing phase [1]. While Figure 2.2 shows the role of MAS in the design process, such system vary significantly by approach, scope and level of sophistication.

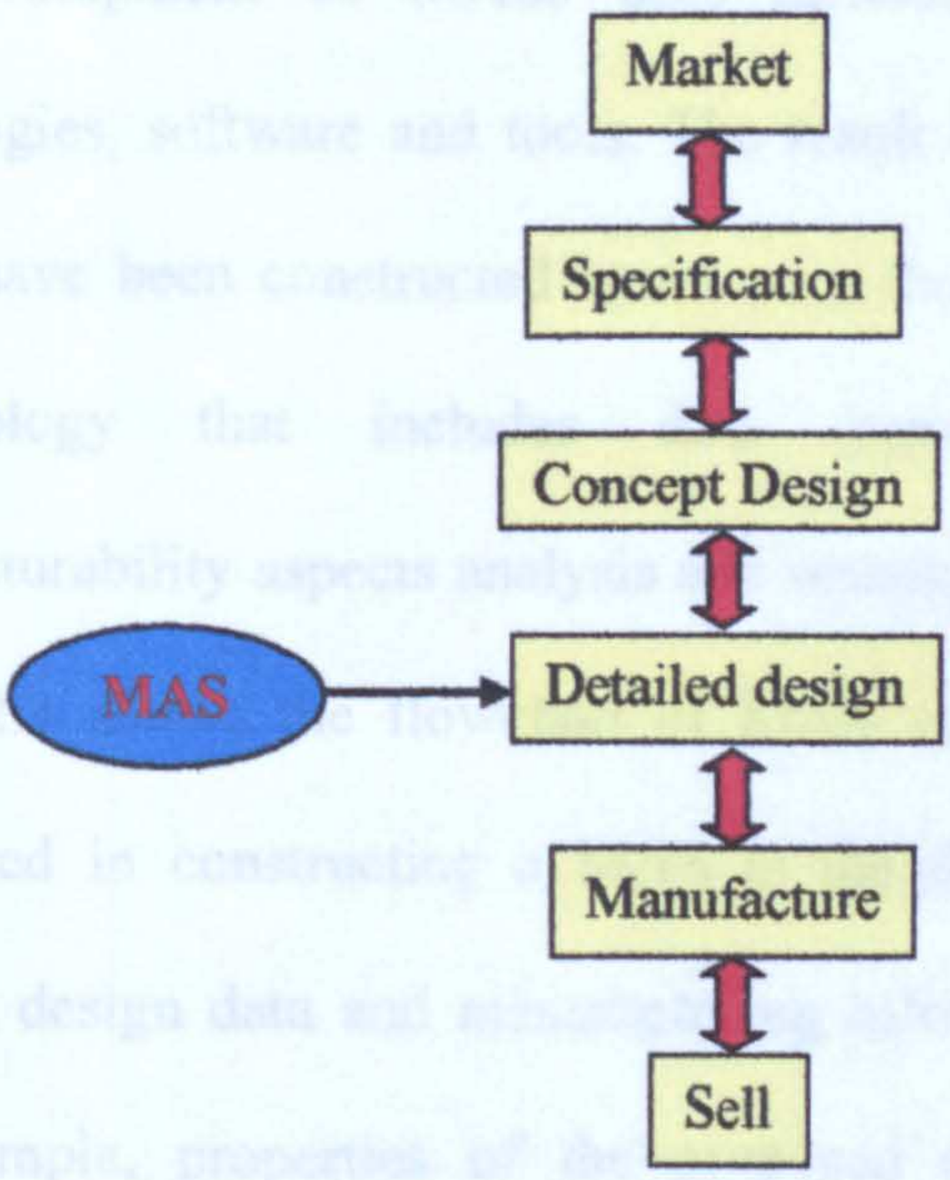

Figure 2.1 Product development life cycle and MAS [49]

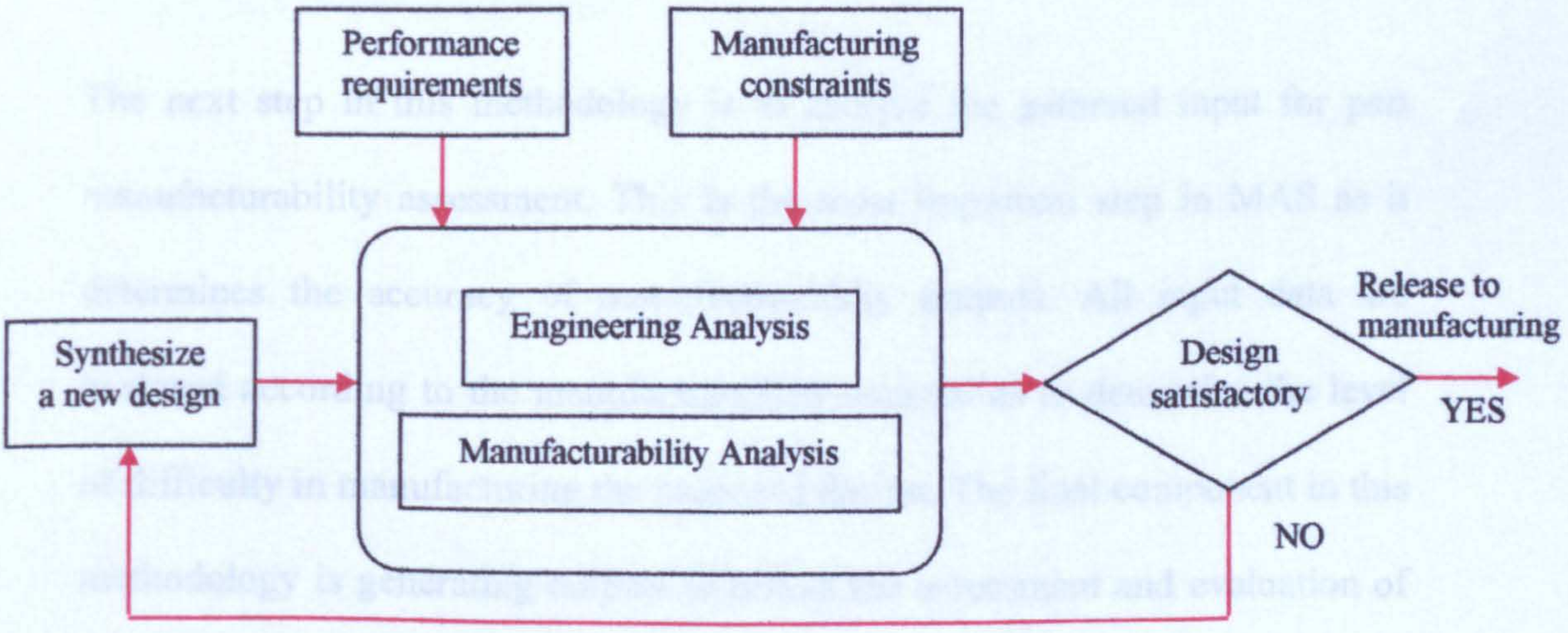

Figure 2.2 Role of manufacturability analysis in the design process [1]

In this section, the discussion is on the methodologies and approaches of MAS construction, output generation, applicability, advantages, limitations and trends.

2.2.1. Approach and methodologies of MAS construction

The development of MASs uses different combination of approaches, technologies, software and tools. The result of this study indicated that most MASs have been constructed based on a three-steps unidirectional flowchart methodology that includes data input mechanisms, engines for manufacturability aspects analysis and reasoning and finally outputs reporting. Figure 2.3 shows the flowchart of MAS construction. The first step to be considered in constructing a MAS is the data input mechanism where all required design data and manufacturing information are fed into the system. For example, properties of the proposed design, such as dimension and tolerance, are input into the system.

The next step in this methodology is to analyse the gathered input for part manufacturability assessment. This is the most important step in MAS as it determines the accuracy of manufacturability outputs. All input data are analysed according to the manufacturability constraints to determine the level of difficulty in manufacturing the proposed design. The final component in this methodology is generating outputs to reflect the assessment and evaluation of manufacturability aspects of the proposed designs and to interactively assist designers in considering manufacturing aspects during the design stage.

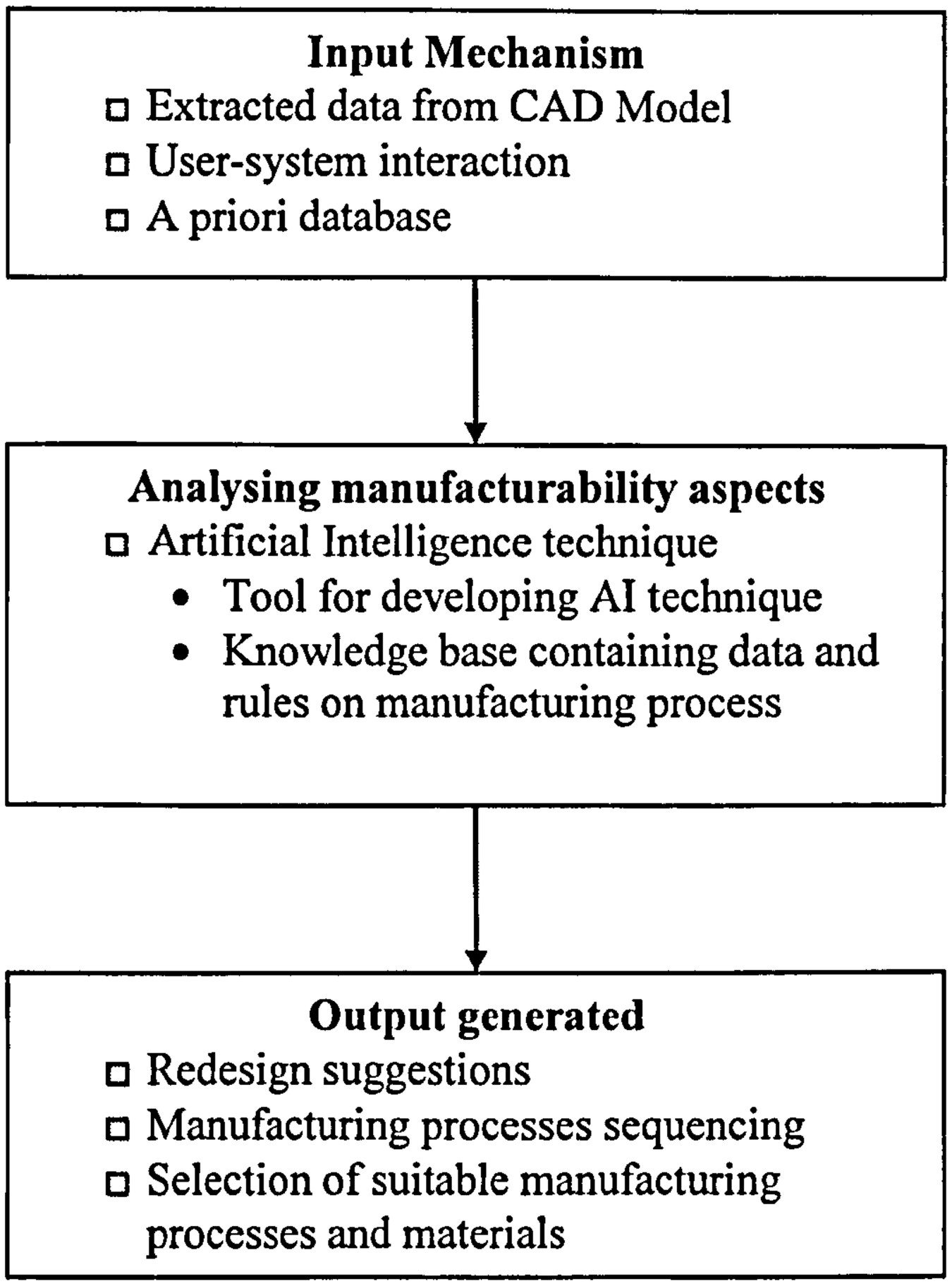

Figure 2.3 Basic methodology of MAS development

2.2.1.1. Data input mechanisms

The current study found that there are three mechanisms that have been implemented in MASs for inputting data into the system: *obtaining data from CAD model*, using *user-system interactions* and *a priori database*. The type of data extracted or collected from the input mechanisms consist of geometrical, material and technological properties of the 'to be analysed' part such as: dimensional, geometrical, tolerance and surface finish specifications, material composition and mechanical properties, production rates and quality control measures.

From the published literature, it can be concluded that there are various techniques that can be used in *obtaining data from a CAD model* such as a feature-based extraction system and neutral files usage such as STEP, IGES and STL. Additionally, data extraction can also be performed via the algorithm embedded into the CAD system such as using Auto LISP [21] and CADKEY [49]. Geometric reasoning technique has also been implemented in order to extract part definition from a CAD model [12-13, 50]. Other techniques developed are 3D recognition model based on the design specifications of CAD model [20, 51-53], attribute extractor [54], CAD modeller [7] and data extraction from process simulation [22, 55]. The data obtained from a CAD model interprets the design details such as geometrical specifications and feeds the needed information to the system. Geometrical specifications, such as features, shapes, dimensions, and technological requirements (tolerances and surface finish) are some of the essential parameters extracted from a CAD model which are considered as main input parameters into a MAS.

Another type of input mechanism is based on *user–system interaction* where the system prompts the user with questions leading towards the collection of information necessary to perform part manufacturability analysis [5, 17, 21, 55-57]. Usual questions are related to workpiece material, part dimensional and geometrical specifications, processing techniques [21] and technological/ functional properties of the component object such as geometric volume, production output rates, expected surface finish, dimensional tolerance, critical surfaces (e.g. wall thickness) [5]. For example, during a consultation session, users input the needed data in the provided interface that, once sufficient, the

program starts to analyse them based on the rules embedded in the knowledge-based (KB) [21]. In this system, important data and information related to the fabrication of a sheet metal component, such as type of material, sheet thickness, minimum corner radius sheet metal part, minimum width of slots along blank profile, shapes and dimensions of holes on the part and maximum dimension (length/width) of component, are gathered from the *user–system interaction* mechanism for the purpose of manufacturability assessment [21].

The last input mechanism is *a priori database* that is embedded into MAS. Data related to manufacturing process, materials and machining tools are available for the user to select during the data input step [4, 55-56]. In this mechanism, users are allowed to choose related data and parameters from the collection of manufacturing information (database) embedded in the system. The difference between this mechanism and the previous one is that all information already exists, and users only have to choose the appropriate one, while in the previous mechanism, users were required to input all needed data through the interface during the interaction.

From the above discussion, it can be concluded that most of the developed MASs used a feature-extraction system to obtain related data from CAD model. Research in this field is rapidly developing to find ways and approaches for accurately extracting design details from the features. One major drawback of this approach is difficulty in appropriately recognising and interpreting the relationship between intersecting features on the analysed part [1, 8, 15, 47, 58-

60]. Other limitations originate from loss of design intent and incompleteness of design and manufacturing information [15, 60].

The other two mechanisms (*user–system interaction* and *a priori database*) are not yet widely used as it involves input activities from the user and then additional effort for gauging/interpreting their applicability in other manufacturing environments. Nevertheless, these two mechanisms are also given significant attention in the research community as they could offer the advantage of inputting more accurate information into a MAS. This is because the input mechanism gets data directly from designer (*user-system interaction*) and from related manufacturing process constraints.

2.2.1.2. Approaches in analysing manufacturability aspects

The next step in this methodology is to analyse the gathered input. This is the most important step in MAS as it determines the output measures on which part manufacturability is assessed. Most developed MASs employ Expert System (ES) techniques to analyse design manufacturability aspects. ES is a computer application system that employs artificial intelligence (AI) to solve problems in a specific domain. ES can provide a relatively inexperienced user with a comprehensible assessment of a problem where an expert is unavailable. In the following the review focuses on the implementation of ES techniques in assisting the analysing of the manufacturability aspects.

Recent studies show that general manufacturability aspects can be analysed automatically using various ES approaches especially at the design stages of

the product realisation. The assessment of manufacturability aspects are done by using different approaches such as: neural network (NN), fuzzy logic (FL), agent-based system (ABS), rule-based system (RBS), object oriented technique (OOT), analytical hierarchy process (AHP) and case-based reasoning (CBR). Manufacturing rules such as processes/materials constraints and properties which are obtained from experts, handbooks, catalogues, experiences and brochures are embedded in the system to be used as guide for assessing the manufacturability of the design. The analysis is made based on rules of manufacturing processes, usual practice of fabrication of specific features or designs, materials/processes constraints and production cost and time.

Approach of expert system modelling

Literature survey on the implementation of ES in developing MAS identified various combinations of specific AI techniques. Statistically analysing the techniques used for building ES it seems that among the most popular approaches (approximately 40%) used RBS [9, 12, 17, 21, 24, 52, 56-57, 59, 61-64]. RBSs use IF-THEN clauses with logical combinations to represent its knowledge base. According to Kusiak and Chen [65], RBS is being frequently applied because the IF-THEN rules are easily acceptable as they are similar to common sense logic and the familiarisation with logic-based languages such as LISP and Prolog. For example, the IF-THEN rules related to the fabrication of sheet metal parts are structured in the KB, then the system interactively searches the list of rules in order to determine which rules are satisfied with the given input [21].

On the other hand, approximately 22% of the researches used OOT in developing the MAS [8, 13, 22, 51, 66-68]. OOTs represent the solution in the form of a program that contains model entities, where each model can be represented by an object. For each object defining the model, it contains data and programming codes that can be performed on those data. In the development of MASs, OOT offers a way of representing objects that are reasoned about, properties and relationships between them. Each of the subclasses of objects has other subclasses related to them and the relationships occurring between them are clearly defined. Using the OOT approach, the analysis is based on the objects and the relations between its sub-classes. For example, electrochemical machining is defined as the main object in the manufacturability model and its machining criteria, such as workpiece material, electrolyte solution, tool electrode, geometric feature and electrochemical machine, are defined as the subclasses [58, 66-67]. This approach has been used for analysing the manufacturability aspects by considering the relationships that occur between the design features and the subclasses stated above.

Another approach used to build ES is AHP which totals up to 16% of the published researches. The AHP is a mathematically based decision-making technique that allows both qualitative and quantitative aspects to be taken into account when making decisions [11, 69]. It not only helps the decision makers to choose the best alternative or solution, but also provides a clear rationale for the choice of AHP by developing and assigning priorities of criteria to judge these alternatives [70]. AHP allows the use of weighting factors to reflect the

functional importance of the features contained in the design [11], or to determine the relative weight [69], for each attribute involved in the estimation of the manufacturability index. This index is a useful indicator of the relative ease of manufacturing parts/features while expressing associated manufacturing difficulties. AHP is implemented to assign weighting factors to features in order to indicate their functional importance, as various features have different roles in supporting the functional requirements of the part [11, 69, 71].

Another approach in modelling ES is called the hybrid approach (HA) in which the assessment is done by a combination of different approaches, among which the implemented HA could be specified as follows: RBS and FL [10], OOT and RBS [5, 16, 18], frame-based and RBS [6], NN, FL and RBS [72], combinations of ABS, OOT and RBS [73], and FL and NN [74].

For example, in a MAS developed by Cherian *et al.* [23], HA is implemented by combining RBS, Bayesian NN and heuristics for assessing the manufacturability aspects. RBS is implemented to evaluate the design geometry while Bayesian NN and heuristics are used to evaluate the material and process parameter selection. The heuristic here is defined as the knowledge of good practice, good judgment, and plausible reasoning in the field of material and process combination. In this study, the overall usage of HA accounted for almost 19% of the reported approaches of ES in MAS development.

Other approaches, accounting for 6% of the research approaches, are NN [59] and ABS [75-78]. NN in ES applications consists of many nonlinear computational elements which form the network nodes and linked by weighted interconnections [79]. It is defined as an interconnected group of artificial neurons (nodes or units) that uses mathematical or computational models for data processing based on a process of adaptation/learning from a set of training patterns [79].

This shows that NN is an adaptive system which changes its structure based on external or internal information flowing through the network [80]. They are usually employed to model any nonlinear mapping between variables and are usually used in classification tasks. Korosec *et al.* [59] used NN to simultaneously evaluate the features complexity in a CAD model with manufacturing capability. In this work, the relationship between surface finish, surface hardness and part manufacturability are expressed as a matrix, which shows a very strong non-linear correlation between the parameters mentioned. Here, NN is capable of analysing the non-linear correlation by sufficient training using calibrated examples while being able to acquire new knowledge from practice.

For ABS, the agent's functionality is defined by the specific needs for the integration of decision-making steps into a common manufacturing decision-making environment. For example [75-76], the manufacturability assessment could be based on several distributed cooperating agents supporting the design, manufacturing and facility assignment activities. Each agent (design agent,

manufacturing agent and facility agent) is related and acts as a decision maker according to its activities.

Figure 2.4 shows an estimative distribution of the 'popularity' of the approaches implemented in modelling ES for MAS development. From the timeline perspective, RBS, OOT and HA have been implemented since 1996 and are still being employed in developing MAS while the most recent techniques, NN, ABS, and AHP are fast expanding.

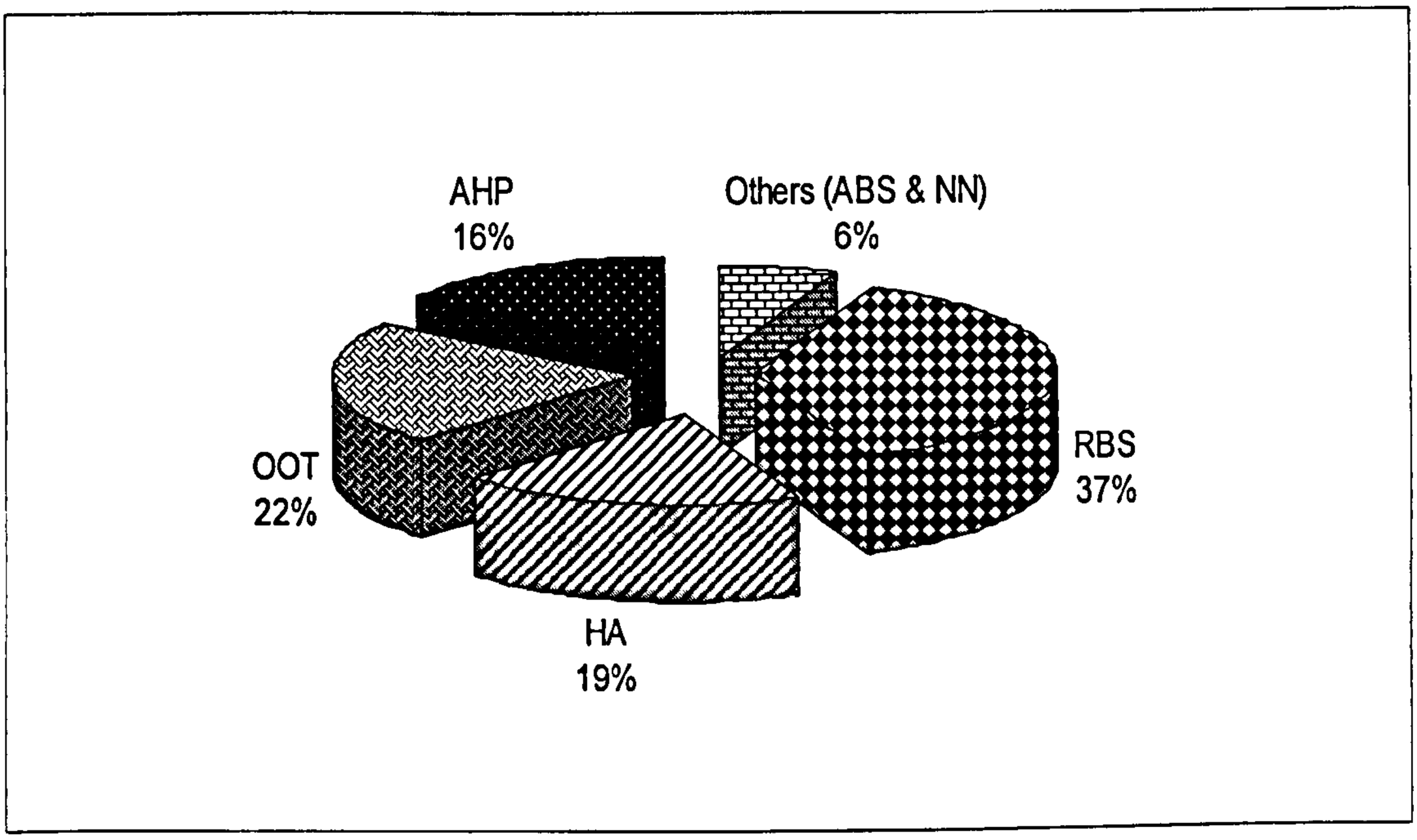

Figure 2.4 Type of approach used for modelling expert system for MAS

Tools to develop expert system (ES)

There are many types of tool, software packages and programming languages available in the market for MAS development using ES. According to Hopgood [79], there are four types of tools available in assisting user to construct ES as follows:

- *ES shells*. It is a complete ES that includes an inference engine (IE), a user interface for programming and for running the system, but it does not provide the KB. Users are required to develop the KB by entering the rules into the system while no supervision is required for the development of IE. Such an approach is easy to use and allows the construction of simple ES; however, the major drawback is the inflexibility in supporting knowledge representation.
- *Toolkits*. These offer almost complete facilities to develop ES such as the features of ES shells, object-oriented programming and AI languages. However, the main drawbacks of the toolkits are as follows:
  - Need of powerful processor, large amounts of disk space and memory (RAM).
  - Costly license fees.
  - 'Embedded knowledge' with reduced flexibility for customisation.

  Among the toolkits available are KEE, ART and Goldworks. Currently, there are some toolkits available in the market that has been built using non AI languages such as C or C++ (Pro Kappa and Nexpert).
- *Programming languages for AI*. A programming language is generated specifically to cater the development of various AI applications. Two important features of AI languages consist of the ability to manipulate symbolic data such as characters, words and numbers and to provide an interactive programming environment. Programming languages that focus totally on AI applications such as LISP and Prolog, offer increased flexibility compared with the above tools.

- *Conventional programming languages*. Programming languages such as C, Pascal and FORTRAN are used as tools for developing the ES. These types of tools require more complicated and tedious program routines compared to the above mentioned tools. Even though it requires complicated programs, they offer the most flexibility in developing AI program.

The distribution of tools usage in developing the ES for MAS based on the four types of tools discussed above is concluded as shown in Table 2.1.

Table 2.1 Distribution of expert system tools

ES shells	Toolkits	Programming languages for AI	Conventional programming languages
• CLIPS [17, 62]	• Nexpert [5, 13, 49, 66-67] • EXPRESS [22, 55]	• Auto LISP [21, 24, 52, 56, 58] • Prolog [9]	• C++ [12, 18, 59, 63-64, 69, 81-82] • Java [57]

Figure 2.5 shows an estimation of the percentage distribution of tools used in developing ES for MAS. The study on the published literature shows that approximately 43% of the developed MAS used conventional programming language, 33% implemented the AI languages, 19% used toolkits to develop MAS and only 5% used ES shells.

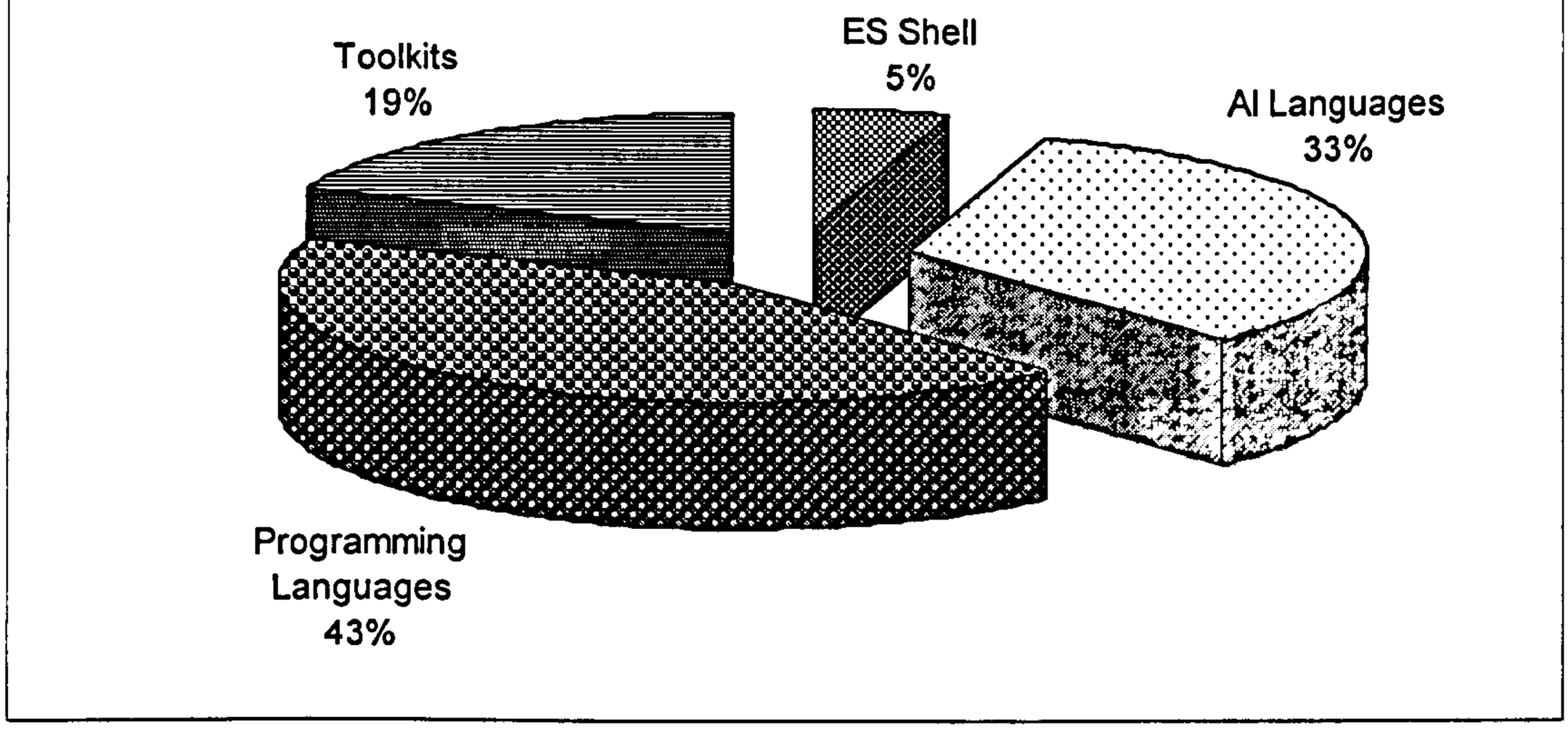

Figure 2.5 Distribution of tools used in developing expert system

2.2.1.3.Outputs generated from MAS assessment

The final component of a MAS generates the outputs as an evaluation of manufacturability aspects which can take the form of: redesign suggestions; selection of processes and materials sequencing setups; estimation of production costs and times; process planning setups. The main objective of MAS is to analyse the manufacturability aspects in determining whether the design can be manufactured or which are the necessary changes on the design to enable its materialisation into a real part. Thus, the results of MAS can take the following forms.

- Redesign suggestion

  During the manufacturability analysis, the users are prompted with suggestions for changes of the part design in order to ensure its manufacturability. The redesign suggestions are usually made after the design has been analysed on the manufacturability aspects, i.e. ES has been run entirely, or during the input session of the design data.

The redesigns suggestions are based on the rules embedded in the KB and are directed to assist designers lacking manufacturability knowledge and thus enabling the reduction of iterations between designs and manufacturing stages.

In a MAS developed by Kumar *et al.* [21], redesign suggestion was provided for the fabrication of die components for sheet metal operations. The advice and suggestion on the design of features were prompted to user from product manufacturability point of view at the initial stage of die design. Among the redesign suggested in this work are changes to minimum corner radius, maximum dimension of the component and the thickness of the sheet metal. While Zha and Du [57] offered advices on how to modify the design of MEMS product that satisfied the constraints of the particular manufacturing processes. The MAS developed by Lee *et al.* [49] was able to provide advice to designer regarding the design of the mould which include feature evaluation. Among the redesign suggestions provided are changes in the size of workpiece, part weight and volume and wall thickness.

From the survey made in this study towards various developed MAS, approximately 56% of them provide redesign suggestions as the MAS outputs [8, 11-12, 16, 18, 21, 49, 57-58, 69]. It can be concluded that redesign suggestion is one of the major outputs of a MAS that can assist designing products correctly with the helps of manufacturing information available at the design stage.

- Provide selection of processes and materials

  MASs can also provide assistance in selecting suitable combinations of processes and materials for the proposed design based on process knowledge and rules. MAS supporting material selection have been reported in relation to the following manufacturing processes:

  - Machining such as milling [5, 54, 62], drilling [5, 62], electrochemical machining [66], grinding [12, 62], turning [9], solid free-form fabrication process (e.g. stereolithography and selective laser sintering) [83].
  - Forming and shaping such as injection moulding [16, 54], powder metallurgy [24], forging [76].
  - Casting: die casting, sand casting [76].
  - Other: LIGA process [64], various manufacturing processes that support the fabrication of MEMS devices such as plastic injection moulding, sheet metal forming, extrusion, die casting, shell mould casting, investment casting and electro-discharge machining [57].

  Usually the material selection is based on the compatibility of the particular groups of materials with types of manufacturing processes such as those stated before. It can be concluded that MAS have been mainly developed for particular processing techniques. This is somehow expected since the relationships between processing techniques and workpiece material have reduced transferability to other processes/environments.

- Process sequencing

  MASs can also identify/propose suitable process sequences in fabricating the proposed design [12, 18, 51, 59, 74, 81-82]. In this approach, the system matches the manufacturing process requirements against existing machine capabilities and availabilities while seeking the reduction of production cost and times. The selection of process sequences are based on the related factors such as process type and capabilities, process sequence applicability and the relationship between features of the analysed part. Thus, process sequencing can be suggested based on the analysis of manufacturability aspects of the design while minimising production cost and time.

- Other outputs

  Additionally, MASs are capable of producing other outputs such as estimation of production cost and time, process planning setup and tooling approaches/orientations. The estimation of production cost and time is generated using mathematical models based on the results of the analysis of the optimised manufacturing processes [5, 47, 54, 62, 66-67, 84]. For example, cost estimation has been developed for die casting based on the mathematical modelling used in the industry practice for this process with input in form of design and process parameters [5]. While parameters such as air travel, cutting length, feeds and hourly rate were adapted in cost estimation module for calculating the value for milling process [54].

Moreover, a process planning setup was generated based on the optimised geometrical and technological properties of the design related to process plan guidelines for specific manufacturing processes [17, 19, 74]. Additionally, by manipulating information related to part geometry and specific tools libraries, a MAS is reported to be capable of providing optimised tooling orientation for a 5-axis sculptured surface machining [85-86].

2.2.2. Applicability of a MAS to various manufacturing processes

Up to now most of the developments of MASs have been related to particular categories of manufacturing processes such as casting, forming/shaping and machining. An overview of the implementation of MAS into various categories of manufacturing processes adapted from Kalpakjian et al. [87] is presented in Table 2.2.

Table 2.2 Categories of manufacturing processes implemented with MAS

	CATEGORY			
	Casting	**Forming and Shaping**	**Machining**	**Others**
Process and literatures related	• Die/Sand casting [5, 13-14, 53, 88]	• Spinning [10, 63] • Forging [5] • Powder metallurgy [23-24, 50] • Roll forming [63] • Injection moulding [4, 15-16, 49, 54, 72] • Blanking/ piercing [17-18] • Fabricating sheet metal [18, 21, 63, 82]	• Turning [9-11] • Milling [4-8, 11, 54] • Drilling [5, 7-8] • Grinding [7, 12] • Wire-electro-discharge [67] • Machining selected to address particular part geometries (e.g. cylindrical, prismatic) [7, 11-12, 56, 58, 74, 84] • Free-form machining [59, 83, 85-86] • Electro-chemical machining [66] • Shaping [7]	• PCB fabrication [22, 55] • MEMS processes [57, 89] • LIGA [64]

Based on the references in this table, it can be noted that most of the developed MAS cater the manufacturability assessment for macro-manufacturing processes while less attention is given to MAS applicability for micro-size product. From the above list of manufacturing processes, it can be concluded that the research in manufacturability assessment can be divided into two broad areas: macro and micro-manufacturing process.

Rough statistical analysis of published work shows that approximately 92% (Figure 2.6) of the researches are focusing on applicability of MAS to macro-

manufacturing processes. Only 8% are targeting the micro-manufacturing processes such as fabrication of MEMS devices [57, 89] and LIGA process [64]. For example, a system that is able to select the 'best combination' of material and process in a concurrent environment for fabricating MEMS devices, based on proposed design and constraints imposed from the material and process selected, is claimed to be developed by Zha and Du [57]. The proposed micro-structures design is dynamically checked by an inference machine supported by rules related to LIGA process that are embedded in KB [64]. In this line, it can be concluded that the major differences between the MAS in macro and micro-manufacturing process lies in the content of the KB developed.

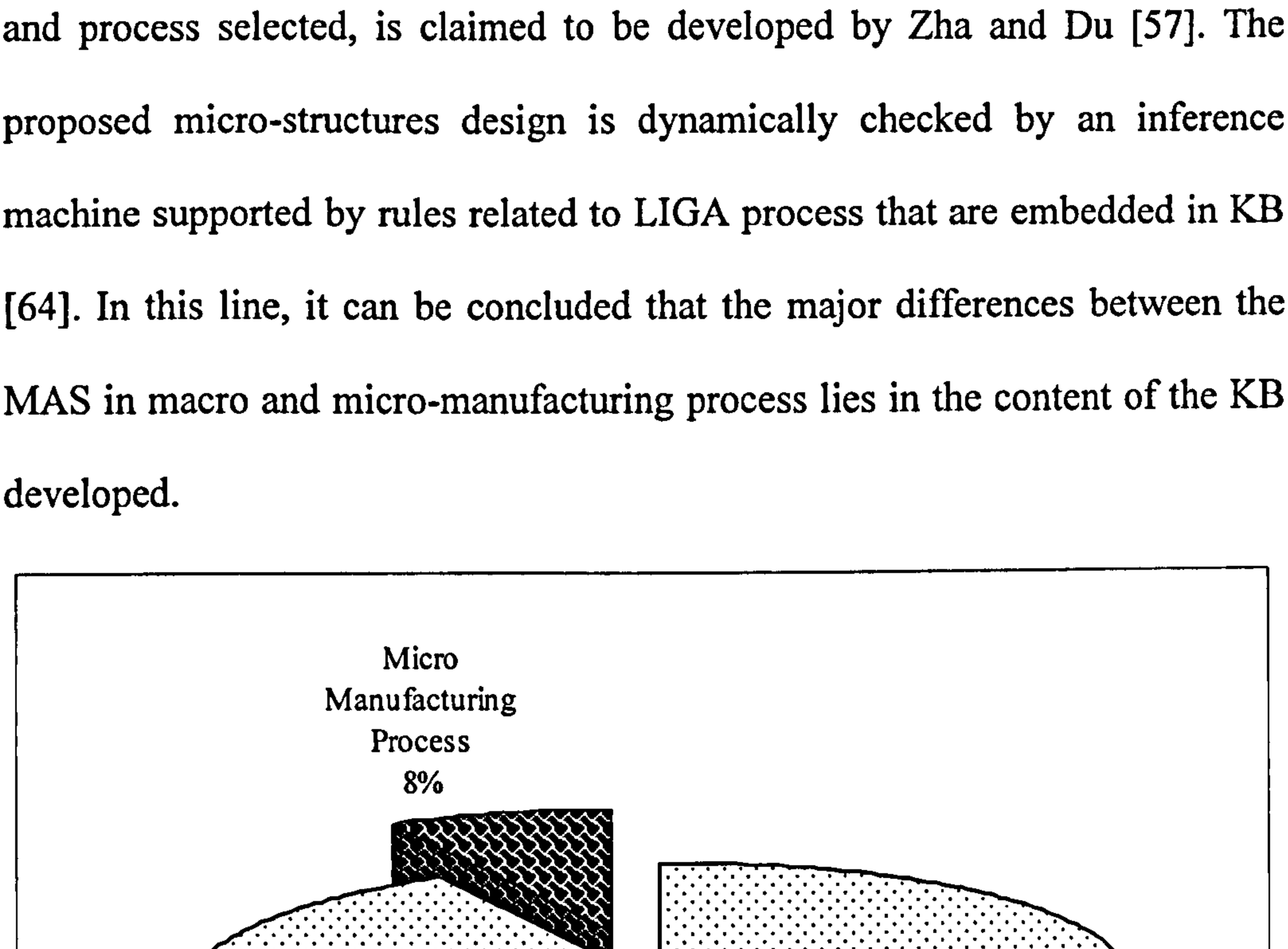

Figure 2.6 Distribution of MAS applicability towards two divisions of manufacturing process

2.2.3. Other aspects that can be analysed through a MAS

MASs can also provide users with indices/indicators to enable the comparison between available processes reflecting the ease of machining unitary/combined features of the analysed part. The manufacturability indices are generated based on geometrical (orientation, intricacy, accessibility, dimensions), technological (workpiece surface finish, part tolerance, employed processing method) [7, 11, 56, 69, 71-72] and assembly (part relationships, type and behaviour of the assembly such as how the mating between features take place) [7].

An index for each feature of a component with respect to each attribute stated above is obtained using parametric fuzzy membership technique [7, 11, 69, 71-72]. Manufacturability indices generated by Yannoulakis [84] are calculated based on the estimated manufacturing times for each feature of a part and then they are used to rank the manufacturing sequences to be employed for the features. The overall manufacturability index is determined from the summation of the indices of the attributes and multiplied by their respective weighting factors [7, 11, 69, 71-72]. Gupta *et al.* [68] also mentioned the development of manufacturability rating to reflect the ease or difficulty of which design can be manufactured but there are no details explanation given. It can be concluded from the current published literature that the assessment of the manufacturability indices are based on the cost and time aspects in order to manufacture the design.

Another important aspect being analysed in MAS is fixturability, where surfaces are rated for fixturing purposes based on related attributes. A fixturability index (FI) is generated based on the summation of the indices from various related attributes such as: surface finish, relation between features, geometrical complexity of surfaces, symmetries, percentage area of the not machined surfaces and orientation of a machined surface with respect to tool direction. The current research suggested that only planar surfaces of the features were considered for fixturability assessment because it provides easy fixturing set-up [69, 71] . The generated FI indicates the suitability of the planer for fixturing purposes.

2.2.4. Advantages of MAS

The assessment of manufacturability aspects of the proposed designs not only acts as a supportive tool to generate designs with the correct measures but it also provides other relevant and useful such as redesign suggestions, material and process selection, process sequencing and set-up of process planning. The implementation of MAS in the design stage is believed to give positive impact to the product development life-cycle as a whole. The main advantages offered by the use of MAS originated from the recent published literature are as follow:

- During the manufacturability analysis, users can be supported with suggestions for critical changes of the designs to enable their manufacture. These redesign suggestions are based on rules embedded in the knowledge-based of the expert system leading towards the reduction of iterations between design and manufacturing stages. Thus, redesign

suggestions represent the major outputs of MASs as it enhances the quality of single/interrelated part designs.

- Provides intelligent assistance in selecting suitable processes and materials based on the compatibility of the proposed designs and built-in knowledge on materials and processes, rules and constraints related to them.
- Assists in determining suitable process sequences for fabricating the proposed designs, this can be done based on contained feature (e.g. holes, slot) in the design and manufacturing interactions, production cost and time criteria for the purpose of production optimisation.
- Represents a key step in incorporating manufacturing issues during design stage to shorten product development time, reduce the number of iteration between design and manufacturing stages, minimises development costs, reduce rework and ensure a smooth transition of designs into production.

2.2.5. Problems and limitations in current MAS

The development and implementation of MAS in the design-manufacturing stage has progressed rapidly over the last decades. From the advantages and applications discussed above, it shows that MAS has a promising future to be implemented in various manufacturing fields especially in assisting designers and manufacturing engineers to minimise the numbers of iterations between corresponding stages of the production routes. Beside all the advantages and its promising future, there are still limitations and challenges occurring in the current MAS.

- **The applicability of MASs is restricted to single manufacturing process**

  Even though MASs have been applied to various types of manufacturing processes, most of the current systems provide assessment to cater for only a single type of manufacturing process. This means that the analysis of manufacturability aspects is done based on that single manufacturing process while the opportunity to take into account the successions, interactions or options with other processes are not considered. This is especially for MAS developed for a particular machine tool which can run other manufacturing processes but not considered in the system. Significant limitations lie in the fact that with fewer manufacturing processes available in the system, the flexibility in assessing the manufacturability aspects is reduced. Besides that, the applicability of MASs is limited to the macro-manufacturing domain *while less attention is given to the new emerging processes such as micro-manufacturing techniques.*

- **Limited outputs produced by MASs**

  Despite various outputs that can be produced by MASs, most studies have only focused on providing a limited number of output combinations. The study shows that approximately 74% of the developed MASs provide only one or two combinations of outputs. Redesign suggestion is the most popular single output provided by developed MASs while the most popular combined outputs are process and material selections supported by cost/time estimations and redesign suggestion combined with manufacturability index. Limited outputs of MASs can be regarded as an

inefficient use of technical database/information built in the system. Choosing to produce a limited number of outputs will reduce the effectiveness, and also the accuracy, of MAS assessments and interactive suggestions.

- **Issues with the input mechanisms**

  Most of the developed MAS applied a feature-extraction system to gather CAD data as input to the MAS. Limitations in using this approach can arise from: imprecision/fuzziness of extracted data, inflexibility of type of data, difficulty in interpreting relationships between various features of the part. Implementation of the latest feature-extraction systems in a MAS that can provide a more accurate input mechanism depend on the on-going research in this field. The development of feature-extraction systems is still a stringent research topic targeted to identify ways to collect accurate and self-sufficient data/design details from the features. Thus, this affects the accuracy of the data being input to the system in assessing manufacturability aspects.

- **Limited capabilities in analysing manufacturability aspects**

  Most researches are limited by focusing solely on the analysing of the manufacturability aspects of the proposed design, while neglecting other important aspects such as part functionality. For example, estimates of design accuracy using the tolerances are made based on the manufacturability aspects only, while the influence on part functionality is totally neglected. Dimensional and geometrical tolerances should be

employed to specify permissible variations for compatibility with the functionality of the proposed design; thus, tolerances are not only design specifications but also play an important role in assessing manufacturability and functionality of parts. Most MASs reported to date consider only manufacturability aspects while sacrificing the functionality aspects in their assessment [12, 47, 58, 63, 69]. Even though the functionality aspects are usually assessed manually or totally neglected, the developed system still reaches the target of producing the proposed design that fulfils the manufacturability aspects but lack of functionality.

It can be concluded that even though MASs offer technical advantages in connecting design and manufacturing engineering, they still have limitations to be tackled. With their significant implications for future practice and industrial exploitation, the limitations highlighted above offer a large incentive for further research development and exploration.

2.3. Uncertainty evaluation modelling (UEM)

Measurement and test results are the basic information underlying the statement of conformity of many products and activities. It is important to have some indication of the quality of the results. For this purpose, it needs 'precise measurements' to ensure high reproducibility in the performance or operation of products and parts. In order to ensure the reliability of measurement, a standard procedure/approach that are accepted and supported worldwide needs to be incorporated. According to *International Vocabulary of Basic and General Terms in Metrology* (VIM) [90], ***measurement*** is defined as "set of

operations having the object of determining a value of quantity". Furthermore, as stated in the *National Institute of Standards and Technology* (NIST) Technical Note 1297 [91], 'the result of a measurement is only an approximation or estimate of the value of the specific quantify in question, that is, the measurand (which is the particular quantity subjected to measurement), and thus the result is complete only when accompanied by a quantitative statement of its uncertainty'. **Uncertainty of measurement** is defined by VIM [90] as a parameter associated with the result of a measurement that characterises the dispersion of the values that could reasonably be attributed to the measurand.

Based on this, it is truly important and necessary to present the result of measurement accompanied with its uncertainty in order to make the measurement comparable, complete and reliable. It is clearly indicated by Desenfant [92] that a measurement or a test result without the assessment of its reliability is completely useless while the comparison between different measurements of the same parameter without knowing the uncertainty is impossible to assess. Uncertainty of measurement when used correctly leads to continuous improvement and often results in improved efficiency, cost reductions and better value for user/customers [93]. The main importance of uncertainty measurement according to Kaarls [94] is providing the opportunity to represent the result of a measurement that gains international acceptance which is important in aspect such as improvement in health care, environment and safety, technical and scientific development, quality assurance, accreditation and certification of products and systems.

There are various procedures and concepts of uncertainty evaluation were proposed and discussed, but in 1993 the publication of Guide to the Expression of Uncertainty in Measurement (GUM) [95] offered a unified method for the evaluation and expression of measurement uncertainties that has been accepted by almost all calibration services worldwide and has become a standard in the field of metrology [96-97]. The basic approach of GUM is to describe a measurement using a model in the form of functional relationship between input and output quantities [93]. The *input quantities* are defined as the aspect that actually determined during measurement process while *output quantities* describe the result of the measurement.

2.3.1. Introduction and definitions

Before venturing into the details of uncertainty evaluation based on the GUM procedures, it is appropriate to define all important terminology employed in this study as the following [90-91, 95, 98]:

- **Measurand** is the particular quantity subjected to the measurement; it is an approximation of the value of the specific quantity to be determined through measurement. The specification of a measurand may require statements about quantities such as time, temperature and pressure. Examples: analysing the cutting force for turning [99], evaluation of shore hardness testers [100], assessing the relative humidity (RH) of the humidity sensor [101].

- **Standard uncertainty** is the estimated standard deviation of each input quantity (sources of uncertainty), which can be evaluated differently for Type A and Type B categories (will be discussed in ***section 2.3.2.1***)

Examples: value of standard deviation of the multiple reading of the dynamometer due to temperature variation [99], standard deviation of the values read by a hygrometer [101].

- **Combined standard uncertainty** is obtained by combining the individual standard uncertainties, calculated based on the *propagation law of uncertainties* (will be presented in ***section 2.3.2.1***).
- **Expanded uncertainty** is the quantity that defines the interval of the measurement result within the value of the measurand that confidently believed to lie. It is obtained by multiplying the *combined standard uncertainty* by a *coverage factor*.
- **Coverage factor** is the numerical factor used as multiplier of the combined standard uncertainty in order to obtain the expanded uncertainty value, typically in the range between 2 and 3. The determination of the coverage factor will be discussed in ***section 2.3.2.1***.

In general, the result of a measurement is only an approximation or estimate of the value of the measurand and thus it is complete only when accompanied by a statement of the uncertainty. The measurement therefore begins with an appropriate specification of the measurand, the method of measurement and the measurement procedure. The uncertainty of the measurement results reflect the lack of exact knowledge of the measurand and it arises from random sources (there are not necessarily independent) such as [95]:

- Incomplete definition of the measurand
- Imperfect measurement of environmental condition
- Improper sampling of the measurand

- Personnel's bias in reading analogue instruments
- Limited instrument accuracy
- Vague values of measurement standards and reference materials
- Assumptions in the measurement procedure
- Variations in repeated observations of the measurand even though taken in the identical conditions

The method of evaluating the uncertainty should be **universal** where it enable the application on a wide range of measurements and measurands, **consistent** which allows its decomposition into lower level components and **transferable** where the uncertainty can be implemented as input to calculate other uncertainties (upper level measurements). Even though the GUM provides the *de-facto* framework in assessing uncertainty, it still depends on the detailed knowledge and deep understanding of the measurand's nature, measurement procedures and input quantities.

2.3.2. Evaluating standard uncertainty

The GUM provides general rules for evaluating and expressing uncertainty in measurement that can be implemented in various fields such as [95]:

- Maintaining quality control and quality assurance in production
- Complying with and enforcing laws and regulations
- Conducting research in science and engineering
- Calibrating standards and instruments and performing tests throughout a national measurement system to achieve the national standards
- Developing and comparing international and physical reference standards

The wide acceptance of the GUM is basically supported by seven renowned international institutional dealing with the fundamentals of metrology [91, 95]:

BIPM	International Bureau of Weights and Measures http://www.bipm.org
IEC	International Electrotechnical Commission http://www.iec.ch
IFCC	International Federation of Clinical Chemistry http://www.ifcc.org
ISO	International Organization for Standardization http://www.iso.ch
IUPAC	International Union of Pure and Applied Chemistry http://www.iupac.org
IUPAP	International Union of Pure and Applied Physics http://www.iupap.org
OIML	International Organization of Legal Metrology http://www.oiml.org

2.3.2.1. Evaluating uncertainty based on GUM framework

The development of uncertainty evaluation which is based on GUM can be summarised into 4 major steps [95]: *(i) Establish the measurement model, (ii) Evaluate the standard uncertainty; (iii) Determine the combined standard uncertainty; (iv) Calculate the expanded uncertainty*. The details of each step are discussed as the following:

- **Establish the measurement model**

  Basically a measurand Y is not measured directly but it is determined from N other quantities $X_1, X_2, \ldots, X_N$ through a functional relationship f:

$$Y = f(X_1, X_2, \ldots, X_n) \qquad \text{Equation 2.1}$$

  The *input quantities* ($X_1, X_2, \ldots, X_N$) which the *output quantity (Y)* depends to, can be classified into:

- Quantities (values and uncertainties) are determined directly during the current measurement. These values are obtained from various ways such as single/repeated observations, determination of corrections to instrument readings and judgement based on experience.
- Quantities (values and uncertainties) are brought into the measurement from external sources such as quantities associated with calibrated measurement standards, certified reference materials an also reference data obtained from handbooks.

As the estimation of the measurement result, if y and $x_1, x_2, \ldots, x_N$ are the estimations of the output (Y) and the input quantities (X_1, X_2, ..., X_N), is given by:

$$y = f(x_1, x_2, \ldots, x_N) \quad \text{Equation 2.2}$$

Once the model has been developed, the next step is to evaluate the standard uncertainties of the estimates input quantities ($x_1, x_2, \ldots, x_N$).

- **Evaluate the standard uncertainty ($u(x_i)$)**

  In this step, the uncertainty of output y (combined standard uncertainty denoted by $u_c(y)$) is determined from the estimated standard deviation of each input estimation (x_i) which is termed as standard uncertainty ($u(x_i)$). The standard uncertainties are evaluated based on the two different methods [91, 95, 97] :

- **Type A**: those which are evaluated by statistical method

  The standard uncertainty evaluation may be based on any valid statistical method for treating data. Examples are calculating the standard deviation of the mean of a series of independent observations; using the method of least squares to fit a curve of data in order to estimate the parameters of the curve and their standard deviations, and carrying out an analysis of variance in order to identify and quantify random effects in certain kinds of measurements.

- **Type B**: those which are evaluated by other means

  Basically the estimate x_i of an input quantity X_i has not been obtained from repeated observations. The evaluation of standard uncertainty is usually based on scientific judgement using all the relevant information available, which may include previous measurement data, experience with or general knowledge of the behaviour and property of relevant materials and instruments, manufacturer's specifications, data provided in calibration and other reports, and uncertainties assigned to reference data taken from handbooks.

- **Determine the combined standard uncertainty ($u_c(y)$)**

  The combined standard uncertainty ($u_c(y)$) is an estimated standard deviation and characterises the dispersion of the values that could reasonably attributed to the measurand Y. By considering that all input

quantities in Equation 2.1 are independent, the $u_c(y)$ of the estimate output y can be calculated based on the propagation law of uncertainties:

$$u_c^2(y) = \sum_{k=1}^{n} \left(\frac{\partial y}{\partial x_i} \right)^2 u^2(x_i) \Rightarrow u_c(y) = \sqrt{\sum_{k=1}^{n} \left(\frac{\partial y}{\partial x_i} \right)^2 u^2(x_i)}$$

Equation 2.3

Where:

$\frac{\partial y}{\partial x_i}$	Describes how the output estimate varies when the value of the input estimates vary
$u(x_i)$	Standard uncertainty evaluated based on Type A or Type B

- **Calculate the expanded uncertainty (U)**

  Although the combined standard uncertainty ($u_c(y)$) can be universally used to express the uncertainty of a measurement result, in some commercial industrial and regulatory applications, it is often necessary to give a measure of uncertainty that defines an interval about the measurement result that may be expected to encompass a large fraction of the distribution of values that could reasonably be attributed to the measurand. The interval is provided by expanded uncertainty (U) which is obtained by multiplying the $u_c(y)$ by a coverage factor k.

$$U = k * u_c(y) \quad \text{Equation 2.4}$$

The result of measurement if then expressed as $Y = y \pm U$ which means that the best estimate of the value attributable to the measurand Y is y with the interval of $y - U \leq y \leq y + U$. U enables the definition of the interval

that covers a large fraction p of the probability distribution characterised by the results and its combined standard uncertainty (p is the level of confidence of the interval). The value of the coverage factor k is based on the level of confidence of the interval and generally in the range 2 to 3. Basically p depends on the coverage factor and subjected to the probability distribution function that models the outputs. As example, for a normal distribution which frequently occurs in practice, k=2 produces an interval that gives a level of confidence of 95% while k=3 provides 99% level of confidence.

Based on the GUM framework, the development of UEM can be summarised as the following (Figure 2.7) [97, 101-104]:

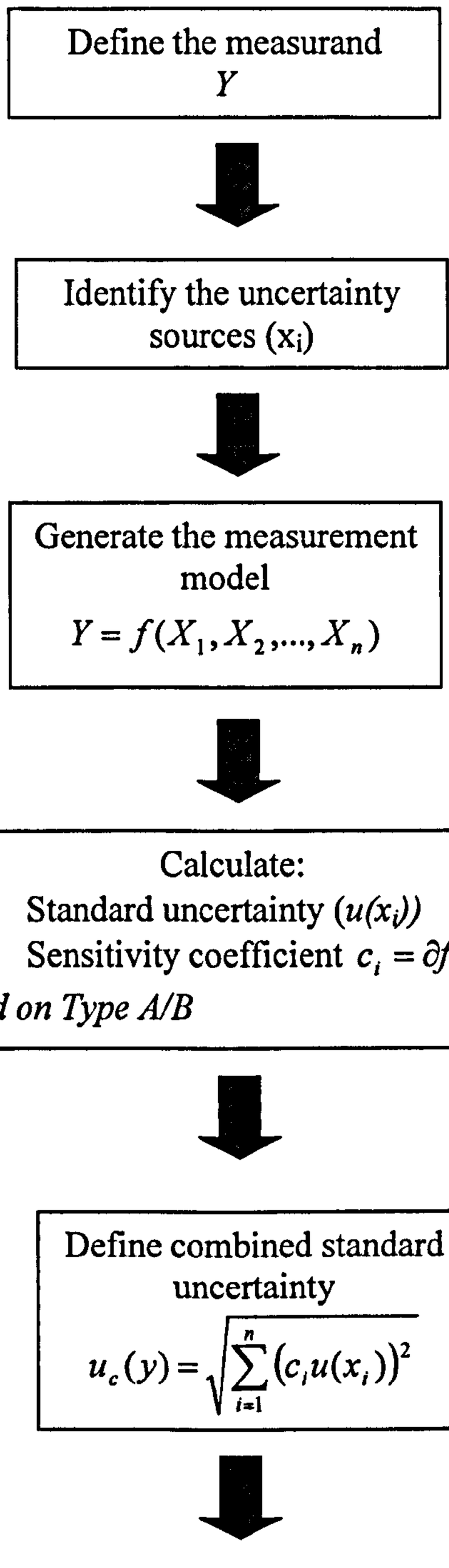

Figure 2.7 GUM framework

2.3.3. Reporting uncertainty

When reporting the result of measurement and its uncertainty, it is preferable to provide a clear description on the methods used to calculate the measurement (e.g. experimental observations, input data) and its uncertainty analysis in details. Specifically, these are the required information in reporting the uncertainty [95, 98]:

- Fully defined measurand (Y)
- How the estimation y was calculated (e.g. number of repeated measurements)
- How the combined standard uncertainty, $u_c(y)$, was evaluated and its components ($x_1 \ldots x_n$)
- List all the uncertainty components and how they were evaluated (Type A or Type B)
- Provide all used constants (if applicable)
- State the coverage interval at the chosen level of confidence
- The measurement should be quoted only to the number of significant figures indicated by the error
- The unit of the measurement of the measurand must be clearly stated

2.3.4. The implementation of uncertainty evaluation

Since the introduction of the GUM framework for evaluating uncertainty in 1993, a considerable amount of literature has been published related to this field. Numerous studies have implemented the GUM framework in evaluating and expressing the uncertainty in measurements in various knowledge

disciplines (e.g. chemistry, health, physics). Among the objectives of evaluating uncertainties stated in these studies are as the following:

- To evaluate the sources of uncertainty and further up to eliminate or at least reduce it [99-100, 105-111].
- To calculate the value of uncertainty for the particular measurement [100-101, 105-106, 108-109, 111-113].
- To compare and assess the uncertainty results with the available standard/guidelines (e.g. ISO) [96, 110].
- To assess the measurement instrument for calibration purposes [100-101, 105, 114-117].

In this section, Table 2.3 presents various examples of study related to uncertainty evaluation implementation with highlights on the objective of the analysis, the determined sources of uncertainty and the results.

Table 2.3 Summary of uncertainty evaluation implementation

Reference	Objective	Source of uncertainty	Type of standard uncertainty evaluation	Results
Castro [105]	• To compute the measurement uncertainty for the positional error calibrator • To minimise the sources of uncertainty of the laser interferometer system	• Laser wavelength inaccuracy • Electronics error • Optics non-linearity • Wavelength compensation • Material thermal expansion • Optics thermal drift • Deadpath error • Cosine error	• Type B	The calculated expanded uncertainty which is based on the evaluation of combined standard uncertainty (u_c) with the coverage factor of 2 (95% level of confidence) is 1.8μm
Su and Wu [101]	• The calibration for uncertainty of humidity sensors testing by means of home-made divided-flow generator was evaluated following the GUM framework at three working temperature points (15, 25 and 35 °C)	• Repeatability of the standard hygrometer • Calibration of standard hygrometer • Repeatability of the humidity sensor device • Calibration of LCZ meter	• Type A • Type B • Type A • Type B	From the analysis, it was concluded that the largest contribution to the uncertainties are from the uncertainty of calibration of standard hygrometer and the uncertainty of calibration of LCZ meter.
Axinte *et al.* [99]	• To propose a procedure for uncertainty evaluation of a single cutting force measurement in turning process	• Error in voltage due to the temperature variation affecting the charge amplifier of the dynamometer • Voltage error due to calibration procedure • Error in voltage evaluation due to the limitation of drift compensation procedure	• Type B	As a result, it was found out that the influence cumulative error from cutting parameters was as important as error from calibration procedure of the dynamometer. Based on this, a model for the expression of cutting forces uncertainty in different cutting conditions was introduced which

		• Error in voltage evaluation due to averaging and rounding procedure in the software • Force error due to variation of depth of cut • Force error due to variation of feed rate		enables the prediction of the uncertainty of cutting for measurements.
Axinte et al. [106]	• To quantify the tool life measurement uncertainty in turning process	• Experimental spread • Uncertainty of flank wear • Uncertainty of depth of cut • Uncertainty of cutting speed • Error due to feed rate • Uncertainty of cutting time measurements	• Type B	From the analysis, it was found that the most relevant contributions to the measurement uncertainty of tool life were experimental spread, then flank wear measurement and variability of cutting data (depth of cut, cutting speed, feed rate).
Xu [116]	• To evaluate the calibration uncertainty of force-measuring devices (load cell-system)	• Uncertainty due to indicator resolution • Uncertainty stemming from rotation effect	• Type B	Both sources have impact towards the uncertainty during the force-measuring device calibration but due to lack of information from the force devices system, the resolution uncertainty is hardly can be reduced. Meanwhile, it was suggested to consider the rotation uncertainty during the force calibration especially when the applied force is in the higher percentage of the capacity.

Misumi *et al.* [117]	• To evaluate the uncertainty in step height measurement of micro-patterned thin films using an atomic force microscope (AFM) equipped with three-axis laser interferometer	• Uncertainty due to repeatability • Stability of laser frequency • Interferometer resolution • Abbe error • Interferometer nonlinearity • Reliable range of parameters for base line	• Type B	The major source of uncertainty in the step height measurements was from the interferometer non linearity which was caused by residual error in an interpolation process.
Pauwels *et al.* [112]	• To propose an uncertainty model to evaluate the reference materials (RM) so that it can be upgraded to Certified RM (CRM) – with certain level of confidence	• Uncertainty stemming from between-bottle variability and measurement repeatability • Uncertainty of the characterisation of the RM batch • Variation from long-term instability (due to storage) • Variation from short-tem instability (during transport)	• Type A • Type B • Type B • Type B	An uncertainty model has been generated based on all sources of uncertainty related in certifying a RM. It can be implemented in characterising a selected homogeneous batch of material with uncertainty values that provide a level of confidence.
Chen [108]	• To evaluate the sources of measurement uncertainty in two thermometers	• Uncertainty due to calibration equation • Uncertainty of the reference standard • Uncertainty due to nonlinearity and repeatability • Uncertainty due to resolution	• Type A • Type A • Type B • Type B	It was found out that the main source of uncertainty in both thermometer measurements is due to calibration equation.
Park *et al.* [109]	• To quantify the uncertainty measurement of thermal expansion of simulated fuel that is measuring using a dilatometer	• Uncertainty of length variation • Uncertainty of the initial sample length (resolution, calibration and temperature variation) • Uncertainty due to system calibration	• Type A • Type B • Type B	As conclusion from the uncertainty analysis, the system calibration was a major contributor to the overall uncertainty in the thermal expansion experiment.

Hoa *et al.* [111]	• To generate a model to evaluate the uncertainty in measurement of semiconductor of piezoresistive sensors • To compare the behaviour between the piezoresistive sensor with polysilicon shield and without the shield	• Influence of relative humidity • Influence of temperature • Error due to intrinsic disturbance • Uncertainty stemming from pressure stimulation	• Type B • Type B • Type A • Type A	The results indicate that temperature-induced exhibit significant uncertainty contributions to the measurement uncertainty of the sensors. The uncertainty in measurement of sensors with polysilicon shield is lower than without the shield.
Uriarte *et al.* [118]	• To establish the uncertainty measurement for the ultraprecision milling machine - ULPREII™ (with tool less than Ø=0.3mm)	• Error due to machine position • Machine trajectory errors • Errors in the spindle, and tool-collets interface • Uncertainty due to tool deflection • Error due to tool wear • Error due to vibration • Error due to burr formation	Not discussed	The following conclusion have been achieved based on the uncertainty analysis for the ULPRE II TM machine: • Tool deflection is the major source of error, followed by collet angular deformation • It was suggested to analyse the influence of these major errors by estimating/defining the system (tool, tool holder, electro spindle and machine) stiffness chain.

Among the challenges in evaluating the uncertainty in measurements that have been raised from these studies are as the following:

- Difficulty in determining the related sources of uncertainty which are relevant to the measurand [107, 110, 112, 115, 119].
- Some of the conventional classification of uncertainty sources stated by the international standard is hardly suitable for applications in accordance with uncertainty models to evaluate the measurement uncertainty [116].
- Lack of reliable and accurate calibration results of instruments used in the measurement [117, 119].
- Doubtful in determining the type of standard uncertainty evaluation (Type A/B) that could affect the calculated uncertainty value (e.g. overestimate/ underestimate) [110].

Based on the provided examples in Table 2.3, it can be concluded that the uncertainty evaluation has been implemented in various fields/purposes. Among the benefits that can be concluded in implementing the uncertainty evaluation are:

- Provide information on the variability measurements that make them comparable, reliable and confidently accepted at the international level.
- Major source/s of uncertainty can be determined from the analysis; this allows actions to be taken to reduce or eliminate the errors occurred that leads to constant improvement of the measurement procedure or the measurand itself.
- It also can offer guidelines via the generated uncertainty model in handling the measurement procedure or instruments [99, 120].

- Provide better approaches or rules related to the measurement procedure that can be implemented in international standard (e.g. ISO)[96].

2.3.5. Software for uncertainty evaluation

Referring to Figure 2.7, it is clear that GUM approach encompasses a tedious and error-prone series of mathematical calculations (e.g. calculation $u(x_i)$ and $u_c(y)$). According to Losinger [121], the implication of manually calculating the $u(x_i)$ and $u_c(y)$ can be horrendous especially when computing the partial derivatives. It can be noted that as the number of the calculations/computations increase, the confidence in the final results tends to decrease. Moreover, users who are involved in uncertainty analysis are aware of the benefits of using a software packages to perform the calculations [122].

Efforts have been made to assist users in evaluating uncertainty with less mathematical error by developing related software that are able to do the analysis especially the tedious calculations. It also allows user to concentrate fully in the more important phase which is determining the *input quantities* and model development. In order to enable the uncertainty analysis, the software should have the following features [123]:

- Provide several important items such as: model equation, input quantities, observations, correlations, budget, report review, import observations and configurations on uncertainty analysis attribute (e.g. setting the coverage factor).

- The analysis is controlled by a standard classification of the input quantities; the result analysis is a clear table of the uncertainty budget that holds all used measurands.
- Perform the classical GUM evaluation of measurement uncertainty which adapt the numerical partial derivates to calculate the sensitive coefficients when error propagation is performed.
- Provide the assigned standard uncertainty and effective degrees of freedom, the sensitivity coefficient derived from the model equation and also the contribution to the standard uncertainty of the result of the measurement.
- The complete result of the analysis is presented as a value with associated expanded uncertainty and automatically or manually selected coverage factors.
- It provides full implementation of Type A and Type B uncertainties.
- It has facilities for structured information that allows documentation of changes and amendments to be recorded in freely editable fields. Any changes made in the data are automatically updated in all related fields in the system.

Among the available software package for computing the uncertainties result based on the GUM framework are GUM Workbench, Assistant and Uncertainty Pro [122].

2.4. Micro-machining

As product development technology becomes more advanced, the size of produced devices decreases and this is where micro-products came into view. According to Brinksmeier *et al.* [124], micro-manufacturing technologies can be distinguished into two categories: micro-system technologies (MST) and micro-engineering technologies (MET) (see Figure 2.8). MST is mainly using processes from micro-electronic technology such as lithography, etching, LIGA while MET utilizes the readapted processes of mechanical and physically material removing techniques such as milling, grinding and laser beam machining.

	Micro-System Technologies (MST)	**Micro-Engineering Technologies (MET)**	
Process	• Lithography • Electroplating • LIGA • Etching	***Mechanical process***	***Energy assisted process***
		• Turning • Milling • Drilling • Grinding	• EDM • Ion/Laser Beam machining

Figure 2.8 Micro-manufacturing technologies [124]

Most of the knowledge that have been utilised in MET are existing technologies adapted to the miniaturisation of structures, devices and systems [26, 31]. Among the examples of this type of micro-machining methods are milling, drilling, grinding and turning where the general principles are similar to those conventional machining operations. Micro-machining is a method of creating miniature devices and components with features that range from tens of micrometers to a few millimetres in size by removing the unwanted material from the workpiece, using the mechanical force of the micro tools [25-26, 30,

35, 125-126]. In this study, focus is given into one of the mechanical process of MET which is micro-milling performed on a custom-made 4-axis Miniature Machine Tool (MMT).

2.4.1. Micro-milling process

In this study, micro-milling process is given the focus in the literature review as it is the main domain for the implementation of the system. According to Bissacco [127], micro-milling is defined as the downscaling of the conventional milling process, involving the use of tools with diameters in the sub-millimetre range. Even though micro-milling can be consider as a rather recent process, not much research interest was focused until the late nineties [127]. Among the advantages of micro-milling are:

- Possibility to machine full 3D micro-structures by high aspect ratio and high geometric complexity [25-28, 30, 128-134].
- High flexibility where the electrical properties of the workpiece do not influence the process so that a variety of materials can be machined (plastics, metallic, composite) in different size, shape and features [25-26, 28, 130-131, 133-137].
- Not requiring expensive set-ups such as in lithographic methods [26, 132] .

Conventional milling is one of the most versatile machining processes and based on this, micro-milling is being analysed and studied to ensure its versatility in generating good quality micro-product. Micro-milling incorporates many characteristics of conventional milling thus, reasonable

limits, a number of issues have been raised concerning the 'size effect' phenomena [27, 30-31, 138]. Different characteristics such as reduced tool dimensions which primarily reduce the tool strength, stiffness and cutting speed, very low material removal rate and increase surface roughness due to built-up edge have been identified due to the downscaling of the existing conventional process which also becoming challenges in micro-milling. Among the problems occurred due to 'size effect' are [127, 135, 139-140]:

- The availability of highly accurate and repeatable machine tools and cutting tools
- Low tool stiffness that makes the system more prone to vibrations
- Process limitations related to minimum chip thickness that can lead to material rubbing
- Low production rate when compared to conventional machining

2.4.1.1. Examples of micro-milling application/implementation

Table 2.4 below presents various literature that utilized micro-milling in producing micro-structure/micro-component.

Table 2.4 Example of micro-milling implementation/application

Reference	Objective	Tools/ Machine	Machining Parameters	Workpiece	Structure/ feature	Results
Popov *et al.* [128]	To implement and verify the machining strategies in milling thin features	Ø=0.2mm end mill; KERN HSPC 2216 micro-machining centre	f_z=0.007mm; V_c=18 m/min; n=39000 rpm; a_p=0.005mm; a_e=0.070mm	Brass	Slot; Pocket; Thin wall	The micro-structure was successfully and accurately machined based on the proposed strategy.
Takacs *et al.* [141]	Identify the optimal process parameters for machining metallic materials	Ø=0.15,0.3,0.4,0.6 mm carbide end mill (z=2)	Not available	Brass; Tempered-grade steel; Carbon steel	Micro-grooves	The results show that metallic materials are able to be machined at an acceptable accuracy and surface quality.
Dimov *et al.* [34]	Optimise machining strategies for a better surface quality by taking into account the specific conditions arose during micro-milling (e.g. side steps, step-over movements)	Ø=0.15mm end mill; KERN HSPC 2216 micro-machining centre	f_z=0.01 mm; V_c=18 m/min; n=40000 rpm; a_p=0.01mm; a_e=0.070mm	Copper C101	Micro-honeycomb structure	It was concluded that machining strategies is one of the important factor in determining the resultant surface finish.
Bissacco *et al.* [39]	Investigate the related issues that affect the part accuracy and surface quality of the machined micro-part in hardened tool steel	Ø=0.2 mm end mill (z=2); 3-axis CNC milling	f_z=0.001mm; V_c=80 m/min; n=127000 rpm; a_p=0.005mm	Hardened tool steel	Micro-structures for micro-injection moulding	The relative accuracy of the machined parts, the surface quality and burr formation are influenced by the low uncut chip thickness to cutting edge radius. A solution was provided by increasing the f_z.

Denkena *et al.* [142]	Analyse the capability of micro-milling in generating micro-structure	Ø=0.5 mm carbide end mill (z=2)	f_z=0.002 mm; V_c=60 m/min; a_p=0.5mm; a_e=0.050mm	Brass; Aluminium	Curved thin wall	Thin wall with minimum thickness of 18μm could be machined without any damages; the curves of the structures increased the wall stiffness.
Lee *et al.* [140]	To characterize the surface quality produced by the micro-milling.	Ø=0.229 mm carbide end mill (z=2); Mori Seiki CNC drilling centre	n=7500, 40000 rpm; a_p=0.06, 0.12 mm	6061 aluminium	Slot	It was found out that tool run-out significantly affect the surface quality, but by using optimal machining parameters, features with good quality can be produced.
Uhlmann *et al.* [143]	Determine the correlation between machining parameters and the characteristics of the workpiece material (Tungsten-copper)	Ø=0.5 mm cemented carbide end mill (z=2) uncoated and TiAlN coated; 3-axis machine tool (type Gamma 303 High Performance)	f_z=0.001 mm; V_c=100 m/min; a_p=0.06mm; a_e=0.05mm	Tungsten-copper (WCu)	Not available	The workpiece material properties (e.g. grain diameter, particle distribution) must be taken into consideration when performing micro-milling From the view of machining parameters, by increasing the f_z, it can provide a better dimensional accuracy.
Keppeler [144]	To propose the manufacturing of CMP pad using micro-milling	Ø=0.127 mm end mill	Not available	PMMA	Column array	The positive mould of CMP was successfully milled on PMMA
Dhanorker *et al.* [42]	Machining of AL 2024-T6 to test and validate cutting force models	Ø=0.635mm carbide end mill (z=2)	f_z=0.15875, 0.3175, 0.635, 1.27, 2.54 μm; V_c=79.8, 119.7, 169.65 m/min; n=40000,60000, 80000 rpm; a_p=0.127 mm	AL 2024-T6 Aluminium	Slot	Large force variations are observed as the diameter of the cutter decreases and the spindle speed increases

Vogler *et al.* [36]	To test the capability of in-house developed MMT in generating 3D micro-structure	Ø=0.5mm carbide end mill (z=2); MMT testbed	V_c=200 m/min; n=125000 rpm	6061 Aluminium; 1018 Steel; 4340 Steel; 316 Stainless Steel; 416 Stainless Steel	Concave and convex feature; Slot	The MMT is able to produce concave and convex portions, while the surface roughness values were found to be in the acceptable range of quality.
Kurita *et al.* [145]	Study the basic performance of the hybrid micro-machine tool	Ø=0.5mm end mill; 3-axis hybrid MMT (milling, EDM, ECM)	V_f=40, 200 mm/s; n=20000,100000 rpm; a_p=0.1 mm	Copper	0.1mm depth groove	Micro-milling process is able to produce the groove on the copper with a better surface roughness when using high speed spindle.
Okazaki *et al.* [146]	Analyse the performance of the custom-made 3-axis desktop micro-milling machine	Ø=0.2mm ball end mill, 0.5mm end mill (z=2); 3-axis desktop micro-milling machine	n=50000, 200000 rpm; a_p=0.1 mm	A7075-T651 (Aluminium Alloy); NAK55 (Hardened steel)	Thin wall; Pocket (honeycomb)	The MMT is capable to generate thin wall and also the honeycomb.
Bang *et al.* [147]	Test the constructed 5-axis milling machine in machining 3D micro-component	Ø=0.1,0.2 mm carbide end mill; 5-axis micro milling machine	n=25000 rpm; a_p=0.005 mm	Brass	Micro-wall; Slot; Micro-column; Micro impeller	Test machining of micro-walls, micro-columns and micro-blades showed that the constructed micro-milling machine is capable of producing practical micro-parts.

Referring to Table 2.4, it shows that micro-milling process has been utilized to produce various type of micro-structure in different materials using a wide range of tool size. The flexibility and efficiency of micro-milling process allows the generation of good quality micro-component. Even though the researches in micro-milling technology have been recently taking shape, a number of micro-parts/components have been successfully produced such as: The 'nature' of mechanically removing the workpiece material for producing parts is well-suited to support the development of micro-injection mould industry because of the promise for accurate, low cost, small batch size processes of 3D moulds using various materials [26]. Among the example of generated micro-moulds are micro-injection moulds made of steel [132], copper [29], stainless steel and aluminium 6061-T6511 [148] and micro-mould for chemical-mechanical polishing pad on polymethyl methacrylate (PMMA) [144]. Moreover, micro-mould for the tyre-rim in micro-car as shown in Figure 2.9 has been successfully machined on steel (SAE H13) [131, 149].

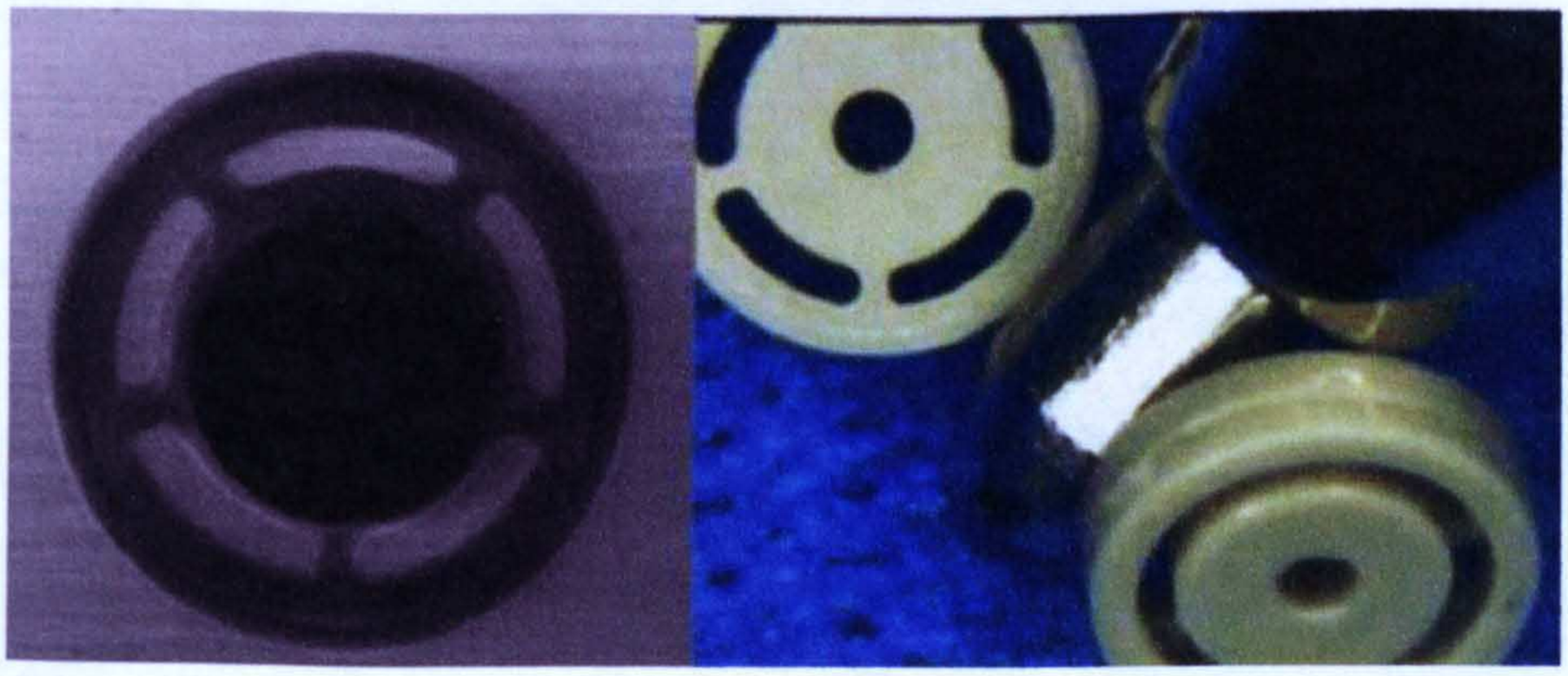

Figure 2.9 Micro-mould (tyre-rim for micro car) on steel (SAE H13) [131, 149]

While the examples in generating micro-embossing dies are: mould made from brass with feature size less than 80μm [150]; master for hot embossing micro-fluidic chips in polymers generated on brass plate (alloy 353) [151] (see Figure 2.10).

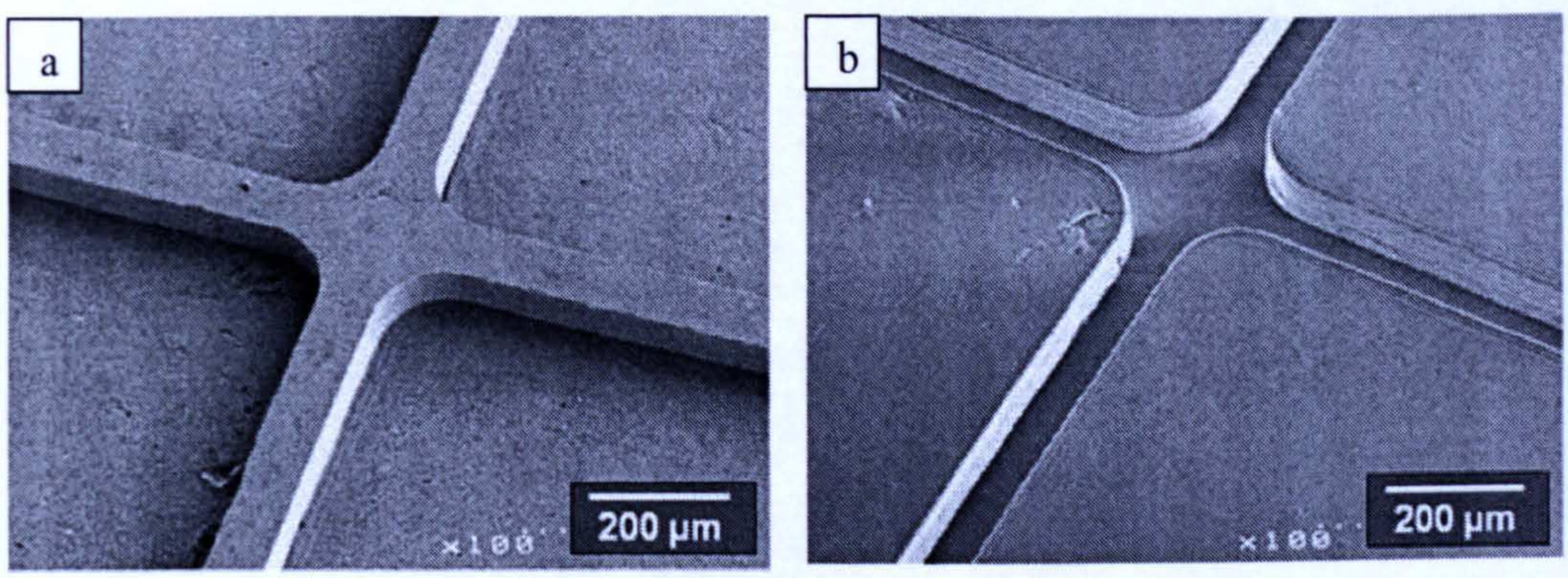

Figure 2.10 Micro-milled mould master on brass (a) Hot-embossed replications on polymer (b) [151]

Another advantage of micro-milling is the capability of generating 3D full features at micro-scale level in a variety of materials also provides new opportunities and applications. The existing published work has presented various of 3D micro-features machined by micro-milling such as three exponential spiral with a single straight trench (height=0.062mm) on PMMA [126] and micro-grooves (width=55μm, depth=40μm) on brass [152]. Beside that, various micro-component have been produced precisely such as micro-turbines (Ø=3.4mm, blade length=0.35mm) [147], micro-gears, neurovascular device components (Figure 2.11) [153], bio-medical devices made from brass with feature size less than 50μm [150], micro-accelerators and gyroscopes made from elastic alloy [154], tooling inserts for micro-filters fabrication [34] and copper electrodes for micro-EDM [29, 143].

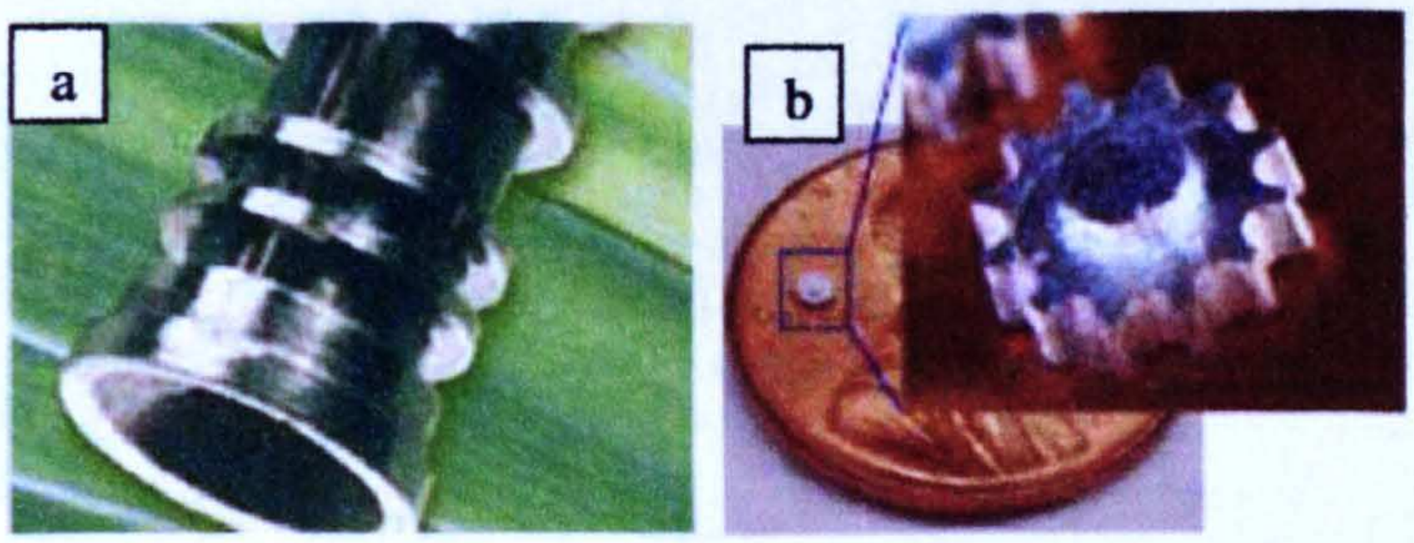

Figure 2.11 Neurovascular device (a) Micro-gear (b) [153]

2.4.1.2. Challenges in micro-milling

Even though micro-milling replicates the conventional process, it is still difficult to predict the operational and the result of micro-milling process. The issues mainly come from the miniaturisation of the components, tools and processes [26]. The main challenges are the following:

- The availability of machine tools

  Precision machine tools are available but at high cost because of their relatively large scale and specialised controlling/motion systems [26, 127]. In contrast with these, the miniature machine tools (MMT) are basically based on the fact that they are cost-effective and have low inertial masses, require low energy [26], easy to achieve high-speed machining and high-precision/rigidity due to reduce inertia [146], encompass lower vibration amplitudes compared to macro-machine [155] and easy deployment around the factory [146]. Among the features that are required for a MMT to support the micro-machining needs are:

  - High spindle speed [26, 127, 133, 135, 141, 149, 156-157]
  - High precision positioning systems [26, 127, 133, 135, 141, 156]
  - Rigidity of the machine structure [26, 127, 156]

Further discussion on the MMT from the previous and current literature will be presented briefly in ***section 2.4.2***.

- The development of micro-tooling

  The size of micro-tools determine the feature size of micro-components; if the diameter can be decreases further, the size of features can be reduced comparable to those produced with lithographic techniques. Since the productivity in micro-machining has been limited by employing low values of cutting parameters (e.g. feed per tooth, axial/radial depth of cuts), tools with improved wear resistance and improved stiffness must be developed to improve the accuracy and repeatability of the process [28]. Among the issues in micro-tool developments are:

  - Tool must be harder than the workpiece material and no thermally activated diffusion has to take place between the tool and workpiece [25, 39].
  - Tool edge radius must be much smaller than the dimension of the cut thickness (with minimum factor of 2) [25, 156].
  - Even though the current commercial micro-tools have a well defined geometry and small tolerance but it has limitation as most of them are designed for steel machining [135]. However, the availability of tungsten carbide tools which are generally used for micro-machining processes provide a better choice for the user due to their high hardness and strength over a broad range of temperatures [26].

- Unpredictable and premature tool life are among the major concerns [29, 150] especially when machining hard materials, such as hardened tool steels [131].
- To enhance the performances of the cutting tools, a variety of coatings (e.g. TiAl, TiAlN, CBN, CBD) have been developed for micro-cutting application; however, with the application of coatings, the cutting edge radius is likely to increase leading to less ability of the cutting edge to remove small amount of materials.
- As the micro-tools require to be replaced frequently, new methods to produce cost-effective tool with quality are a necessity.

- The nature of the workpiece material properties

  The effects of material properties of the workpiece (e.g. hardness, grain size effect) are considered highly important because in micro-machining the material removal process is ruled by the interfacial interaction between the cutting edge and the workpiece [158]. Moreover, in micro-machining usually the chip forms within a single grain at a time compared to the conventional machining where the chip formed by several grain, as in micro-machining the material grain size is not downscaled with the process dimensions. This issue has been extensively reported in various literatures [127-128, 130, 158-159]. The distinct difference between micro and macro-machining are the assumption of homogeneity in workpiece material properties is not valid because, in micro-machining, the grain size could be of the same order of magnitude with the depth of cut/radius of the cutting edge (Figure 2.12). Popov et al. [128] suggested that refinements of the grain structure could lead to more 'favourable' conditions during tool-

material interactions. The preferable grain structure of material for micro-machining is homogeneous workpiece of very fine composition with narrow grain size distribution and without internal stresses [127, 131, 158]. It was also proposed for the cutter edge radius of the tool not to be smaller than the average grain size of the material [141].

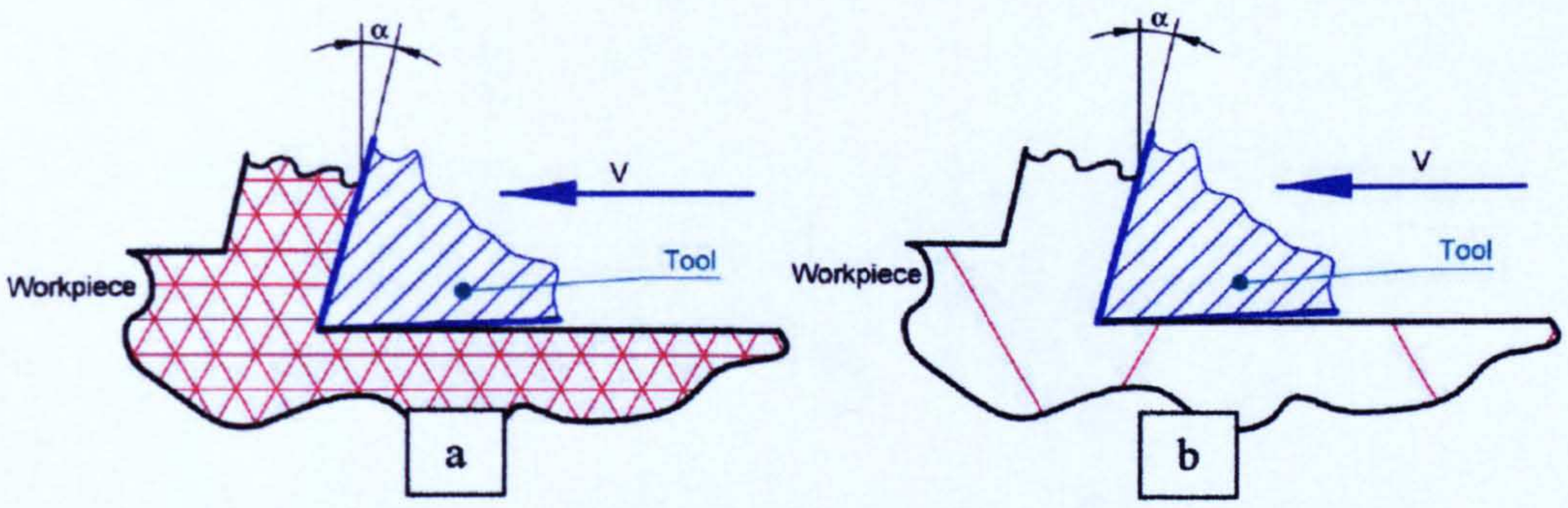

Figure 2.12 Relation between grain size and chip thickness for conventional milling (a) and micro-milling (b) [127]

- The quality of the generated surface

  Burr-free machining strategies have to be developed as it is difficult to handle the machined micro-parts after the machining process have been completed [25, 30, 39, 128, 131, 135, 152, 160]. In machining ductile metallic materials such as brass, the burr occurrence is higher when the feed per tooth (f_z) is low and when utilizing the down milling approach [131, 141, 160]. At lower f_z, the rubbing and compression (ploughing mechanism) of the material take place instead of cutting and this generates more burrs [131, 160]. De-burring process as practiced in macro-machining are unfeasible at micro-scale as it can destroy the delicate micro-features. One of the causes of low quality surfaces is tool wear and high tool wear

occur when machining hard materials which change drastically the tool condition and consequently the process performance [135].

- Machining thin-walled or minimal structural dimensions

  Generating thin features represents a major challenge in micro-milling because of the instability of the machining operation [128, 142, 154, 161]. By making features thin, their stiffness decreases which could result in the occurrence of vibration during machining. This could lead to the deterioration of the component's accuracy and poor surface quality [128]. Listed below are the suggested strategies in machining thin walls and small dimension structures [126, 128, 142]:

  - The toolpath should be selected in such a way that the cutting should process from the least supported area toward the best supported thin features in the micro-component.
  - In producing filleted thin features, it should be machined in a number of subsequent passes by removing the material layer by layer that are carried out with a sufficiently low spindle speed to prevent vibration.
  - Avoid sharp corners and introduce fillets for this minimal structural dimensions and thin wall.

The following are examples of thin walls that were generated in various literatures:

- Thin wall (height=0.01mm, width=0.008mm) has been machined on PMMA [126].
- Trench made by micro-slotting (width=15μm, depth=150μm) and thin wall between slots (width=55μm, height= 150μm) [134].

- Thin wall (width=65.5μm, length=3.43mm, height=778.7μm) has been machined on Mg-Zn-Y alloy which was used for biomedical application [161].
- Micro-component with thin wall (length=0.02mm, height=0.31mm and width=0.8mm) was successfully machined on brass [128] (Figure 2.13).

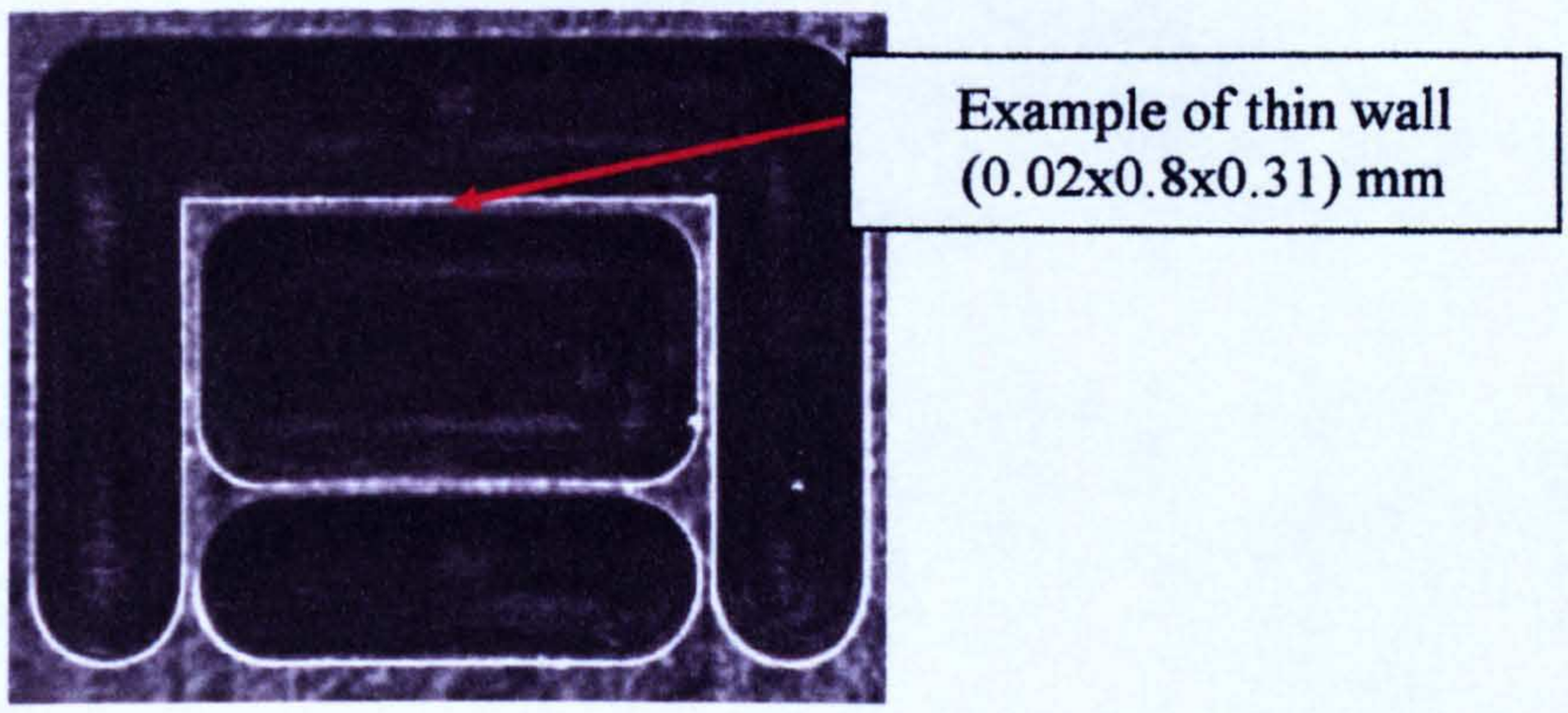

Figure 2.13 Example of thin wall on brass [128]

- In order to avoid tool breakage and to maintain the desired tolerance, the depth of cut is often less than the critical minimum chip thickness [26, 30, 39, 41-42, 131, 136]. The major challenge in micro-machining processes is the limits that have to be imposed on the resulting machining forces that may influence the accuracy of the process because of the elastic deformations of the micro-tools and/or parts [25-26, 28, 35, 130]. As example, in micro-end mill, the machining forces exerts a larger influence on accuracy because the main direction of the force is perpendicular to the tool axis [35]. Even though there are various models have been developed to predict the cutting forces for conventional milling, but none can be successfully implemented for micro-milling. Various researches have been

developing the cutting force models especially for micro-machining that can accommodate the requirement for various materials and cutting conditions [26, 28, 40, 130, 135]. From these literatures, the aspects that were suggested to be considered in the micro-cutting force analysis such as the chip thickness model [26, 28, 41, 131, 162], the workpiece material's elastic-plastic effect and tool run-out [40, 140] and the static deflection of the tool and cutting edge radius [39].

- Furthermore, small depths of cut and cutting edge radii increase the friction between the tool and the workpiece that resulted in thermal growth and wear which can also cause ploughing phenomena. This phenomena leads to material rubbing that produce a rough surface and elastic recovery of the workpiece [26, 28, 30, 130, 135].
- In micro-milling, the effect of tool run-out is clearly noticed as it creates a great problem for the dimensional accuracy and surface quality of the micro-milled part, shorter tool life and higher tool breakage [40, 140]. For a conventional macro-scale machining, the run-out which is typically in the order of micrometers has a small effect and often being negligible on the dimensional accuracy of the machined feature. Due to 'size effect', the value of the tool run-out to tool diameter ratio becomes larger than the conventional milling. The tool run-out is caused by the imperfect tool alignment, asymmetric tool geometry, mismatch between tool and machine tool and vibration of tools during machining. Since the tool is not accurately and asymmetrically oriented relative to the surface being cut, the loading of the cutting edges will vary and this provide negative impact towards the surface roughness, tool wear and vibration [40, 141].

Even though micro-machining imitates conventional machining in many ways (e.g. operational, process), due to the differences/challenges discussed above, the existing knowledge and experience on current macro-machining cannot be directly applied and adapted to the micro-scale. In order to make micro-machining more flexible, robust and productive, it is essential to understand and tackle the differences and issues occurred between the macro and micro-machining. The adaptation of the knowledge from conventional process can be materialised in micro-machining with the conditions stated below:

- Deep understanding of micro-phenomena
- Extensive investigation in chip removal processes
- Detailed approach of analysing the micro-cutting force prediction
- Thorough study of the workpiece material properties effect
- Systematic approach on the process of handling/inspecting the produced micro-product

2.4.2. Development of miniature machine tool

Although manufacturing of such miniature features and components can be achieved on large-scale Precision Machine Tools (PMTs), the design and construction of Miniature Machine Tools (MMTs) is acquiring great interest due to the recent advancements in Micro-Electro Mechanical Systems (MEMSs).

From the concept of miniaturization of machine tools has emerged the use of small-scale all-in-one manufacturing systems called micro-factories. Okazaki et al. [155] defines the term "micro-factory" as an entirely new approach to design and manufacture that minimizes production systems to match the requirements of miniature parts. Such systems leads to reduction of space and energy as well as the minimisation of investment and operational costs, aiming to achieve light and agile manufacturing systems that are optimized for current manufacturing needs in producing micro-components.

On the other hand, the interest has recently focused on use of MMTs for specific chip removal processes such as turning, milling, drilling and grinding as well as Electro Discharge Machining (EDM) and Electro Chemical Machining (ECM) in order to understand the mechanics of micro-machining process and optimize the process parameters. Liu *et al.* [130] states that there are a number of issues that prevail in micro-scale machining. Such issues are fundamentally different from macro-scale machining and influencing the underlying mechanisms of the process, resulting in changes in the chip-formation process, cutting forces, vibrations and process stability, and hence leading to significant influences on the surface topography of the machine surfaces and dimensional accuracy of the produced components. Thus, dedicated MMTs are currently built for analysis of the aspects of precision, accuracy, stability and reconfigurability of MMTs as well as their integration with MEMSs for in-situ inspection and metrology purposes.

Table 2.5 gives a summary of selected examples of MMTs and systems while Figure 2.14 shows examples of developed MMT from the literature. Although there are a number of works on building micro-factories and multi-purpose MMTs for implementing several machining operations using the same machine tool, the majority of research is related to construction of dedicated MMTs for conducting specific operations for the generation of components with complex geometries. This is due to the fact that the process mechanics can be well understood and the stand-alone characteristics of such dedicated machine tools can be investigated extensively.

Table 2.5 Examples of selected micro-factories and miniaturised machining systems

Reference	**Developed System and addressed machining operations**	**Machine Size (mm)**
Kussul et al.[163]	3-axis Micro-factory (turning, milling, drilling, grinding)	130x160x85
Asad et al. [164]	3-axis Micro machining centre (milling, turning, grinding)	1500x1100x1900
Kurita et al. [145]	3-axis Hybrid MMT (milling, EDM, ECM)	557x604x655
Azizur et al.[165]	3-axis MMT (milling, turning, drilling, grinding, EDM)	600x560x660
Vogler et al. [36]	3-axis MMT (milling and drilling)	250x150x200
Ashida et al. [166]	3-axis Micro-milling machine	119x119x102
Okazaki et al. [146]	3-axis Desktop micro-milling machine	450x380
Iijima et al. [167]	Micro-turning machine	150x100
Ho Bae et al. [168]	Micro-lathe	45x44x39
Kitahara et al.[169]	Micro-turning machine	32x25x30.5
Ashida et al. [166]	Micro-forming machine	111x66x170

Hirano et al. [170]	Desktop micro-ECM machine	600x650x750
Shi et al. [161]	3-axis MMT	400x320x100
Mishima [171]	Micro-factory (lathe, press, milling)	600 x 900
Subrahmaniam and Ehmann [172]	Meso-scale Machine Tools (milling)	90x60x60
Bang et al. [147]	5-axis micro milling machine	294x220x328

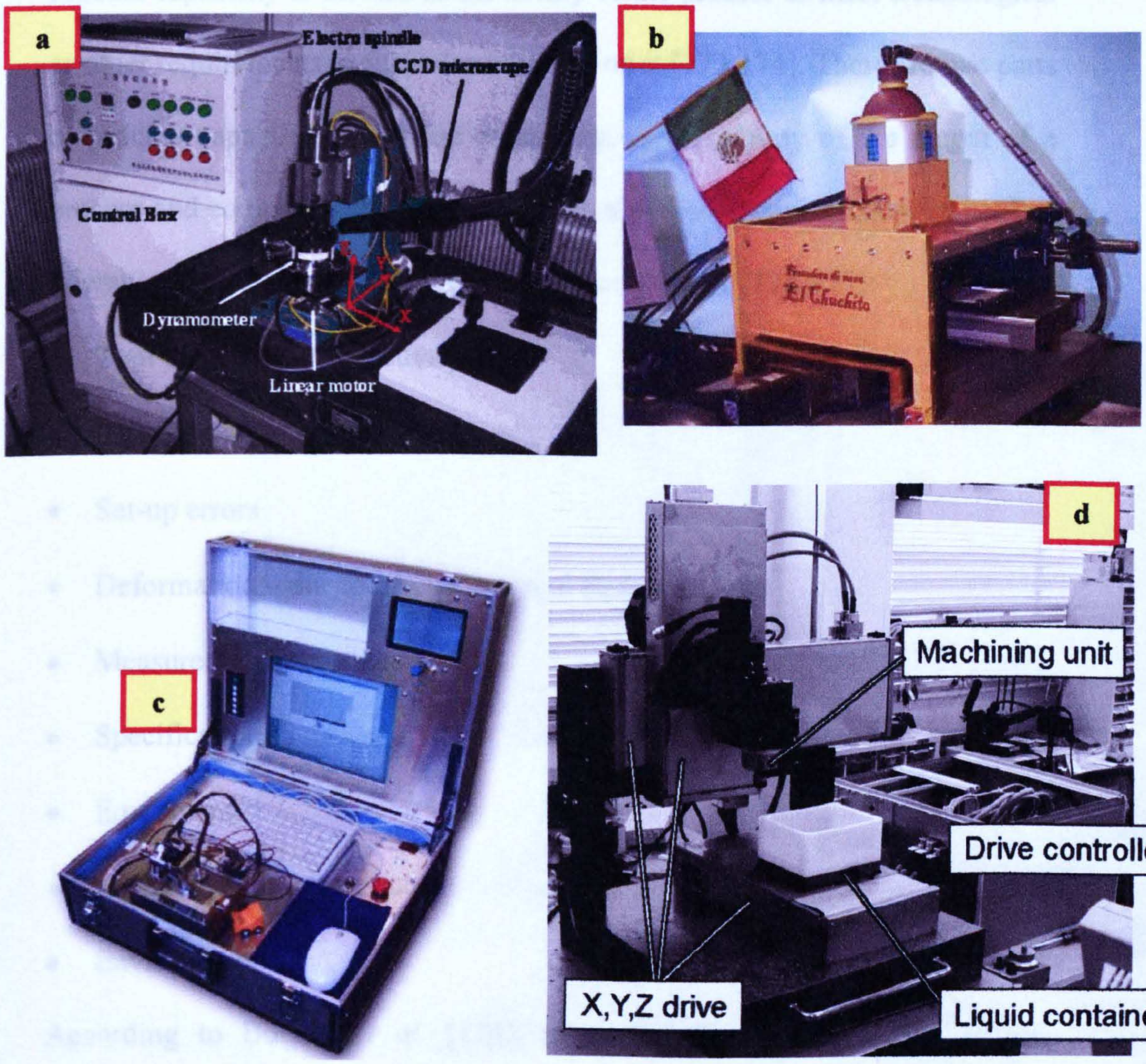

Figure 2.14 Example of MMT: (a) 3-axis MMT [161]; (b) 3-axis Desktop micro-milling machine [146]; (c) Micro-turning machine [167] (d) 3-axis Hybrid MMT [145]

It can be seen from Table 2.5 that the overall size of MMTs are varying significantly. Therefore, the construction of a MMT with optimal features and characteristics is of significant importance not only to achieve the required technical performances in a particular setup, but also to consider handling and versatility aspects.

Process capability is defined as the ability of the process to meet technological or other requirements to fulfil demands put on it [173-174]. There are two parts of process capability which are measuring the variability of the output of a process and comparing the variability with a proposed specification or product tolerance. Among the variability factors or criteria are [174-175]:

- Tool and functional accuracy
- Operator
- Set-up errors
- Deformation – due to mechanical and thermal effects
- Measurement impurities
- Specifications
- Equipment
- Method or job instructions
- Environment

According to Booker *et al.* [174], in analysing a design at the concept development or early detailing stage, it is only necessary to focus on the main variabilities associated with manufacturing process. Based on this, in reviewing the literature related to the custom-made MMT, it was found out that in order to assess the capability of the machine tool, the surface quality and the

geometrical accuracy of the machined part (e.g. groove, thin wall, honeycomb) were selected to be the main evaluation criteria [36, 145-147, 161]. Various tool and workpiece materials were utilized in machining parts using in-house developed MMTs and the results indicate their capabilities to produce surfaces of acceptable quality and geometrical accuracy. Another important finding was that the machine tools were also able to machine full 3D features; one of the examples is shown in Figure 2.15 where a micro-impeller was successfully generated from a 5-axis micro-milling machine tool [147]. Moreover, based on the listed machine size in Table 2.5, it is believed that most of the MMTs can be categorized as portable desktop machines which allow flexible deployment around the workshop/factory.

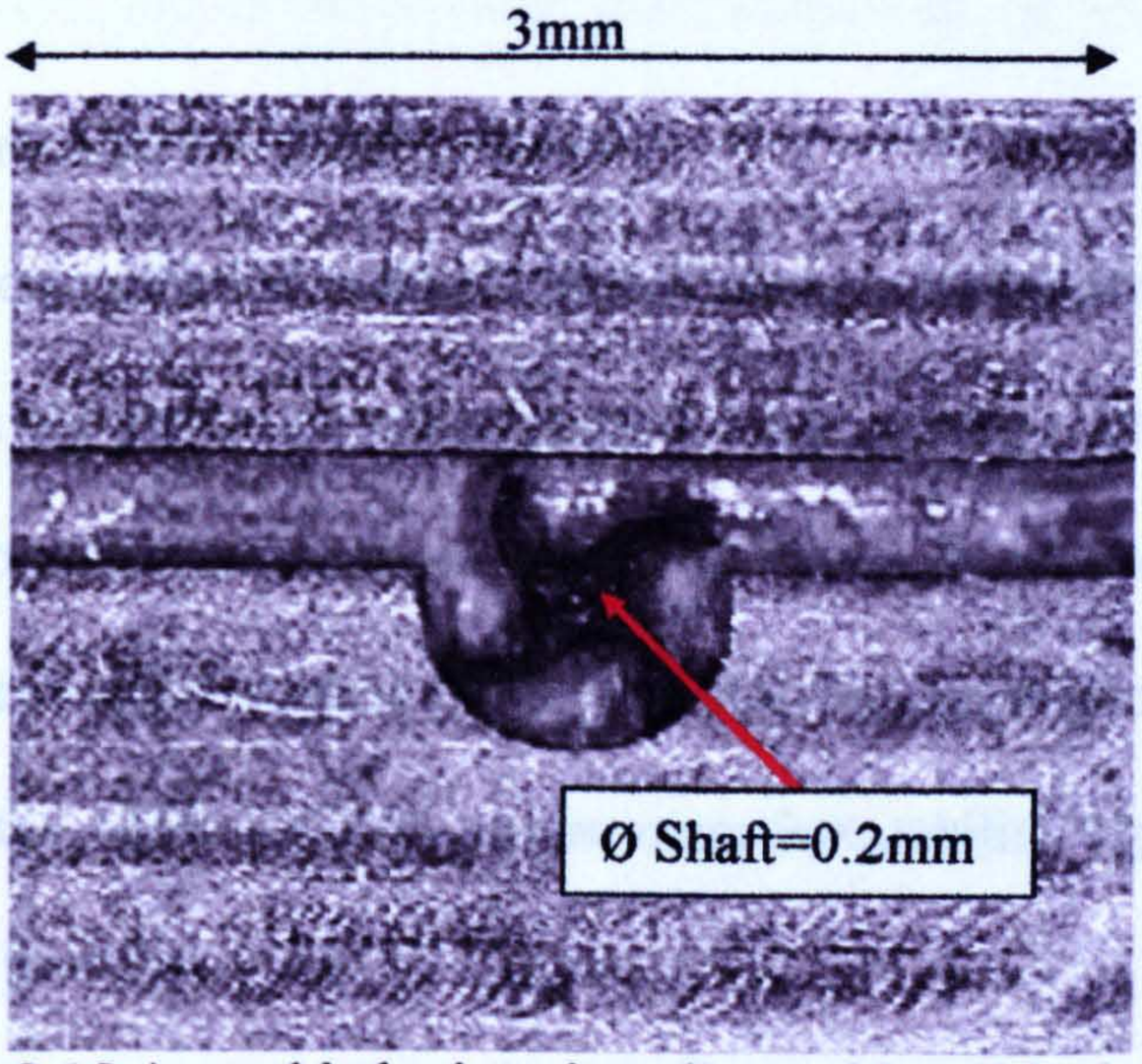

Figure 2.15 Assembled micro-impeller and base block [147]

2.5. Knowledge gaps and discussion

From the extensive literature review it can be noted that the development of Manufacturability Analysis System (MAS) should be able to assist the user in assessing the CAD model at the design level to ensure that the product can be manufactured. The main advantage of implementing MAS is providing

supports for the user with suggestion of critical changes for the design to make it easy to manufacture. Furthermore, it also represents a solution in integrating manufacturing issues during the design stage that helps to shorten the product development time by reducing the iteration between the design and manufacturing stages. However, despite all the advantages offered by the MAS implementation, there are still areas of improvement that can be explored to enhance the MAS capabilities. Therefore, to fully appreciate the MAS implementation towards assisting the user/designer in producing product which is manufacturable at the design stage, the research gap must be filled to enhance the knowledge in micro-product manufacturing. Among knowledge gaps to be addressed in this study are as following:

2.5.1. MAS for micro-milling process

MASs have been applied to various types of manufacturing processes and most of them are in the macro-manufacturing domain and less attention has been given to micro-manufacturing processes. As MASs has proved to work for macro-manufacturing processes [19-21, 23-24], an implication of this is the possibility of the MAS to check micro-manufacturability aspects for micro-manufacturing process.

A few publications claim that MAS for micro-domain have been developed, however, it is not very encouraging because they are mainly for Micro-System Technologies (MST) processes such as MEMS [57, 89] and LIGA [64]. So far, there is no clear evidence of MAS implementation for Micro-Engineering Technologies (MET) processes such as micro-milling/drilling/turning. More

importantly, with the current demands in producing micro-product via the MET processes [124], it prompts the requirement of a systematic approach in the design stage so that the manufacturing information can be considered and make the micro-product easy to manufacture. The development of MAS for micro-milling process where various aspects (e.g. materials used, acceptable and suitable tolerances and dimensions) can be assessed to allow the design being compatible with the production needs that leads to improved quality of machined micro-product. In this study, MAS can be defined as a system that assists the MMT user in generating micro-part based on the manufacturability analysis of a CAD model. The manufacturability aspects being considered are dimensions, tolerances, tool size, surface roughness, features interactions, impact of uncertainty in machining the recognized primitive feature and material. At the same time, it also can boost the confidence in applicability of MET processes in producing micro-component.

Although MET is adapted from conventional macro-processes, the differences generated due to 'size effect' has made it emerge as a new process which give strong grounds why MAS specifically for micro-domain is needed. Due to this fact, a new MAS for micro-milling process was proposed to be developed in order to assess the applicability of MAS in this area which appears to be missing from the literature. Moreover, to make this MAS development in this study more appealing and interesting, the custom-made 4-axis Miniature Machine Tool was selected to be the main domain of the system application. This is somehow in line with the call for a system that can assist users in generating micro-component using this MMT with better judgement.

2.5.2. New technique for data input and manufacturability assessment

The input mechanism plays an important role in providing data needed for manufacturability analysis. In order to feed the system with accurate and relevant data, it is necessary to investigate and develop efficient and comprehensive combinations of input mechanisms. Currently, the literature reports that *feature-extraction system* is mainly used in extracting related CAD data into MAS, and this approach has been limited by vagueness of collected data [1, 8, 15, 47, 58-60], incomplete design and manufacturing information being extracted [15, 60] which is laborious for the user. Furthermore, the development of this method is still a stringent research topic targeted to identify ways to collect accurate and self-sufficient data/design details from the features. Thus, this affects the accuracy of the data being input to the system in assessing manufacturability aspects. Therefore, the development of new techniques in gathering data from CAD model and, at the same time, to assess its manufacturability can lead to improving the data reliability.

Moreover, the combination of *user–system interaction* and *a priori database* can be introduced and adapted for inputting the required data into the MAS. Prior studies in the literature have shown that these two methods of data gathering were not given much attention by MAS developers and this makes them worth to explore.

2.5.3. Development of uncertainty evaluation model (UEM) for Miniature Machine Tool (MMT)

Uncertainty evaluation has been proved through several publications that it can provide the analysis for calculating the uncertainty value and on the same time to identify the main source of the errors with the intention to assist the user to eliminate or reduce them. This helps to enhance the quality and reliability of the analysed measurand and can possibly propose a better approach for the measurement procedure.

Based on this fact, a better understanding is required as to how the construction of the MMT can influence the geometrical accuracy of the machined micro-part by employing the uncertainty evaluation. Even though a similar study made by Uriarte *et al.* [118] has reported the uncertainty analysis made for an ultraprecision milling machine, but the focus is mainly for the errors which occurred during the micro-milling process itself such as the tool, tool holder and machine stiffness during machining.

From the literature, there is no evidence that the implementation of uncertainty analysis has been made to evaluate the errors stemming from the construction of the MMT and its effect towards the machined micro-part. More importantly, this study also proposes to provide an uncertainty model and method/procedure to account for the errors when constructing any similar in-house MMT systems where knowledge concerning this matter is scarce and limited in the current literature. The developed model can provide a better

understanding in assessing errors that affect the quality of the final machined micro-parts.

2.5.4. Integration between MAS, UEM and micro-machining

Most of the developed MAS are limited by solely focusing on assessing the manufacturability aspects based on the proposed design while abandoning other aspects such as tolerances, materials, dimensions, tooling, tools/parts orientations and process capabilities in determining the level of manufacturability. Moreover, as mentioned in the limitation of current MAS, not much attention has been given towards enriching the knowledge /recommendations that can assist the end-user of the system in making more comprehensive technical decisions regarding the manufacturing of the proposed designs. However, most MASs evaluate the functionality aspects manually or totally neglected [12, 47, 58, 63, 69]. It would be worth considering this aspect during the design stage as it also plays an important role in determining the function of the design.

Therefore, in order to enhance the capacity of MAS in assessing manufacturability aspects, the results from micro-machining experiments and uncertainty evaluation towards the MMT will be integrated in the system's database. This is to fully understand the capabilities of the MMT which is the main scope of the developed MAS.

CHAPTER 3: METHODOLOGY

3.1. Introduction

In this chapter, the methodology to achieve the aims and objectives of this study are described in detail. Principally, there were four important phases in the proposed methodology for this study:

(i) Development of the system (MicroMAS)

(ii) Analysis of uncertainty evaluation model (UEM)

(iii) Micro-machining experiments

(iv) Integration of MicroMAS, UEM and micro-machining experiments

This chapter begins with a synopsis of overall research approach that briefly describes each phase. Following this, each phase has been presented in detail and all the related procedures, objectives, ideas, software packages, tools, technologies used to facilitate the development are also discussed.

3.2. Overall research approach

Table 3.1 presents the synopsis of each phase of the methodology; it lists the components, contents, objectives, approaches, technologies/tools and software used in this study. More detailed explanation on the each phase will be laid out throughout this chapter.

Table 3.1 Synopsis of each phase related to the research methodology

Phase	Component	Content	Objective/ Details	Approach	Software/ Tool
System development	Data input module	- user-system interaction - a priori database	- To gather data such as PFs dimensions, material, tolerances and surface roughness of the PFs and overall part.	Users input the required data. Feedbacks are provided in verifying the given input.	- VB
	Manufacturability assessment module	- Primitive Feature Identification (PFI) - Single and Coupled Feature Analysis (S/CFA) - Manufacturability Indices (MI)	- PFI: to assess and analyse the inputs. - S/CFA: to analyse the single and coupled primitive features and to define their interactions. - MI: to generate manufacturability indices based on single/coupled feature analysis, material, quality measures (e.g. tolerance, surface roughness).	Rule-based System (RBS) with IF-THEN clauses. MIs are expressed by a rating convention.	- VB
	Outputs generation module	- Redesign suggestions - MIs - Material selection	- Provides the results (MIs, suggestion) from the manufacturability assessment.	-------	- VB

Phase	Component	Content	Objective/ Details	Approach	Software/ Tool
System development (continued)	Database	Related rules and constraints on PFs, interactions and index ranges.	- To provide all related rules and constraints developed based on literature, handbooks, workshop and factory standard, and experiences from the experts, catalogues and brochures, micro-machining experiments, UEM analysis's results	Listing of all rules and constraints.	- VB - RBS - MS Access
Uncertainty Evaluation Model	---	Modelling of uncertainty evaluation for geometrical accuracy.	- To investigate the possible errors that affects the geometrical accuracy of the machined parts in MMT. - To develop uncertainty evaluation model based on the results of the investigations on the aspects stated above.	GUM framework; CMM analysis; ISO guidelines	- GUM
Micro-machining Experiments	Machining of 'adapted standard' micro-testpieces	Producing various micro-parts/ components to assess the capability of the MMT and to populate relevant data for MicroMAS	- To assess the capability of the MMT in terms of producing the 'adapted standard' micro-testpiece. - To analyse the generated surface quality and geometrical accuracy. - To validate the UEM results.	Micro-milling; geometry and texture analysis of micro-machined surface; geometrical accuracy of machined workpiece.	- MMT - Talysurf - Optical micro-scope - CMM
	Generating micro-slots and thin wall		- To assess the capability of the MMT in generating micro-slots and thin walls. - To analyse the surface quality and geometrical accuracy of the generated micro-slots and thin walls. - To generate index range for manufacturability indexes (tolerance and surface roughness).		

Phases	Component	Content	Objective/ Details	Approach	Software/ Tool
Micro-machining Experiments (cont)	Micro-milling of a micro-component		- To study the ability of the MMT in generating 3D micro-components. - To investigate the surface quality and geometrical accuracy of the generated micro-component. - To assess the analysis of MicroMAS on the same micro-component.		
Integration	MicroMAS; UEM; Micro-machining experiments	Integration of all the relevant results into the MicroMAS	- To integrate results from micro-machining experiments and UEM into MicroMAS, this is to make certain that the system emulated its domain (the MMT).	RBS with IF-THEN clauses.	- VB

LEGEND:

VB	Visual Basic.NET
GUM	GUM Workbench
RBS	Rule-based system
MMT	Miniature Machine Tool
CMM	Coordinate measuring machine

3.3. System development

As the prime phase, the objective of this stage is to develop the concept of MicroMAS for micro-machining environment addressed to a custom-made 4-axis Miniature Machine Tool (MMT). The development of the system is based on the three-step unidirectional which was divided into three modules/components (Figure 3.1): (i) data input module, (ii) manufacturability assessment module, (iii) output generation module. The exclusiveness of this approach for MicroMAS is relying on the content of each module, which is the combination of approach/tool/software used to develop the system. As summarized in Table 3.1, each module has its own purpose and contribution towards the development of MicroMAS.

The **data input module** is where all the relevant and related data were feed into the system. In this study, two approaches were selected and combined which were the *user-system interaction* and *a priori database*. In the *user-system interaction* method, the system prompts the user with enquiry leading towards the collection of related information. While for the second method, the users are allowed to choose related data and parameters from the manufacturing information in the system's database. The difference between this method and the previous one is that all information was already embedded, and users only have to choose the appropriate one. While in the previous method, users were required to input all needed data through the interface during the interaction.

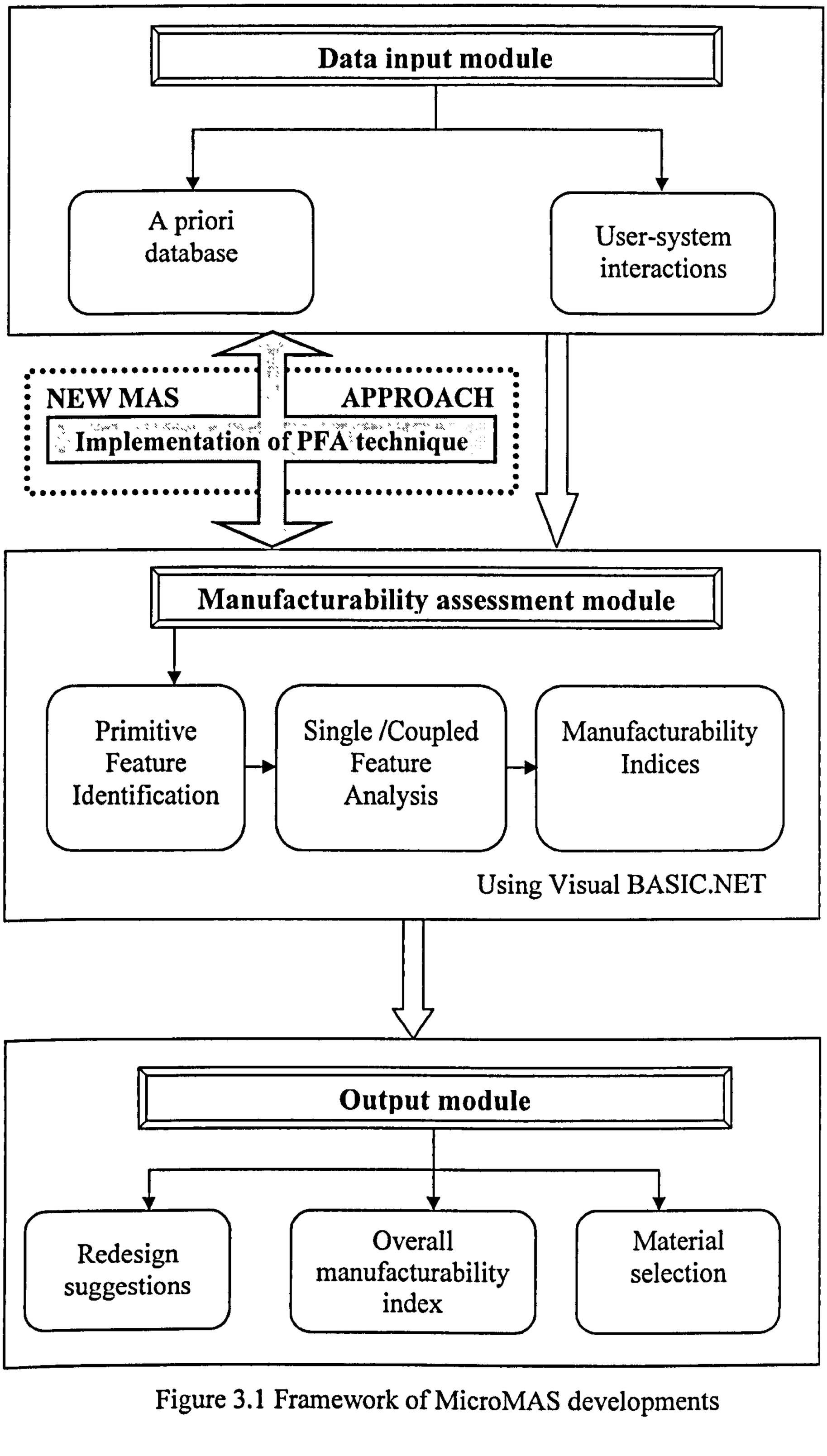

Figure 3.1 Framework of MicroMAS developments

In the **manufacturability assessment module,** the approach chosen to assess the manufacturability of the proposed CAD model was by using the conventional programming language provided in the Visual Basic.NET® (VB) software. VB was derived from BASIC programming language and enables the development of graphical user interface (GUI) applications and access to database. GUI is a type of user interface which allows the user to interact with the developed system with images and text commands. VB was selected as the backbone of this system development as it provides user-friendly environment for developing interfaces and linkages that suits the overall MicroMAS approach and requirement.

Figure 3.2 presents an example of the VB integrated development environment (IDE), where the windows application for the MicroMAS is being generated.

The four items in the IDE which is essential for developing a project in VB are as following:

- Designer – The area where the designing of the forms/interfaces and also the related codes are generated.
- Toolbox – Provides list of user-interface controls (e.g. button, list box, text box, label, menu).
- Solution Explorer – Gives an overview to the user of the developed project such as generated files, forms while allowing switching between coding and designing forms/interfaces.
- Properties – A useful tool to configure the related items such as selected user-interface controls, forms and database development in the application during design time.

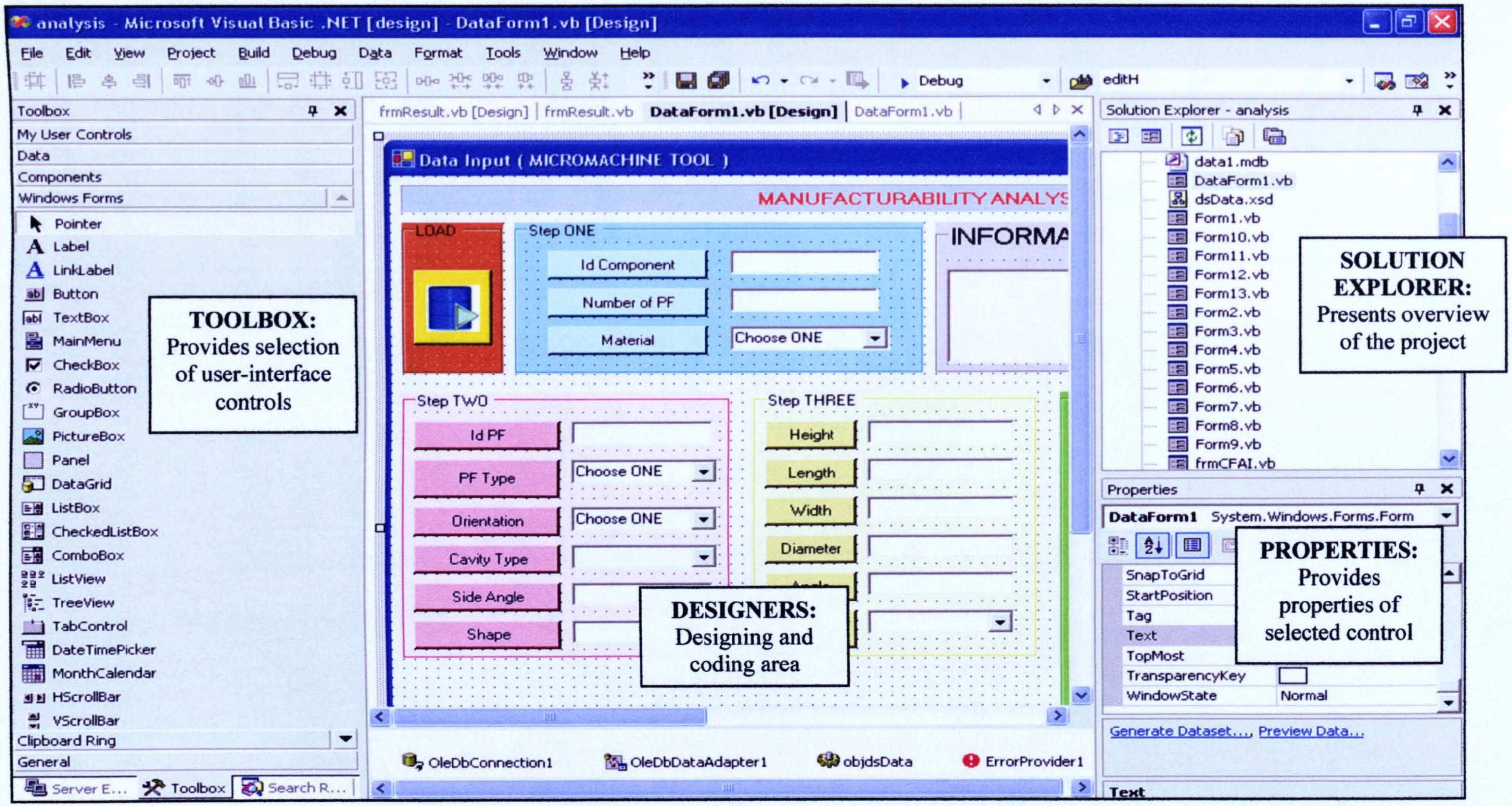

Figure 3.2 Interface of VB.NET integrated development environment

In this module, the development of the manufacturability assessment was divided into three elements: *Primitive Feature Identification (PFI)*, *Single/Coupled Feature Analysis (S/CFA)* and *Manufacturability Indices*. The details of these elements will be presented in ***Chapter 4***.

Furthermore, the *Ruled-based System (RBS)* was implemented to assist the decision making in the manufacturability assessment through the IF-THEN clauses. It helps to control the analysis of MicroMAS and represents the systems' knowledge base via logical combinations. RBS has been applied in manufacturing based inference engines because the IF-THEN rules are similar to common sense logic [65]. Moreover, the concept of RBS and IF-THEN clauses can be implemented in any programming language or software packages including VB. In this study, the related rules and conditions correlated to micro-milling, the MMT and primitive features elements are saved in the form of IF-THEN clauses. All the rules and conditions stored in database are interactively being searched based on IF-THEN clauses in order to determine which rules satisfy the inputs.

Finally, in the third module, the **output generation**, provides the outputs from the manufacturability assessment such as redesign suggestion, overall MI and selection of materials. This result was displayed in various types of interfaces (e.g. pop-up window, reports, forms) generated using VB.

The database is the medium where all the data and information needed for the analysis is stored; it was developed using Microsoft Access (MS ACCESS) and

linked to the VB. Figure 3.3 illustrated the relationship between the software (VB.NET, MS ACCESS, GUM Workbench) and the practical aspects (machining experiments, uncertainty analysis) of the work. All related manufacturing information and rules are embedded in the database to be used as guide for assessing the manufacturability of the proposed design.

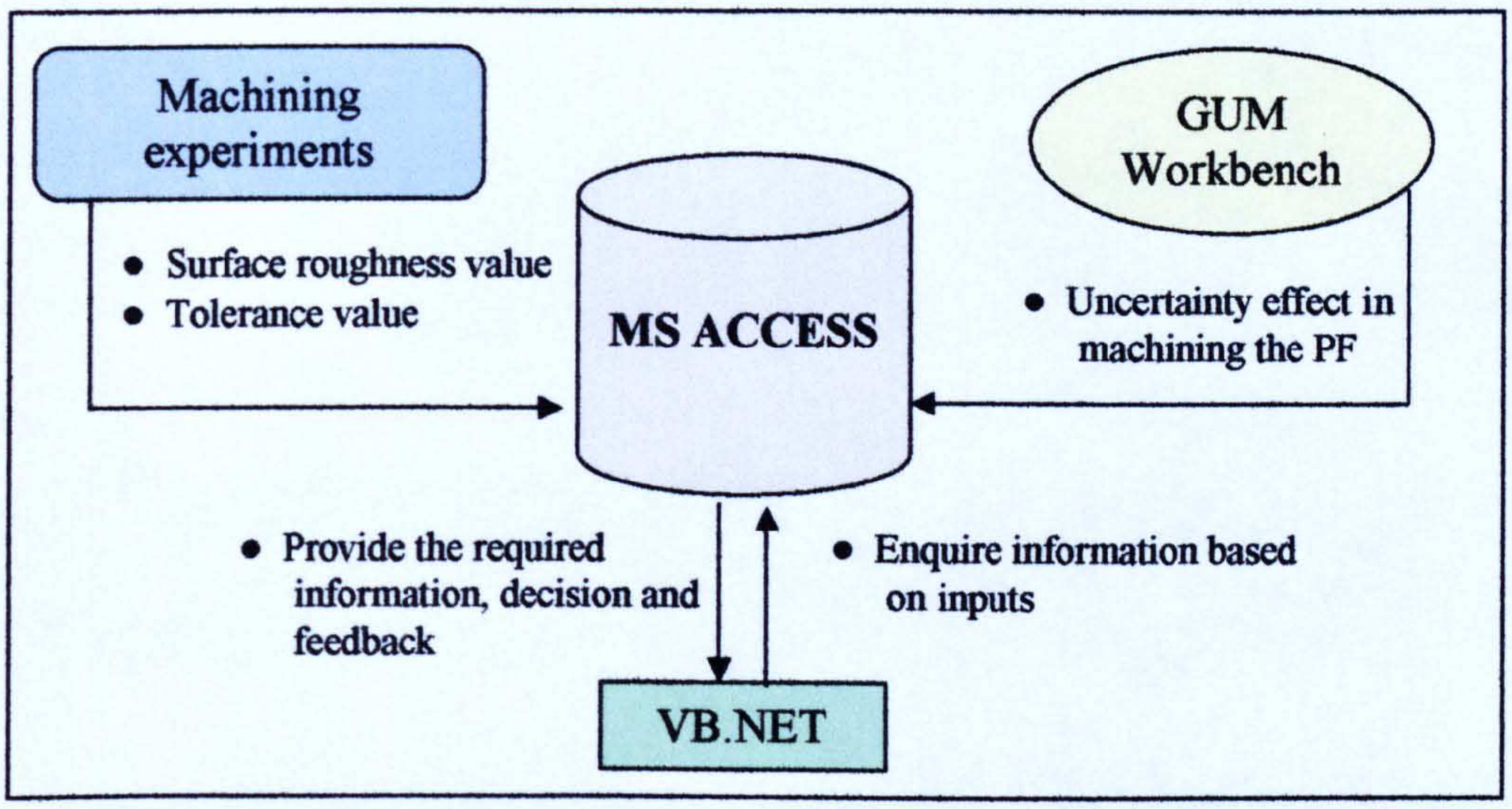

Figure 3.3 Schematic of relationship between the VB.NET, MS ACCESS, GUM Workbench and Machining experiments

For this study, a new approach which is the Primitive Feature Analysis (PFA) technique was introduced for data gathering and manufacturability evaluation in between the data input module and manufacturability assessment module as shown in Figure 3.1. The details of the system generation will be discussed in ***Chapter 4*** for the development of the PFA technique and ***Chapter 7*** for the implementation of the MicroMAS.

3.4. Micro-machining experiments

As stated before, the domain of the MicroMAS application is the in-house developed MMT which provides the micro-machining environment for the system implementation. In this study, MicroMAS is also developed to cater the needs of the MMT that requires a system to support a robust and efficient generation of micro-parts. In order to understand the MMT response in producing micro-product and, on the same time, to populate relevant data into the MicroMAS, a series of experiments have been carried out using various materials and cutting tools. Furthermore, these experiments are based on the recommended machining parameters from the tool manufacturers (Sandvik Coromant) and it was not the aim of this study to seek for any further optimisation of cutting parameters. Among the proposed experiments are:

- Machining the 'adapted standard' micro-testpiece
- Generating micro-slots and thin walls
- Producing a micro-component demonstrator

These experiments have been carried out on different materials (e.g. Stainless steel, Steel, Titanium Alloyed), using various machining parameters and micro-cutting tools (end-mill with Ø between 0.5 and 0.8mm).

3.4.1. Miniature machine tool (MMT)

The custom-made 4 axis Miniature Machine Tool (see Figure 3.4) has been used for all the micro-machining trials performed within this study. This 4-axis Miniature Machine Tool (MMT) addresses the machining of micro-parts, i.e. dimensions at or sub millimetre range with high dimensional and geometrical accuracies, through mechanical chip removal processes (micro-milling) was

developed with purpose to investigate its capability and contributions to this field.

Figure 3.4 (a) shows the illustration of the 4-axis MMT that was constructed and used as the benchmark of the MicroMAS development for micro-machining environment, while Figure 3.4 (b) shows the complete MMT (with the cover of the machine has been removed) which has been set-up in a micro-machine lab, University of Nottingham – MCM group.

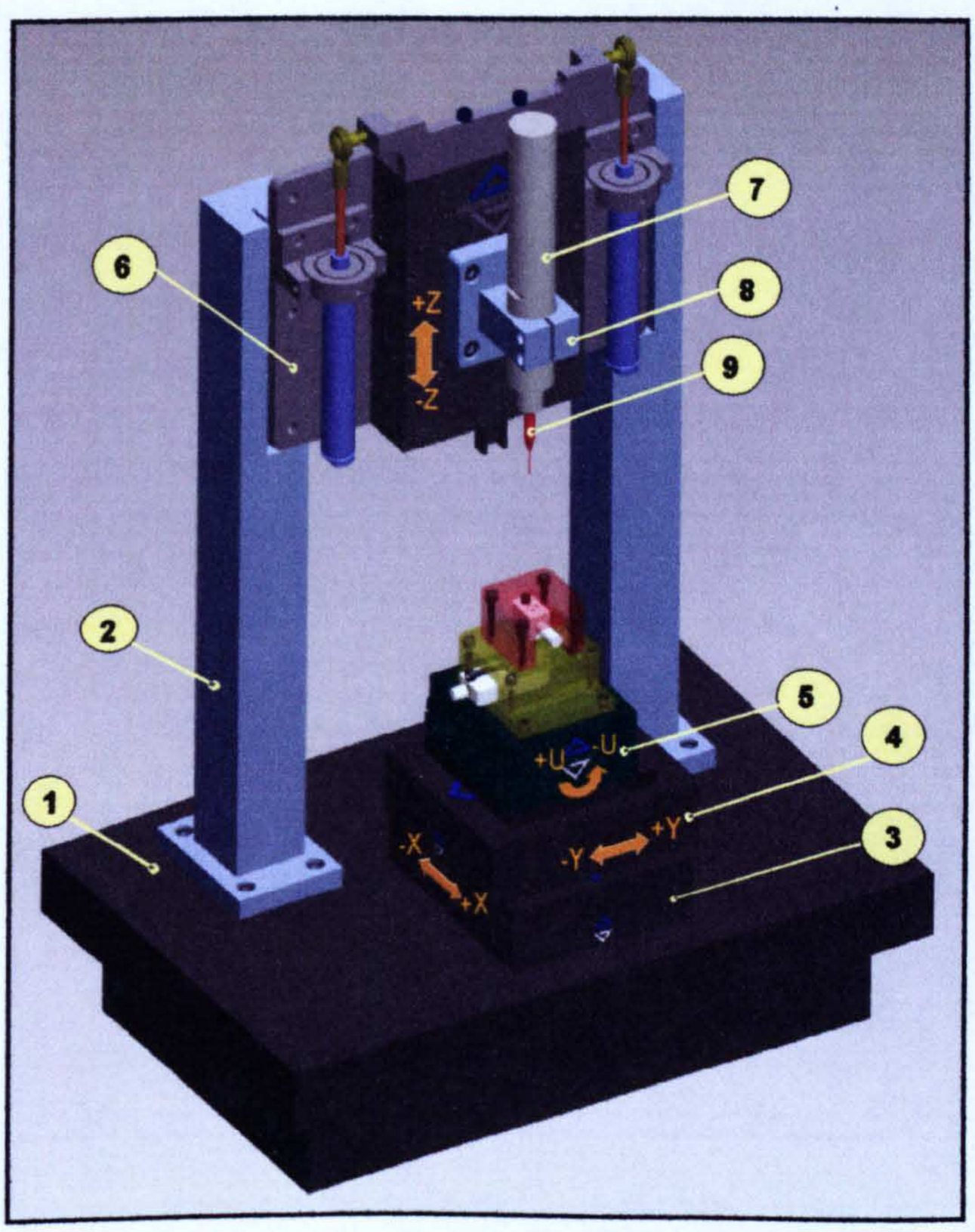

	Component
1	Granite base
2	Machine frame
3,4	Linear stage (X and Y axis)
5	Goniometre (U axis)
6	Dual counter-balance head (Z axis)
7	Brushless motor spindle
8	Spindle arm
9	Cutting tool

Figure 3.4 (a) Illustration of 4-axis Miniature Machine Tool (Source :[38])

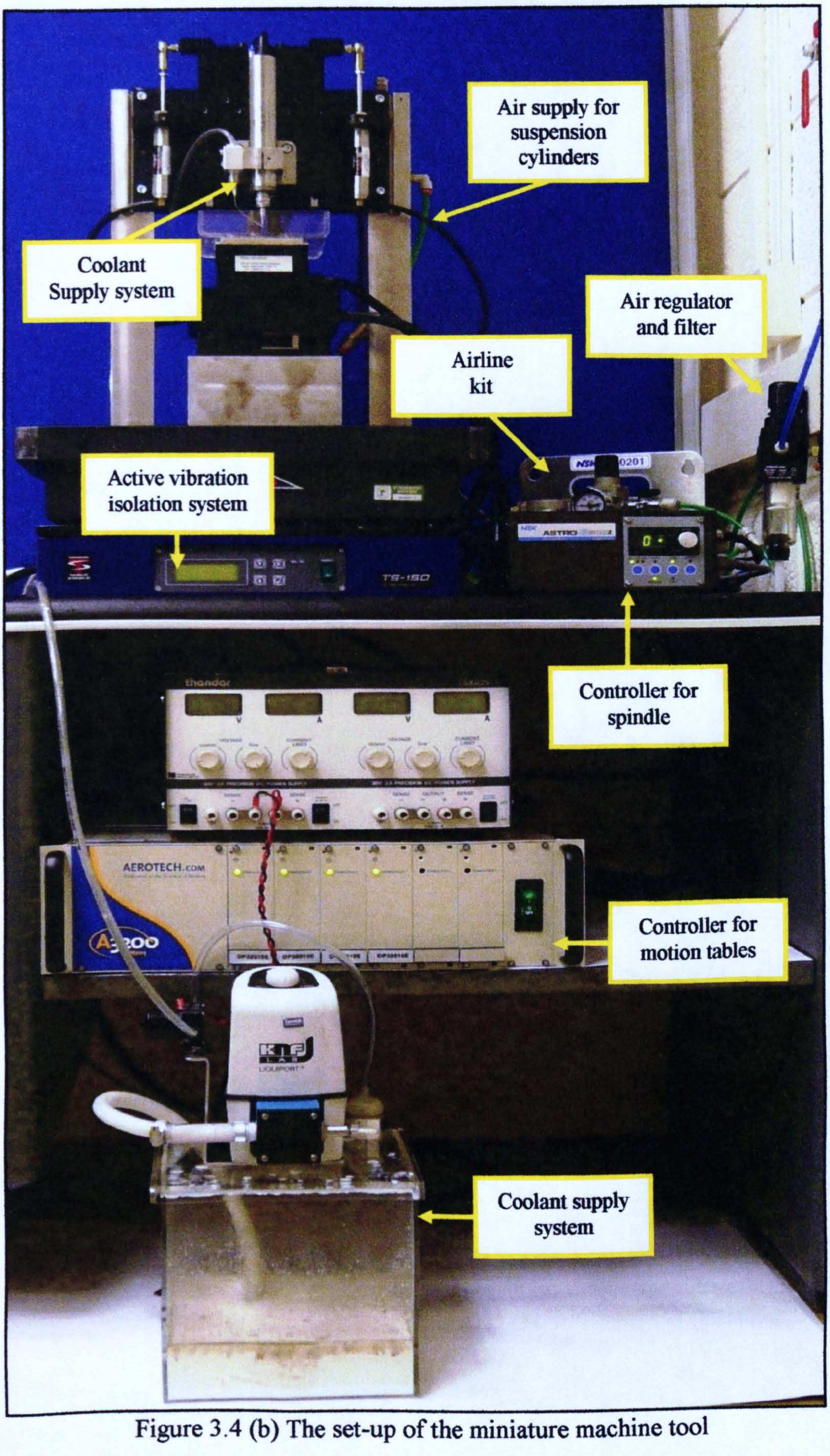

Figure 3.4 (b) The set-up of the miniature machine tool

3.4.1.1.MMT components

In the development of the MMT, a gantry configuration has been adopted for construction of the system in order to allow easy access to the working space and to exploit the advantages offered by the new-technology miniature weight-compensated linear stages. Details on the major components of the MMT are described as the following:

- **Machine tool frame**

  The frame was manufactured of INVAR 36 alloy (INVARiable Ni - 36%, Fe-63%) that was particularly chosen due to its low thermal expansion coefficient ($1.3x10^{-6}$ $°C^{-1}$ between 20-100°C), thus minimising the dimensional errors due to temperature variations.

- **Machine base**

  The gantry frame was mounted on a granite base (Figure 3.4) that with its low thermal expansion coefficient ($8.6x10^{-6}$ $°C^{-1}$ between 20-100°C) not only minimises the effect of temperature variation on the dimensional chain of the MMT system but also has, to some extent, the capability to damp external vibrations (140-1600Hz) [173].

- **Positioning tables**

  The realisation of the 4-axis of MMT has been achieved by employing high resolution positioning stages (manufactured by Aerotech) with technical capabilities presented in Table 3.2. Two linear motor stages (ALS130-025) assembled perpendicular to each other provide 25mm travel in X and Y directions. The direct drive goniometre (ANT-20G-90) placed on top of linear stages enables swivel (rotary) action of 20° in U direction. In addition, the vertical movement of 25mm in Z direction is

achieved using a dual counter-balanced linear motor stage (ALS130-025) that is fed by regulated dry air for suspension inside the cylinders at both ends to ensure smooth and stable operation of the stage.

Table 3.2 Characteristics of the positioning system and spindle units of the 4-axis MMT

Characteristics of the multi-axis motion system of the 4-axis MMT	
X and Y axis tables: Linear motor stages	
Total travel:	25 mm
Drive system:	Linear Brushless Servomotor
Feedback:	Noncontact Linear Encoder
Resolution:	0.005 – 1.0 μm
Max. travel speed:	300 mm/s
Max. linear acceleration:	10 m/s^2
Max. load:	12 kg (horizontal); 10 kg (side)
Repeatability:	±0.1 μm
Nominal stage weight:	3.0 kg
U axis table: Direct drive goniometre	
Transverse axis radius:	90 mm
Travel:	20°
Resolution:	0.00082 arc sec
Repeatability:	±0.5 arc sec
Max. load:	2.0 kg
Velocity:	150 °/sec
Nominal stage weight:	1.1 kg
Z axis table: Dual counter-balanced linear motor stage	
Total travel:	25 mm
Drive system:	Linear Brushless Servomotor
Feedback:	Noncontact Linear Encoder
Resolution:	0.005 – 1.0 μm
Max. travel speed:	300 mm/s
Repeatability:	±0.1 μm
Characteristics of the spindles of the 4-axis MMT	
AC brushless motor spindle	
Spindle speed:	Up to 50,000 rpm
Spindle accuracy:	within 1 μm

Max. output power:	250 W
Weight:	1,067 g (w/cord)
Collet chuck:	Ø1mm; Ø3 mm; Ø6 mm
Air driven spindle	
Spindle speed	Up to 200,000 rpm
Spindle accuracy	within 1 μm
Weight	200g
Air pressure	0.3MPa
Collet chuck	Ø1.6 mm

- **Motor and spindle unit**

  A brushless motor-spindle unit with controller and airline kit (ASTRO-E 500Z) was chosen (Table 3.2). Brushless motor-spindle unit with ceramic bearings (EMS-3057) is an integrated motor and spindle solution with high speed rotation of 50,000rpm and low tool run-outs (<1μm). The controller (NE147) enables high degree of control over the speed while the airline kit (AL-0201) supplies dry and regulated air into the spindle. The spindle unit was attached to the dual counter-balanced head via the spindle arm that was manufactured of INVAR 36.

- **Cooling system**

  The cooling system designed for the MMT which consists of two sections: the suction/pumping system and the plastic container able to allow wet machining condition to be run in the MMT. The suction/pumping system functions are to deliver and to pump out the cooling liquid from the machining area and also to filter the coolant. The plastic container which comprises of two parts (the tray cover and the working tray) takes the role in protecting the motion tables. The coolant that will be used in this study is Hocut 3380 high lubricity chlorine and

sulphur free soluble oil blended with severely refined mineral oils. The resultant rich milky emulsion is very low foaming and suitable for high pressure coolant systems which associated with modern CNC machine tools. It was recommended to use between 4% and 6% concentration for general machining [174].

- **Active vibration isolation system**

  To ensure high degree of insulation of the working environment from the external sources of vibrations, an active vibration isolation system (TS-150) has been used as a dedicated table for the MMT. The active vibration isolation table has been placed under the granite base of the micro-machining system (Figure 3.4(b)).

3.4.2. Materials

The workpiece materials that were selected are AISI 1040 Steel, 316L-Stainless Steel and Titanium Alloyed (TiAl6V4) which are widely used in machining of wide range of micro-products, forms and finishes. As example: Mild and 316L steels have been used for developing micro-moulds [39, 127, 131-132, 148-149] while 316L and TiAL6V4 have been utilized in producing medical devices such as such as micro-spray valve for precise aseptic and sterile fluid applicant [175].

In this study, these materials were used for generating the micro-testpiece, machining micro-slots and thin walls and also producing micro-component demonstrator. The material properties are important to be analysed, as example

the hardness has a significant impact in terms of the tool capability to machine them as it is essential for the tool to be harder than the workpiece material. Table 3.3 displays the basic characteristics of the materials used in the experimental part of this study.

Table 3.3 Material properties [87]

Property	Steel (AISI 1040)	316L – Stainless Steel	Titanium Alloyed (Ti-6Al-4V)
Composition (WT %)	C: 0.37 - 0.44, Mn: 0.6 – 0.9, P: 0.04, S: 0.05	C: 0.07, Cr: 16 – 180, Fe: 61.9 – 72.0, Mn: 2, Ni: 10.0 – 14.0, P: 0.045, Si: 1.0, Mo : 2.0-3.0	C: 0.08, Al: 5.5 – 6.75, Fe: 0.3, H: 0.01
Density (kg/m^3)	6920 – 9130	8000	4430 – 4700
Hardness (HRc)	7.4 – 12.0	10.5 - 18	32.8 – 34.5

3.4.3. Cutting tools

In this study, the selected cutting tools are Sandvik Coromant flat end mill cutters with diameters between 0.5 and 0.8mm. These solid carbide milling cutters (CoroMill® Plura) are commercially available and suitable for wet or dry machining. The cutting edges had a rake angle of 10° and a helix angle of 30°.

As suggested by the manufacturer, these tools are compatible for general machining (e.g. shoulder/face/slot-milling) and also profile-milling in most materials. Figure 3.5 presents an example of the specifications of a flat end

milling cutter with diameter of 0.6mm. **Appendix 3.1** illustrated the specifications of the other tools employed (e.g. cutter diameter of 0.5 and 0.8mm). Figure 3.6(a) shows the tools used in this study, while Figure 3.6 (b) presents the magnified version (X100) of 0.6 mm cutter.

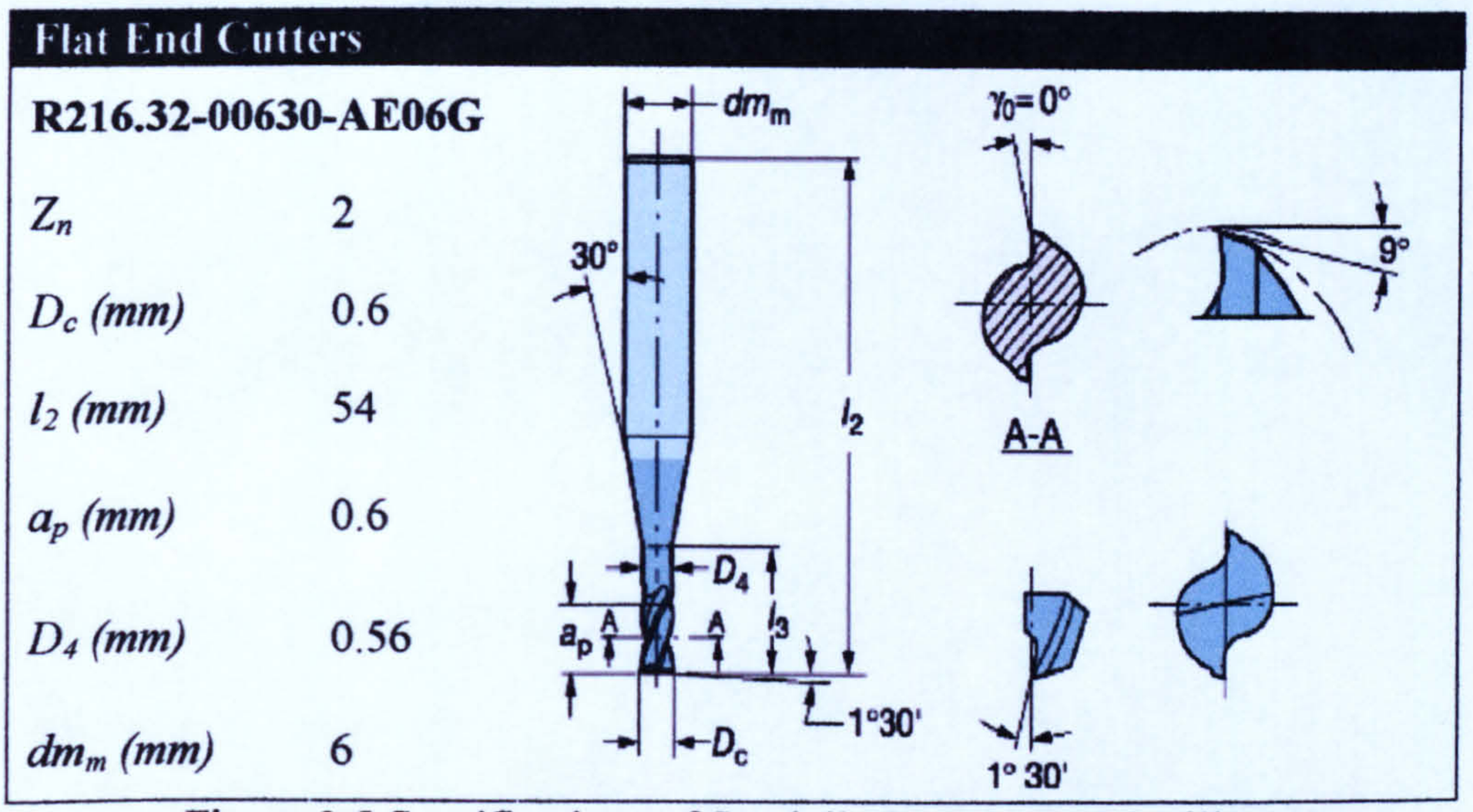

Figure 3.5 Specifications of Sandvik-Coromant end mill cutter

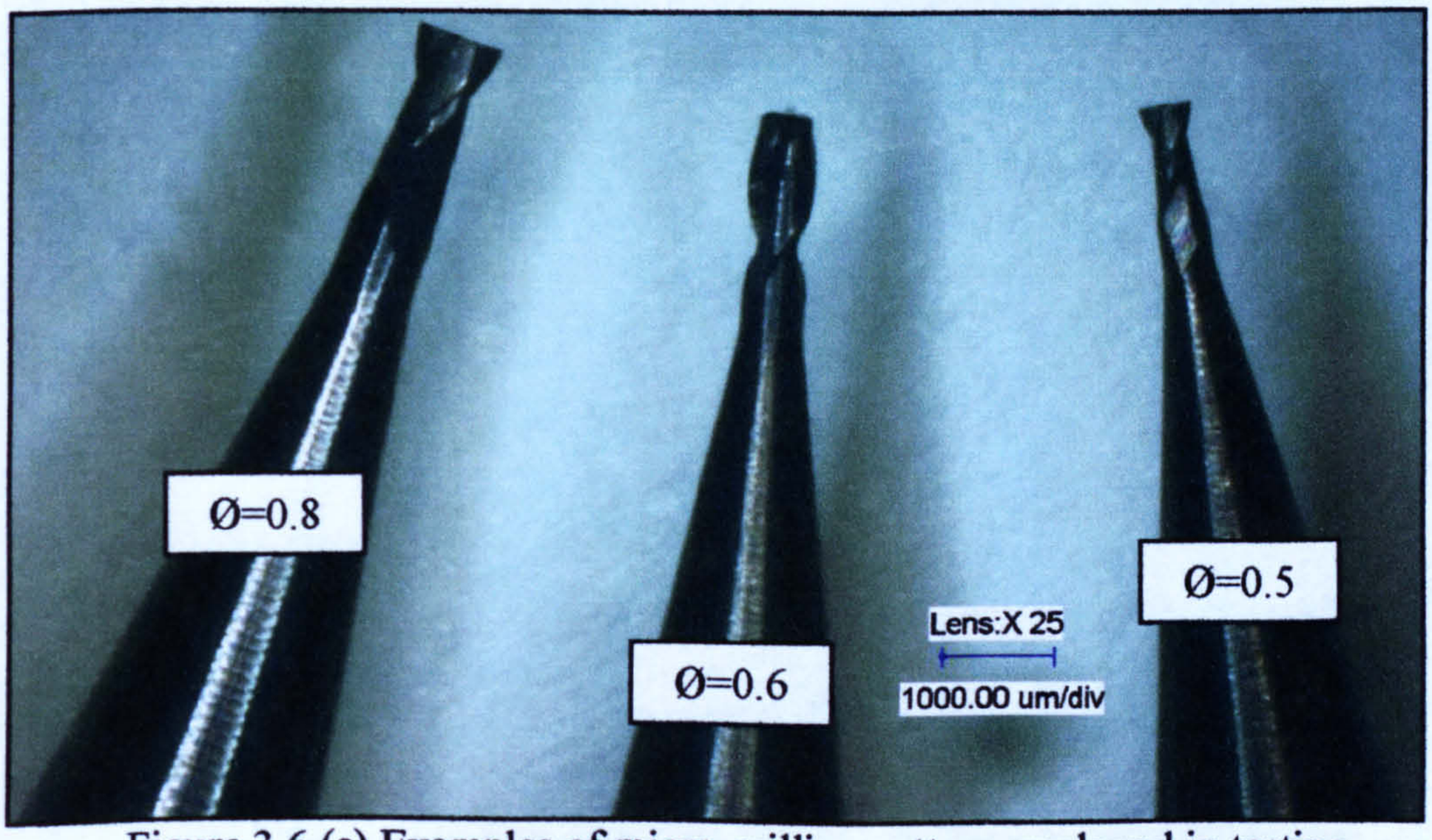

Figure 3.6 (a) Examples of micro-milling cutters employed in testing

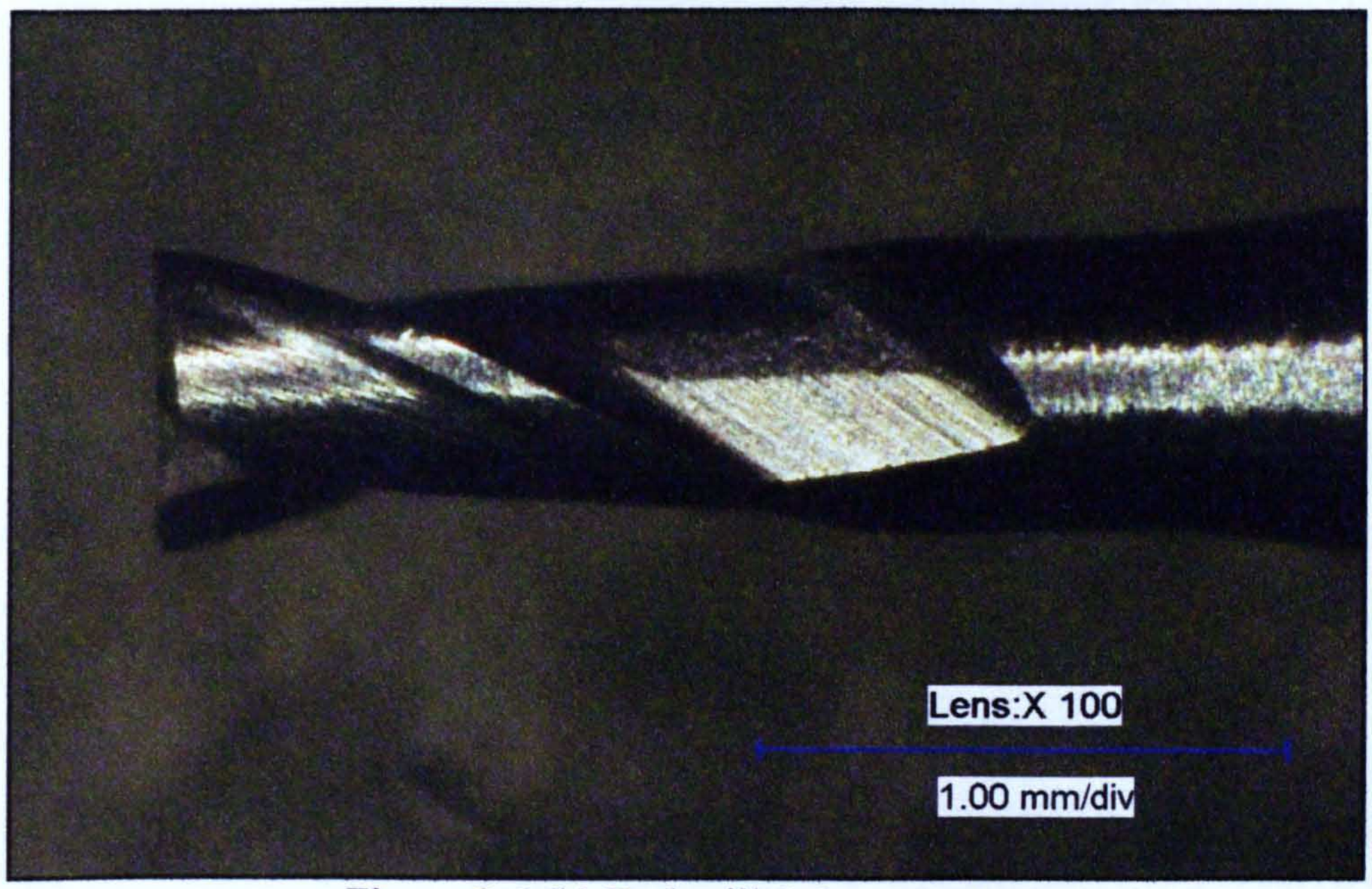

Figure 3.6 (b) End mill 0.6 mm cutter

3.4.4. Machining of the 'adapted standard' micro-testpiece

In order to assess the cutting accuracy of the MMT, an 'adapted standard' micro-testpiece which is similar to the one suggested in ISO 10791-7:1998 (Test conditions for machining centres- Part 7: Accuracy of a finished testpiece) has been selected [176]. For the purpose of assessing the capability of the MMT, the defined standard micro-testpiece was scaled down appropriately as shown in Figure 3.7. It carries all the significant features of the machining standard and would be an appropriate example for assessing cutting accuracy of the MMT. Some of the significant features are:

- Circularity with the inner circle.
- Linearity or straightness of the outer square.
- Perpendicularity at the corners.
- Angular accuracy (45° at the edge of the inner diamond with outer square).
- Parallelism with the opposite sides of a square.

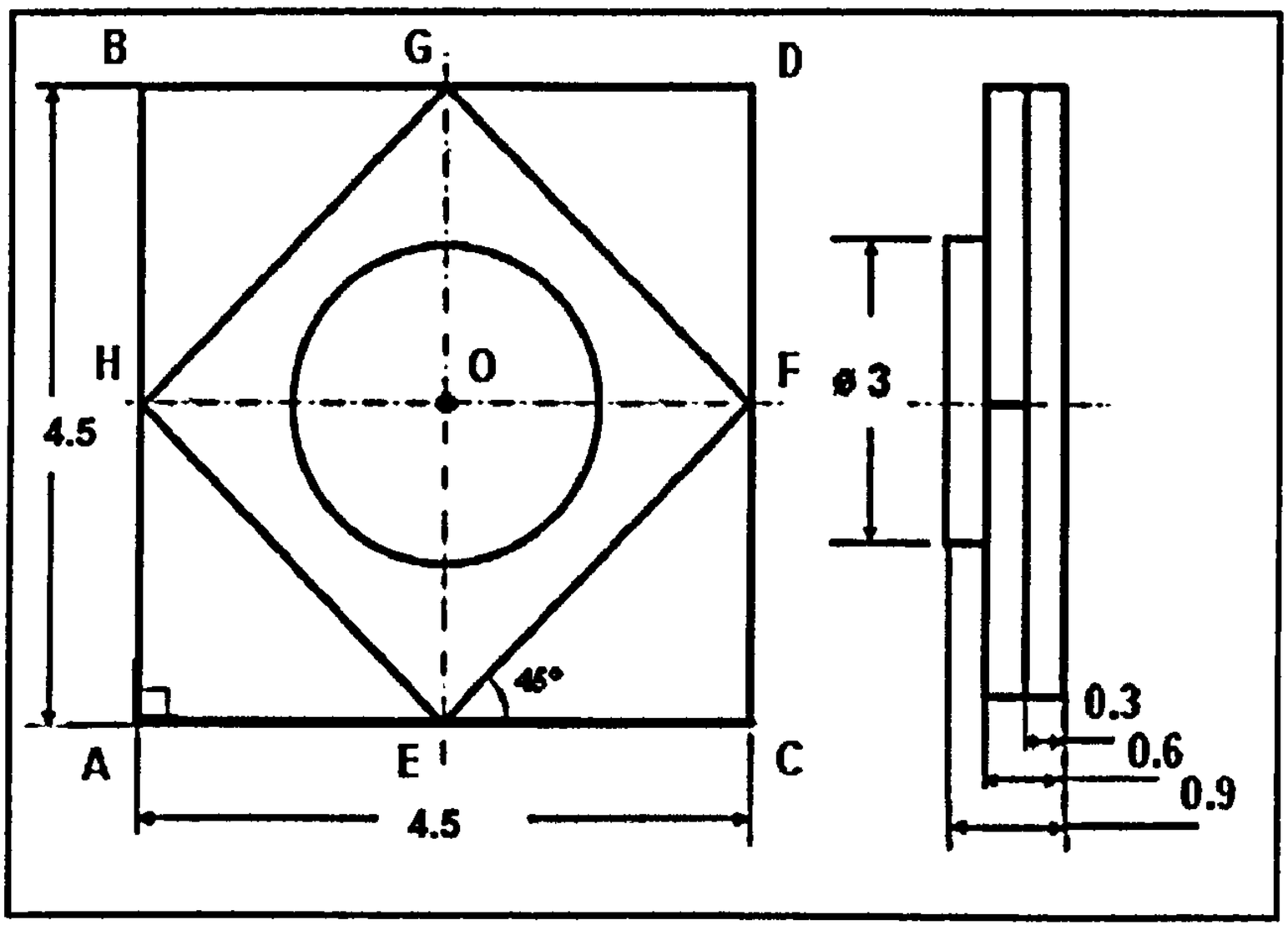

Figure 3.7 The 'adapted-standard' micro-testpiece (in mm)

On completion of machining the micro-testpiece, the workpieces were evaluated for their geometrical accuracy and surface quality. In the following paragraphs, the procedures and criteria of these assessments are demonstrated. The results from these evaluations can provide an overview on the capability of the MMT in producing micro-part.

Geometrical accuracy analysis

Two approaches were implemented for the geometrical accuracy assessment: firstly by using the coordinate measuring machine (CMM) and secondly via a Keyence VHX-Optical Digital Microscope. The AISI 1040 sample was evaluated using a Carl Zeiss F25 Microsystem CMM (Figure 3.8(a)) with 0.3 mm stylus diameter. The 3D CMM which is supported on air bearing with a measuring volume of one cubic decimetre is capable of measuring micro-system components at a resolution of 7.5nm. The silicon stylus was developed based on a 6.5 x 6.5 mm silicon chip membrane and integrated piezo-resistive

elements. As shown in Figure 3.8 (b), an additional camera aids visualisation when probing the miniaturised features, thus simplifying part programming. Figure 3.8(b) also presents the example of AISI 1040 micro-testpiece sample being evaluated via the Carl Zeiss F25 Microsystem CMM.

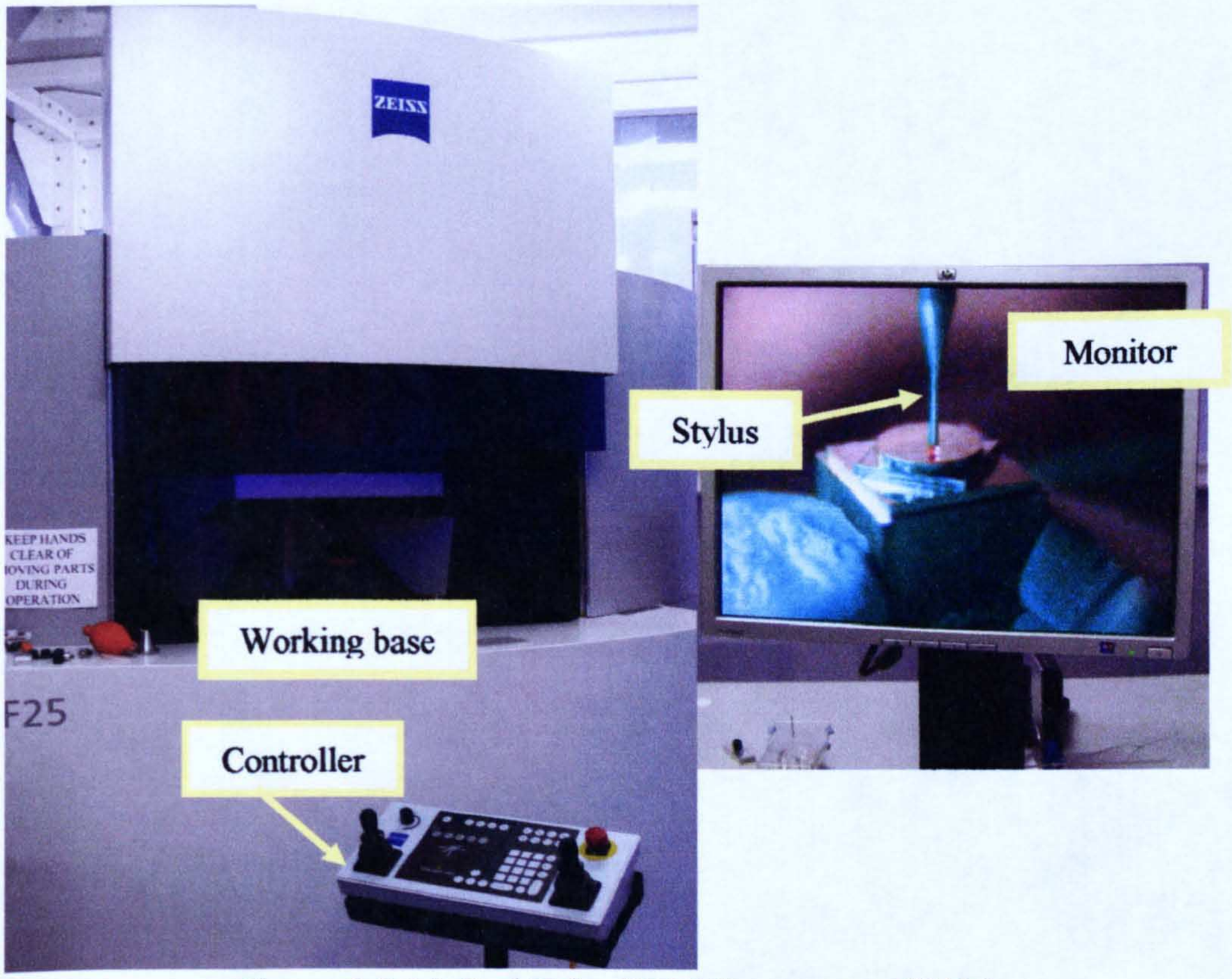

Figure 3.8 (a) Carl Zeiss F25 Microsystem CMM

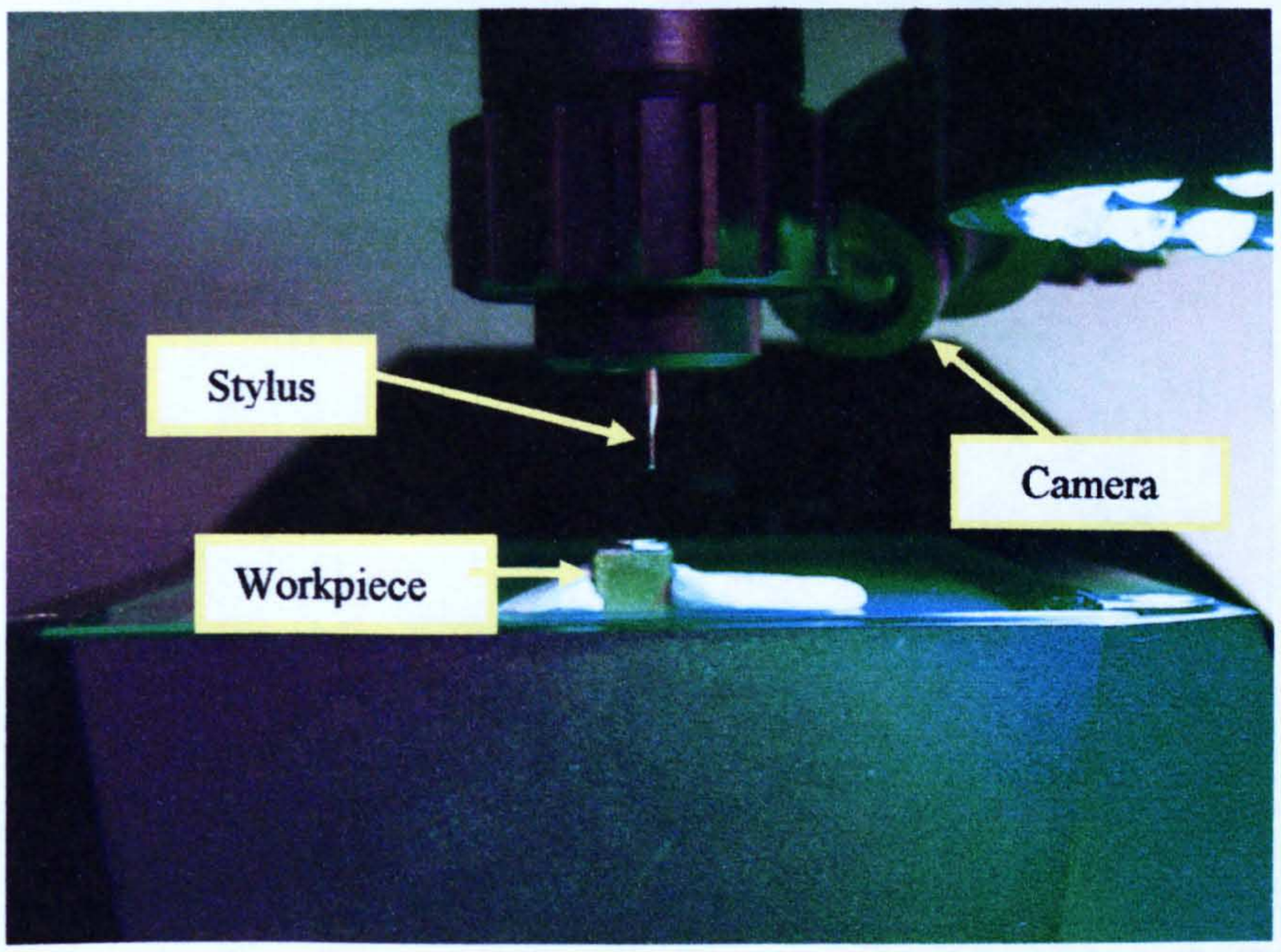

Figure 3.8 (b) AISI 1040 micro-testpiece being evaluated via CMM

Aspects that are being focused on the CMM analysis of the AISI 1040 micro-testpiece are:

- Circularity of the circle (from top of the cylinder)
- Straightness of outer square and the diamond shape
- Perpendicularity at the corners
- Angular accuracy (45° at the edge of the inner diamond with outer square)
- Flatness on top of cylinder

For the Keyence VHX-Optical Digital Microscope (Figure 3.9) evaluation, TiAl6V4 sample was analysed based on the aspects listed below:

- $\emptyset_{\text{Cylinder}}$
- $\angle A, \angle B, \angle C$ and $\angle D$
- $\angle FEC$
- $\|\text{AB}\|$, $\|\text{AC}\|$, $\|\text{CD}\|$ and $\|\text{BD}\|$

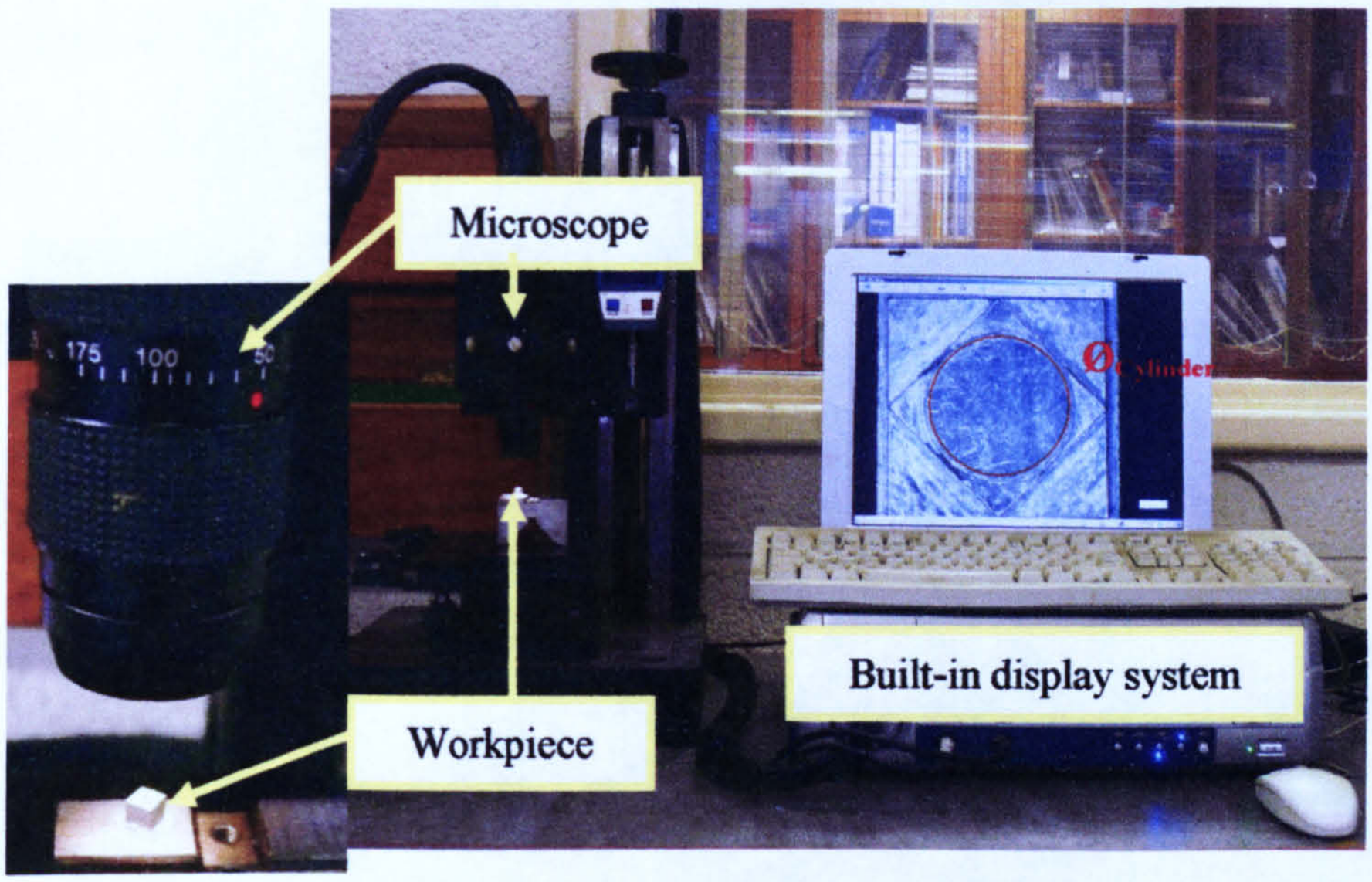

Figure 3.9 Keyence VHX-Optical Digital Microscope

Figure 3.10 shows the example of on screen image of measuring the diameter of the cylinder under the microscope. All aspects mentioned above are being repeatedly measured (3 to 5 times) and the results are being averaged with standard deviation values are included.

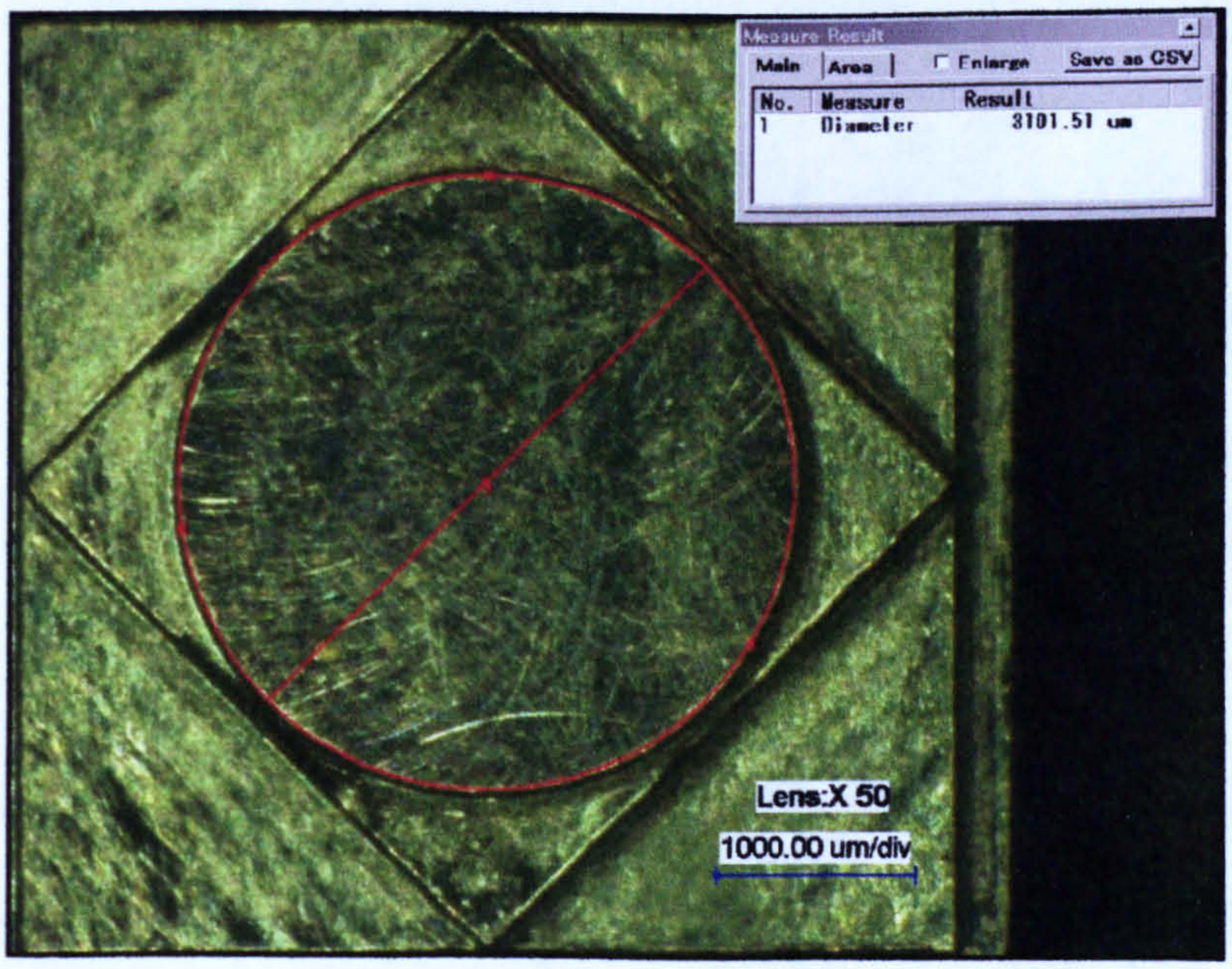

Figure 3.10 The example of on screen image of measuring the cylinder

Surface quality measurements

For the surface quality assessment, the machined micro-testpieces were analysed using a Taylor Hobson Talysurf CLI 1000 (Figure 3.11) equipped with an inductive gauge (stylus tip radius 2μm - with resolution of 40nm). It is a scanning surface topography instrument that moves the workpiece under a stationary gauge head. Data is collected one point at a time with each point having a discrete X, Y, Z location. For the inductive gauge (also shown in Figure 3.11), a diamond stylus which is attached to a lever arm is drawn over the surface. Vertical movement of the stylus (when it travels across the peaks and valleys) is converted into an electrical signal by the inductive gauge [177].

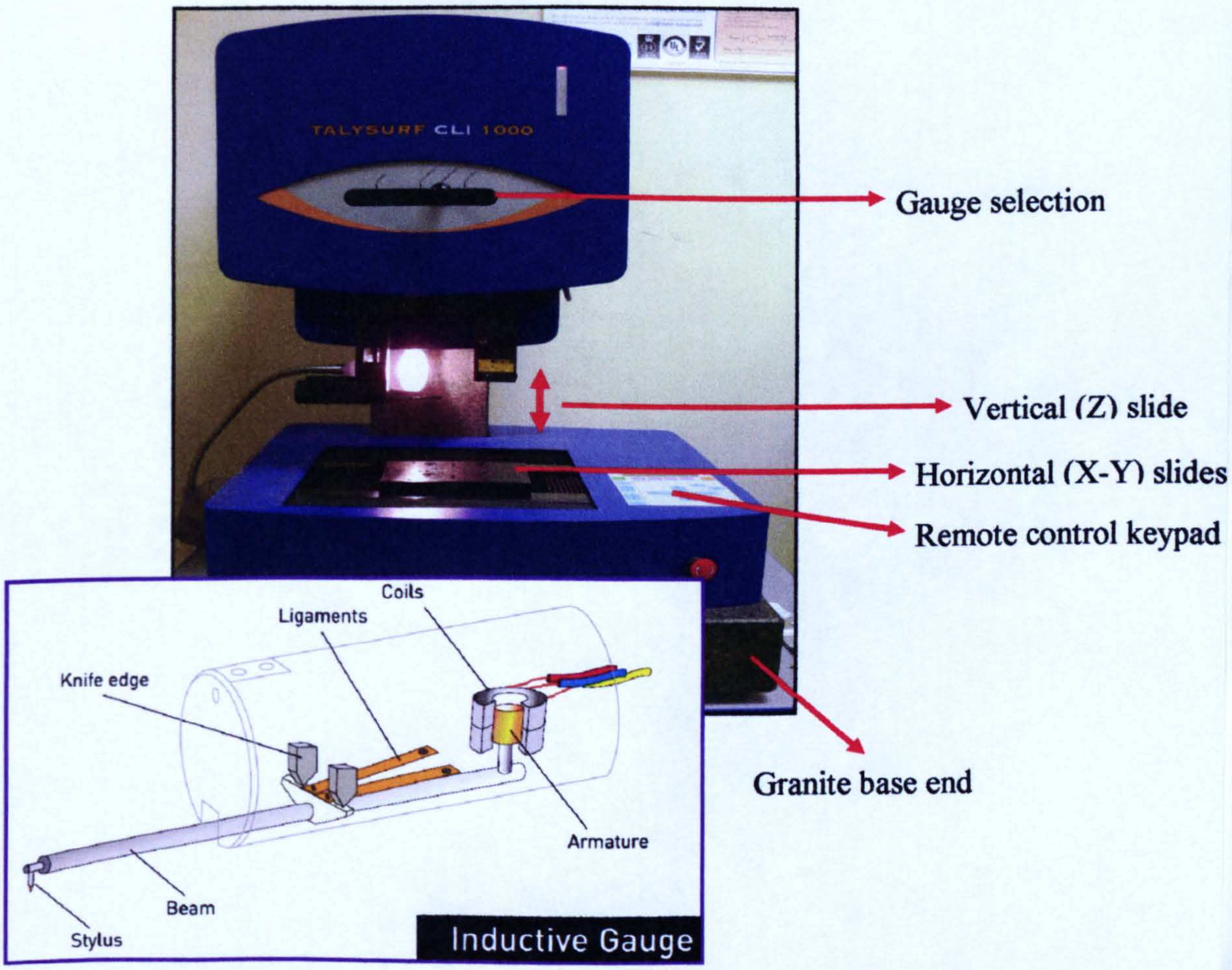

Figure 3.11 Talysurf CLI 1000 system for surface quality analysis [177]

The procedures in analysing the surface roughness of the micro-testpieces are described as below:

- The inductive gauge was placed on top of the cylinder (Figure 3.12(a))
- The surface profile was analysed at 8 different positions as shown in Figure 3.12(b).

The parameters used to evaluate the surface quality were the arithmetic average roughness (R_a) and also the average maximum height of the analysed profile (R_z). Surface roughness values (R_a and R_z) were averaged results of 8 measurements executed across the cylinder's top surface with sampling length =0.8mm and cut-off value of 0.04mm.

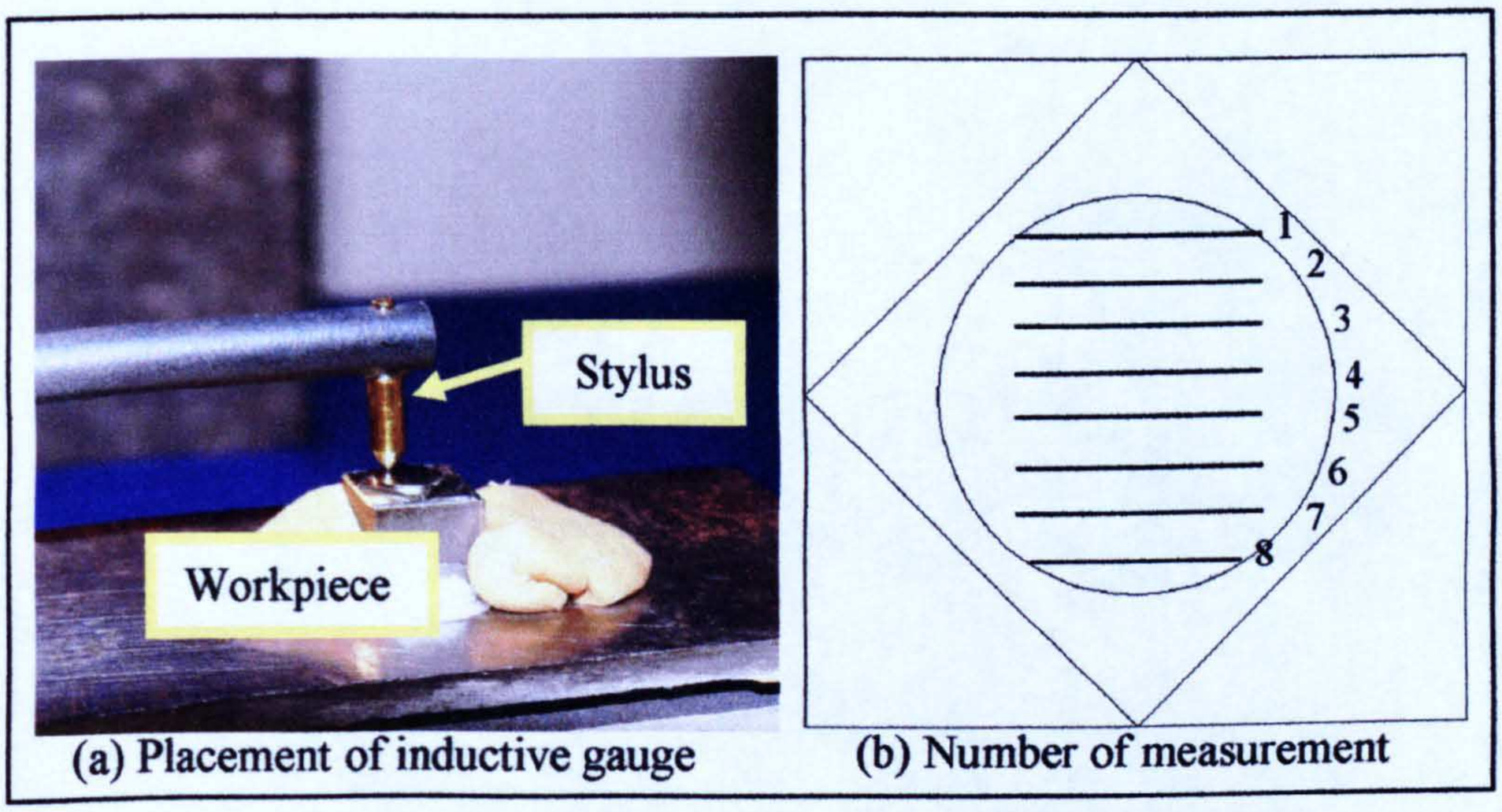

(a) Placement of inductive gauge (b) Number of measurement

Figure 3.12 Measurement procedure using Talysurf CLI 100

The details of machining procedures and parameters will be discussed in Chapter 6.

3.4.5. Machining micro-slots and thin walls

Another crucial attribute in assessing the ability of a machine tool is to produce thin features because they represent one of a major challenge in micro-machining [128]. To address this, the experiment of producing thin walls between two micro-slots was proposed in this study. The experiment was performed by machining different dimension (for different cutters diameter) of the micro-slots and thin walls in various materials. The selected materials for these trials were 316L and TiAl6V4. Table 3.4 shows the dimensions for micro-slots and thin walls that have been proportionately determined based on the cutter's size. The dimensions of the thin wall and micro-slot were determined based on the previous study that produced milled thin walls and slot in micro-levels [134, 154, 158, 161, 178-180].

The width of the thin wall was determined based on 20% of the cutter's size while the height was the maximum depth of cut recommended by the tool manufacturer. Whereas for the micro-slots, the width was determined based on the ratio of 1.2 of the cutter's size while the height follows the maximum depth suggested by the tool manufacturer.

Table 3.4 Dimension of thin wall and slot

Tool diameter (mm)	Thin wall (WxHxL) in mm	Slot (WxHxL) in mm
0.5	0.10 x 0.50 x 5.00	0.60 x 0.50 x 5.00
0.6	0.12 x 0.60 x 5.00	0.72 x 0.60 x 5.00
0.8	0.16 x 0.80 x 5.00	0.96 x 0.80 x 5.00

Besides analysing the thin wall and micro-slots, this set of experiments also give an opportunity for surface roughness aspect to be analysed and more data for MicroMAS being collected. In order to do so, by using the same tool after producing the micro-slots and thin walls, an area of surface profiling were machined at the end of the workpiece. Figure 3.13 illustrates the proposed micro-slots, thin wall and surface profiling area to be machined on the workpieces.

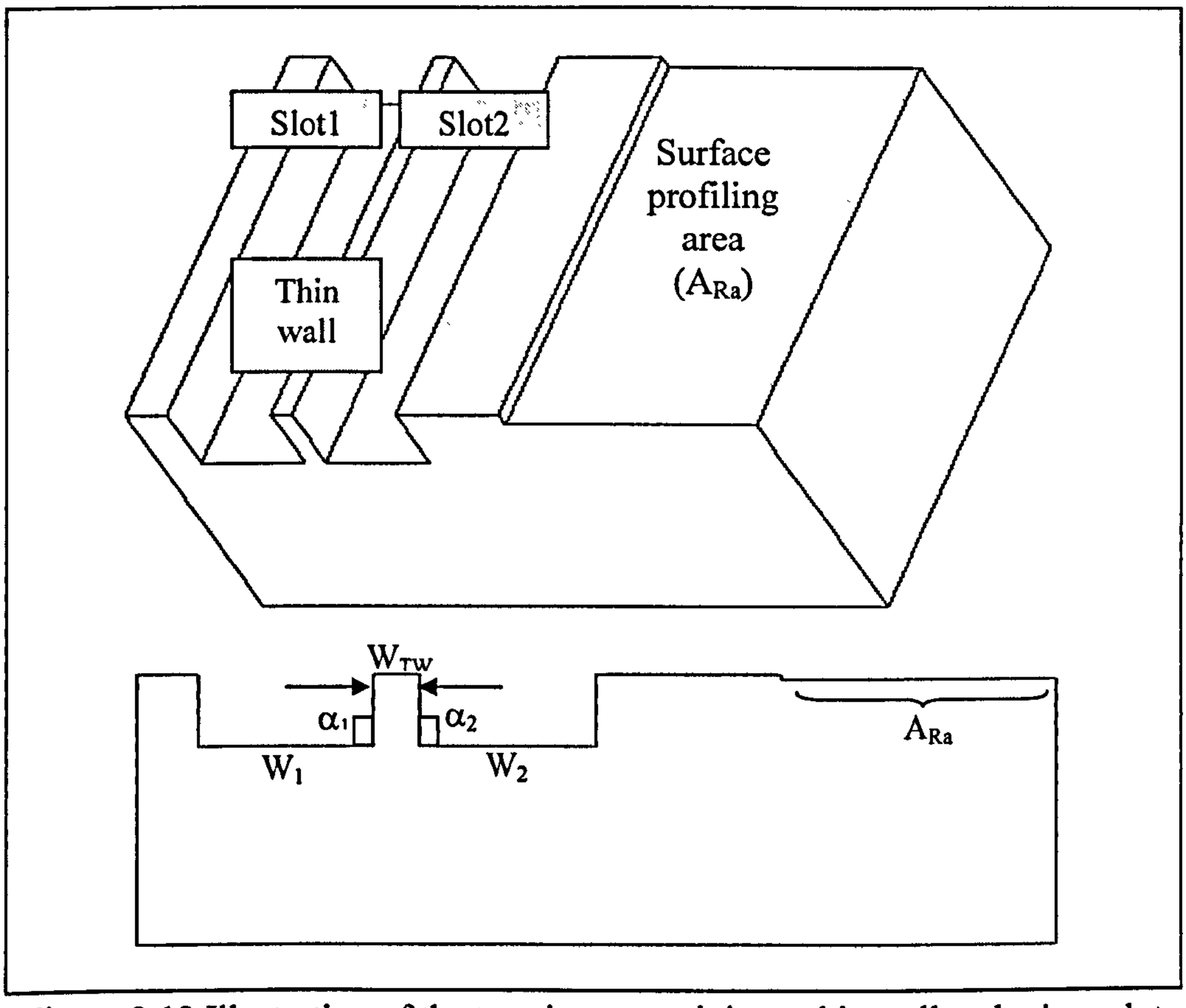

Figure 3.13 Illustration of the testpiece containing a thin wall and micro-slots

The procedure of evaluating the geometrical accuracy of the thin walls, micro-slots and also the surface quality of the surface profiling area is presented in the following section. The details of the machining procedures and parameters implemented to generate this sample demonstrator will be discussed in ***Chapter 6***.

Geometrical accuracy analysis

For the geometrical accuracy measurement, these samples are measured using a Keyence VHX-Optical Digital Microscope (Figure 3.9) (x25 – x175 magnifications) on the dimensions of the generated micro-slots and thin walls. The accuracy of the angles (α_1, α_2), the width of the micro-slots (W_1 and W_2) and of the thin walls (W_3) were measured 3 times, the average and standard deviation values were then calculated.

Surface quality measurement

The surface roughness measurement was performed using a Talysurf CLI 1000® (inductive gauge) at the area (A_{Ra}) as shown in Figure 3.13 in 10 different locations along the A_{Ra} (Figure 3.14). Surface roughness values (R_a and R_z) were averaged with sampling length of 0.8mm and cut-off length of 0.025mm.

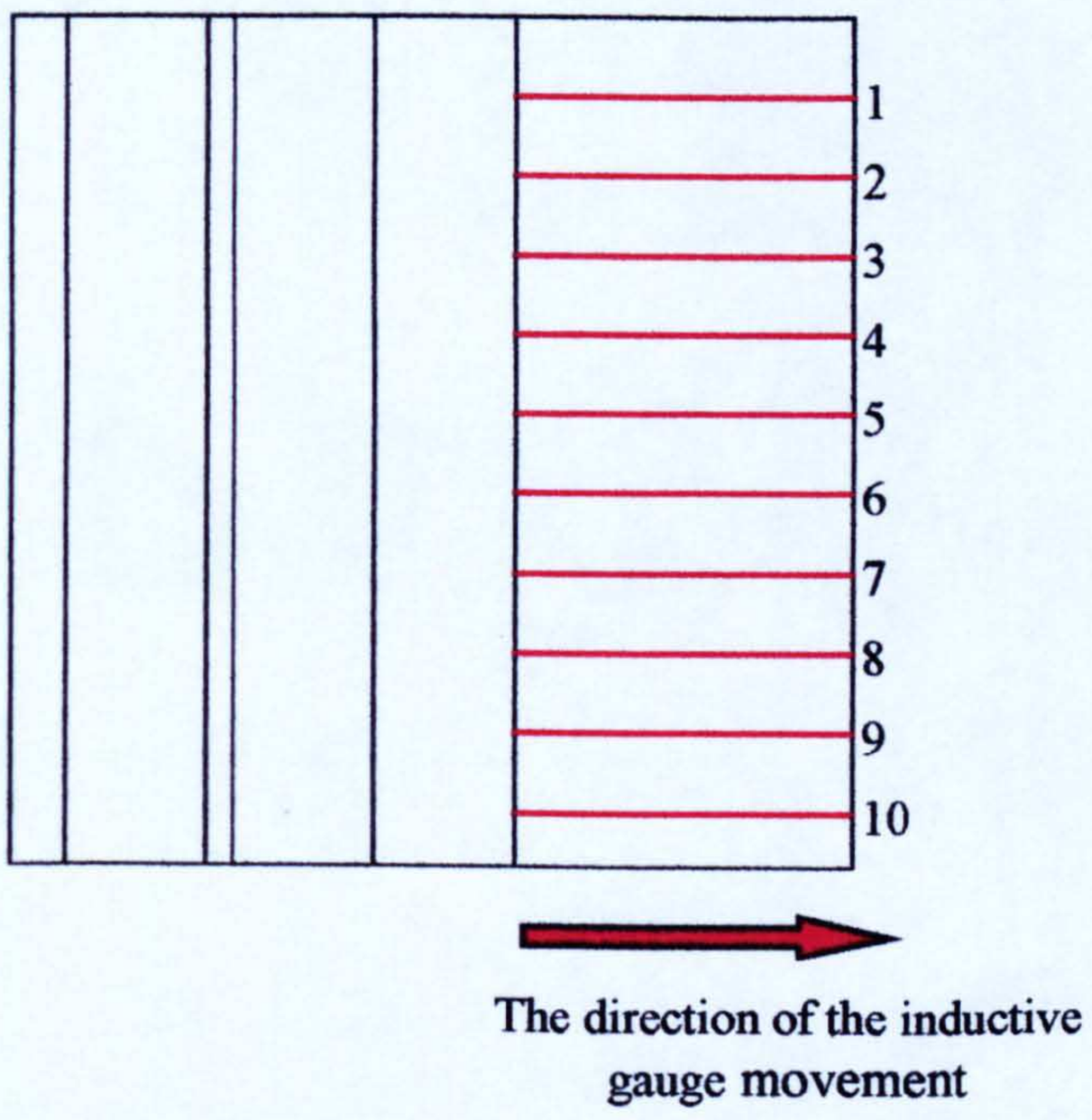

Figure 3.14 Measurement procedures (from top view of the workpiece)

3.4.6. Producing the micro-component demonstrator

To further understand the ability of the MMT, a generic micro-component that includes various features/shapes such as blind cavities (holes), slots and bosses is employed for machining. This micro-component is proposed to be machined in a difficult-to-cut material such as TiAl6V4. Figure 3.15 shows the dimensional details of the selected micro-component.

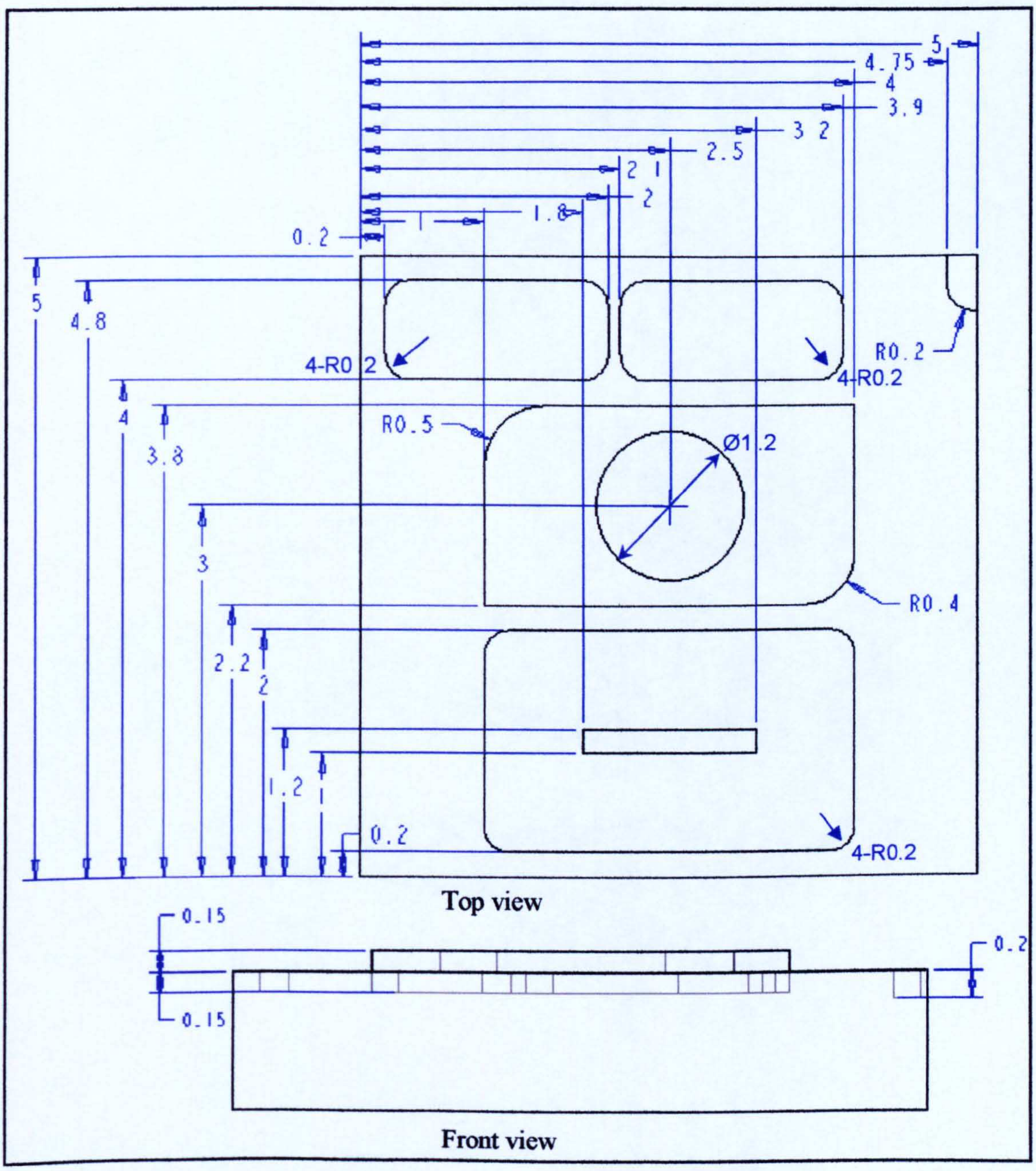

Figure 3.15 Details dimensions of the micro-component demonstrator

On completion of machining operations, the micro-component was assessed for its geometrical accuracy and surface quality. The methods and criteria of the evaluations are presented in the following paragraphs, while the machining procedures and parameters will be discussed in ***Chapter 6***. The results from this assessment can provide an indication of the ability of the MMT in producing micro-component.

Geometrical accuracy analysis

For the geometrical accuracy assessment, all features (as illustrated in Figure 3.16) were measured using a Keyence VHX-Optical Digital Microscope (Figure 3.9) as the following:

- Width - W_{F1}, W_{F2}, W_{F3}, W_{F5}, W_{F6}, W_{F7}, W_{TW}=Thin Wall between F2 and F3.
- Length - L_{F1}, L_{F2}, L_{F3}, L_{F5}, L_{F6}, L_{F7}
- Radius – R_{F4}.

All measured values were averaged results of 3 to 5 measurements with standard deviation values (σ - 99% of confidence interval) are being considered.

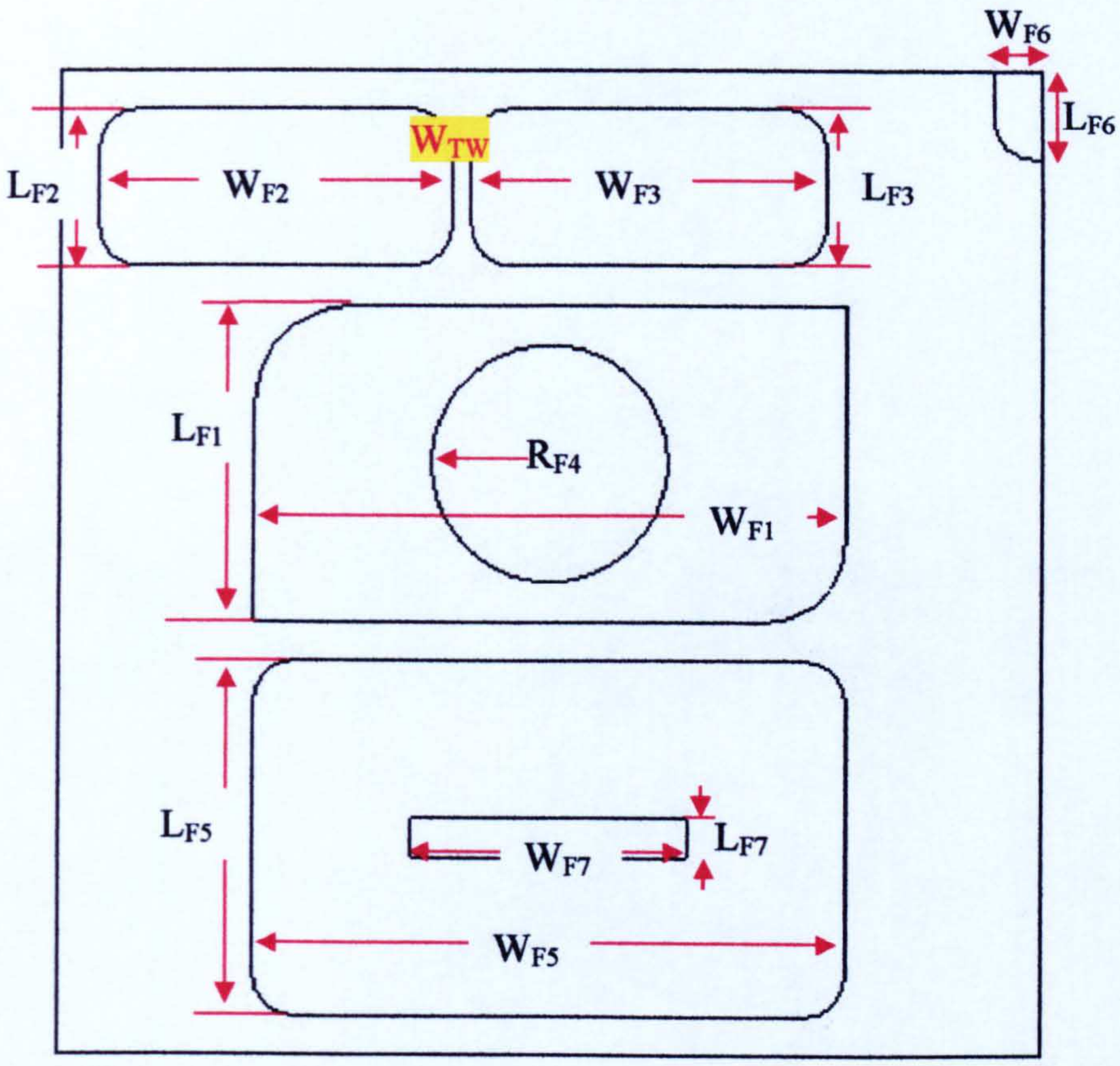

Figure 3.16 Dimensions measured from the machined micro-component

Surface quality measurement

The surface roughness measurement was again performed using a Talysurf CLI 1000® (inductive gauge).The stylus was located on the top of workpiece at four different areas (outer part of F1, within F2, F3 and F5) as highlighted in Figure 3.17. The arrows in the figure indicate the direction of the inductive gauge in measuring the surface profile. Surface roughness values (R_a and R_z) were averaged from 3 measurements with sampling length between 0.5 and 0.8mm and a cut-off length of 0.025mm.

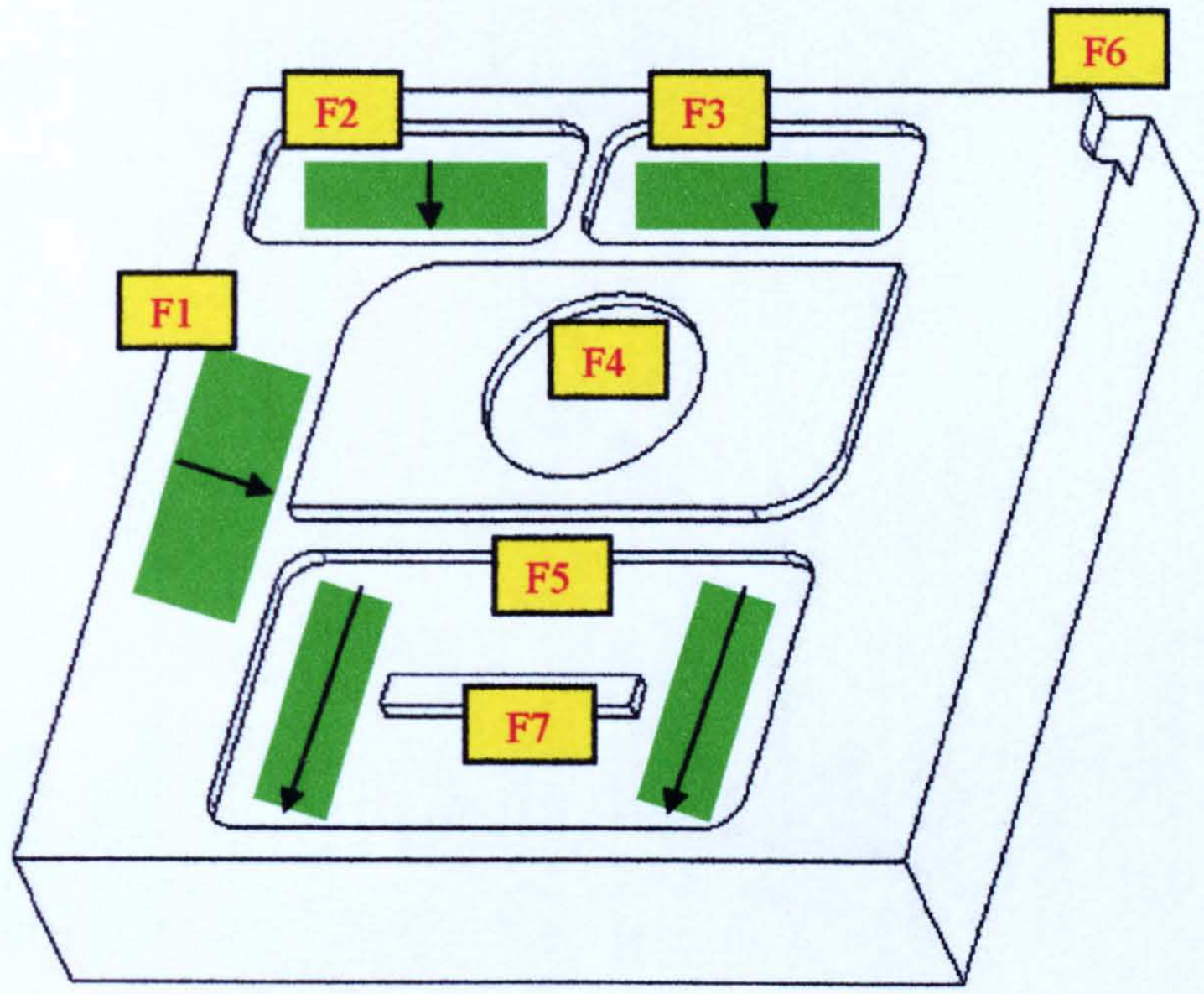

Figure 3.17 Area of surface roughness measurements indicating the directions of the inductive gauge

3.5. Uncertainty evaluation model (UEM)

In the third phase, the development of the UEM was considered to analyse the influence of the occurred errors in constructing the MMT on the geometrical accuracy of the machined micro-parts. Furthermore, it also allowed on understanding of how these errors are transferred into kinematic (tool path generation) flaws. However, the errors occurring/generated during machining (e.g. tool deflections, tool wear, vibrations) are not considered in this study.

Besides developing a model/method that can predict errors of a (custom-made) machine tool, the results from this analysis is proposed to be integrated into the MicroMAS. The integration can portray the real condition of the MMT in the developed MicroMAS. For this reason, the effect of flaws in the MMT

construction is taken into consideration in determining the MIs. The details of this approach will be discussed in ***Chapter 4*** and ***Chapter 5***.

Figure 3.18 shows the steps taken to develop the UEM which is based on the ISO GUM [95, 102]. The analysis of the UEM is carried out in GUM Workbench which is a software tool for evaluation of uncertainties in measurements. Basically, the approach taken to develop the UEM is divided into three main phases: model development, model analysis and finally simulation and validation.

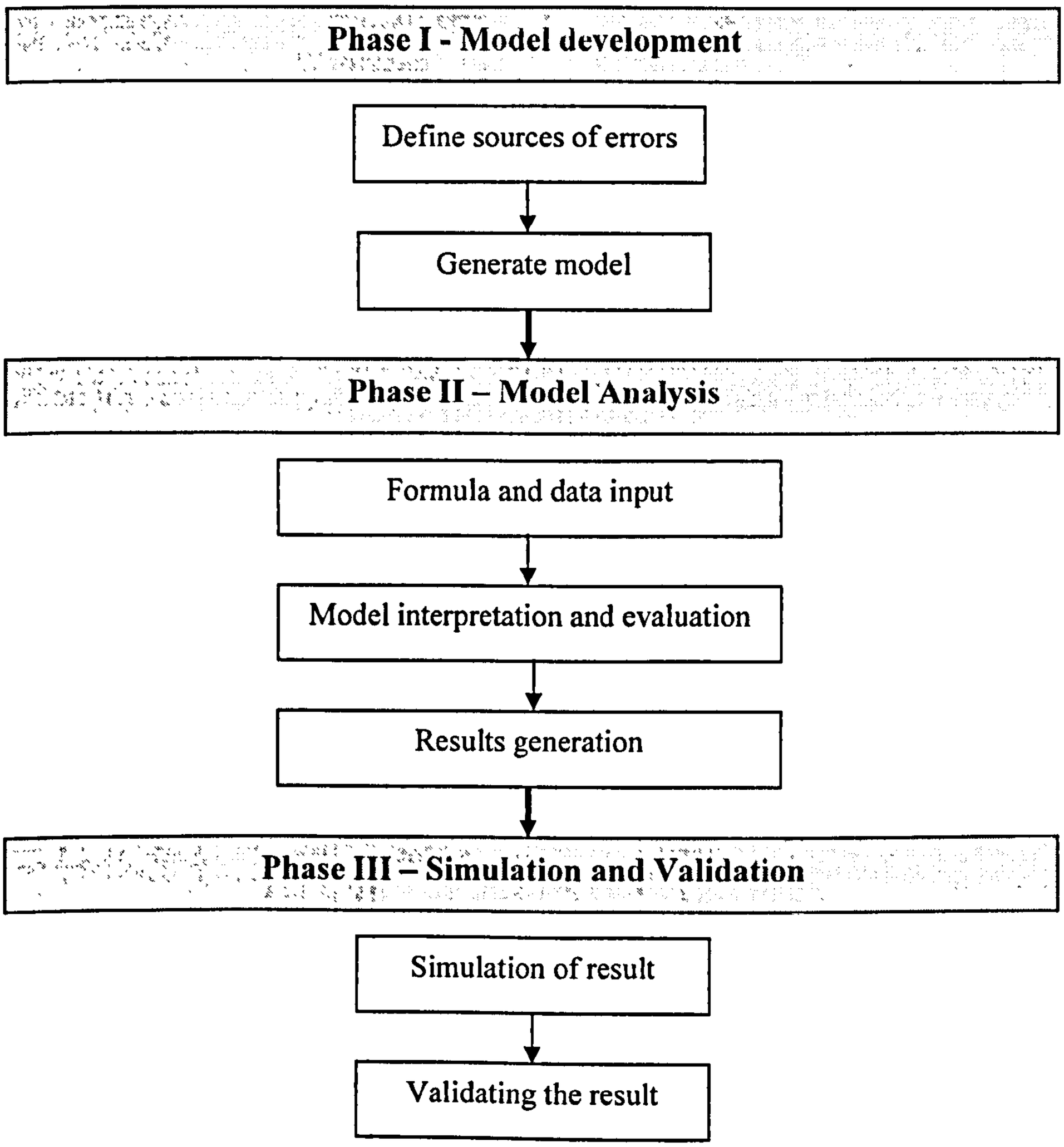

Figure 3.18 The UEM development phases

Referring to the above figure, the UEM is developed based on the following description:

3.5.1. Phase I: Model developments

3.5.1.1.Define the output quantity or the measurand (Y)

The first step in developing the uncertainty model is to define the measurand Y which is the particular quantity to be determined. In this study, Y is defined as the coordinates (x, y, z) from the tool path of generating a cylinder using spiral milling movement. The measurand Y is often not measured directly but determined from N other quantities: X_1, X_2, ..., X_N through a functional relationship f as described in ***Equation 2.1*** [95]:

$$Y=f(X_1, X_2, ..., X_N) \quad \text{(Refer to Equation 2.1)}$$

The input quantities in the measurand model can be evaluated during the current measurement or can be themselves function of other low level quantities. From here, the estimate of the measurand Y denoted by y is obtained by Equation 2.1 using *input estimates* x_1, x_2, ..., x_N for the values of the N quantities X_1, X_2, ..., X_N. Thus the *output estimate* y, which is the result of the measurement, is given by ***Equation 2.2***:

$$y = f(x_1, x_2, ..., x_N) \quad \text{(Refer to Equation 2.2)}$$

3.5.1.2.Define the input quantities ($x_1, x_2, ..., x_N$)

Next is to identify and fully define the errors (variables) stemming from the MMT construction that affect the geometrical accuracy of the generated micro-parts. All essential information regarding the identified errors should be taken into consideration. In order to identify the errors, the MMT was placed under

the CMM for metrological analysis. The CMM used was a Mitutoyo Euro-C-A121210 CMM with a 2mm stylus diameter (Figure 3.19(a)). Initially the CMM must be calibrated with a dedicated sphere ball to ensure the measurements are to be accurate. The MMT was placed on the CMM machine table and the error minimisation procedures on the MMT assembly will be discussed in details in Chapter 6 (Figure 3.19(b)).

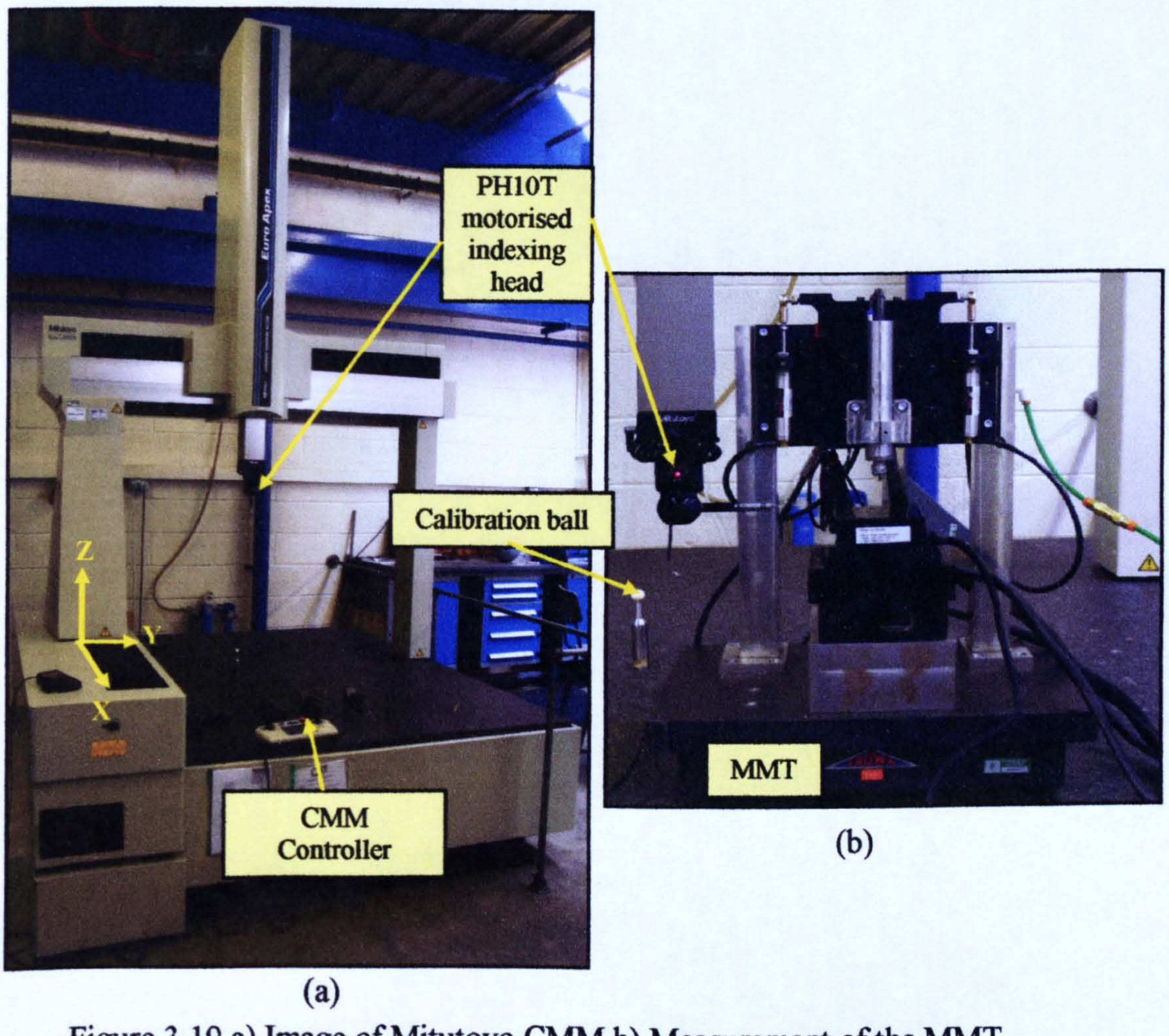

Figure 3.19 a) Image of Mitutoyo CMM b) Measurement of the MMT

Beside the CMM evaluations, the errors were also identified from the in-work MMT observations, previous literatures and related standards (e.g. ISO 230 – Test code for machine tools).

3.5.1.3.Establish the measurement model

Once the errors were identified, the uncertainty model was derived from: the outcome of the CMM evaluation, in-work MMT observations, reported values, manufacturer's specifications, handbooks and general knowledge. In this, the uncertainty of output y which is a combined standard uncertainty was obtained from the estimated standard deviation of each input estimation x_i that is termed as standard uncertainty. The purpose of this step was to evaluate the standard uncertainties of the estimates (x_1, x_2,...x_N) of the input quantities where each of them were evaluated differently based on its type (A or B) [95, 123].

3.5.2. Phase II: Model analysis (GUM Workbench)

As a well-established approach in evaluating the measurement uncertainty, the GUide to the expression of uncertainty in Measurements (GUM) was chosen as the dedicated uncertainty analysis environment for this study. The GUM approach involves a tedious and error-prone series of calculations, but by using GUM-software package to perform them, removed from all the difficulty in analysing the measurement of uncertainty [122-123].

In this study, GUM Workbench which is one of the available commercial GUM based software package that has been developed by Metrodata GmbH, Germany [123] was selected to estimate uncertainty measurement for errors in constructing the MMT. This software is available from the Metrodata website (http://www.metrodata.de/download_en.html) and it can be freely used for educational purposes. Moreover, based on the discussed features in ***section 2.3.5*** (Chapter 2), GUM Workbench claimed to own all of them [121-123,

181]. This software tool is used to analyse the uncertainty of physical measurements and calibrations based on the internationally recognised GUM-method. It supports a systematic procedure in building an uncertainty analysis starting with the mathematical equation which models the physical relationship of quantities in the respective measurement. The analysis process is controlled by the appropriate classification of the input values according to the available information that are based on the procedures and formula given in the following publications [121, 181]:

- Guide to the expression of uncertainty in measurement (GUM).
- Expression of the Uncertainty of Measurement in Calibration (EAL R2).
- ISO/DTR 14253-2: "Geometrical Product Specifications (GPS) – Inspection by measurement of workpieces and measurement equipment – Part 2: Guide to the estimation of uncertainty of measurement, in calibration of measuring equipment and in product verification" (PUMA – method).
- NIST Technical Note 1297 Guidelines for Evaluating and Expressing the Uncertainty of NIST measurement Results.

GUM Workbench was claimed to be very intuitive, easy, user-friendly and systematic [121-123]. Based on the experience of using the GUM Workbench, Jalukse et al. [181] described this software as a very good program for modelling measurement procedures which allows the main sources of uncertainty to be highlighted and suitable for a wide range of measurement problems from very simple to very complex procedures. It also provides a very clear interface in presenting the formulas and its definition and offers a

standard format of uncertainty report. While Axinte *et al.* [99, 106] has also successfully carried out uncertainty evaluation in both quantifying tool life measurements for turning process and also expressing the uncertainty in cutting force measurement which takes into account process-related contributions.

3.5.2.1. Model input in GUM Workbench

The generated model as in ***Equation 2.2*** is then inputted into the GUM Workbench for the uncertainty analysis by considering the details of all the input quantities (x_1, x_2,...x_N). Figure 3.20 shows the example of the *model equation interface* in GUM Workbench where all the parameters in the developed model ***(Equation 2.2)*** and its descriptions (e.g. units) are being input.

GUM Workbench

File Edit View Option Tools Help

Model | Observation | Correlation | Budget | Previous

Title | Model equation | Quantities

Equation:

Σδ.. Rename

```
R=sqrt(X^2+Y^2);
X=a*(cos(ω*(t*0.0377)))+ΔX1+ΔX2+ΔX3+ΔX4;
ΔX1=L*(sqrt(cos(α)^2-cos(γ)^2));
Y=a*(sin(ω*(t*0.0377)))+ΔY1+ΔY2+ΔY3+ΔY4;
ΔY1=ΔY0+L*sin(α);
```

Area to declare the developed model

Quantity	Unit	Definition
R	mm	the radius of a circle
X	mm	the x value
Y	mm	the y value
a	mm	radius
ω	rad/sec	angular velocity
t	sec	time
ΔX_1	mm	Uncertainty due to X,Y,U planes deviation for X
ΔX_2	mm	Uncertainty due to original position deviation of table movement for X
ΔX_3	mm	Uncertainty due to temperature deviation for X
ΔX_4	mm	Uncertainty due to worktable accuracy for X
L	mm	Tool length
α	rad	Angle between Tool (Z) and side of U table
γ	rad	Angle between Tool (Z) and top of U table
ΔY_1	mm	Uncertainty due to X, Y and U planes deviation for Y
ΔY_2	mm	Uncertainty due to original position deviation for Y
ΔY_3	mm	Uncertainty due to temperature deviation for Y
ΔY_4	mm	Uncertainty due to worktable accuracy for Y
ΔY_0	mm	value of shifted planes

Table to define each declared parameters

Figure 3.20 Example of model equations interface

Following the completion of providing the generated model into the *model equation interface,* the details of each declared parameter are required in the *Quantities interface* as shown in Figure 3.21. As stated in Chapter 2, each input quantity can be classified as either Type A (repeated observed quantity) or Type B (non-repeated observed quantity/known uncertainty). In GUM Workbench, for Type A, it is evaluated by a statistical analysis of a series of observations (e.g. experimental results). While for Type B, it can be associated with different type of probability distributions (e.g. Normal, t-distribution, rectangular, u-shaped, triangular and trapezoidal). It is very important to classify the input quantity as each type (A and B) has different approach of evaluation.

Then, the uncertainty analysis towards the generated model is being done by selecting the ***Budget*** button (as shown in Figure 3.21). In here, the GUM approach calculation of standard uncertainty, sensitivity coefficient, combined standard uncertainty, degrees of freedom, coverage factor and expanded uncertainty are being made.

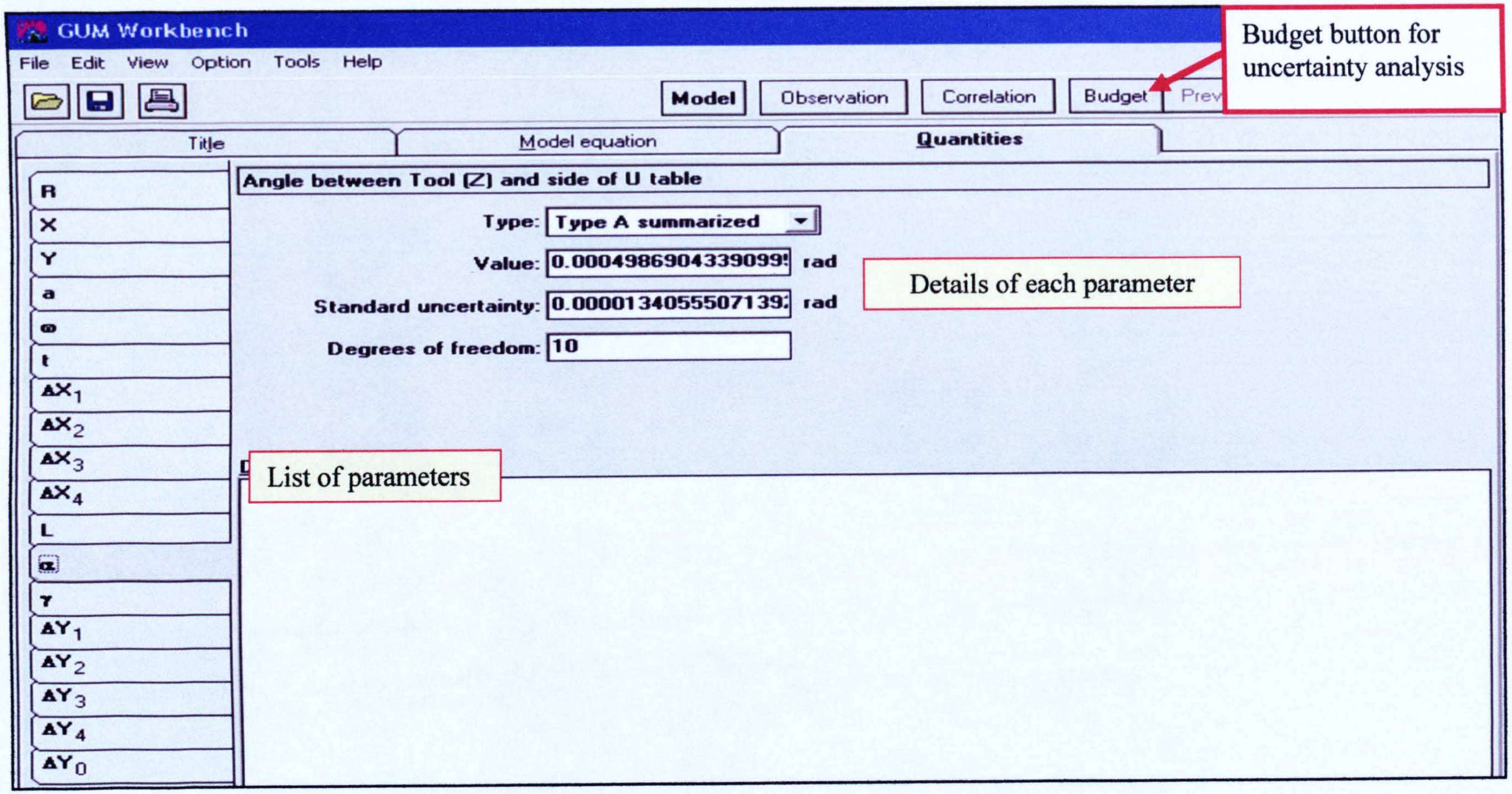

Figure 3.21 Example of quantities interface

The result of the analysis is clearly defined on a table that contains all variables with their symbols and values, the assigned standard uncertainty and actual degrees of freedom, the sensitivity coefficient worked out by the model equation and their contribution to the standard uncertainty of the measurement's result. Finally, the complete result of the uncertainty analysis is presented as a value with the connected expanded uncertainty and automatically selected coverage factor.

3.5.3. Phase III: Simulation and validation

The generated uncertainty results obtained from the GUM Workbench analysis were simulated and validated via machining experiments and observations.

i. In order to simulate the validity of the uncertainty model, the spiral milling tool path was performed without cutting while stopping the tool at particular time intervals and the tool tip position was evaluated using CMM.

ii. The results from the CMM measurements have been compared with those obtained with the uncertainty model in terms of errors in roundness and height of the cylinder on which spiral milling was simulated.

3.6. Integration of MicroMAS, micro-machining experiments' results and UEM's results

In the final phase, it was the aim of the study to incorporate the results from micro-machining experiments and UEM analysis into the developed MicroMAS. This was to ensure that the system emulated its domain (the MMT). Table 3.5 summarised the contribution of UEM and micro-machining experiments into the MicroMAS. Figure 3.22 shows the overall built of the

MicroMAS where it presents the contributions and relationship between the UEM, micro-machining experiments and MicroMAS.

Table 3.5 Contributions of UEM and micro-machining experiments into MicroMAS

Aspect	Contributions/Relationship
Micro-machining experiments	• Provide surface roughness and geometrical accuracy values for the related MIs. • Validate the UEM analysis when spiral milling of a cylinder. • Present the overview of the MMT capability in producing various types of micro-features.
UEM analysis	• Propose a model/method that can predict the errors of a custom-made machine tool. • Visualise the real condition of the MMT construction. • Provide the effect of the errors in the MMT construction through MIs.

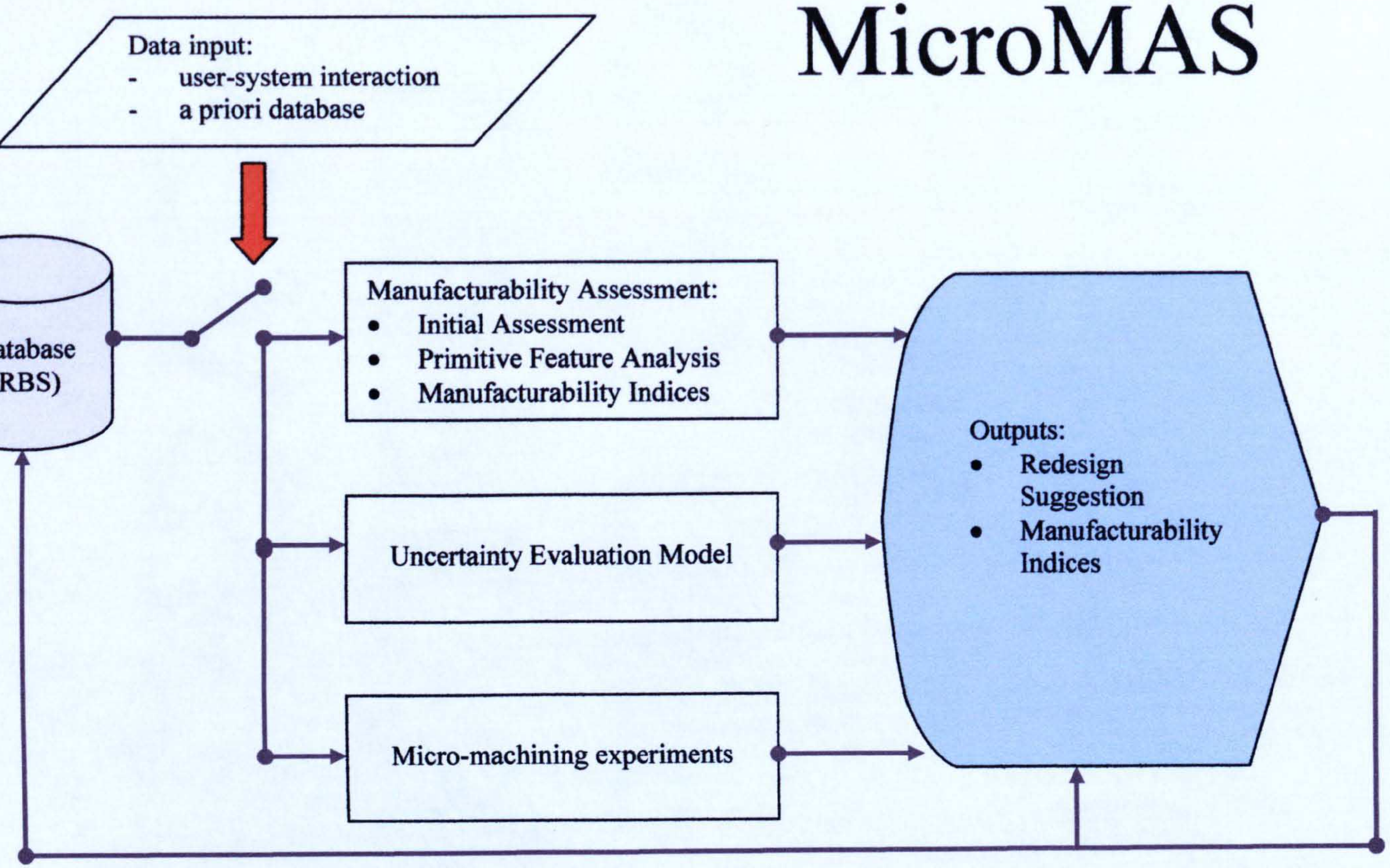

Figure 3.22 Relationship between MicroMAS, UEM and micro-machining experiments

CHAPTER 4: PRIMITIVE FEATURE ANALYSIS TECHNIQUE

4.1. Introduction

In developing the Manufacturability Analysis System (MAS), the feature analysis approach is one of the methods used to extract information from proposed design (CAD model) for its manufacturability assessment purposes. A new technique called **"Primitive Feature Analysis"** (PFA) has been developed in this study for gathering essential data from CAD models and to further analyse their manufacturability. Furthermore, this is the technique that is implemented in the developed MicroMAS explicitly for micro-milling process run on the custom-made 4-axis Miniature Machine Tool (MMT) for the above mentioned purposes (data gathering and manufacturability assessment).

This chapter describes and illustrates the mechanism of the PFA technique which consists of three phases: primitive feature identification, Single Feature Analysis (SFA) and Coupled Feature Analysis (CFA). The concepts, objectives and flowcharts of each phase are discussed. Then, the implementation of the PFA technique's algorithm on a CAD model is described and demonstrated. Finally, the execution of the PFA technique in the developed MicroMAS is defined and briefly discussed.

4.2. Description of Primitive Feature Analysis (PFA) technique

Instead of using laborious methods of data extraction from CAD models and to address the limitations of other methods (e.g. feature-based extraction system,

neutral files usage) mentioned in Chapter 2, this study proposes a new structure for MASs that relies on a "translation" of CAD essential information into a set of algebraic primitive features whose manufacturability are analysed in a singular and interrelated (i.e. coupled) manner. In contrast with the common approach that focuses on extracting the data based on a wide range of single entity features (e.g. holes, slots, pockets, steps, dovetails, counter bores/sinks), this study proposed the opportunity of feature analysis based on a reduced number of algebraic primitives (e.g. box, sphere, cylinder, cones). The introduction of Primitive Feature Analysis (PFA) technique manifests a new opportunity in obtaining data from CAD models and further to analyse their manufacturability as a prerequisite for more efficient MASs. In CAD systems, Primitive Feature (PF) is a known concept and by using this as the foundation for the feature analysis in PFA technique, it is believed MAS users will define the parts easier.

In this study, the PFA technique is implemented by gathering data from CAD models and being executed throughout the entire MicroMAS for the purpose of manufacturability aspects assessment. PFA is defined as a method for assessing the manufacturability of singular PF as well as their interactions (coupled PFs) in making possible the realisation of the CAD models and further enabling the manufacturability analysis of the part. In this study, the selected PFs are: box, sphere, cylinder and cone (as illustrated in Table 4.1).

The approach of the PFA technique is to define and to gather data from the proposed CAD models, based on the contained PF, and further to express their existence as bosses (positive PF) or pockets (negative PF) on the analysed parts. Furthermore, once the manufacturability of each negative/positive PF is evaluated, the next step is to interact them by assessing their degree of compatibilities which lead to the evaluation of part manufacturability by use of aggregate indexes that will be discussed in this chapter.

Table 4.1 Illustration of Primitive Features

Type	Primitive Feature (PF)
Box	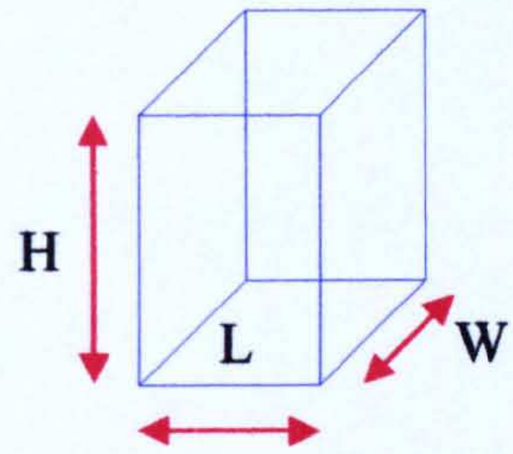
Cylinder	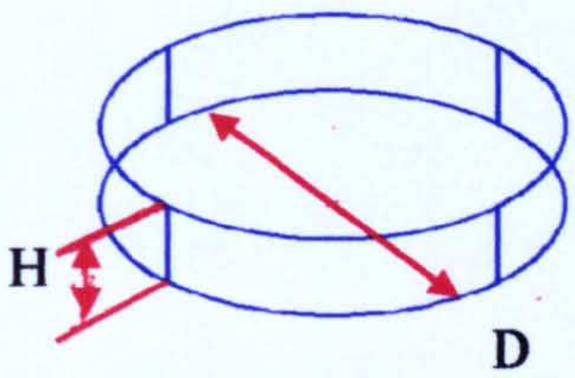 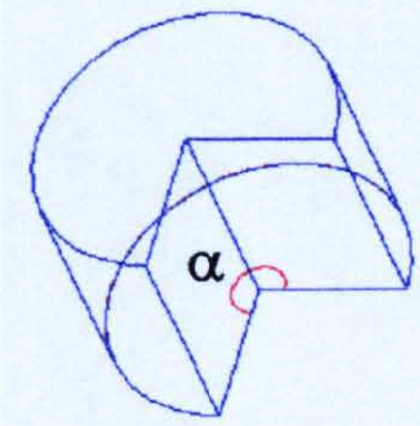
Cone	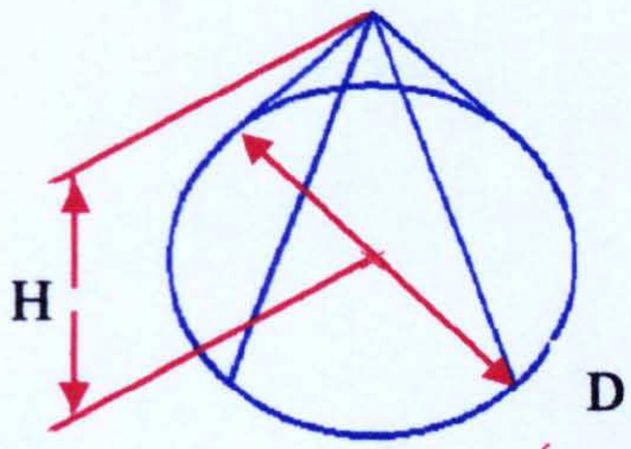
Sphere	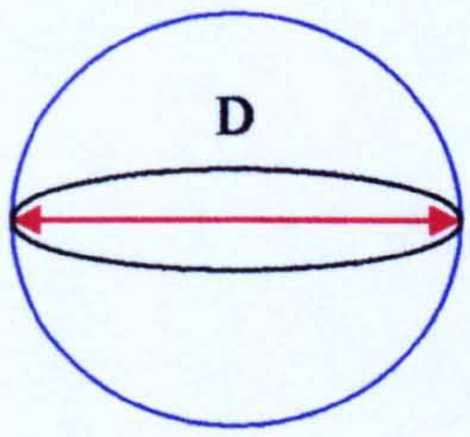 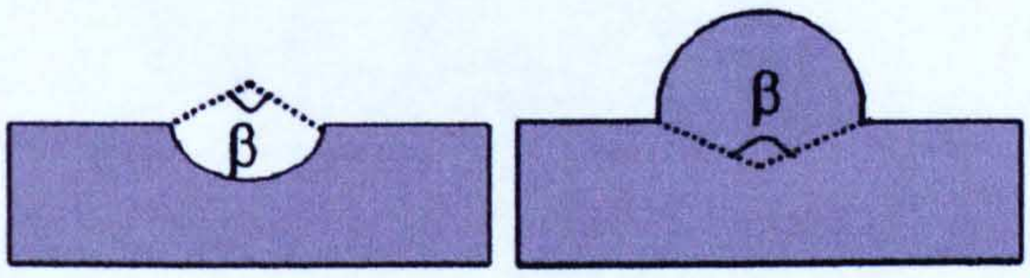

Legend:

- L – Length
- W - Width
- H - Height
- D - Diameter
- α_e - Extension angle of the cilindrical surface
- β - Surface angle = Angle made from the surface to the centre point

4.3. Manufacturability indexes

The manufacturability analysis which is based on the PFA technique is expressed through specific Manufacturability Indexes (MIs). MIs reflect the relative ease of machining of the component based on associated ratings of

various aspects such as PF characteristics, surface roughness, tool dimension, tolerances, machinability of selected materials and also uncertainty effect in machining the micro-feature using the custom-made 4-axis Miniature Machine Tool (MMT). The MMT is being highlighted because it is the domain for the MicroMAS where the PFA technique is being implemented in this study.

MI evaluations are based on the results from Single Feature Analysis (SFA) performed for each PF that is followed by Coupled Feature Analysis (CFA) to reflect their interactions. In calculating MI at SFA level, there are five key characteristics that have been considered: form of singular PF (as in Table 4.1), uncertainty impact in machining the feature, surface roughness, tolerances and tool diameter effect on machining the PF's minimum curvature. For each key characteristic an MI value is assigned.

MI for singular PF (MI_{PF}) reflect the level of manufacturability based on the geometrical aspects of a PF such as: orientation of the PF (boss or cavity), shape (straight, negative or positive tapered) and end-corner specifications. MI for surface roughness (MI_{Ra}), tolerances (MI_{TOL}) and tool dimension effect (MI_{DIM}) emulate the quality measures of the part as chosen by the user. While the UEM impact is represented by MI_{UEM}, where this index justifies the real condition of the MMT will be discussed in ***Chapter 5.*** The simulation of determining all the MIs will be presented in ***sections 4.4*** and ***4.5***.

All these indexes are summed up to an index (MI_{SFA}) that reflects the level of manufacturability for the analysed PF as shown in Equation 4.1. A weighting factor ($0<K_i\leq1$) is assigned to each index based on the user decision in

determining which key characteristics are more important when considering the manufacturability of the PF.

$$MI_{SFA} = \frac{\sum K_i . MI_i}{5}, \qquad \text{(Equation 4.1)}$$

Where i= PF, Ra, TOL, DIM, UEM

The indexes are represented by a rating convention generated based on micro-machine specifications, recommended cutting parameters, previous manufacturability evaluations [7, 11, 69, 71-72] and feature analysis [60]. The following rating convention for any output measure (e.g. MI_{PF}, MI_{Ra}, MI_{UEM}, MI_{DIM}, MI_{TOL} and MI_{SFA}) has been implemented throughout the entire PFA technique (single and coupled features as well as overall analysed part):

- **Medium** level of manufacturability; **for 0.5< MI ≤ 1.0**
- **Harder** level of manufacturability; **for MI ≤ 0.5** (Equation 4.2)
- **Easier** level of manufacturability; **for MI >1.0**

The calculations of indexes for all the output measures are described throughout this chapter and simulated in ***section 4.5***.

4.4. PFA framework and mechanism

The PFA technique is developed based on primitive features concept, machining experiences/observations and also results from micro-machining experiments and/or from related literature. Figure 4.1 shows a flowchart with additional graphical representations of analysis done at each phase of the PFA

technique: Phase 1 - PF identification, Phase 2 - Single Feature Analysis (SFA) and Phase 3 - Coupled Feature Analysis (CFA).

The objective of SFA is to assess the level of manufacturability for each defined PF based on their orientation, shape and end-corner specification while the aim of CFA is to analyse the relationships between the PFs based on their relative distances and type of interaction (e.g. attached PF). The results from the SFA determine the MI_{SFA} for each identified PF and while the results from the CFA level conclude the MI_{CFA} and $MI_{OVERALL}$ for the micro-part.

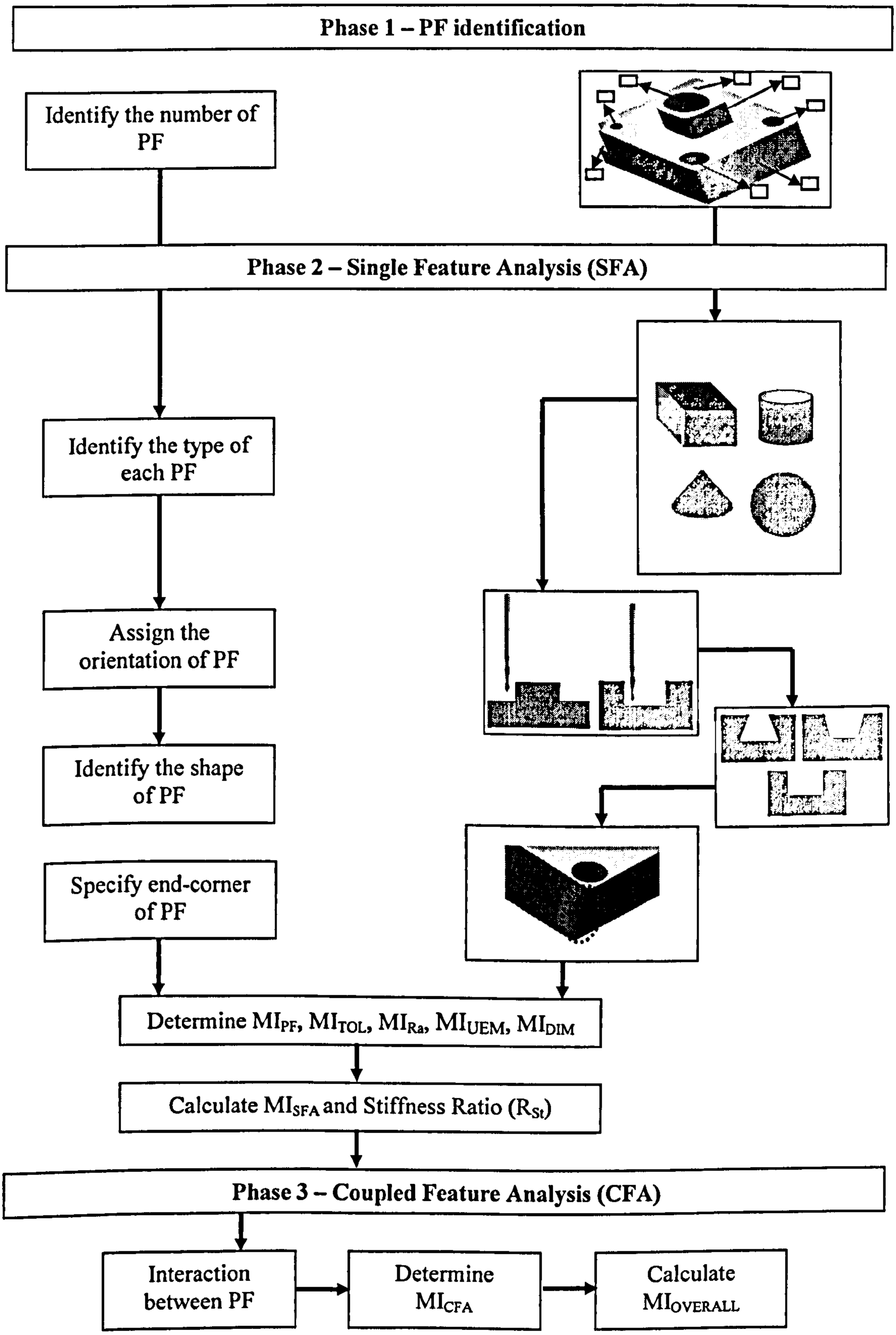

Figure 4.1 Flowchart and illustration of PFA technique

4.4.1. PF identification

In the first phase, each of the PF contained in the proposed CAD model is identified and a number is assigned to each of them that act as the unique reference for future analysis in the PFA process. In this phase, the user has to recognize all the PF contained in the proposed design and to identify their geometrical characteristics. If there are features that cannot be considered, in a simplified way, as PFs, the user will "decompose" them to fit the requirements of the system.

Table 4.1 presents the essential geometrical data required from each PF to assist the analysis process. The data collected are then used for the manufacturability analysis based on the mechanisms discussed in the following part.

4.4.2. Single feature analysis (SFA)

For the second phase, the evaluation of MI_{SFA} is the key elements of SFA that stem from the analysis of PF as follows (Figure 4.2):

(i) Assign the orientation for type of each PF

(ii) Assign the shape of PF

(iii) Specify the type of end-corner

(iv) Analyse tolerance, dimension, UEM impact and surface roughness

(v) Evaluate the stiffness ratio (R_{St}) of related PFs

Referring on the flowchart and illustrations in Figure 4.1 and 4.2, SFA approach for identifying and analysing PFs can be describes as follows:

i. Type of PF orientation.

For each PF, their orientation is assigned whether it is a boss or a cavity as described in Figure 4.2(a). Boss is a feature that is generated by removing the material outside of it while a cavity is generated by removing the material inside of it. If the feature is assigned as a cavity, its type is determined based on whether it is a blind or through cavity as illustrated in Figure 4.2(b).

ii. Shape of PF.

This is determined based on the side angle value provided by the user during the input data session. The category assigned to each PF is whether a positive-tapered, negative-tapered or straight shape. Figure 4.2 (c) illustrates different types of the side angle (θ). A positive-tapered is defined when $\theta > 90°$ while when $\theta < 90°$ is considered as negative-tapered and a straight shape when $\theta = 90°$.

iii. End-corner specification.

It is based on the type of end-corner's shape which is classified as sharp, radiused or fillet corner as presented in Figure 4.2(d).

iv. Analyse quality measures of PF.

To enable the evaluation of MI_{SFA}, the tolerances, surface roughness of the PF, the tooling dimensions have to be specified by user and also the impact of the UEM analysis. These values are associated with ratings indexes as specified in Equation 4.2, the way how each index is calculated for each of these output measures will be discussed in ***section 4.5***.

v. Evaluate the stiffness ratio (R_{St}) of PF.

As discussed in Chapter 2, one of the challenges in micro-milling is producing thin features/walls because it involved the stability of the

machining operation. For this reason, the stiffness ratio of the particular PF is evaluated by comparing the calculated ratio with pre-set values. The pre-set values are determined from various sources (e.g. machined micro-parts on the MMT, machining experiences, the MMT capability). Basically by making a feature thinner, their stiffness decreases which could result the occurrence of vibrations during machining and this leads to deteriorations of the process accuracy that affect the part quality. Figure 4.2(e) shows the example of R_{St} calculations for box and cylinder which is based on the Length (Width/Diameter)-to-Height ratio.

Aspect	Graphical representation
(a) Boss and Cavity	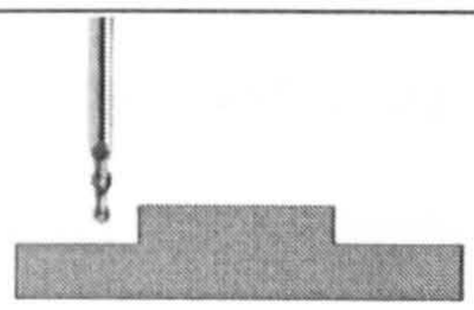 **Boss:** Feature generated by removing the material outside. 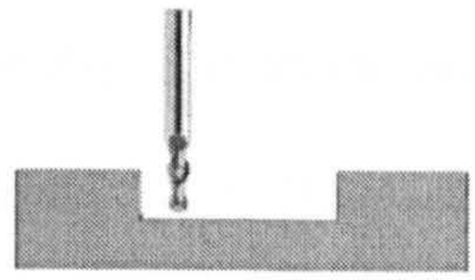 **Cavity:** Feature that is generated by removing the material inside
(b) Type of cavity	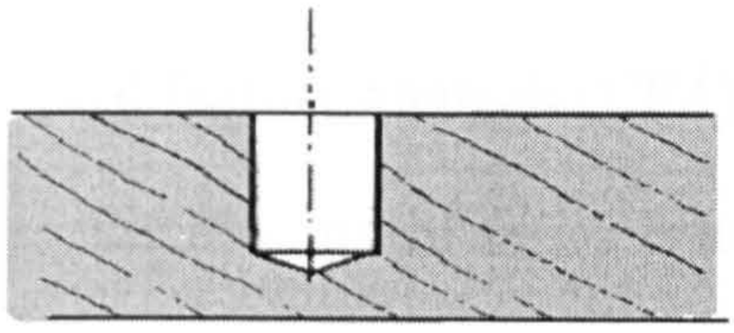 Type: Blind 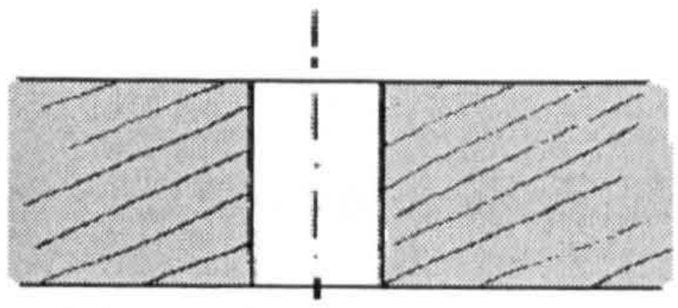 Type: Through
(c) Side Angle	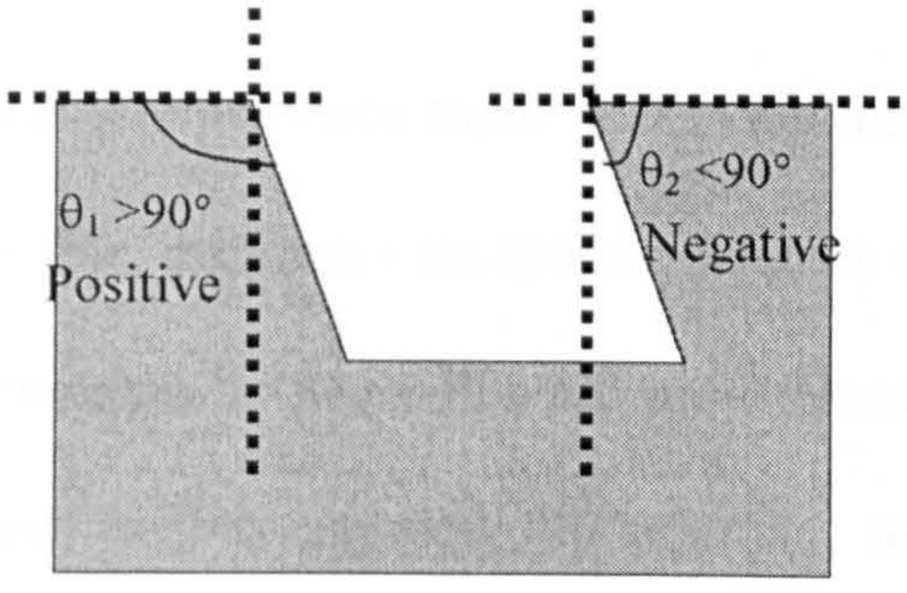 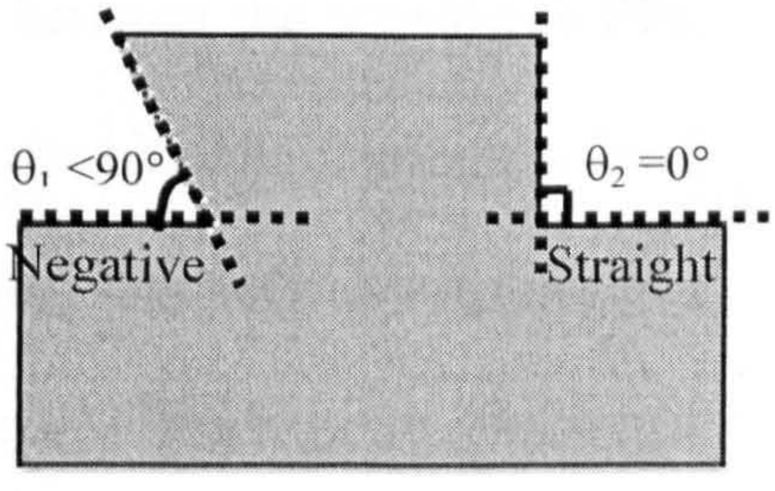
	θ_1, θ_2 = side angle (defines the shape of the features)
d) End-corner	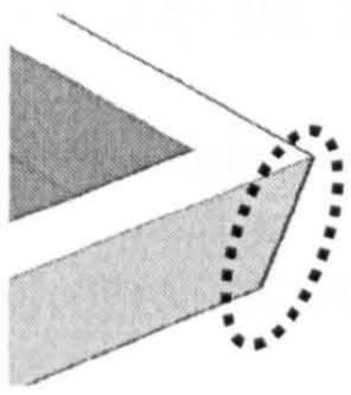 Sharp 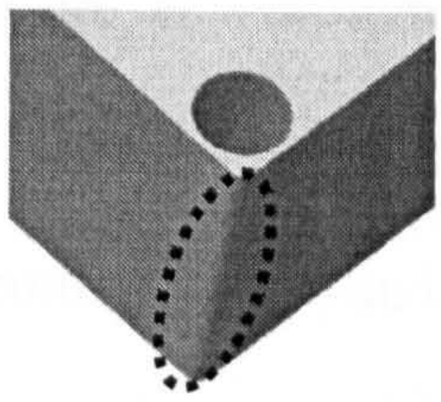 Radiused 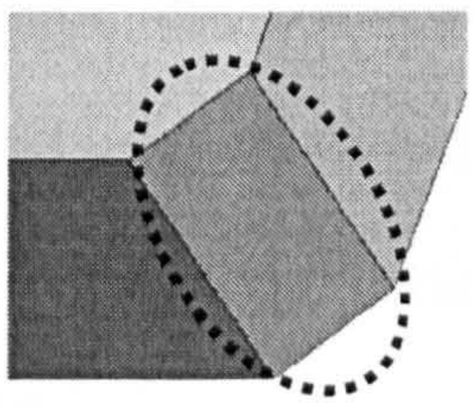 Fillet
(e) Stiffness Ratio (R_{St})	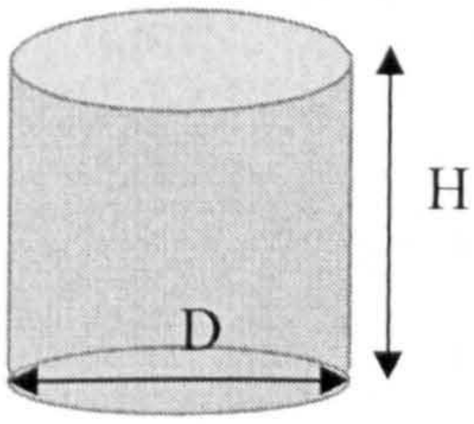 $R_{St}=\frac{D}{H}$ 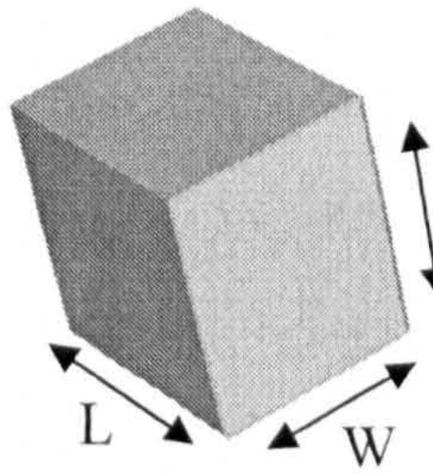 $R_{St}=\frac{LorW}{H}$

Figure 4.2 Single Feature Analysis terminologies

Finally, after these selections/specifications, MI_{SFA} values are made for each PF (Equation 4.1) and their ratings expressing the difficulty to manufacture are evaluated based on the convention specified in Equation 4.2. Examples of calculation of MI_{SFA} values are presented in ***section 4.5***.

4.4.3. Coupled feature analysis (CFA)

In this phase, the determined MI_{SFA} is taken at the upper level of analysis, i.e. evaluation of MI_{CFA}. The CFA aims to determine the level of relationship among PFs by taking into consideration the relative distance (RD) and the type of interactions between them. RD is the distance between the considered PFs. Besides that, minimum acceptable distance (MD) used in determining the level of relationship between PFs are pre-defined earlier. The MD was determined based on various aspects, for example, the distance between two negative boxes (slots) can result in a thin wall that can preserve its geometrical characteristics only the features are at a minimum distance; this could be dependent on workpiece material (strength), tool run-out (inducing vibrations), cutting parameters (influencing cutting forces) and accuracy of the MMT. The types of interactions between PFs are illustrated in Figure 4.3.

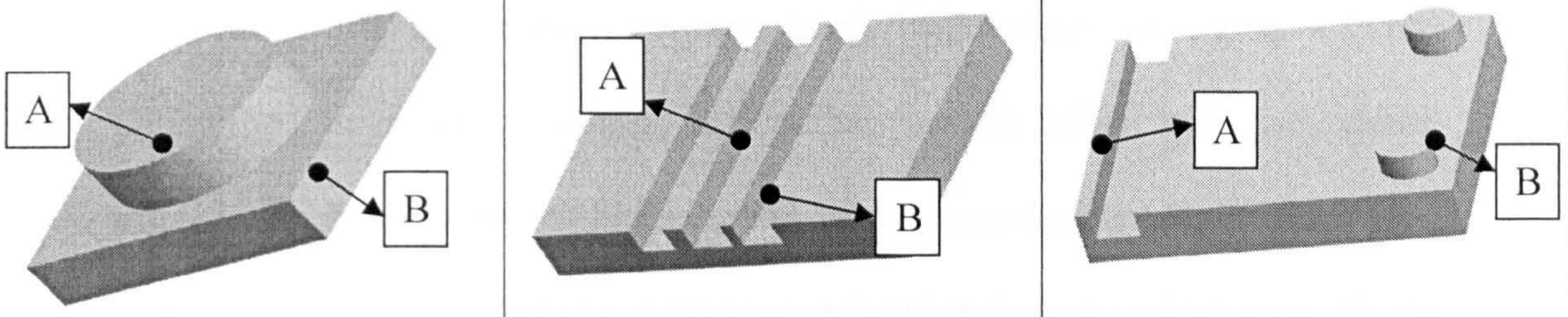

(a) Attached | (b) Adjacent | (c) Independent

Figure 4.3 Types of PFs interactions

i. Attached PFs

PFs that are joint or manufacture related when their relative distance (if any) might affect the machining operations and tool path/processing strategies. Figure 4.3 (a) shows an example of attached PF between a cylinder (PF_A) and a box (PF_B) where both share the same surface.

ii. Adjacent PFs

PFs that are not joint but positioned next to each other with the relative distance between them that is within the range of MD. Figure 4.3(b) shows the example of adjacent PF between a "negative" box (PF_A) and a "positive" box (PF_B).

iii. Independent PFs

PFs that are not joint or next to each other in which case the relative distance between them are out of the MD range value. Figure 4.3(c) shows the example of independent PFs: "positive" box (PF_A) and "positive" cylinder (PF_B).

The calculation of MI_{CFA} is subjected to the specifications shown in Table 4.2; this is done by multiplying MI_{SFA} with pre-defined coefficients (K_{RD}) that

depend on the comparison between RD and MD as well as the type of feature interactions. In this study, the suggested K_{RD} values in Table 4.2 are determined based on machining experiences on the MMT and also related previous literature/practices in producing micro-components [34, 60, 128, 134, 182]. Furthermore, the listed values are not fixed and can be adjust accordingly to fit other machining process or machine tool.

Table 4.2 Specification of K_{RD} for calculating CFA index (MI_{CFA})

Feature Classification	**Distance between PFs (mm)**	**MI_{CFA}=MI_{SFA} x K_{RD}**
Attached	RD < MD	MI_{SFA} x 0.65
	RD = MD	MI_{SFA} x 0.75
	RD > MD	MI_{SFA} x 0.90
	No RD	MI_{SFA} x 1.00
Adjacent	RD < MD	MI_{SFA} x 0.55
	RD = MD	MI_{SFA} x 0.70
	RD > MD	MI_{SFA} x 0.85
Independent	RD ≤ MD	MI_{SFA} x 1.00
	RD > MD	MI_{SFA} x 1.00

Note: RD – Relative Distance
MD – Minimum Acceptable Distance

Example of calculating MI_{CFA} is presented in the following section. Finally, the overall part manufacturability index, $MI_{OVERALL}$, is evaluated. This is done by taking into consideration MI_{CFA} and the machinability index of the workpiece material (MI_{MAT}) as referred in the literature [183-184]. Therefore, $MI_{OVERALL}$ of the proposed design is calculated as shown in the Equation 4.3 and the example of calculating $MI_{OVERALL}$ is also shown in the following topic.

$$MI_{OVERALL} = \frac{MI_{MAT} + \sum_{n=1}^{n+1} MI_{CFA}}{n}, \qquad \text{(Equation 4.3)}$$

Where n=number of PFs

4.5. Example of PFA implementation

A micro-component has been selected for the purpose to simulate the PFA mechanism discussed above which has been machined on the in-house developed MMT. Figure 4.4 shows a design of a generic micro-component that comprises singular and coupled features such as through/blind cavities (holes), slots and bosses. Figure 4.5 shows the detailed dimensions of the selected micro-component. This CAD model is analysed based on the PFA mechanism and its results are shown in Tables 4.3, 4.4, 4.5 and 4.6. The complete result of this simulation is listed in **Appendix 4.1**. Figure 4.4 also presents the identified PFs which are labelled with PF_1 to PF_8.

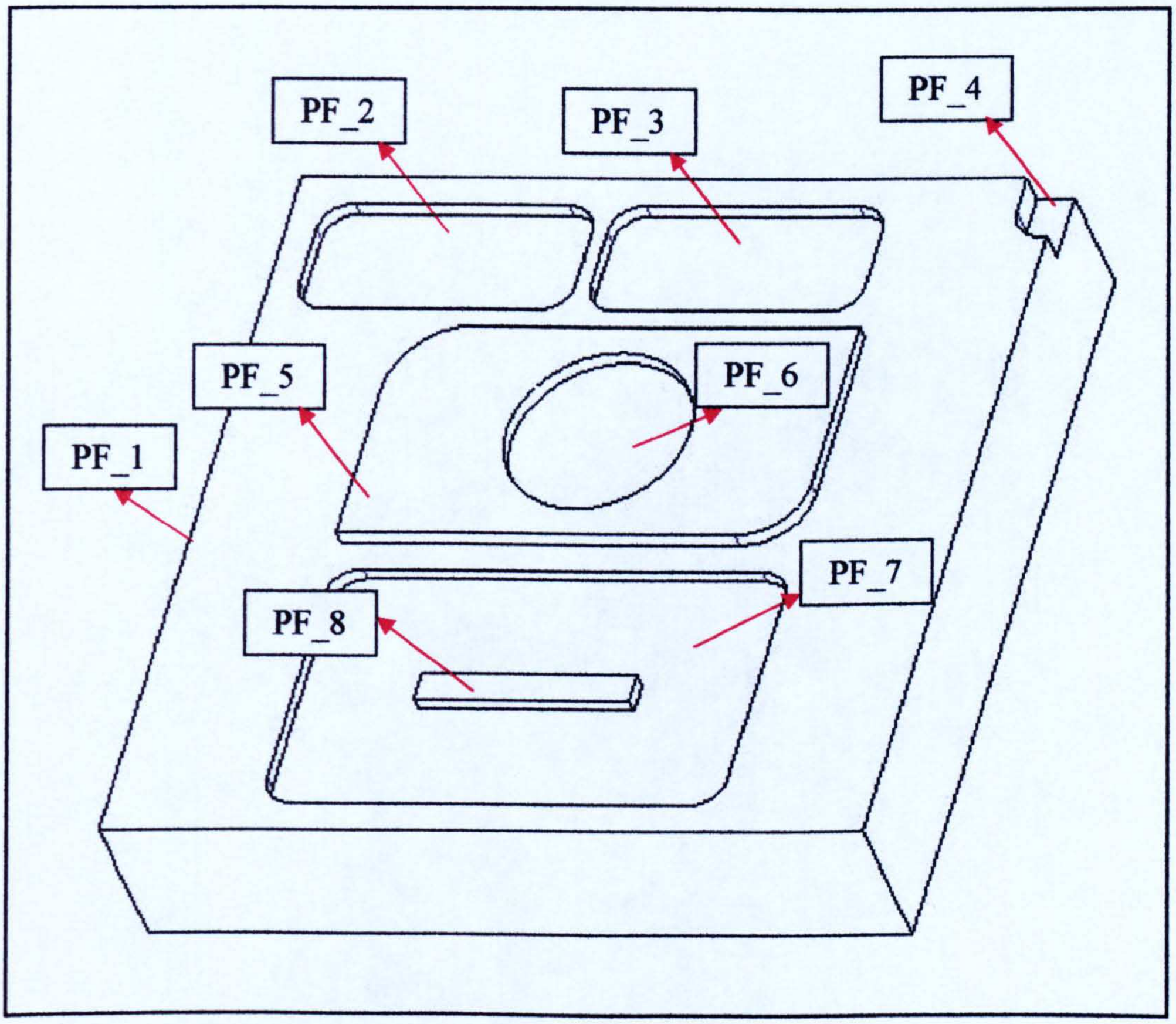

Figure 4.4 Proposed micro-component

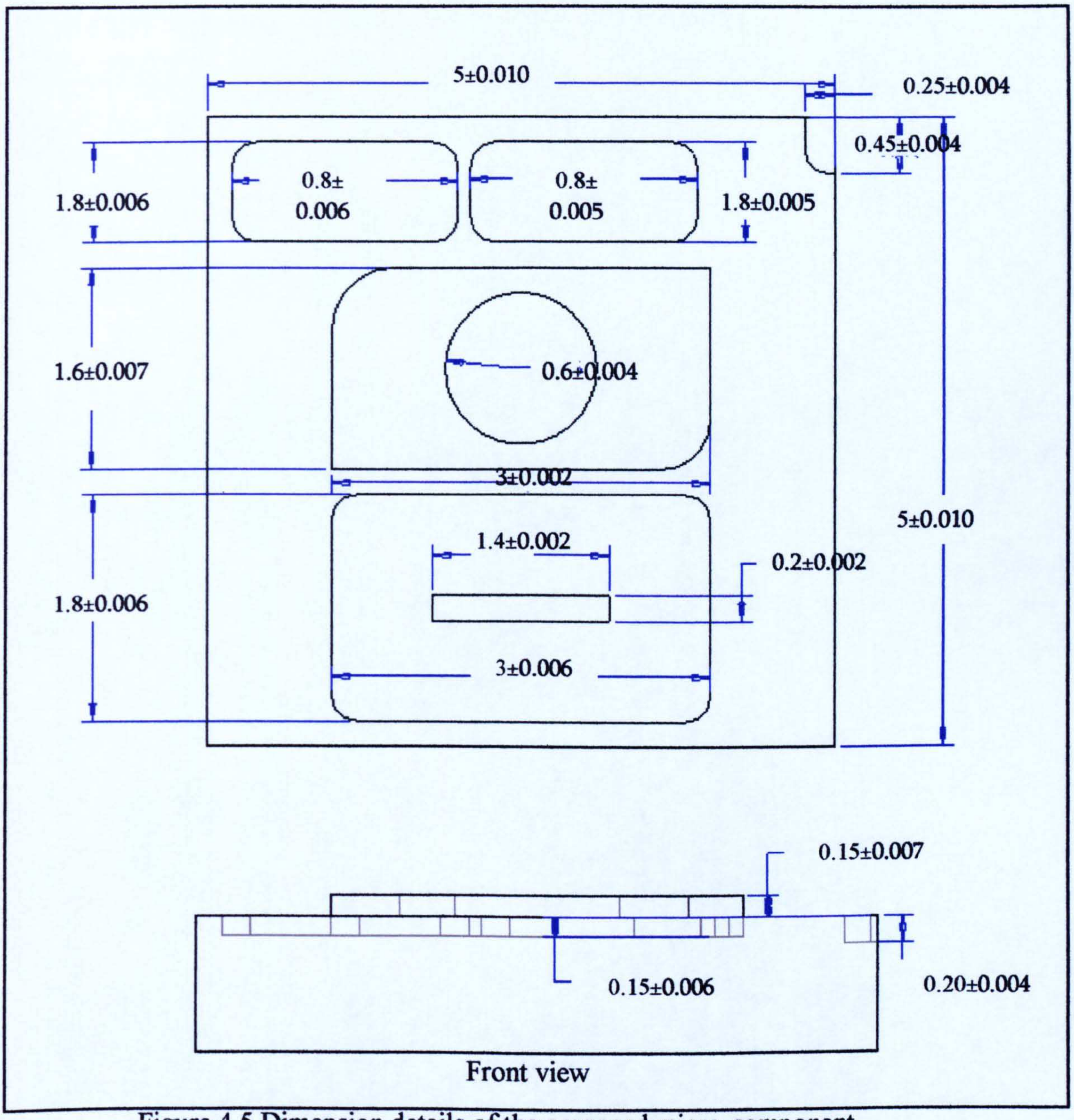

Figure 4.5 Dimension details of the proposed micro-component

Referring to the phases in the flowchart (Figure 4.1), the above proposed design is firstly analysed based on SFA and the summarised results are listed in Table 4.3. The complete overall analysis of this micro-component is listed in **Appendix 4.1**.

MI_{PF} for each PF is based on the combination of results from each element discussed in the SFA phases: type, orientation and shape of PFs as well as end-corner specifications. **Appendix 4.2** presented the complete list of MI_{PF} analysis based on all possible combinations of the discussed elements for all selected PFs used in this technique.

Table 4.3 Results from Single Feature Analysis

PF	Type of PF	PF Orientation	Type of Cavity	PF Shape	End-corner	MI_{PF}	Stiffness Ratio (R_{St})
PF_1	Box	Boss	N/A	Straight	Sharp	1.5	3.33
...	...	...	...	...	...	...	...
...	...	...	...	...	...	...	...
PF_6	Cylinder	Cavity	Blind	Straight	None	1.0	8.00
PF_7	Box	Cavity	Blind	Straight	Radiused	1.0	12.00
PF_8	Box	Boss	N/A	Straight	Sharp	1.0	1.33

Note: N/A – not applicable

The determination of MI_{PF} started with the exploration of results as illustrated in Table 4.3 (refer to the arrows). The MI_{PF} index range (refer to **Appendix 4.2**) was generated based on all results of SFA elements which are combined and analysed based on pre-defined IF-THEN clauses (this concept will be presented in detail in ***Chapter 7***). The index range was populated dependent on machining experiences, MMT specifications, geometrical effects, part quality measures, feature analysis, usual practice of machining specific features, material and process constraints and handbooks. Each PF has its set of SFA elements' combinations which determine the MI_{PF} values based on the pre-defined conditions. Figure 4.6 magnified the determination of the MI_{PF} for PF_5 and also the calculation of the stiffness ratio.

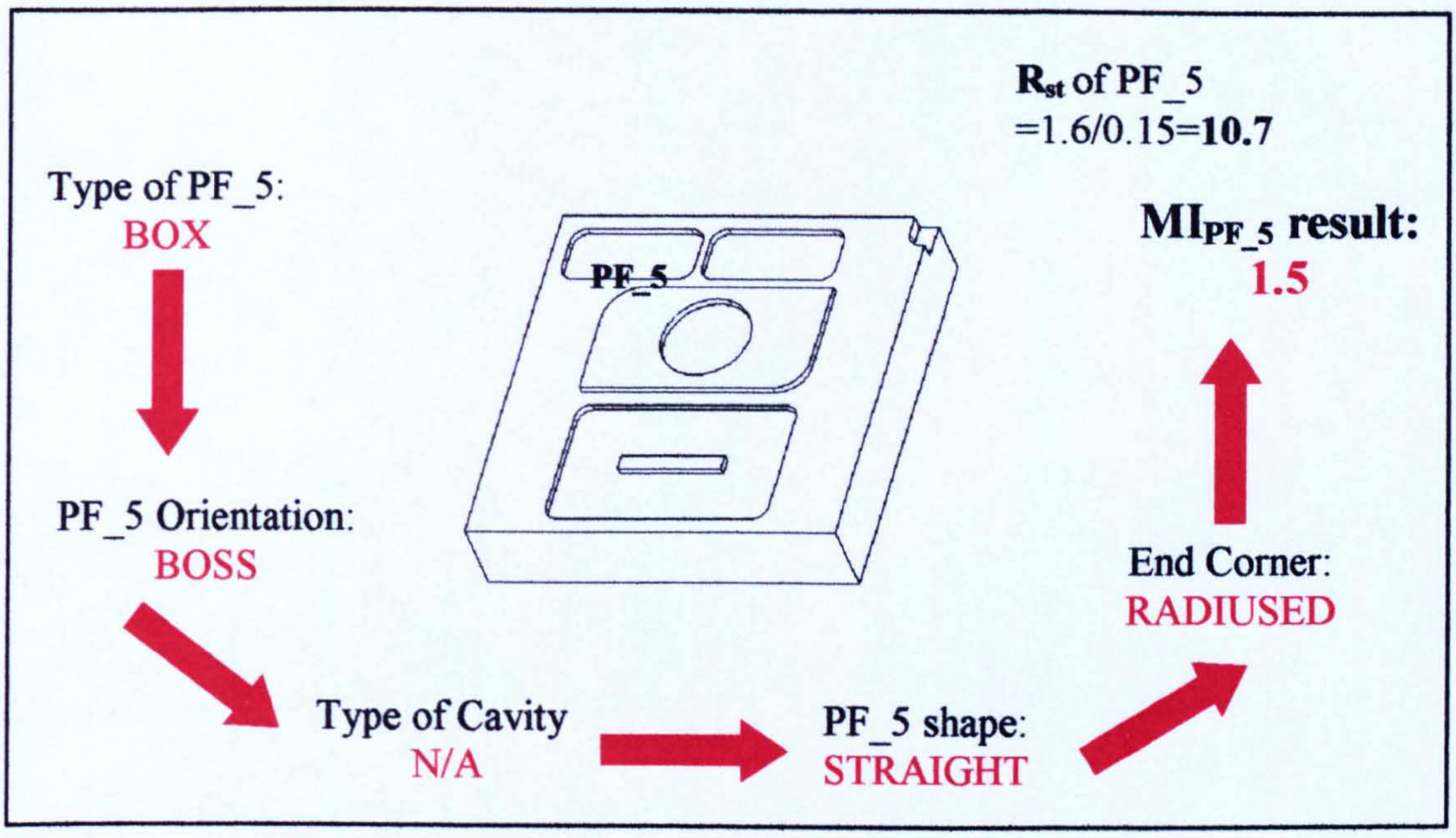

Figure 4.6 Example of MI_{PF} determinations (PF_5)

Table 4.4 presents some of the conditions when a box is considered as primitive feature while the detail conditions for other primitive features are listed in **Appendix 4.2**.

Table 4.4 An example of PF analysis: A box condition

Type of PF	PF orientation	Type of Cavity	PF Shape	End-corner	MI_{PF}
Box	Boss	N/A	Straight	Radiused	1.5
		N/A	Negative-tapered	Radiused	0.5
		N/A	Positive-tapered	Radiused	1.0
	Cavity	Through hole	Straight	Radiused	1.5
		Blind	Straight	Radiused	1.0
		Through hole	Negative-tapered	Radiused	0.5
		Blind	Negative-tapered	Radiused	0.5
		Through hole	Positive-tapered	Radiused	1.0
		Blind	Positive-tapered	Radiused	1.0

Note: N/A – not applicable

As example, for PF_1, the combination result is as follow: PF type - "Box"; PF orientation - "Boss"; PF shape - "Straight"; End-corner specifications -"Sharp". This combination leads to an index of 1.0 for MI_{PF} which means that PF_1 has

the level of *medium to manufacture*. As for PF_5, the outcome of MI_{PF} is 1.5 which defines that the level of manufacturing as *easy*. This resulted from the combination of each element in SFA which are: PF type - "Box"; PF orientation - "Boss"; PF cavity type- "N/A"; PF shape -"Straight" and End-corner specifications - "Radiused".

Beside MI_{PF}, the other manufacturability indices that are taken into consideration in determining the MI_{SFA} (Equation 4.1) are MI_{DIM}, MI_{TOL}, MI_{Ra} and MI_{UEM}. In determining the index range for these MIs (e.g. ***easier***, ***medium*** and ***harder*** to manufacture), the first step is to select the nominal value (N) for the particular MI that will be considered as ***medium to manufacture*** with MI = 1.0 (results of dividing N by N). Then, based on Equation 4.4, this selected N is used to calculate the MI value for any other selected value (denoted as S) such as tolerance, surface roughness, UEM effect.

$$MI_x = \frac{S}{N} \quad \text{(Equation 4.4)}$$

The calculated MI_x will then determine the level of manufacturability based on the agreed convention stated in Equation 4.2. By utilizing this approach, the generation of index range for MI_{DIM}, MI_{TOL}, MI_{Ra} and MI_{UEM} are described as the following:

1. Dimension Index (MI_{DIM})

MI_{DIM} rates the size of cutter used to generate the PFs and is based on the following considerations:

- The availability of the cutting tool diameter that can be employed on the MMT on which MicroMAS is implemented.

- The minimum radius of curvature of PFs' should be larger than the diameter of the cutter, this is to allow the generation of the smallest milled features.

Figure 4.7 (a) shows the variation interval of MI_{DIM} based on the cutting tool diameters. In this study, the value of MI_{DIM} is determined based on the cutting tool diameter with assumption that the minimum radius of curvature is based on the size of the cutter. The generation of MI_{DIM} is straightforward, for example, if the users select a tool with Ø=0.8μm, the MI_{DIM} will be 0.8.

2. Tolerance Index (MI_{TOL})

This index is adapted from the International Tolerance Grades (ITG) based on the tolerance grade/class of precision [185-186]. In addition, the results from the experiment of analysing the geometrical accuracy of the machined micro-slots and thin walls using the MMT are also considered in here. These experiments are part of various set-ups in populating relevant data for the MicroMAS. From the analysis and the obtained results that will be discussed in ***Chapter 6***, the MI_{TOL} index range was divided into series of different feature sizes and also adaptation from ITG with assumptions that micro-machining result in fine tolerance grades (e.g. 2 - 6). Figure 4.7(b) shows the generated range of MI_{TOL}.

The series of feature size intervals was generated according to the size of the proposed micro-slots and thin walls. Based on this, the nominal value(s) for MI_{TOL} for each interval is determined based on the calculated standard

deviation which is generated from the measurements on the thin walls and micro-slots. As an example, for feature size between 0.5 and 1.0 mm, the nominal value selected is 0.0046mm. Based on the discussed approach in determining the MIs (Equation 4.4), if the tolerance value selected by the user is 0.007mm, then the MI_{TOL} is equal to 1.52. This is derived from the calculations of 0.007 divided by 0.0046 and the level of manufacturability in this case is *Easy to manufacture*. However, the methodology of determining the index can accept other relevant tolerance values.

3. Surface Roughness Index (MI_{Ra})

This index rates the difficulty of obtaining a minimum workpiece surface roughness as specified by the user when employing micro-milling in the specified conditions (part geometry, workpiece material). Here, the determination of the MI_{Ra} range is based on the results of the surface quality analysis from the micro-machining experiments using the MMT (will be discussed in ***Chapter 6***). The MI_{Ra} index range was divided into categories that also have influence in the obtained surface quality, such as the type of the workpiece material and also the size of the cutter selected by the user. This range was generated based on the rating convention in Equation 4.2 and shown in Figure 4.7(c). The index range was generated based on the R_a measurements on the experiment of machining micro-slots and thin walls. The average values of R_a were considered as the nominal value for the particular index range according to the type of workpiece material and also cutter's size. As an example, for machining on 316L material using Ø=0.5mm cutter, the nominal value that has been selected is 0.033μm. Based on the discussed approach in

determining the MIs (Equation 4.4), if the R_a value selected by the user is 0.016μm, then the MI_{TOL} is equal to 0.48. This is derived from the calculations of 0.016 divided by 0.033 and the level of manufacturability in this case is *Hard to manufacture*.

4. Uncertainty effect in machining the primitive feature (MI_{UEM})

This index is implemented to partly reflect the real condition of the MMT which is the main domain of the MicroMAS implementation. It considers the uncertainty effects in machining the PF based on the Uncertainty Evaluation Model (UEM) analysis on the occurred errors stemming from the construction of the MMT which affects the accuracy of the forms/shapes of the machined micro-features (e.g. PF). From the analysis and the generated UEM results (that gives the expected uncertainties in form/shape machining), it can be concluded that the smaller the size or dimension of the PF, the bigger the impact of this uncertainty impact towards the machined forms/shapes.

The foundation of MI_{UEM} index range is similar to MI_{TOL} where it was divided into a series of different features size intervals according to the size of the proposed micro-slots and thin walls. The index range for the MI_{UEM} is generated based on the expanded uncertainty value obtained from the UEM analysis in machining the cylinder using the spiral milling tool path (will be discussed in ***Chapter 5***). The nominal value(s) for MI_{UEM} for each interval is determined based on the average value of the obtained expanded uncertainty. As an example, for feature sizes between 0.5 and 1.0 mm, the nominal value selected is 0.0055μm. Based on the discussed approach in determining the MIs

(Equation 4.4), if the uncertainty effect selected by the user for the particular PF is 0.0085 μm, then the MI_{UEM} is equal to 1.55. This is derived from the calculations of 0.0085 divided by 0.0055 and the level of manufacturability in this case is *Easy to manufacture*. Figure 4.7(d) presents the generated index that reflects the real condition of the MMT due to the error on constructing it.

a) Value of MI_{DIM}

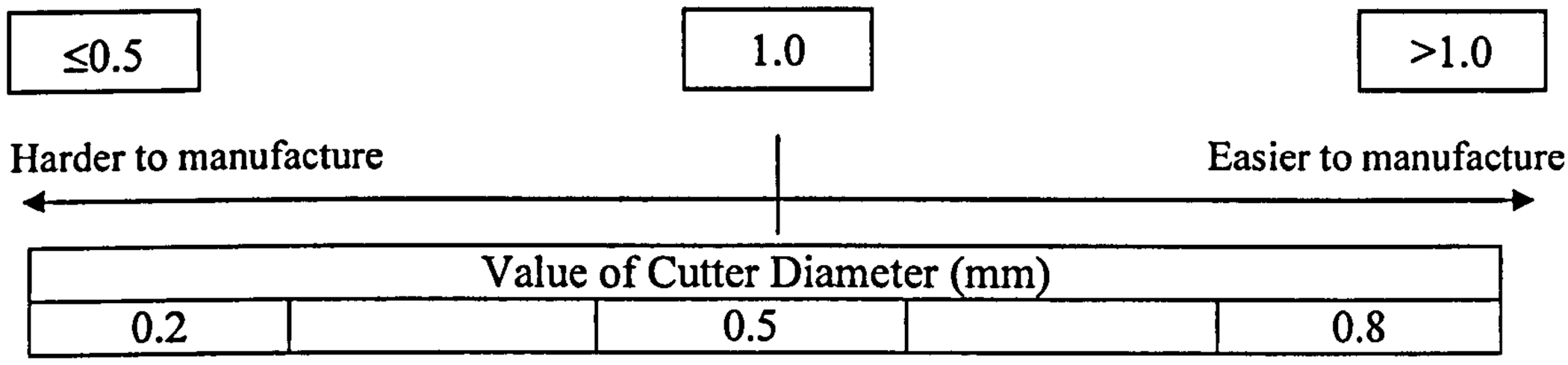

(b) Value of MI_{TOL}

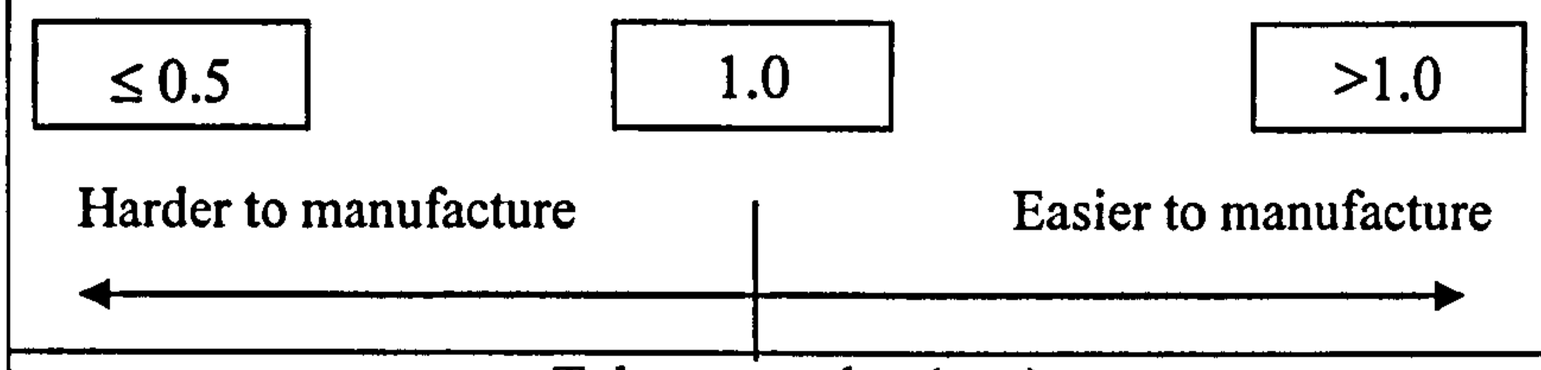

Feature size (mm)	Tolerance value (mm)		
0.0 – 0.5	0.0012	0.0030	0.0060
0.5 – 1.0	0.0020	0.0046	0.0070
1.0 – 1.5	0.0024	0.0049	0.0078
1.5 – 2.0	0.0030	0.0062	0.0086
> 2.0	0.0034	0.0078	0.0092
Tolerance class*	2	4	6

*Standard from International Tolerance Grade

(c)Value of MI_{Ra}

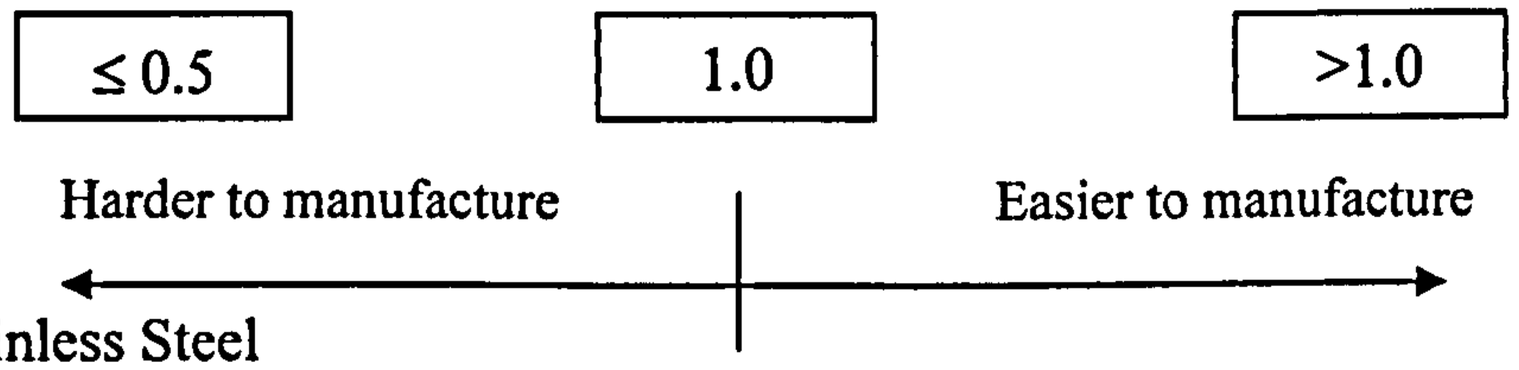

Material: 316-Stainless Steel

Cutter's size	R_a value (μm)		
0.5	0.016	0.033	0.043
0.6	0.008	0.018	0.028
0.8	0.009	0.019	0.029

Material: Titanium Alloyed

Cutter's size	R_a value (μm)		
0.5	0.019	0.039	0.049
0.6	0.024	0.049	0.059
0.8	0.020	0.040	0.050

Material: Steel (AISI 1040)

Cutter's size	R_a value (μm)		
0.5	0.022	0.045	0.055
0.6	0.016	0.032	0.042
0.8	0.018	0.039	0.049

d) Value of MI_{UEM}

Feature size (mm)	≤ 0.5	1.0	>1.0
	Harder to manufacture ←		→ Easier to manufacture
	Uncertainty effect (μm)		
0.0 – 0.5	0.0035	0.0065	0.0095
0.5 – 1.0	0.0025	0.0055	0.0085
1.0 – 1.5	0.0020	0.0045	0.0075
1.5 – 2.0	0.0015	0.0035	0.0065
> 2.0	0.0010	0.0030	0.0045

Figure 4.7 Index ratings for MI_{DIM}, MI_{TOL}, MI_{Ra} and MI_{UEM}

Based on the Figure 4.7, Table 4.5 shows the summarised MIs for each PF which are utilized to calculate MI_{SFA} (based on Equation 4.1) with the weight factor (K_i) for each MI is considered as 1.

Table 4.5 Summary of MI_{SFA} results for each PF

PF	MI_{PF}	MI_{TOL}	MI_{DIM}	MI_{Ra}	MI_{UEM}	MI_{SFA} (Eq.4.1)
PF_1	1.0	1.28	1.0	1.54	1.3	1.20
...	...	...	...	...	...	...
...	...	...	...	...	...	...
PF_6	1.0	0.76	1.0	1.03	0.9	0.94
PF_7	1.0	0.97	1.0	1.28	1.1	1.04
PF_8	1.0	0.67	1.0	0.52	0.8	0.80

The results of MI_{CFA} (Table 4.6) are based on the conditions stated in Table 4.2 and taking into consideration the relative distances between PFs shown in Figure 4.8. As an example, PF_2 is *adjacent* to PF_3 with the RD=0.10mm and based on the condition in Table 4.2, the initial value of MI_{SFA} for PF_2 (1.02) is recalculated to 0.87 (MI_{SFA} x 0.85), the pre-defined MD in this example is ≤ 0.08mm.

Table 4.6 MI_{CFA} results

1st PF	2nd PF	Interactions analysis	Distance (mm)	PF	MI_{CFA}
PF_1	PF_4	Attached	-	PF_1	1.20
PF_2	PF_3	Adjacent	0.10	PF_2	0.66
...	...	...	...	...	...
...	...	...	...	...	...
PF_5	PF_6	Attached	0.20	PF_6	0.85
PF_5	PF_7	Adjacent	0.20	PF_7	0.62
PF_7	PF_8	Attached	-	PF_8	0.60

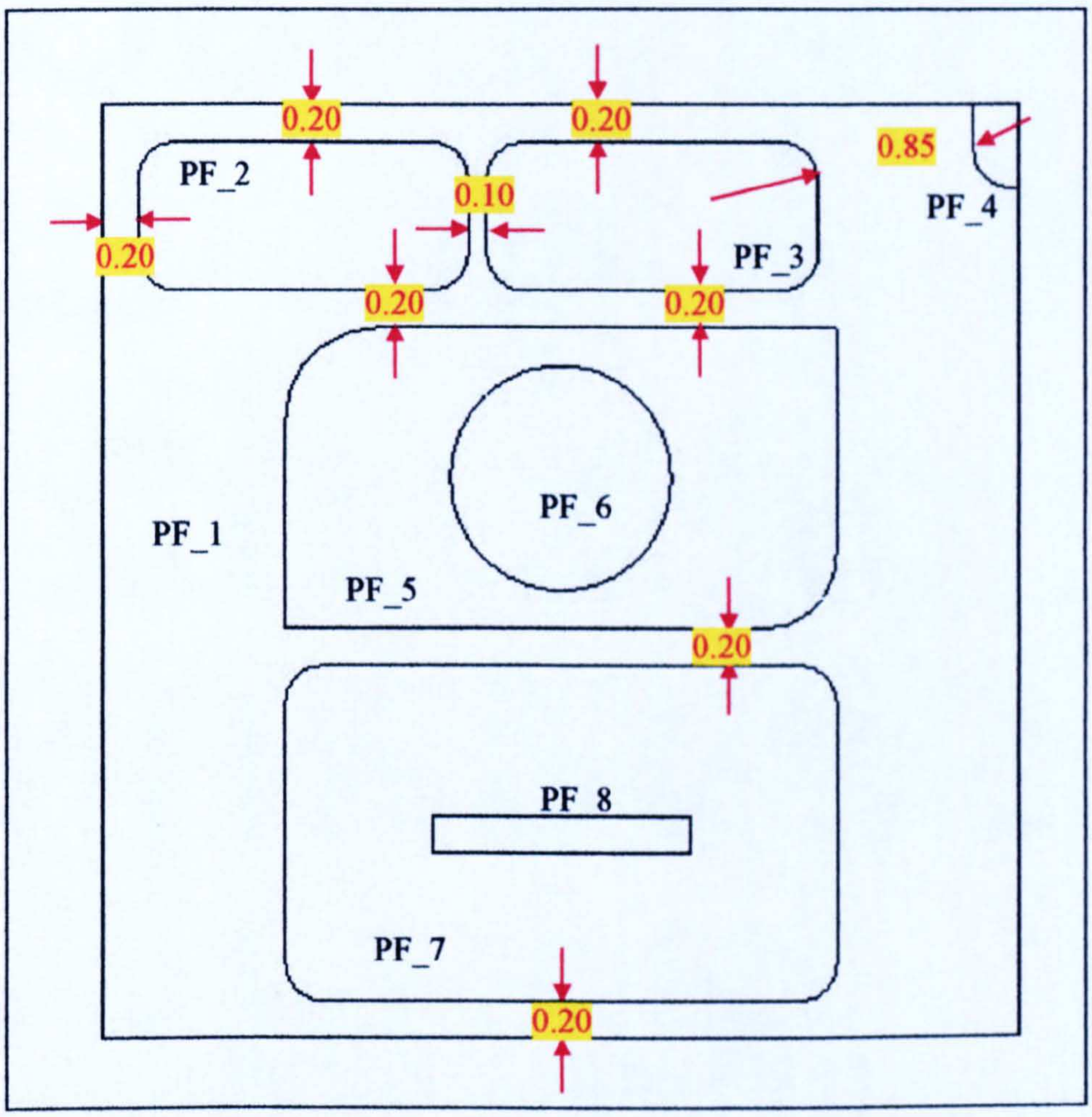

Figure 4.8 Examples of relative distances between PFs (mm)

Based on the PFA technique's algorithm, Table 4.7 shows the overall result of manufacturability assessment for the considered examples indicating a **medium** level of manufacturability since $MI_{OVERALL}$ is **0.84**. Referring to the $MI_{OVERALL}$ result, for medium and hard level of manufacturability,

recommendation or suggestion can be given in order to increase the MI and on the same time to make the part easier to manufacture. Generally, the final generated outputs are in the form of feedbacks to user in terms of relevant redesign suggestions such as reviewing the K_i for each MI in SFA phase, redefine the quality measures aspect (e.g. surface roughness, tolerance and uncertainty effect) and selecting materials with higher MI that represent easier to machine.

Table 4.7 $MI_{OVERALL}$ results

PF MI_{CFA}	PF_1	PF_2	PF_3	PF_4	PF_5	PF_6	PF_7	PF_8
	1.20	...	...	...	...	0.85	0.62	0.60
Material :	Titanium Alloyed				**MI_{MAT} :**		1.05	

$$MI_{OVERALL} = \frac{MI_{MAT} + \sum MI_{CFA}}{8} = \frac{1.05 + 6.72}{8} = 0.84$$

Generally, the simulation of the PFA technique above is based on micro-parts to be machined in the MMT, there are possibilities for the coefficients and other rules can be adjusted to be fit to analyse other machining processes or machine tool.

4.6. Implementation of PFA into MicroMAS

MAS has been developed using different combination of approaches, technologies, software and tools. In this study, MicroMAS which is a manufacturability analysis system dedicated for micro-milling process is developed based on a three-step unidirectional flowchart methodology that includes data **input mechanisms, inference engines for manufacturability analysis** and **outputs reporting.**

The first is the development of the **input mechanism** where all the required design data and manufacturing information are fed into the system. The next step is to analyse the gathered input for performing part **manufacturability assessment**, here data are analysed according to the manufacturability constraints and rules to determine the difficulty level for manufacturing of the proposed design. The final component in MASs' methodology consists in **generating the outputs** to reflect the evaluation of manufacturability aspects of the proposed designs while interactively assisting the operators in (re)considering manufacturing aspects at the design stage.

In developing MicroMAS, the PFA technique is introduced in this methodology for the purpose of gathering essential data from CAD models and also analysing its manufacturability aspects. The PFA technique is suggested to be integrated in between of the first (input mechanism) and second (manufacturability analysis) steps as highlighted in Figure 4.9.

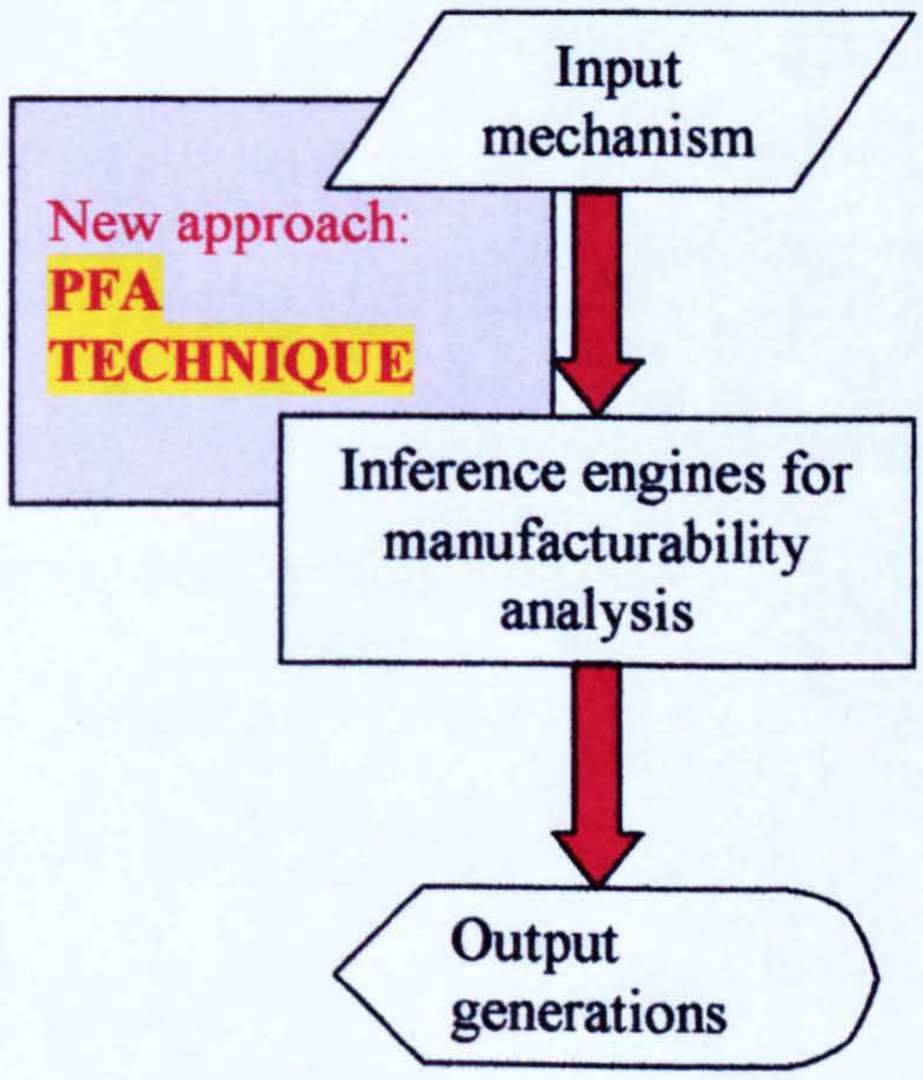

Figure 4.9 Flowchart of MicroMAS developments

The stages of PFA for implementation in MicroMAS are transformed to four main sequentially stages: (i) Initial Assessment (IA), (ii) Single Feature Analysis (SFA), (iii) Coupled Feature Analysis (CFA), (iv) Output generated. The details of the PFA technique implementation in MicroMAS will be discussed thoroughly in ***Chapter 7***.

4.7. Summary

This chapter described the PFA technique and simulated its implementation on a CAD model. The backbone of the PFA technique is the Primitive Feature (PF) concept which is combined with the positive (bosses) and negative (pockets) scheme to define the components and produced meaningful interpretations. PFA technique consists of two crucial phases which are SFA and CFA in defining the micro-parts and analysing its manufacturability.

SFA was used for gathering essential data from the CAD model that are further "enriched" with part quality measures which is efficient in providing "necessary and sufficient" input data to MAS. Furthermore, SFA provided an efficient way (MI_{SFA}) to evaluate the manufacturability of each PF of the analysed part. Since the analysed part has many PFs, the PFA technique provides a systematic way to interact them and to assess the manufacturability (MI_{CFA}) of coupled features. This enables the manufacturability analysis of the part as a result of multi-feature interactions and not as an outcome of a single entity (rigid) assessment commonly used in the most reported work in previously developed MAS.

A new sequential Manufacturability Indexes scheme is introduced to indicate the level of manufacturability for each PF and also for the overall micro-part. Based on the generated indexes convention, the level of manufacturability for each PF (Equation 4.1) is determined based on several aspects such as PF (e.g. orientation, shape, type), dimensional tolerance, surface roughness, UEM analysis impact, tools diameters and selected workpiece material. $MI_{OVERALL}$ which indicates the overall manufacturability (Equation 4.3) of the micro-component is calculated based on the aspects analysed above and also the interactions occurred between PFs. These indexes are presented by a rating convention that is divided into three levels (as described in Equation 4.2): **Harder** to manufacture, **Medium** to manufacture and **Easier** to manufacture.

In this study, the PFA technique is being executed in the domain of micro-parts through MicroMAS and its implementation will be simulated in ***Chapter 7*** where the development phases are expanded to four stages where each of them provides progression or outputs that can reflects the manufacturability assessment of the proposed CAD model.

The execution of the PFA technique in MicroMAS is an opportunity to take into consideration the manufacturing aspects and analyse them at the early stage of product development life cycles in the micro-milling domain run in a custom-made 4-axis Miniature Machine Tool.

CHAPTER 5: UNCERTAINTY EVALUATION MODEL FOR A MINIATURE MACHINE TOOL FOR MICRO-MACHINING

5.1. Introduction

This chapter presents the development of Uncertainty Evaluation Model (UEM) in assessing the errors stemming from the construction of a Miniature Machine Tool (MMT) that might affect the geometrical accuracy of the machined micro-parts. Although the machining process (micro-milling) is, in general terms, similar to conventional milling, the great reduction in dimensions gives a big impact in its cutting conditions (e.g. minimum chip thickness, tool stiffness, ratio between depth of cut and material grain size). However, there is another aspect to consider when utilising an in-house developed machining system. In this line, the error budgeting through UEM is highly important for the MMT as there is a critical need to understand the origin of the errors (either from the machine itself or from the machining process) that affect the quality of the machined part. Furthermore, through this analysis, it provides a method or approach to understand the sources of errors that affect the produced quality of the final machined part from any similar custom-made MMT.

This chapter begins with the explanation of the objectives and the approach taken in developing the uncertainty analysis model for the MMT. Then the generated uncertainty models from the identified sources of errors in constructing the MMT that influence the geometrical accuracy of the machined micro-parts were discussed. Furthermore, the analysis and results of the

generated uncertainty model that have been analysed in a Guide to the expression of uncertainty in Measurements (GUM) software are also provided. Finally, the results from the uncertainty analysis were discussed and its significant contribution to the developed MicroMAS is presented.

5.2. Objectives and approach

5.2.1. Objectives

Uncertainty Evaluation Model (UEM) has been developed to understand the influence of the errors in constructing the MMT on the geometrical accuracy of the machined micro-parts. In any micro-machining domain, there are many aspects (e.g. machining parameters, machine tool characteristics, materials, tooling) to be taken into consideration, which might not be important in the macro-machining area. Therefore, it is important to analyse any errors related to the construction of the MMT; these errors might not be of high importance in the case of using a conventional macro-machine tool but in this case it can significantly affect the quality of the machined micro-parts.

The main objective of the UEM development was to analyse the errors stemming from the construction of the MMT and to understand how they are transferred into kinematic (tool path generation) errors. However, the errors generated during machining (e.g. tool vibration/wear) are not considered into this model.

5.2.2. Approach

The approach taken to develop UEM is divided into three main phases: (i) model development, (ii) model analysis, (iii) simulation and validation (**Figure 3.18**). These phases have been discussed in ***Chapter 3***.

5.3. UEM development

5.3.1. Sources of errors

Figure 5.1 presents a summary of the sources of errors in the micro-part generation with an emphasis of the uncertainties stemming from the MMT construction which is the focus of this analysis. However, this summary of errors should be considered as an example originating from the analysis of a particular setup, i.e. MMT, that can be even further translated into recommendations for machine tool verifications. Anyway, the highlighted source of errors (Uncertainties of (micro) machining process) in Figure 5.1 was not being considered in this study.

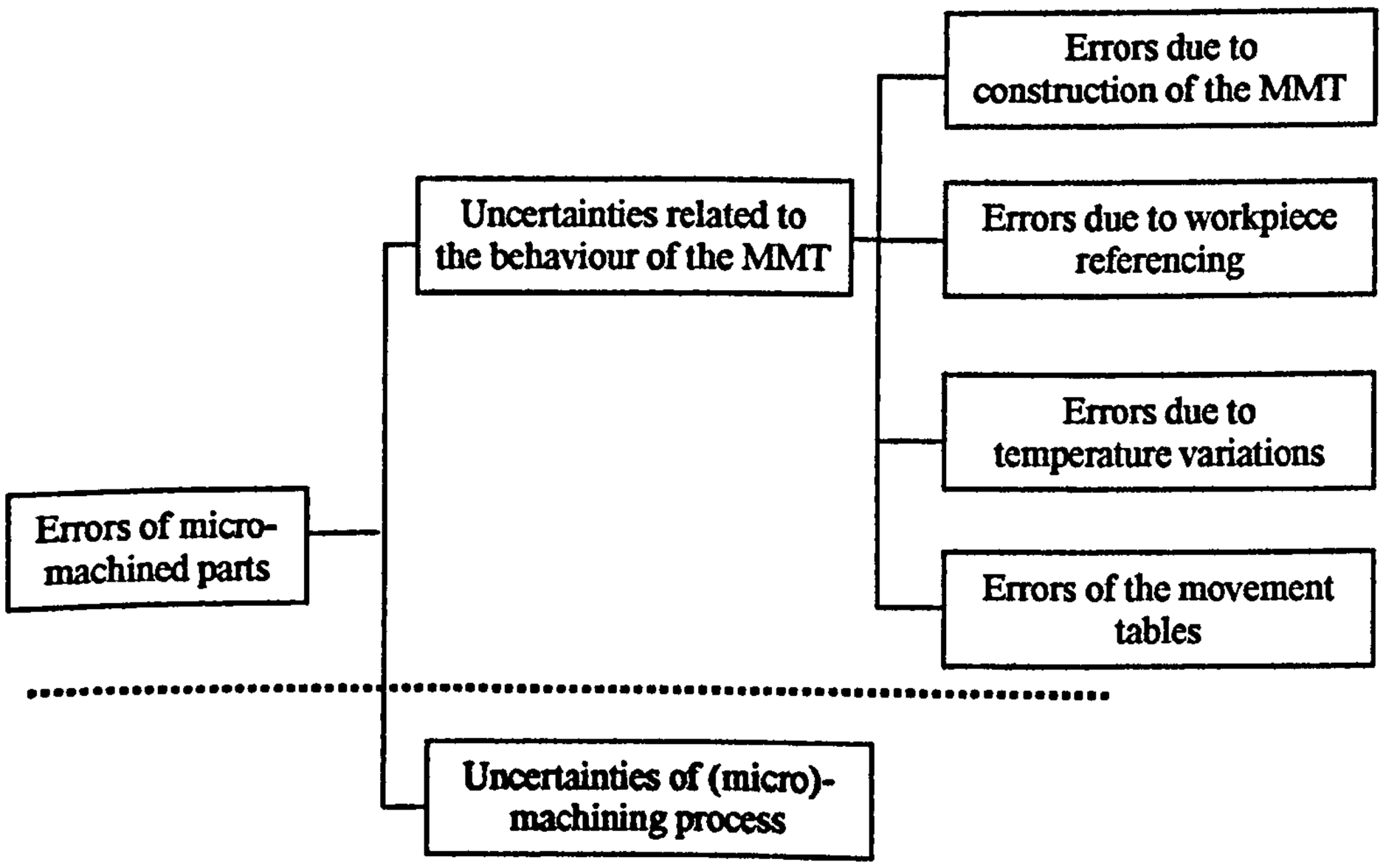

Figure 5.1 Summary of the sources of uncertainties that affect the part accuracy machined on the MMT

Based on the Figure 5.1 and also the discussion that will be made in Chapter 6 on the errors on constructing the MMT, the identified sources of errors are listed below and will be discussed thoroughly throughout this chapter:

- Errors due to construction of the MMT
    - Geometrical deviations (e.g. flatness in X/Y/Z planes) of the gantry frame as well as additional errors when assembling it on the granite base plate.
    - Combined positioning errors of the z axis (tool/spindle axis) from the reference place due to the possible errors in assembling the z-motion table and the spindle (through its holder) on the gantry frame.
    - Deviations on the top of the working table from the reference place due to the stack of the X, Y and U motion tables that were mounted on the granite base plate.
- Errors related to the evaluation of workpiece reference point
- Errors related to the temperature variations
- Errors originating from the positioning inaccuracies of each table

5.3.2. Model development and analysis

In developing the uncertainty model, two important aspects are taken into consideration: (i) **static evaluation** such as standard guidelines on uncertainty evaluation on machine tool (ISO 230 series - Test code for machine tool series) and (ii) **dynamic evaluation** such as tool path generation (e.g. linear/ circular/ spiral milling movement) and CMM assessment.

Moreover, in order to understand how these errors are transferred into flaws in tool path generations, the model is generated based on the x, y and z coordinates. The tool movement is represented by these coordinates so that the generated errors can be illustrated through them. For the model development, Equation 5.1 simulated the actual position (X, Y, Z) of the cutter that is calculated based on the theoretical position (x, y, z) that are affected by the errors listed above.

$$X = x + \Delta x_1 + \Delta x_2 + \Delta x_3 + \Delta x_4$$
$$Y = y + \Delta y_1 + \Delta y_2 + \Delta y_3 + \Delta y_4 \qquad \text{Equation 5.1; with}$$
$$Z = z + \Delta z_1 + \Delta z_2 + \Delta z_3 + \Delta z_4$$

X, Y , Z	Actual position of the cutter
x, y , z	Theoretical position of the cutter
$\Delta x_1, \Delta y_1, \Delta z_1$	Errors due to construction of the MMT
$\Delta x_2, \Delta y_2, \Delta z_2$	Errors related to workpiece reference point
$\Delta x_3, \Delta y_3, \Delta z_3$	Errors related to temperature variations
$\Delta x_4, \Delta y_4, \Delta z_4$	Errors originating from table inaccuracies

5.3.2.1 Errors due to construction of the MMT (Δx_1, Δy_1, Δz_1)

As stated before, the error sources originate from the MMT constructions such as geometrical deviations of the gantry frame, positioning errors of the Z axis from the reference plane and also deviations at the top of working table from the reference place.

Based on the CMM evaluations that will be discussed in ***Chapter 6***, Figure 5.2(a) gives an exaggerated indication of the positioning errors of a dummy tool axis relative to XYZ space. It can be noted that the tool axis is not perpendicular to the XY plane, and it is tilted in space from both XZ and YZ planes as well as from theoretical Z axis; however, the average deviation angles from the perfect (orthogonal) position are very small in values. Figure

5.2(b) presents a schematic representation of the magnified errors of the spindle axis in 3D space where $\|A'E\|$ is the length of the spindle system (from its holding point on the Z-motion table) with its axis making angles α ($\angle EA'G$) and γ ($\angle EA'H$) with the XZ plane and Z axis respectively; the angle with YZ plane is dependent of the represented information. From the figure, it can be noted that not only the tool axis is spatially tilted but also does not intersect the Z axis, meaning that it is shifted with a distance of Δy_0 from the XZ plane.

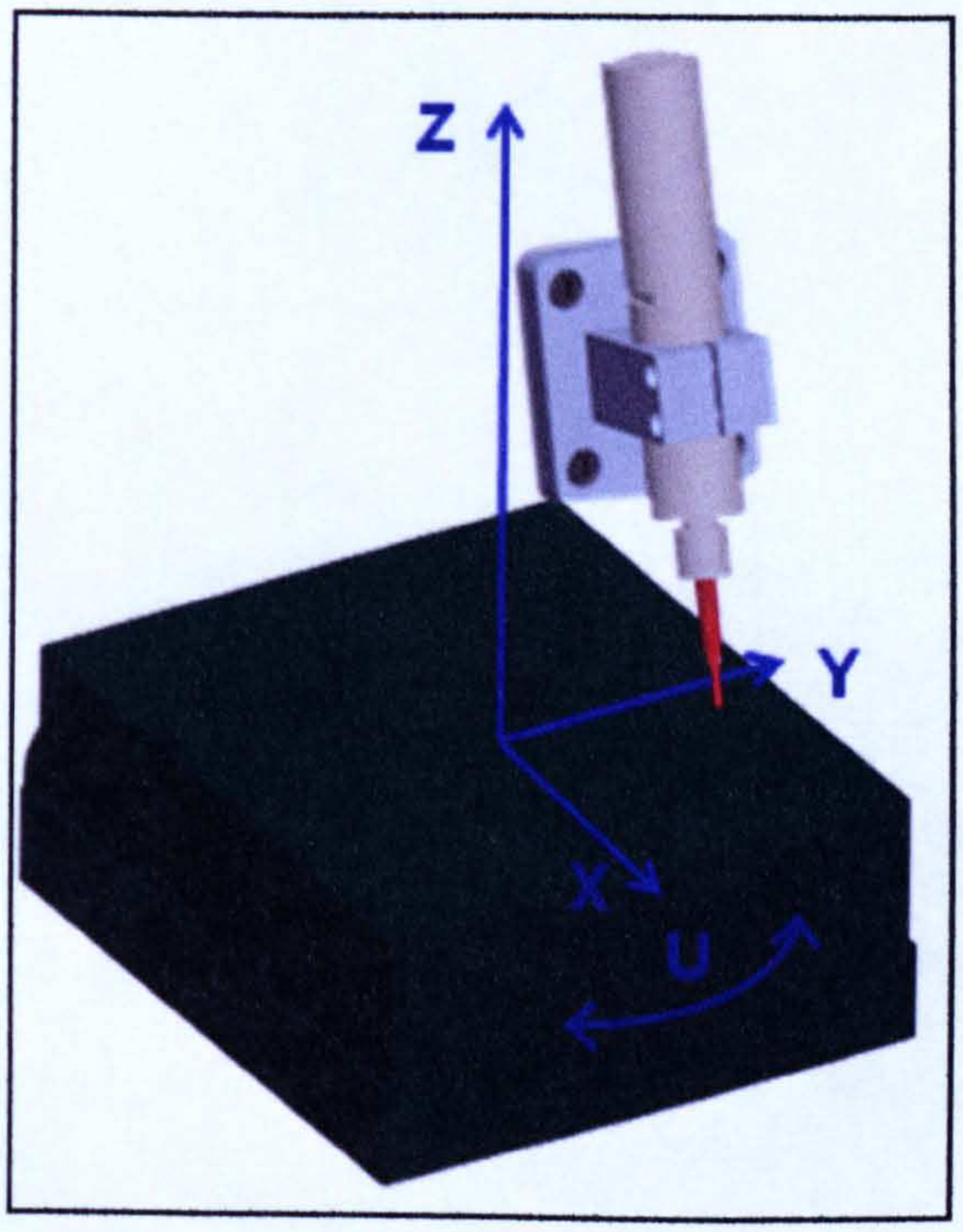

Figure 5.2 (a) An exaggerated defective orientation of the spindle in 3D space

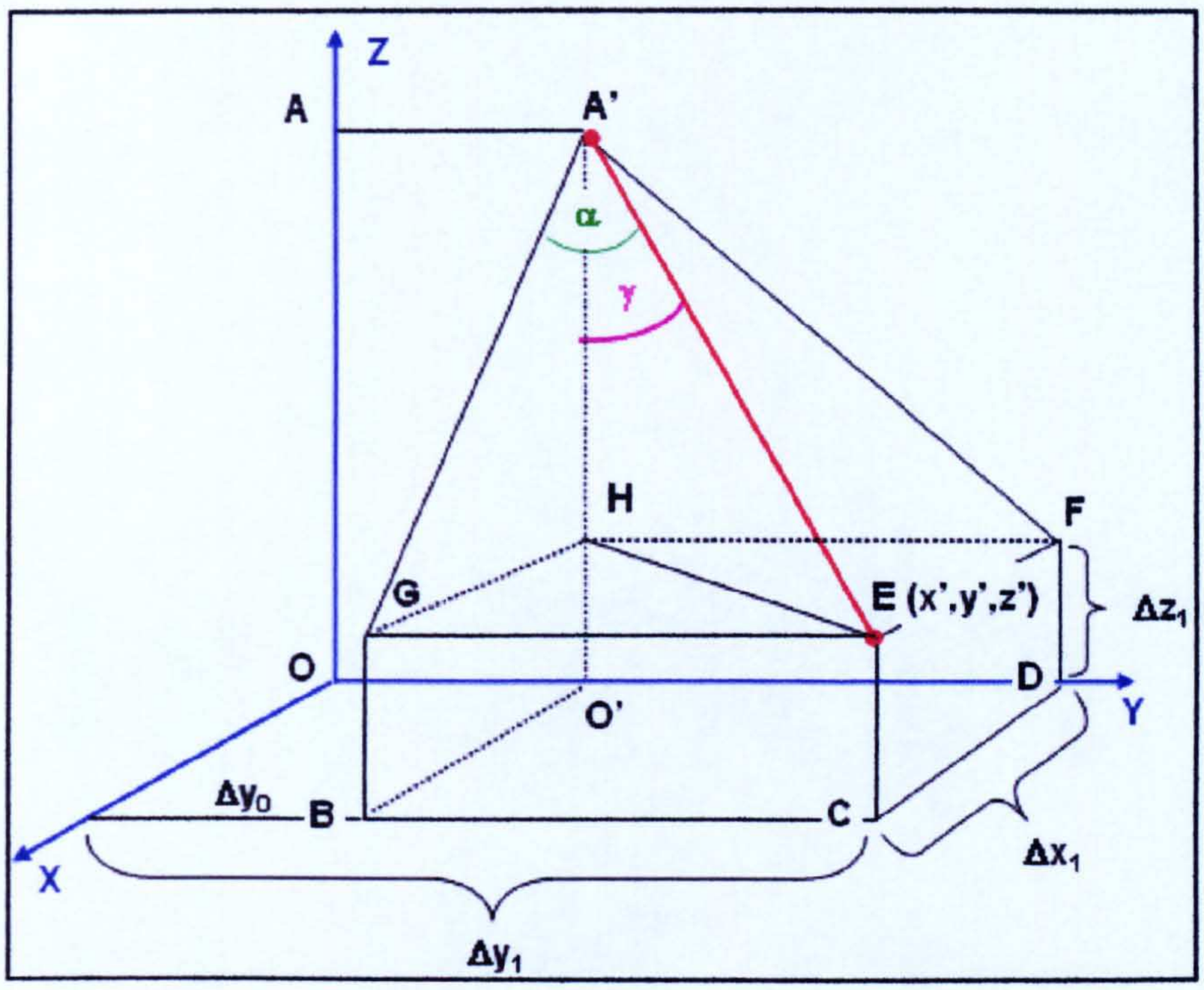

(b)

Figure 5.2 (b) Geometrical representations for calculating positioning errors

Based on the information given in Figure 5.2(b), it can be said that the spatial tilt of the spindle results in overall positioning errors (Δx_1, Δy_1, Δz_1) of the tip of the cutter relative to the upper surface of the XY-motion platform (i.e. where machining takes place). This states that the spindle system should ideally be $\|AO\|$, with O as tool tip; instead, it is taken as $\|A'E\|$ (with $\|AO\| \equiv \|A'O'\| \equiv \|A'E\|$).

As the length of the spindle-tool system, $\|A'E\| = L$ is a known distance, the angular (α,γ) and linear (Δy_0) deviations are also known as average values obtained by repeated CMM evaluations (will be presented in ***Chapter 6***). Therefore, the positioning errors of the tip of the cutter relative to the upper surface of the XY-motion platform can be calculated as shown in Table 5.1, while Equation 5.2 summarizes the positioning errors occurred for each axis.

Table 5.1 Calculation of positioning errors for each axis

Z axis	X axis	Y axis
$\Delta z_1 = O'H = O'A' - A'H$; $A'H = A'E\cos\gamma$ $\Delta z_1 = A'E - A'E\cos\gamma$ $= L - L\cos\gamma$ $\Delta z_1 = L(1-\cos\gamma)$	$\Delta x_1 = EF$ or GH ; where $GH = \sqrt{GA'^2 - A'H^2}$ $GA' = A'E\cos\alpha$; $A'H = A'E\cos\gamma$ $GH = \sqrt{(A'E\cos\alpha)^2 - (A'E\cos\gamma)^2}$ $\Delta x_1 = A'E\sqrt{\cos^2\alpha - \cos^2\gamma}$	$\Delta y_1 = \Delta y_0 + HF$ or GE $GE = A'E\sin\alpha$ $\Delta y_1 = \Delta y_0 + L\sin\alpha$

$$\Delta x_1 = L\sqrt{\cos^2\alpha - \cos^2\gamma}$$
$$\Delta y_1 = \Delta y_0 + L\sin\alpha \qquad \text{Equation 5.2}$$
$$\Delta z_1 = L(1-\cos\gamma)$$

Based on extensive measurements, the averaged values of the quantities specified in Equation 5.2 have been obtained as follows:

- $\alpha = 0.0286°$
- $\gamma = 0.0653°$
- $\Delta y_0 = 7.0\times10^{-4}$mm, and thus;
- $\Delta x_1 = 5.12\times10^{-3}$mm; $\Delta y_1 = 3.19\times10^{-3}$mm; $\Delta z_1 = 3.15\times10^{-6}$mm.

From the aspect of dynamic evaluation, it is interesting to point out that with a 3D tool path, the errors Δx_1, Δy_1, Δz_1 combine themselves into a generation error of the machined components; of course, the generation error depends on the parametric equations of the 3D tool path. Taking for example the generation of a cylinder (radius, r=1.5mm) generated through spiral milling (Figure 5.3), the tool path can be parametrically described by Equation 5.3:

$$x = r\cos\omega t = r\cos(\frac{V_f t}{r}) = r\cos(\frac{f_z.z.n}{r}t)$$

$$y = r\sin\omega t = r\sin(\frac{V_f t}{r}) = r\sin(\frac{f_z.z.n}{r}t) \qquad \text{Equation 5.3;}$$

$$z = V_z t$$

With:

- V_z – feed speed of the tool along z axis
- V_f – tangential speed of the cutter in xy plane to follow a circle of radius r
- ω– angular speed of the cutter
- f_z – feed per tooth
- z – number of teeth of the milling cutter
- n – spindle speed
- t – cutting time

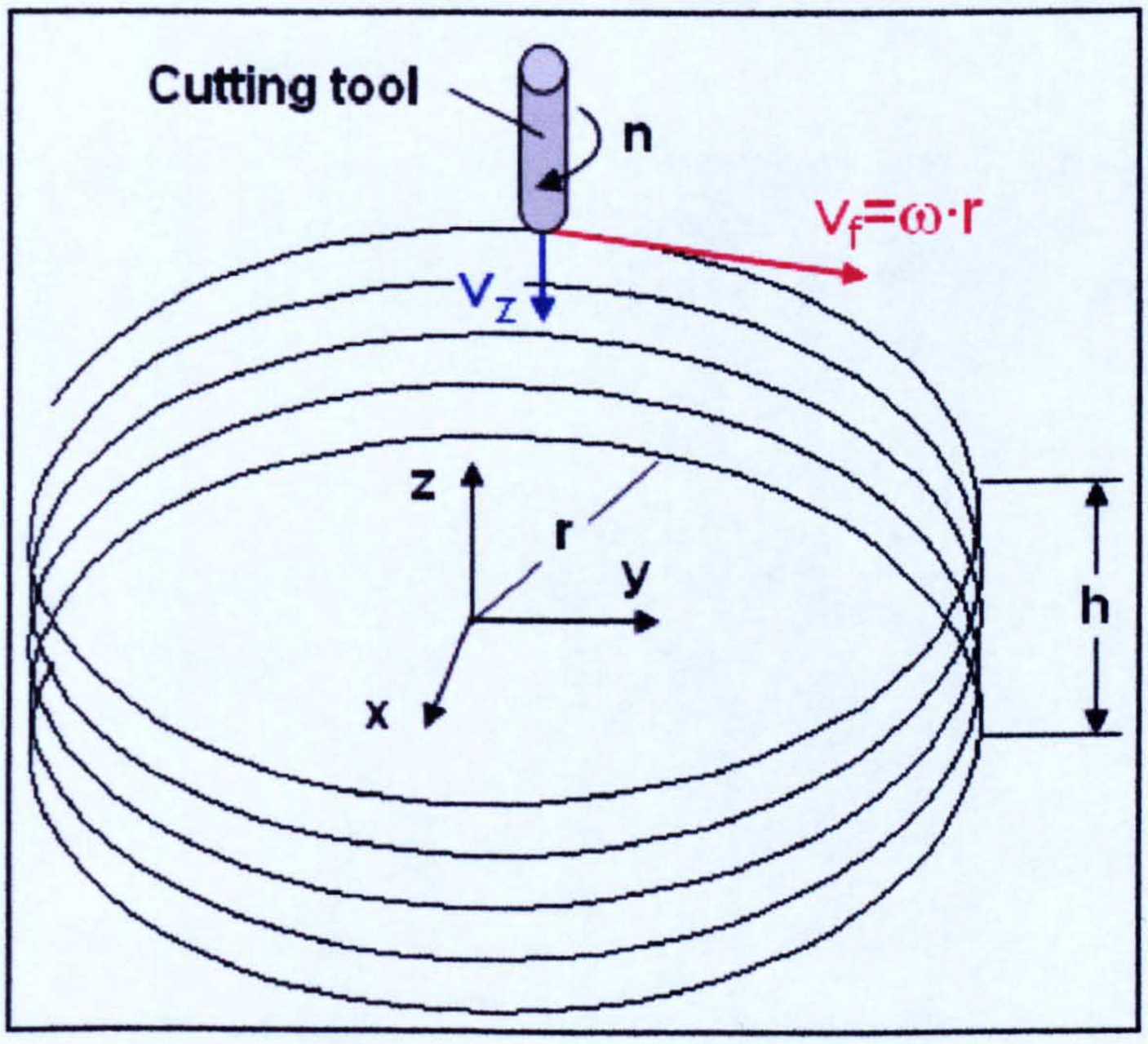

Figure 5.3 Spiral path of the milling cutter

It should be noted that x, y, z represent the theoretical positions of the tool reference point along its path which is necessary for spiral milling the required cylinder. However, these successive positions (at different cutting times, t) are affected by the generation error originating from Δx_1, Δy_1, Δz_1 errors due to the spatial tilt of the cutter as described in Equation 5.2. Therefore, when the cutter follows the tool path characterised by Equation 5.3, the errors presented in Equation 5.2 lead to geometrical deviations from the theoretical cylinder of radius r and height h (which is equal to distance in z).

However, apart from the generation error, the MMT system can also be affected by other sources of uncertainties as discussed below.

5.3.2.2. Errors related to the evaluation of workpiece reference point (Δx_2, Δy_2, Δz_2)

Apart from the tool path generation errors, the MMT system can also be affected by other source of uncertainties such as errors stemming from the workpiece reference point. These are mainly related to the resolution of the sensing/probing system that detects the moment of contact between the workpiece and the tool. In this study, an innovative probing system based on electrical contact between the tool tip and the workpiece has been employed that led to satisfactory part referencing (will be discussed in ***Chapter 6***). Based on this, and for the purpose of UEM analysis, twelve repeated measurements were taken for the uncertainty observation of this type of error. Table 5.2 listed the measurements made on referencing a part for each axis (X, Y and Z).

Table 5.2 Measurements for each axis (in mm)

No	X	Y	Z
1	0.00010	0.00009	0.00009
2	0.00009	0.00010	0.00005
3	0.00008	0.00012	0.00007
4	0.00007	0.00011	0.00010
5	0.00011	0.00008	0.00008
6	0.00012	0.00007	0.00009
7	0.00010	0.00006	0.00006
8	0.00008	0.00009	0.00012
9	0.00011	0.00008	0.00010
10	0.00007	0.00013	0.00007
11	0.00006	0.00009	0.00008
12	0.00008	0.00007	0.00011

5.3.2.3 Errors related to the temperature variations (Δx_3, Δy_3, Δz_3)

These errors are mainly related to the uncertainties introduced by the expansion/contraction of the motion tables with the varying temperature while those that might originate from the MMT frame/table have been neglected (as they are made of low thermal expansion materials). Such errors have been evaluated for a temperature variation interval of 5°C. The assumption made here for the uncertainty due to temperature effect is based on the proposed value in ISO 230-3:2001 – Test code for machine tools – Part 3: Determination of thermal effects during CMM measurement [187]. It is suggested that based on a typical room temperature, it resulted with the uncertainty value of 2.0×10^{-3} mm.

5.3.2.4 Errors originating from the positioning inaccuracies of each table (Δx_4, Δy_4, Δz_4)

Such errors are indications of the positioning repeatabilities of the motion tables given in the manufacturer's data sheet. Following the specification of linear and swivel stages provided by Aerotech, the standard uncertainty value suggested for the positioning accuracy of the worktable was 3.0×10^{-4} mm.

Thus, in the case of spiral milling a cylinder (Figure 5.4), the actual position (X, Y, Z) of the cutter is based on the theoretical position (x,y,z) that is affected by errors as described through Equation 5.4, where the quantities from Equations 5.2 and 5.3 have been substituted.

$$X = x + \Delta x_1 + \Delta x_2 + \Delta x_3 + \Delta x_4 = r\cos(\frac{f_z.z.n}{r}t) + L\sqrt{\cos^2\alpha - \cos^2\gamma} + \Delta x_2 + \Delta x_3 + \Delta x_4$$

$$Y = y + \Delta y_1 + \Delta y_2 + \Delta y_3 + \Delta y_4 = r\sin(\frac{f_z.z.n}{r}t) + (\Delta y_0 + L\sin\alpha) + \Delta y_2 + \Delta y_3 + \Delta y_4$$

$$Z = z + \Delta z_1 + \Delta z_2 + \Delta z_3 + \Delta z_4 = v_z t + L(1 - \cos\gamma) + \Delta z_2 + \Delta z_3 + \Delta z_4$$

(Equation 5.4)

As a cylinder is spiral milled, the quantities from Equation 5.4 should follow the conditions shown in Equation 5.5 where r and h are the radius and the height of the cylinder.

$$r = \sqrt{X^2 + Y^2}$$
$$h = Z \qquad \text{(Equation 5.5)}$$

5.4. Model analysis using GUM Workbench

GUM Workbench which is a GUM-based software package has been selected to perform the uncertainty evaluation for the positioning errors of the cutting tool through spiral tool path at a series of time based on the generated Equations 5.1 to 5.5. Figure 5.4 shows the flow of the model analysis being done in the GUM Workbench.

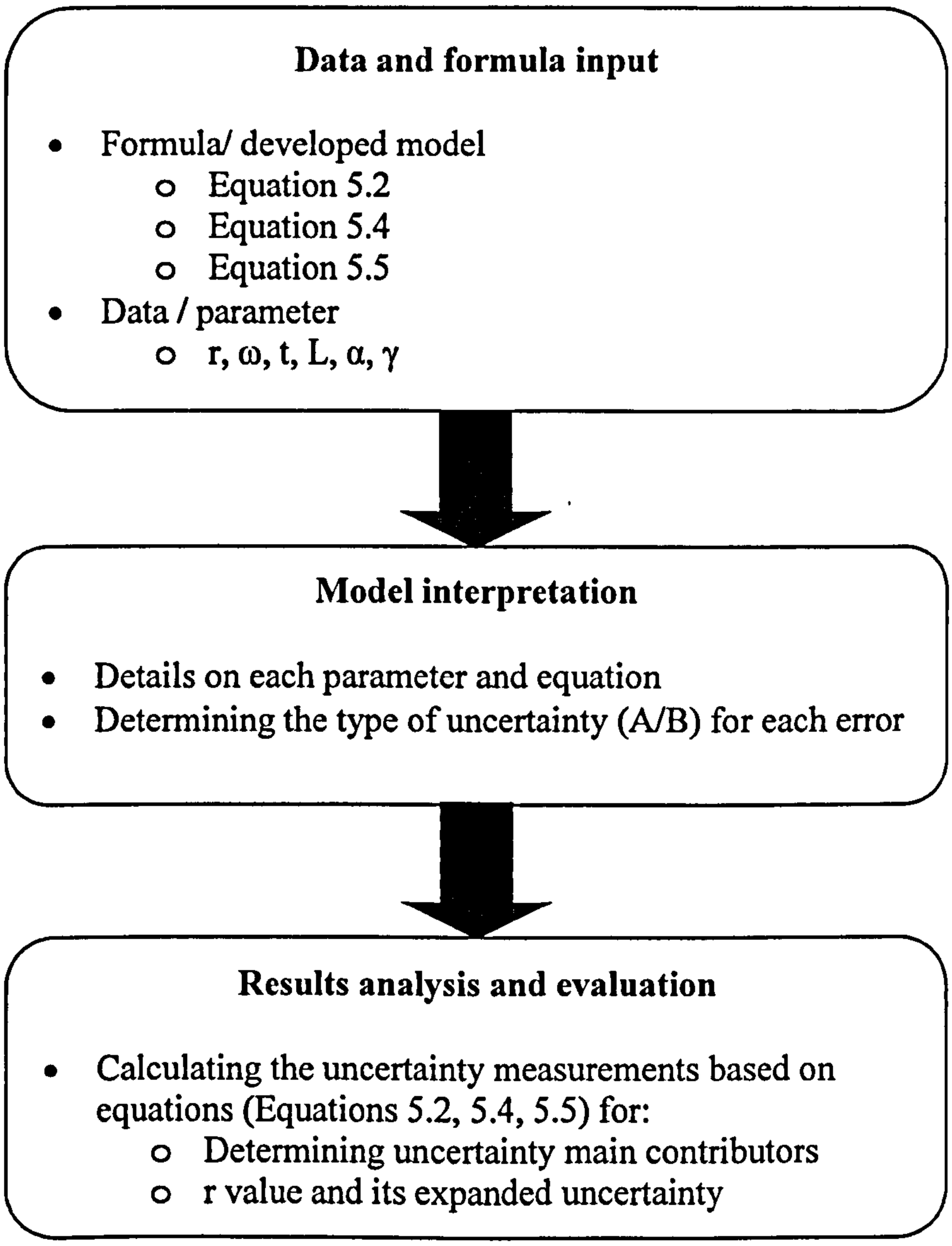

Figure 5.4 The flow of the uncertainty evaluation model analysis phase

5.4.1. Data input and model interpretation

Based on the generated equations (Equation 5.2, 5.4, 5.5), all the required and related data, parameters, definitions are being input into the GUM Workbench. In this study, the analysis of X and Y axis are merged in one model ($r = \sqrt{X^2 + Y^2}$) and based on Equation 5.4. While for Z axis it was analysed in another model which is also based on Equation 5.4. Table 5.3 summarized all the input into the GUM Workbench for X and Y axis while Table 5.4 listed the details for Z axis in order to allow its uncertainty analysis.

Table 5.3 Input into GUM Workbench (X and Y axis)

Parameter	**Explanation**	
R	Radius of the cylinder (mm)	
ω	Angular velocity of the cutter (rad/s)	
T	Time (s)	
α	Angle between tool and side of xz plane (rad)	
γ	Angle between tool and z axis (rad)	
		Type of uncertainty
Δx_1	x error in tool positioning due to deviation of xy plane	Type A
Δx_2	x error in tool positioning due to evaluation of reference point	Type A
Δx_3	x error in tool positioning due to temperature variations	Type B
Δx_4	x error in tool positioning due to positioning error of x table	Type B
Δy_1	y error in tool positioning due to deviation of xy plane	Type A
Δy_2	y error in tool positioning due to evaluation of reference point	Type A
Δy_3	y error in tool positioning due to temperature variations	Type B
Δy_4	y error in tool positioning due to positioning error of y table	Type B
X	$X = x + \Delta x_1 + \Delta x_2 + \Delta x_3 + \Delta x_4 = r\cos(\frac{f_z \cdot z \cdot n}{r}t) + L\sqrt{\cos^2\alpha - \cos^2\gamma} + \Delta x_2 + \Delta x_3 + \Delta x_4$ (Eq.5.4)	
Y	$Y = y + \Delta y_1 + \Delta y_2 + \Delta y_3 + \Delta y_4 = r\sin(\frac{f_z \cdot z \cdot n}{r}t) + \Delta y_0 + L\sin\alpha + \Delta y_2 + \Delta y_3 + \Delta y_4$ (Eq.5.4)	

Table 5.4 Input into GUM Workbench (Z axis)

Parameter	**Explanation**	
v_z	Feed speed of the tool along z axis (mm/sec)	
T	Time (sec)	
γ	Angle between tool and z axis (rad)	
		Type of uncertainty
Δz_1	z error in tool positioning due to deviation of z axis	Type A
Δz_2	z error in tool positioning due to evaluation of reference point	Type A
Δz_3	z error in tool positioning due to temperature variations	Type B
Δz_4	z error in tool positioning due to positioning error of z table	Type B
Z	$Z = z + \Delta z_1 + \Delta z_2 + \Delta z_3 + \Delta z_4 = v_z t + L(1-\cos\gamma) + \Delta z_2 + \Delta z_3 + \Delta z_4$ (Eq.5.4)	

The type of uncertainty for each error is determined based on how the parameters/variables are being observed. In this analysis, it involved four types of parameters that represent the errors. For the errors due to the tool path generations that stem from the construction of the MMT (Δx_1, Δy_1, Δz_1), it has been classified as Type A because values of this parameter were obtained through CMM evaluations as will be discussed in ***Chapter 6***. While for the errors related to the evaluation of workpiece reference point (Δx_2, Δy_2, Δz_2), it also falls under the same classification as the previous error (Type A) because it involved series of measurements on the innovated probing system as also will be mentioned in ***Chapter 6***.

Furthermore, for the errors related to temperature variation (Δx_3, Δy_3, Δz_3) and also errors originating from the positioning inaccuracies of each table (Δx_4, Δy_4, Δz_4), they have been classified as Type B because the uncertainty values are known based on the data given by the manufacturer of the motion tables (Aerotech) and also referring to ISO standards on temperature variations.

In GUM Workbench, there are two important steps that involved two different interfaces for data input and model interpretations:

- Model Equation interface

Figure 5.5 presents the example of the *Model Equation* interface where all the generated models (Equation 5.2, 5.4, 5.5) and descriptions for each of them are being stated in the *Equation Area*. While the parameters involved in each model are being listed and defined in the *Quantity* table as also pointed in Figure 5.5. Basically this interface holds the model equation and

also its definition, symbols and related units.

- Quantities interface

  This interface as shown in Figure 5.6 provides the medium for all the parameter being supplied in the *Model Equation* to be interpreted in detail. Among the information required are the type of uncertainty, value (if it is constant), method of observation and type of distribution. Table 5.3 (for X and Y) and Table 5.4 (for Z) supplied some of the required information into this interface. Figure 5.6 provides the example of the input required for parameter α which is the angle between the tool holder (Z axis) and the side of XZ plane.

GUM Workbench

File Edit View Option Tools Help

Model | Observation | Correlation | Budget | Previous

Title | Model equation | Quantities

Equation:

Σδ.. | Rename

R=sqrt(X^2+Y^2);

X=a*(cos(ω*(t*0.0377)))+ΔX1+ΔX2+ΔX3+ΔX4;

ΔX1=L*(sqrt(cos(α)^2-cos(γ)^2));

Y=a*(sin(ω*(t*0.0377)))+ΔY1+ΔY2+ΔY3+ΔY4;

ΔY1=ΔY0+L*sin(α);

Eq. 5.5

Eq. 5.4 for X

Eq. 5.2 for X

Eq. 5.4 for Y

Eq. 5.2 for Y

Quantity	Unit	Definition
R	mm	the radius of a circle
X	mm	the x value
Y	mm	the y value
a	mm	radius
ω	rad/sec	angular velocity
t	sec	time
ΔX_1	mm	Uncertainty due to X,Y,U planes deviation for X
ΔX_2	mm	Uncertainty due to original position deviation of table movement for X
ΔX_3	mm	Uncertainty due to temperature deviation for X
ΔX_4	mm	Uncertainty due to worktable accuracy for X
L	mm	Tool length
α	rad	Angle between Tool (Z) and side of U table
γ	rad	Angle between Tool (Z) and top of U table
ΔY_1	mm	Uncertainty due to X, Y and U planes deviation for Y
ΔY_2	mm	Uncertainty due to original position deviation for Y
ΔY_3	mm	Uncertainty due to temperature deviation for Y
ΔY_4	mm	Uncertainty due to worktable accuracy for Y
ΔY_0	mm	value of shifted planes

Definition (including unit) of each declared parameter/quantity

Figure 5.5 Example of Model Equation interface

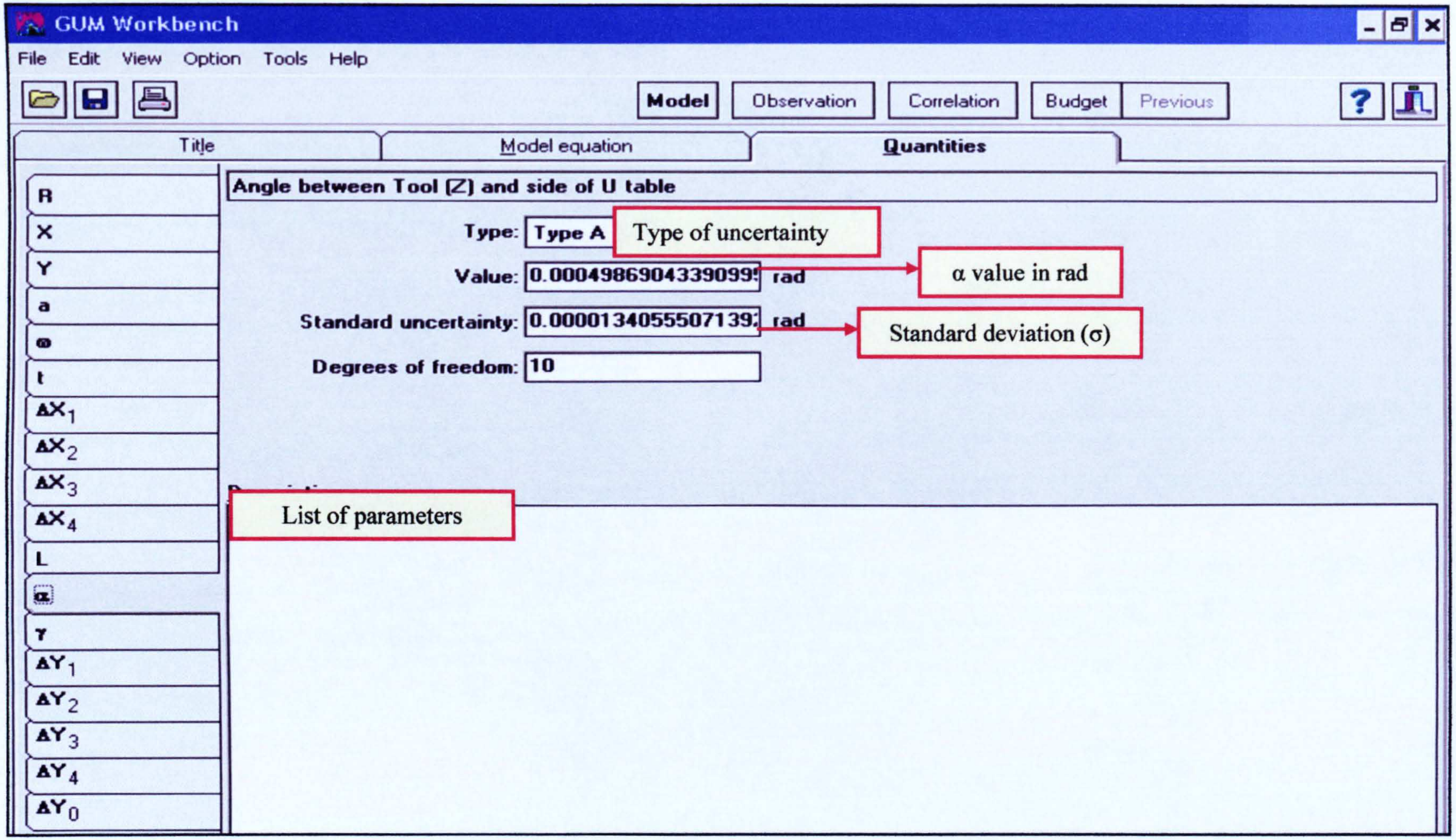

Figure 5.6 Example of Quantities interface (details of parameter α)

5.4.2. Results analysis and evaluation

The main objective of this phase is to evaluate the uncertainties of the positioning errors of the cutting tool (UX, UY, UZ - expanded uncertainty) for three spiral rotations based on the inputted Equations 5.2, 5.4 and 5.5 into the GUM Workbench. In order to evaluate the uncertainty above, the analysis is made for 30 times with the incremental values of the cutting time (Δt=0.0377s). In this section, an example of the analysis at t=1.131s is simulated.

Figure 5.7 shows the *Uncertainty Budget* interface where detailed results of the analysis are being presented once the *Budget* button (as pointed out in Figure 5.7) is selected. The analyses were performed based on the GUM framework/method in calculating and defining the uncertainties measurements. Beside that, GUM Workbench provides facilities to print a structured report which follows the rules given by the EAL and also the ISO-guides (**Appendix 5.1**).

GUM Workbench

File Edit View Option Tools Help

Model | Observation | Correlation | Budget

Budget button – for uncertainty result

Spherical movement model

Uncertainty budget:

Quantity	Value	Standard uncertainty	Degrees of freedom	Sensitivity coefficient	Uncertainty contribution	Corr.-coeff.	Index
X	-0.74443 mm	$2.13 \cdot 10^{-3}$ mm			(a)		(b)
Y	1.302755 mm	$651 \cdot 10^{-6}$ mm					
a	1.5 mm						
ω	5.555400 rad/sec	$115 \cdot 10^{-6}$ rad/sec	∞	$-2.51 \cdot 10^{-3}$	$-290 \cdot 10^{-9}$ mm	0.00	0.000
t	10.0 sec						
ΔX_1	$4.97 \cdot 10^{-3}$ mm	$2.13 \cdot 10^{-3}$ mm					
ΔX_2	$89.17 \cdot 10^{-6}$ mm	$5.43 \cdot 10^{-6}$ mm	11	-0.496	$-2.69 \cdot 10^{-6}$ mm	0.00	0.000
ΔX_3	$200.00 \cdot 10^{-6}$ mm	$5.77 \cdot 10^{-6}$ mm	∞	-0.496	$-2.86 \cdot 10^{-6}$ mm	0.00	0.000
ΔX_4	$300.00 \cdot 10^{-6}$ mm	$8.66 \cdot 10^{-6}$ mm	∞	-0.496	$-4.30 \cdot 10^{-6}$ mm	0.00	0.000
L	4.850000 mm	$115 \cdot 10^{-6}$ mm	∞	$-75.7 \cdot 10^{-6}$	$-8.74 \cdot 10^{-9}$ mm	0.00	0.000
α	$499 \cdot 10^{-6}$ rad	$134 \cdot 10^{-6}$ rad	7	5.39	$723 \cdot 10^{-6}$ mm	0.57	0.324
γ	$1.140 \cdot 10^{-3}$ rad	$383 \cdot 10^{-6}$ rad	7	-2.73	$-1.05 \cdot 10^{-3}$ mm	-0.82	0.676
ΔY_1	$3.119 \cdot 10^{-3}$ mm	$650 \cdot 10^{-6}$ mm					
ΔY_2	$90.83 \cdot 10^{-6}$ mm	$6.09 \cdot 10^{-6}$ mm	11	0.868	$5.29 \cdot 10^{-6}$ mm	0.00	0.000
ΔY_3	$200.00 \cdot 10^{-6}$ mm	$5.77 \cdot 10^{-6}$ mm	∞	0.868	$5.01 \cdot 10^{-6}$ mm	0.00	0.000
ΔY_4	$300.00 \cdot 10^{-6}$ mm	$8.66 \cdot 10^{-6}$ mm	∞	0.868	$7.52 \cdot 10^{-6}$ mm	0.01	0.000
ΔY_0	$700.00 \cdot 10^{-6}$ mm	$1.15 \cdot 10^{-6}$ mm	∞	0.868	$1.00 \cdot 10^{-6}$ mm	0.00	0.000
R	1.50045 mm	$1.27 \cdot 10^{-3}$ mm	12				

Result: (c)

Value: 1.5004 mm ± Expanded uncertainty: $2.8 \cdot 10^{-3}$ mm | Coverage factor: 2.2 | Coverage: t-table 95%

Figure 5.7 Interface of the generated uncertainty result

Based on the uncertainty result interface in Figure 5.7, the important information obtained from the analysis are the values of the Standard Uncertainty, Uncertainty Contribution's and also its index, overall result, expanded uncertainty based on the selected coverage factor. The value of the Standard Uncertainty provides the result of the uncertainty measurement for each analysed parameter. The value of the Uncertainty Contribution (Figure 5.7 (a)) is automatically evaluated by GUM Workbench, and all *important contributions* in the uncertainty measurement are highlighted with yellow background. In GUM Workbench, parameters are considered as *important contributions* when it is being part of the contributor those add up to 99% of the standard uncertainty.

While for the Uncertainty Contribution's index (Figure 5.7(b)), it shows the percentage of the parameters contributions towards the overall standard uncertainty. From here, the parameters (variables) that contribute most to the uncertainty measurement is/are indicated.

Finally, at the bottom of the interface (Figure 5.7 (c)), it provides the overall result of the measurement analysis together with the expanded uncertainty and the coverage factor that was used. In determining the coverage factor it is assumed that the distribution of the result can be described with a t-distribution while the value of the coverage factor is taken from a t-table with a coverage probability (in this example it is 95%).

Example of uncertainty analysis

Based on the analysis made, Table 5.5 presents an example of a summary for uncertainty budgeting exercise considered for a particular position of the cutter, at a cutting time of t=1.131s (30xΔt), when following a spiral path (with r=1.5mm, ω=5.5554rad/sec, V_z=10mm/min radius). While Table 5.6 shows an example for Z-axis uncertainty analysis results.

Table 5.5 An example of uncertainty evaluation of the errors of X and Y when the cutter follows a spiral path, implication on the uncertainty of the cylinder radius (r)

Uncertainty evaluation for X and Y coordinates				
Parameters	Value	Standard Uncertainty	Uncertainty Contribution	Index
X	-0.7443 mm	2.43×10^{-3} mm		
Y	-1.2952 mm	94.4×10^{-6} mm		
R	1.5 mm			
ω	5.5554 rad/sec	115×10^{-6}rad/sec	267×10^{-9} mm	0.000
T	t=1.1310 sec			
α	498.7×10^{-6} rad	13.4×10^{-6} rad	**-41.9×10^{-6} mm**	**0.133**
γ	1.1402×10^{-3} rad	38.3×10^{-6} rad	**-106×10^{-6} mm**	**0.856**
Δx_1	5.127×10^{-3} mm	215×10^{-6} mm		
Δx_2	89.17×10^{-6} mm	5.43×10^{-6} mm	-2.71×10^{-6} mm	0.001
Δx_3	200.00×10^{-6} mm	5.77×10^{-6} mm	-2.86×10^{-6} mm	0.001
Δx_4	300.00×10^{-6} mm	8.66×10^{-6} mm	-4.31×10^{-6} mm	0.001
Δy_1	3.1935×10^{-3} mm	67.0×10^{-6} mm		
Δy_2	90.83×10^{-6} mm	6.09×10^{-6} mm	-5.28×10^{-6} mm	0.002
Δy_3	200.00×10^{-6} mm	5.77×10^{-6} mm	-5.01×10^{-6} mm	0.002
Δy_4	300.00×10^{-6} mm	8.66×10^{-6} mm	-7.51×10^{-6} mm	0.004
Δy_0	700.00×10^{-6} mm	1.15×10^{-6} mm	-1.00×10^{-6} mm	0.000
Result $r = \sqrt{X^2 + Y^2}$ (Eq. 5.5)				
Value of r (mm)	Expanded Uncertainty (mm)	Coverage Factor	Coverage	
1.49387	250×10^{-6} mm	2.2	t-Table 95%	

From the table above, it can be concluded that at t = 1.1310 sec, the generated value for r is *1.49387±0.00025mm*, while the expanded uncertainty is *0.00025*

mm with the coverage factor of *2.2*. From the point of coordinate position for X and Y and also its positioning error of the cutting tool (X±UX, Y±UY), the result are as follow:

- X- axis = (-0.7443±0.00243)
- Y-axis = (-1.2952±0.0000944)

For this particular coordinates, the main parameters that mostly contribute to the positioning errors in this case are identified as the γ and α angles which provide 98% of the overall uncertainty contribution.

Table 5.6 An example of uncertainty evaluation of the errors of Z when the cutter follows a spiral path, implication on the uncertainty of the cylinder height (h)

Uncertainty evaluation for Z coordinate				
Parameters	Value	Standard Uncertainty	Uncertainty Contribution	Index
v_z	0.1768 mm/sec	$34.6x10^{-3}$ mm	$13.1x10^{-6}$	0.047
T	t=1.1310 sec			
γ	$1.1402x10^{-3}$ rad	$38.3x10^{-6}$ rad	$86.6x10^{-6}$	0.921
Δz_1	$3.15x10^{-6}$ mm	$2.12x10^{-6}$ mm		
Δz_2	$85.00x10^{-6}$ mm	$5.97x10^{-6}$ mm	$5.77x10^{-6}$	0.010
Δz_3	$200.00x10^{-6}$ mm	$57.7x10^{-6}$ mm	$5.97x10^{-6}$	0.020
Δz_4	$300.00x10^{-6}$ mm	$8.66x10^{-6}$ mm	$2.12x10^{-6}$	0.001

Value of Z (mm)	Expanded Uncertainty (mm)	Coverage Factor	Coverage
0.06724	$120x10^{-6}$	2.2	t-Table 95%

While the result for the Z axis is more straightforward, the value for the Z coordinate and its positioning error of the cutting tool (Z±UZ) is (0.06724±0.00012) with the coverage factor of 2.2. The main parameters that contributes most to the positioning errors for Z axis is the γ angle which provide 92% of the overall uncertainty contribution.

The above generated results are based on one position of X, Y and Z at t cutting time. Repeating this procedure at different cutting times, a series of points with their errors (X±UX, Y±UY, Z±UZ) simulating the spiral tool path have been obtained. For this purpose, at incremental values of the cutting time (Δt=0.0377s), the positioning errors of the cutting tool UX, UY, UZ (expanded uncertainties, k=2.2 coverage factor) have been evaluated by repeating the analysis for 30 different cutting time. The result for each cutting time is presented in **Appendix 5.2** with details on standard uncertainty and their contribution to the standard uncertainties' results.

5.5. Simulation and validation

For the final phase in evaluating the uncertainty of the positioning errors of the cutting tools, the generated models and the results obtained from GUM Workbench is being validated. In order to evaluate the validity of this uncertainly model, the spiral tool path, simulated for the evaluation of positioning uncertainties, has been performed on the MMT without cutting while stopping the tool at particular time intervals when the tool tip position (X, Y, Z) was evaluated using Coordinate Measuring Machine (CMM).

In here, the results from the measurements (CMM) have been compared with those obtained from the uncertainty model (analysed in GUM Workbench) in terms of errors in roundness (from X and Y axis analysis) and height of the cylinder (from Z axis analysis) on which spiral milling was simulated, it was found that the predicted errors have been smaller by 32% for roundness and 18% for height when compared with the real data. Though these comparative

results show that the proposed uncertainty model can be an effective tool to predict the sources of geometrical inaccuracies of milled surfaces, the differences between similar values can be accounted by factors that have been considered constant (e.g. error of the dummy tool, rounding errors in the MMT control system) as well as those that depend on the accuracy of the CMM.

However, using the proposed uncertainty model, further errors can be accounted for the improvement of the overall prediction of the geometrical errors of machined micro-parts manufactured on the MMT.

5.6. Discussion

There are two major aspects that can be concluded from the uncertainty analysis above:

- In developing a custom-made MMT, it is important to understand the sources of errors when generating the machines surfaces, this can be facilitated by the development of uncertainty models that allow the evaluation of the contribution of the MMT constructive errors on the accuracy of the tool path and ultimately on the generated surfaces. Through the UEM analysis, it provides the opportunity to implement a methodology to evaluate the uncertainties of any in-house developed machine tools in identifying the main sources of the overall errors of the machines performance that affect the quality (e.g. geometrical accuracy) of the final product. It is essential to investigate the sources of errors that affect the final product especially for custom-made machine tool because usually there is no standard or guidelines available for the machine. In this study,

the uncertainty evaluation has been made by analysing the errors stemming from the MMT construction and simulated through the spiral milling tool path in machining a cylinder.

- The main sources of the uncertainties based on the evaluation of the errors stemming from the construction of the MMT have been indicated through the development of the UEM. This is made through the uncertainty evaluation for the positioning errors of the cutting tool for spiral milling tool path. From the series of results generated in GUM Workbench, it can be concluded that the main source of errors from the MMT construction are α=0.0286° and γ=0.0653°. However, based on the obtained expanded uncertainty values, it shows that these errors do not contribute any significant effect towards the geometrical accuracy of the machined part.

From the 30 repetition analysis, it shows clearly that γ contributed 80% of the uncertainty while α takes the rest 20%. This is presented in Table 5.7 that listed the uncertainty contribution index value for α and γ based on the 30 different cutting times (yellow highlighted columns show that γ is the main contributor, while red highlighted columns represents α as the main contributor).

Table 5.7 Uncertainty contribution index for α and γ

No	Uncertainty contribution Index (α)	Uncertainty contribution Index (γ)	No	Uncertainty contribution Index (α)	Uncertainty contribution Index (γ)
1	0.007	0.993	16	0.007	0.993
2	0.000	1.000	17	0.000	1.000
3	0.005	0.995	18	0.005	0.995
4	0.035	0.965	19	0.035	0.964
5	0.126	0.873	20	0.129	0.871
6	0.384	0.616	21	0.394	0.606
7	0.878	0.121	22	0.892	0.107
8	0.911	0.089	23	0.899	0.101
9	0.554	0.446	24	0.542	0.458
10	0.324	0.676	25	0.317	0.683
11	0.198	0.802	26	0.195	0.805
12	0.125	0.875	27	0.123	0.877
13	0.078	0.922	28	0.076	0.923
14	0.046	0.954	29	0.045	0.955
15	0.0230	0.977	30	0.022	0.978

5.7. Contribution to MicroMAS

This analysis provides the opportunity to partly portray the real condition of the MMT in the developed MicroMAS. For this purpose, it is proposed to integrate the results from the UEM analysis in the MicroMAS by taking into consideration the uncertainty effect in machining the particular form/shape of PF in calculating the manufacturability indexes (MI) in MicroMAS. As the analysed micro-part in MicroMAS is being decomposed to primitive features (e.g. box, cylinder, sphere), in order for its manufacturability aspect to be assessed, the uncertainty effect is suggested to be integrated in the Single Feature Analysis (SFA) phase.

In calculating the Manufacturability Index for Single Feature Analysis (MI_{SFA}), another MI is added which is the Manufacturability Index for Uncertainty Evaluation Model (MI_{UEM}), where the uncertainty effect in machining the

shape/form of the particular PF is incorporated for each identified primitive feature (PF) as presented in the formula below (Equation 4.1).

$$MI_{SFA} = \frac{\sum K_i . MI_i}{5}, \qquad \text{(Equation 4.1)}$$

where i= PF, Ra, TOL, DIM, **UEM**

In this study, the UEM development was analysed based on the machining of a cylinder in the MMT using a spiral milling tool path. Even though the impact of the generated error can be considered small and insignificant towards the geometrical accuracy of the machined micro-part, it is a value added approach to take this effect into consideration as it provides a better judgement towards the determination of the MIs.

As an example of considering the uncertainty effect in MicroMAS, the MI_{UEM} index range is generated from the expanded uncertainty values obtained from the UEM analysis of evaluating the spiral milling tool path of a cylinder. Assumption has been made that the smaller the size or dimensions of the PF, the bigger the impact of the uncertainty. Furthermore, the average of the expanded uncertainty from the 30 repetitions of cutting time is considered as the nominal value for the MI_{UEM}.

Therefore, as a conclusion, the calculation of MI_{SFA} has taken into consideration the uncertainty effect by introducing it into the formula

(*Equation 4.1*) and the details of the MI_{UEM} range value was presented in ***Chapter 4***.

5.8. Summary

This chapter has involved a discussion on the development of the UEM and its analysis involved in determining the sources of errors stemming from the construction of an in-house developed MMT that might affect the geometrical accuracy of the machined micro-part. Four sources of main errors have been identified which are: errors due to the MMT construction; errors related to evaluation of workpiece reference point; errors related to temperature variations and errors originating from positioning inaccuracies of each table. In order to evaluate the uncertainties stemming from the identified errors, the uncertainty model/equations are generated based on the spiral milling tool path in machining a cylinder. From the analysis made in the GUM Workbench, it shows that these errors do not contribute any significant impact towards the dimensional accuracy of the machine micro-parts.

The model and methodology developed in analysing the errors above provide a proof that uncertainty analysis is able to understand the sources of errors from a custom-made machine tool that affect the quality of the final machined part. Moreover, once this model/methodology is developed, the geometrical errors can be evaluated in any situation when other (more) complex surfaces are generated. However, one should note that the existing model does not account for the errors associated with machining process (e.g. tool/part deflection, tool

wear, etc.) as it mainly focuses to highlight a method to account for the errors when constructing similar MMT systems.

From here, it can be concluded that the crucial contribution of this study is a model/methodology was successfully designed which can assist in predicting the sources of errors when generating a machined surfaces for a custom-made machine tool and also can provide a fundamental guidance for developing a MMT.

Furthermore, in order for the developed MicroMAS to mirror the real condition of the MMT in the system, the impact of UEM analysis is taken into consideration for calculating the Manufacturability Index for Single Feature Analysis (MI_{SFA}). The Manufacturability Index for Uncertainty Evaluation Model (MI_{UEM}) is introduced and being considered in the MI_{SFA} formula for each identified primitive feature (PF). With this scheme, the manufacturability analysis in MicroMAS is more significant as it consider the uncertainty effect in machining the shape/form of the PF.

CHAPTER 6: MINIATURE MACHINE TOOL: AN EXAMPLE OF MICRO-MACHINING ENVIRONMENT FOR MICROMAS

6.1. Introduction

In order to clearly visualise the micro-machining environment in the developed MicroMAS, a miniature machine tool was devoted for this task. This chapter describes the main domain of the MicroMAS application which is an in-house developed 4 axis Miniature Machine Tool (MMT). Given that the MMT is a custom-built machine, it has been put through a series of machining experiments and observations in order to identify its limitations and capability. The discovered limitations are discussed thoroughly together with its solutions. Beside that, the advantages of the MMT and its contribution on the micro-machining domain are also commented later in this chapter.

For the purpose of envisaging the MicroMAS implementation in a micro-machining setting, this chapter also discusses in details all the proposed experimental procedures and set-ups. The main objectives of these experiments are to assess the capability of the MMT and at the same time to populate relevant data for the developed MicroMAS. Among the proposed experiments are:

- Machining the "adapted standard" micro-testpiece
- Producing thin walls and micro-slots
- Generating a micro-component demonstrator

Furthermore, from these experiments the surface quality and geometrical accuracy of the surfaces that can be machined via the MMT are evaluated. The

machining procedures, parameters and results are comprehensively discussed in this chapter. Finally, the integration of these results and their significant contribution to the developed MicroMAS are also presented.

6.2. The custom-made 4-axis Miniature Machine Tool (MMT)

The custom-made 4 axis miniature machine tool (see ***Figure 3.4***) has been used for all the micro-milling trials performed within this study; the detailed descriptions of the MMT have been discussed in ***Chapter 3***.

6.2.1. Problems and limitations

In developing a custom-built miniature machine tool for the generation of complex micro-features via chip removal processing there are concerns in ensuring that the machine can be operated as precisely as possible. Since there are no standards, guidelines or user manual to refer to in operating the MMT, a series of machining experiments and observations in order to discover its limitations have been conducted. Furthermore, as the MMT is assembled from various "off-the-shelf" components their integration should be taken with serious consideration as it can limit the performance of the MMT. In the following are the revealed problems and limitation of the MMT:

6.2.1.1. Errors in constructing the MMT

As mentioned before, the construction of the MMT is based on the integration of various components. Thus, this gives potential for operational error to occur in the MMT. The analysis of the errors in constructing the MMT is based on the following practical facts:

- The machine (gantry) frame can have its geometrical deviations (e.g. flatness in X/Y/Z planes) as well as encountering additional errors when assembled on the granite base plate. Thus, the gantry frame can have compounded errors relative to the reference system of the MMT.
- Assembling the Z-motion table and the spindle (through its holder) on the gantry frame can result in combined positioning errors of the Z axis (tool/spindle axis) of the MMT from the reference plane.
- The X, Y and U motion tables that are stuck on top of each other and mounted on the granite base plate can result in deviations at the top of the MMT (top) working table from the reference plane.

Due to the reduced dimensions of the system, an error minimisation procedure has been performed by placing the MMT on the table of a CMM (Figure 6.1) to assemble its modules while intermediately performing the metrological checks through the following steps:

- The gantry frame has been ground, in a single hit fixture, on the critical surfaces: those by which the frame is fixed on the machine platform and the surface against which the spindle holder is mounted.
- The frame was mounted on the granite base, and then the subassembly has been assessed by CMM in relation to the reference plane followed by error compensation through adding liners and controlling the torque when fastening the bolts.
- The Z-motion table was mounted on the gantry frame, and its positioning errors relative to the reference plane were evaluated through CMM by

moving the table in different locations (e.g. max., min. and middle z positions with 5 repetitions) followed by errors compensation [188].

- The spindle, through its holder, was mounted on the Z-motion table followed by CMM evaluation and errors minimisation as previously described.
- The X-motion table was mounted on the machine platform and its positioning errors relative to the reference plane were evaluated through CMM for different positions of the table (max., min., and middle X positions with 5 repetitions) followed by errors compensation. After this, the same procedure was employed when mounting the stacking of Y and U motion tables.

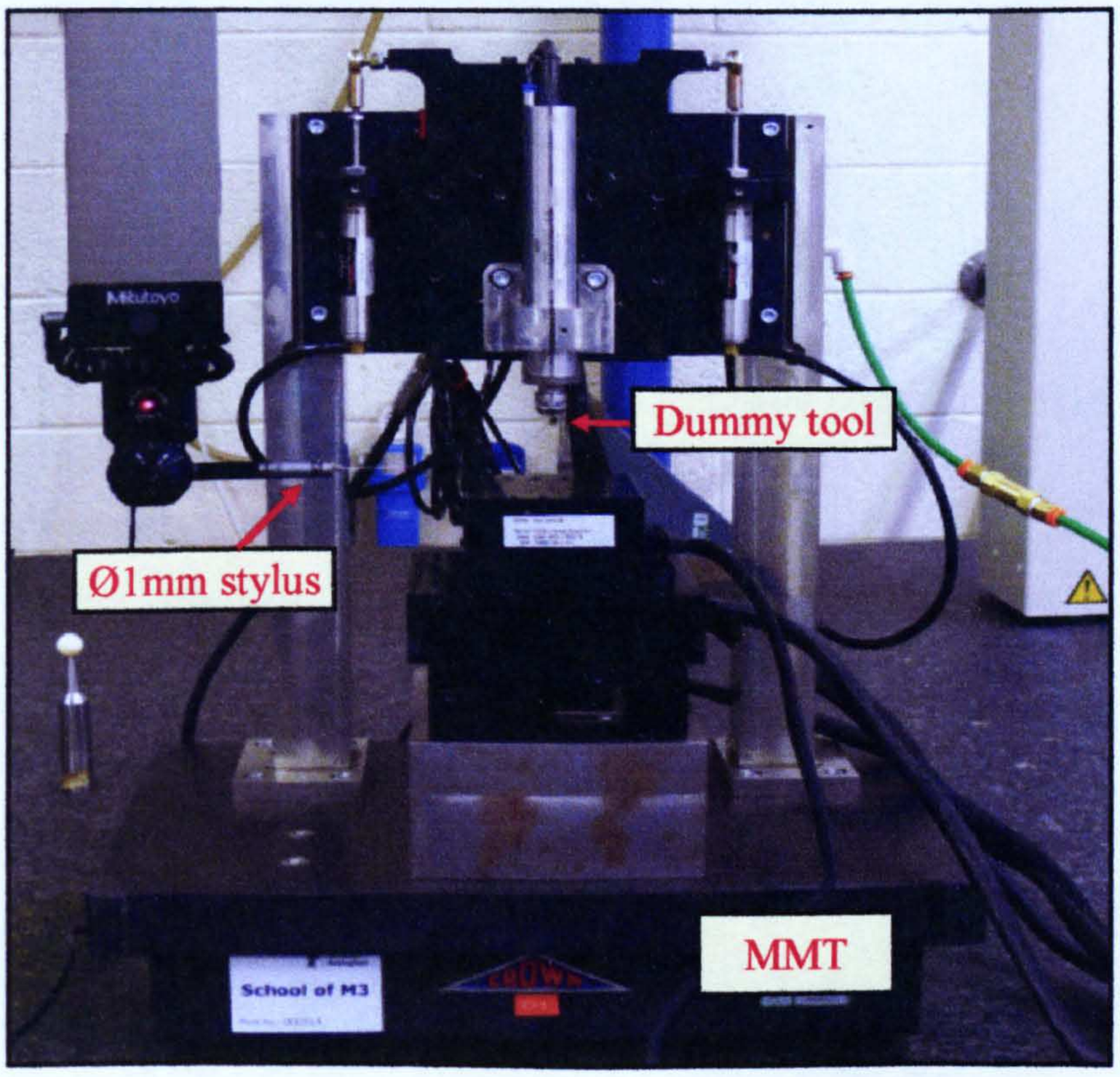

Figure 6.1 Metrological evaluation of the MMT

Once this error minimisation procedures were completed, further CMM measurements were carried out to evaluate the resulting positioning errors of the axis of a dummy tool mounted on the spindle relative to the XYZ plane, these positioning errors lead to the generation of part geometrical inaccuracies when the tool follows a 3D cutting path (this error was considered further in ***Chapter 5*** during development of the Uncertainty Evaluation Model (UEM)).

From the CMM evaluation procedure discussed above, the errors that were identified are listed below, together with the corrections being made:

- The gantry frame was found out to be deviated from the reference plane; as the spindle unit that holds the cutting tool was attached to the frame, this deviation can possible cause errors to the generated tool path. In the domain of micro-machining, a small error in the construction of the machine tool can contribute to big errors when machining the micro-parts. Based on this, the correction for the problems were made by shimming the slideways attached to the frames and clocked it again (via CMM) to ensure the accuracy of the frame position.
- There are combined positioning errors of the Z axis (tool/spindle axis) from the reference place due to the assembled Z-motion table and the spindle (through its holder) on the gantry frame.
- It was found out that the top of the U-motion table was not parallel with the X and Y motion tables. From the CMM evaluation, it shows that the position of the U-motion table is tilted and this can contribute flaws in machining the micro-parts. The correction was made by setting the new

home position for the U-axis which is parallel with the rest of the motion tables.

6.2.1.2. Determining the new machine working space

The machine work space has been defined in the previous work as reported in [38], and Figure 6.2 illustrates the determined travel and *original* home position. The working space (i.e. reached by the maximum allowable travel of the tables) is defined in accordance with the "machine zero point", which refers to the point when all the axes are at their home position. The "safe travel" which is the maximum allowable space that each table can travel was also defined based on their minimum and maximum movements (denoted as X_{min} and X_{max}, Y_{min} and Y_{max}, Z_{min} and Z_{max}, and U_{min} and U_{max}) as shown in Table 6.1.

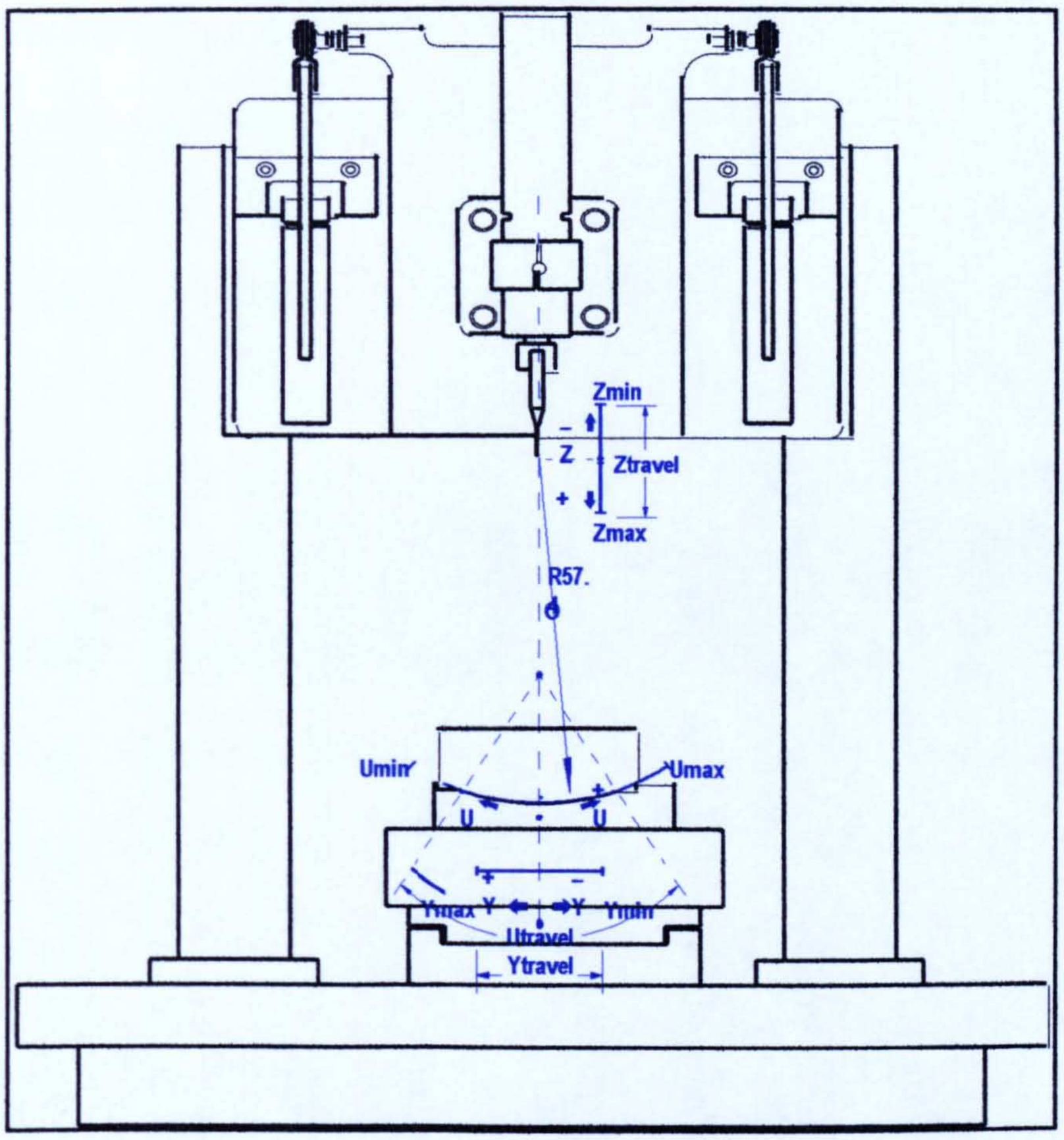

Figure 6.2 The travel and home position for each axis (Source: [38])

Table 6.1 Previous home position and safe travel for the tables (Source: [38])

Axis	Min.	Max.	Safe Travel	Home Position
X	-2.66	27.71	30.37	**12.525**
Y	-2.32	27.33	29.65	**12.505**
Z	-2.15	27.14	29.29	**12.495**
U	-10.70	8.68	19.38	**-1.010**

The values for X, Y and Z axes are in mm whereas those for U axis are in degrees.

$Safe\ Travel = \|\|Max| + |Min|\|$ ***and*** $Home\ Zero = |0.5 * (|Max| - |Min|)|$

The point where the home position of each axis coincides is the "machine zero" point.

Based on the current setting as stated in Table 6.1, it was discovered that there were limitation in the allowable space for Z-axis movement as illustrated in Figure 6.3(a). The current home position (in the middle of the safe travel area) has restrained the travel space for the Z-axis and also limits the reach of the tools towards the workpieces placed on top of U-motion tables. In order to solve this limitation, the setting of the home position for the Z-axis has been changed. The new home position for the Z-axis is shown in Figure 6.3(b) and also presented in Table 6.2. This resulted for the Z-axis to be able to reach the top of the U-axis in its safe travel space, which means more allowable space for Z-axis movement.

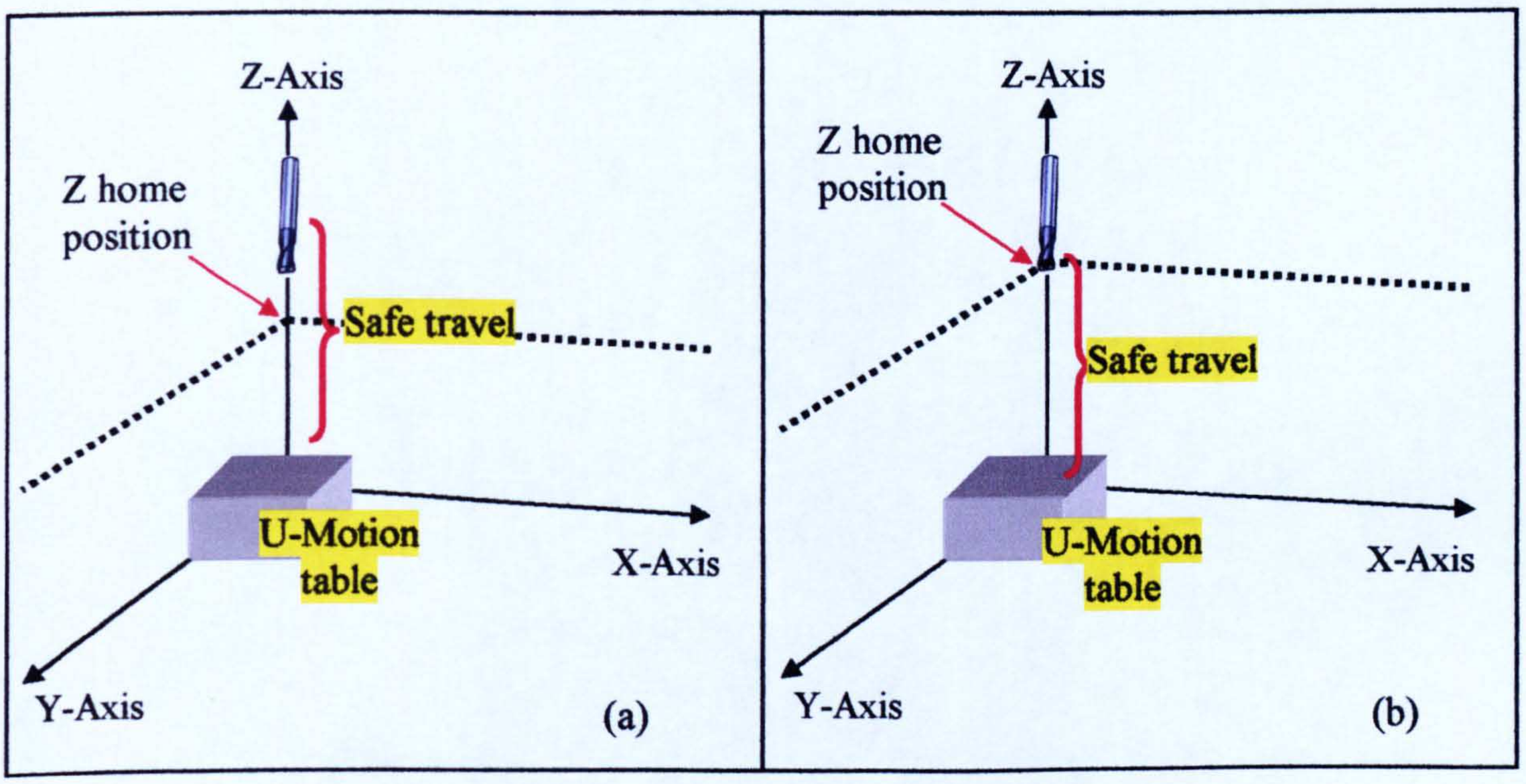

Figure 6.3 Previous and current travel space for Z-Axis

Moreover, the correction made (by setting the new home position) to ensure that the U-motion table is parallel with the X and Y motion tables was also presented in Table 6.2.

Table 6.2 New working space for the MMT

Axis	Min	Max	Safe Travel	Home position
X	-2.66	27.71	30.37	12.525
Y	-2.32	27.33	29.65	12.505
Z	-29.28	0.01	29.29	0.00
U	-9.21	10.17	19.38	1.5455

**The values for X, Y and Z axes are in mm whereas those for U axis are in degrees*

6.2.1.3. Integration between machine controller software (Nview) and CNC software (MasterCAM)

MasterCAM is a CAD/CAM application that can be use to design parts and create complete machining operations. In this study, MasterCAM has been chosen to generate machining tool paths and further to produce the CNC code for the MMT based on the specific post-processor. The developed post-processor has taken into consideration all aspects of the MMT (machining space, safe travel distance) and also the Nview requirement. In developing the specific post-processor, a problem has been discovered involving the Z-axis virtual pivot point to be perfectly in line with the MasterCAM zero (Y=0) when the datum is set. This problem occurred whenever U-axis is involved in the machining, but for 3-axis machining (X, Y and Z) this is not relevant.

In order to solve this problem, the distance between the Z virtual pivot and the MasterCAM zero (top of the workpiece) needs to be measured every time the U-axis is involved in the machining. The distance to be measured is between the machine virtual pivot (tip of tool) and the MasterCAM workpiece zero

datum (which is fixed 13.36 mm from the top of U-axis table when U=0) as presented in Figure 6.4. The measured distance which can be varied depends on the positioning of the tool is being fed manually on the MasterCAM interface before generating the tool path. The problem is believed to be sourced from the swivel movement of U-axis to meet the position of the X=0, Y=0 and Z=0 at the same point, however further work is needed to address this issue.

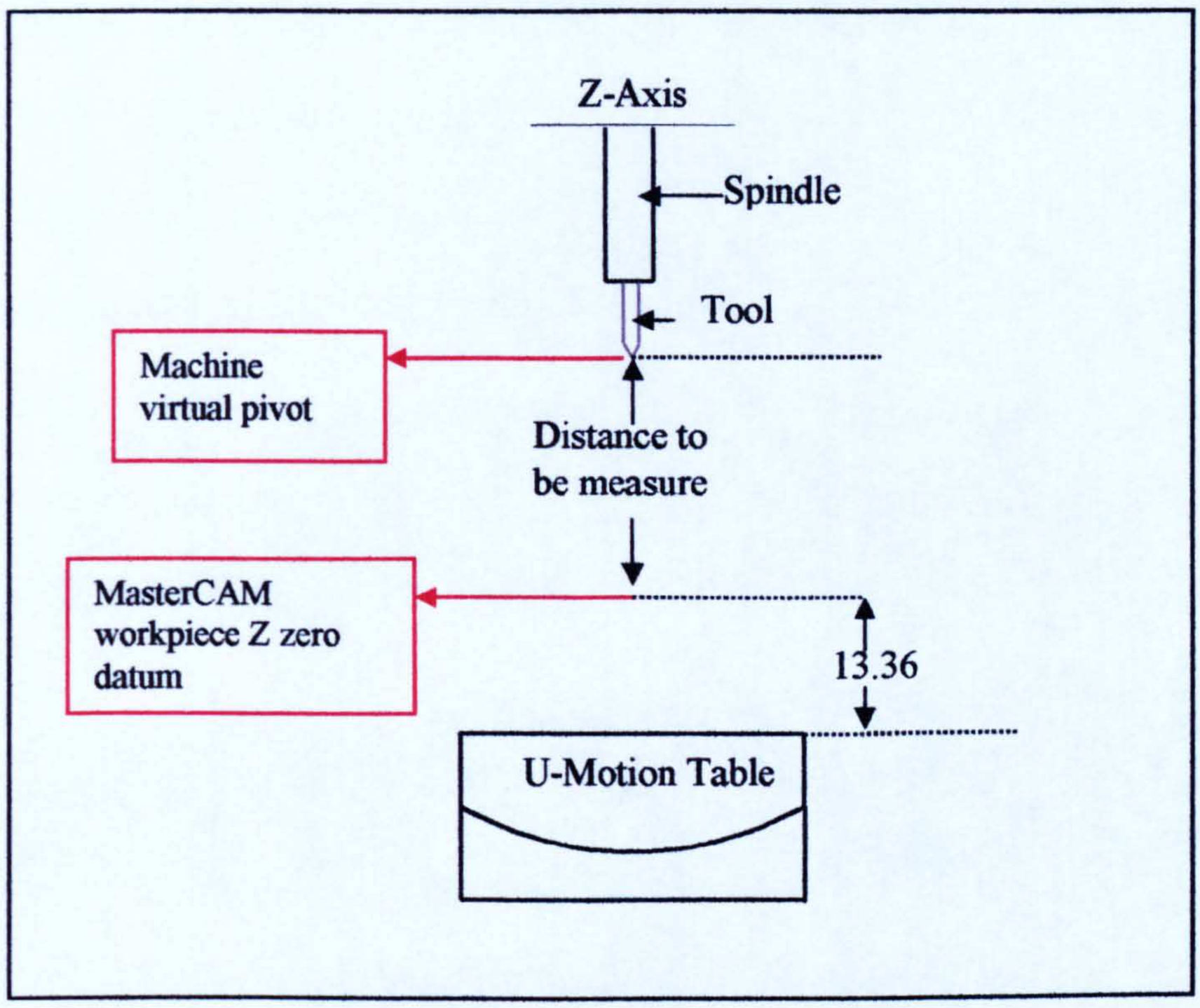

Figure 6.4 Distance to be measure

6.2.1.4. Workpiece home positioning

Another limitation that has been observed is in setting the position of the workpiece on the MMT to coincide precisely with the tool position at its zero point. This problem is solved by using a multimetre as the sensor/probe that detects the moment of contact between the workpiece and the tool. In this study, the probing system is based on the electrical contact between the tool tip

and the workpiece. ***Appendix 6.1*** shows the set-up of the multimetre for detecting the home positioning of the workpiece.

6.2.1.5. The cooling system and the suction/pumping system

The MMT is constructed from motion tables that employ a non-cogging linear motor as the driving element. This means the produced chips tend to get stuck/trapped between the slides of the table. Besides that, the stacking of the motion tables could possibly caused the machined chips to be trapped between the tables. This can result in failure of the MMT operation. Initially the MMT was designed to operate under the dry condition but, through one of the machining observation, running on a wet-environment machining helps to maintain a longer tool life and produce a better part quality. In order to solve this limitation and to allow wet condition machining, the design of the MMT had to be reconsidered.

As proposed by Limvachirakom [189], a cooling system that is able to retain the fluid in a container without deteriorating the stacked X, Y and U motion tables (which are not water proof) has been designed. A plastic container to protect the motion tables and the suction/pumping system has been fabricated for this purpose. The function of the suction/pumping system is basically to deliver the cooling liquid to the machining area and also to filter the coolant. In addition, it is also used to ensure that the machining area is clear from the chips. The plastic container (consists of two parts: the tray cover and the working tray) was designed to allow wet machining condition to be run on the

MMT. Figure 6.5 shows the new suction/pumping mechanism implemented on the MMT.

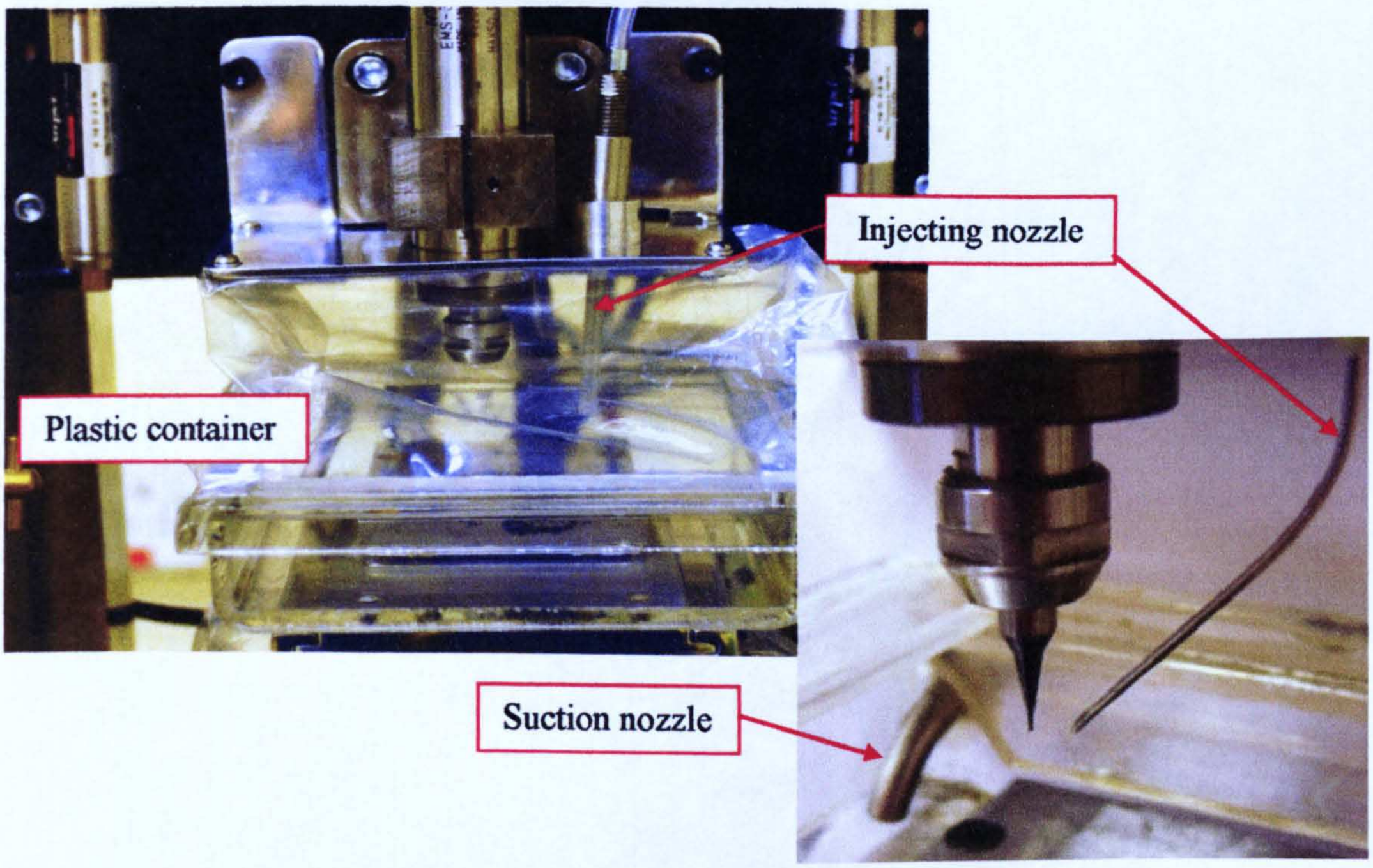

Figure 6.5 Plastic container and suction/pumping system

6.3. Micro-machining experimental details

Based on the current MMT set-ups and also considering all discussed limitations, the custom-built MMT is believed to be able to perform micro-milling process at an acceptable degree of accuracy. In order to demonstrate the capability of the MMT and at the same time to provide relevant information into the developed MicroMAS, various experiments for generating micro-parts of different shapes and dimensions have been conducted. As discussed in ***Chapter 4***, there were five important aspects being considered in determining the Manufacturability Indexes (MIs). These are: the Primitive Feature Index (MI_{PF}), Surface Roughness Index (MI_{Ra}), Tolerance Index (MI_{TOL}), UEM

impact Index (MI_{UEM}), and Dimension Index (MI_{DIM}). The experiments can be utilized to determine the range for MI_{Ra} and MI_{TOL} indexes based on the obtained results of R_a and geometrical accuracy.

As presented in ***Chapter 3***, there are three important types of experiments that were being considered in this study. Among the proposed experiments were machining the 'adapted-standard' micro-testpiece, generating micro-slot and thin walls and finally producing micro-component demonstrator. These experiments have been carried out in different materials (e.g. Stainless steel (316L), Steel (AISI 1040), Titanium Alloyed (TiAl6V4)), using various machining parameters and micro-cutting tools (end-mill with Ø = 0.5 – 0.8mm from Sandvik Coromant).

6.3.1. Machining the 'adapted-standard' micro-testpiece

The objective of machining the 'adapted-standard' micro-testpiece (Figure 3.7) was to assess the capability of the MMT in term of surface quality and geometrical accuracy. The surface quality was assessed using surface profile analysis (e.g. R_a and R_z), while the geometrical accuracy was obtained via a Coordinate Measuring Machine (CMM) and also a Keyence VHX-Optical Digital Microscope.

6.3.1.1. Machining procedures and parameters

In machining the micro-testpiece, each of the main features (cylinder, diamond shape and also the outer square) were generated by implementing the

contouring function from MasterCAM at respective depths for each layer. The steps taken in machining the micro-testpiece are described below:

- First, the cylinder was generated and Figure 6.6 shows the layout of the milling operation using the machining parameters shown in Table 6.3 in a wet condition (coolant=Hocut 3380).

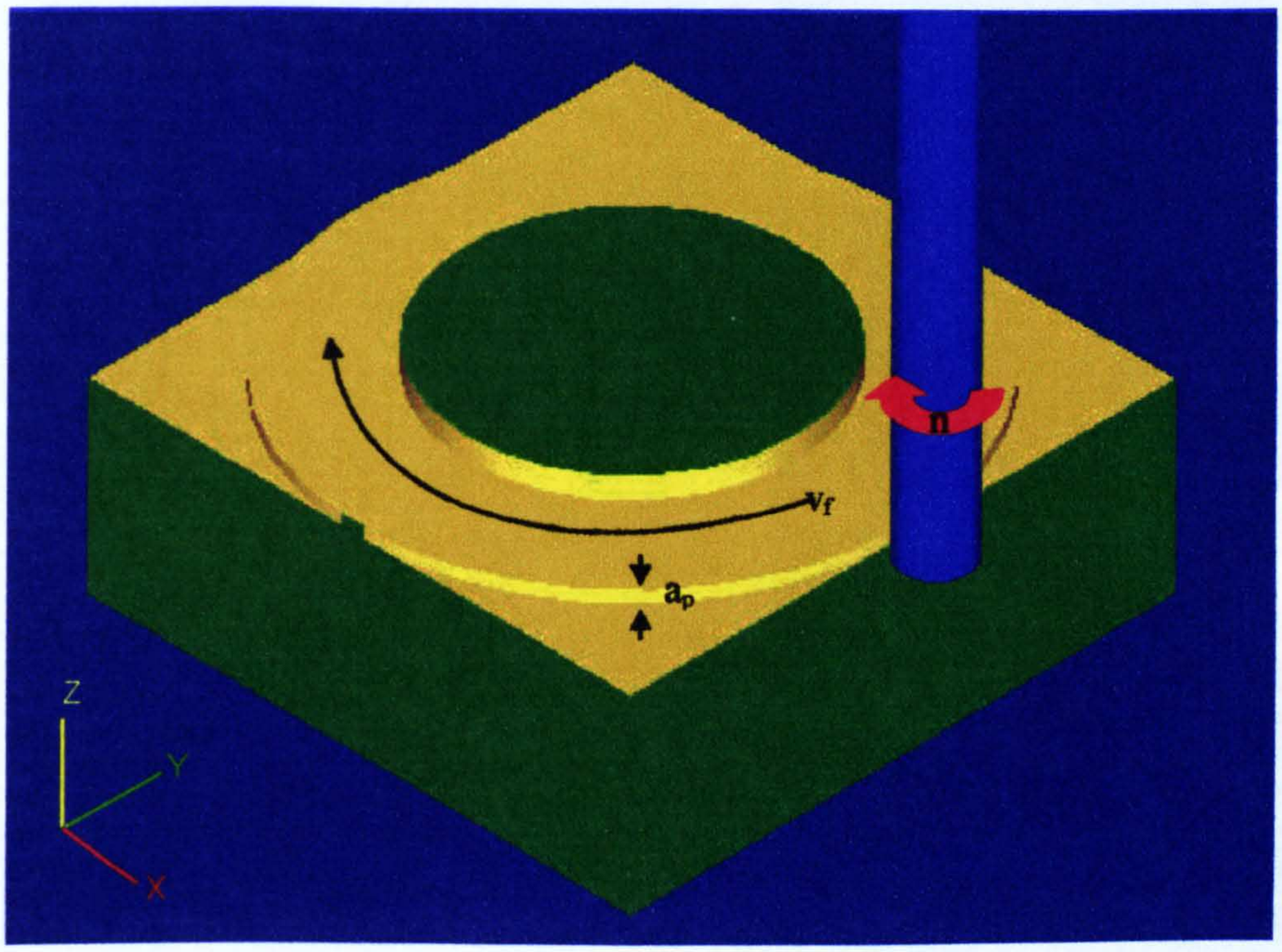

Figure 6.6 Layout of the cylinder machining operation

- After completing the machining of the cylinder, a diamond shape was then milled based on the layout shown in Figure 6.7.

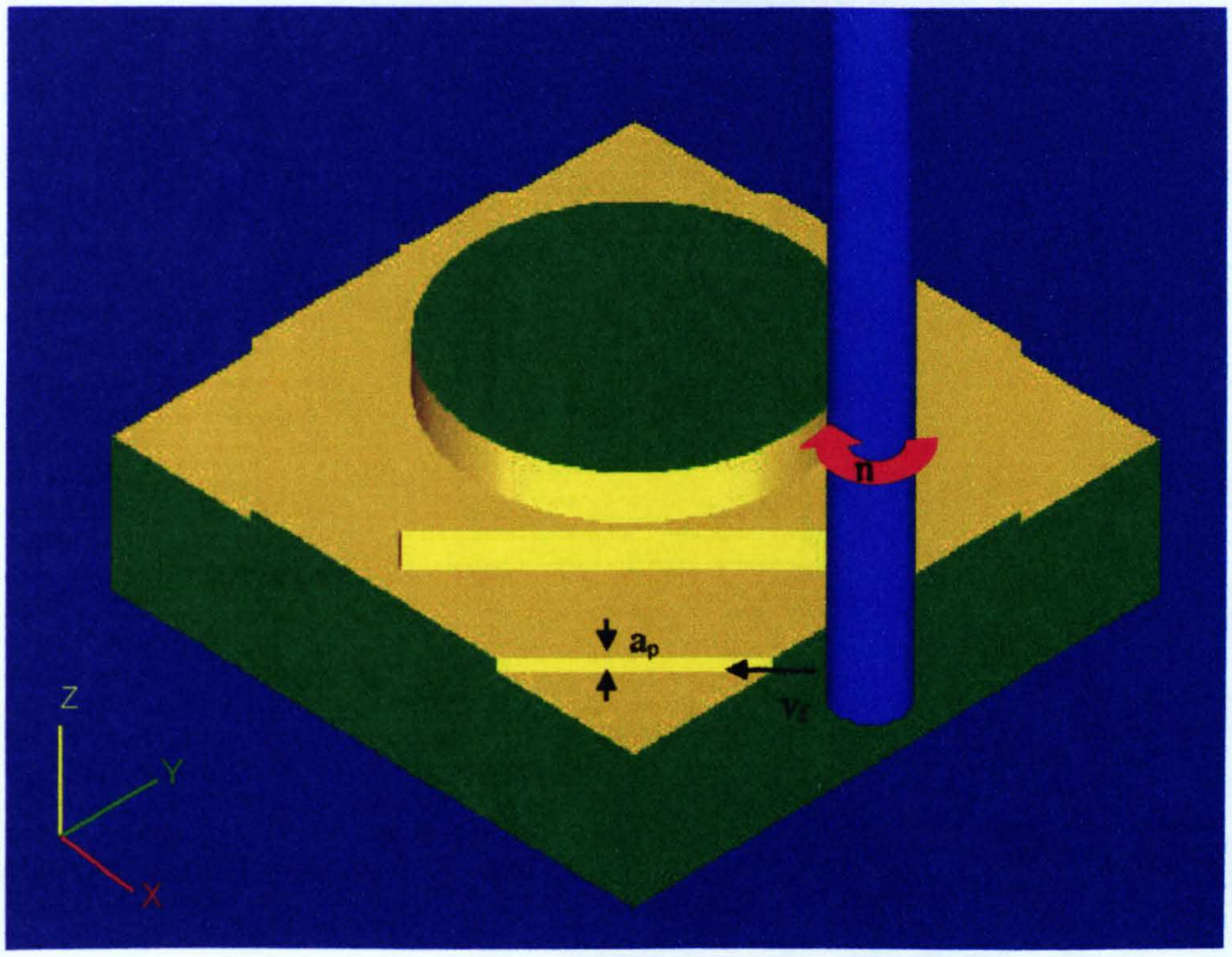

Figure 6.7 Layout of the diamond shape feature machining operation

- Finally, the outer square of the micro-testpiece was then machined via the layout illustrated in Figure 6.8.

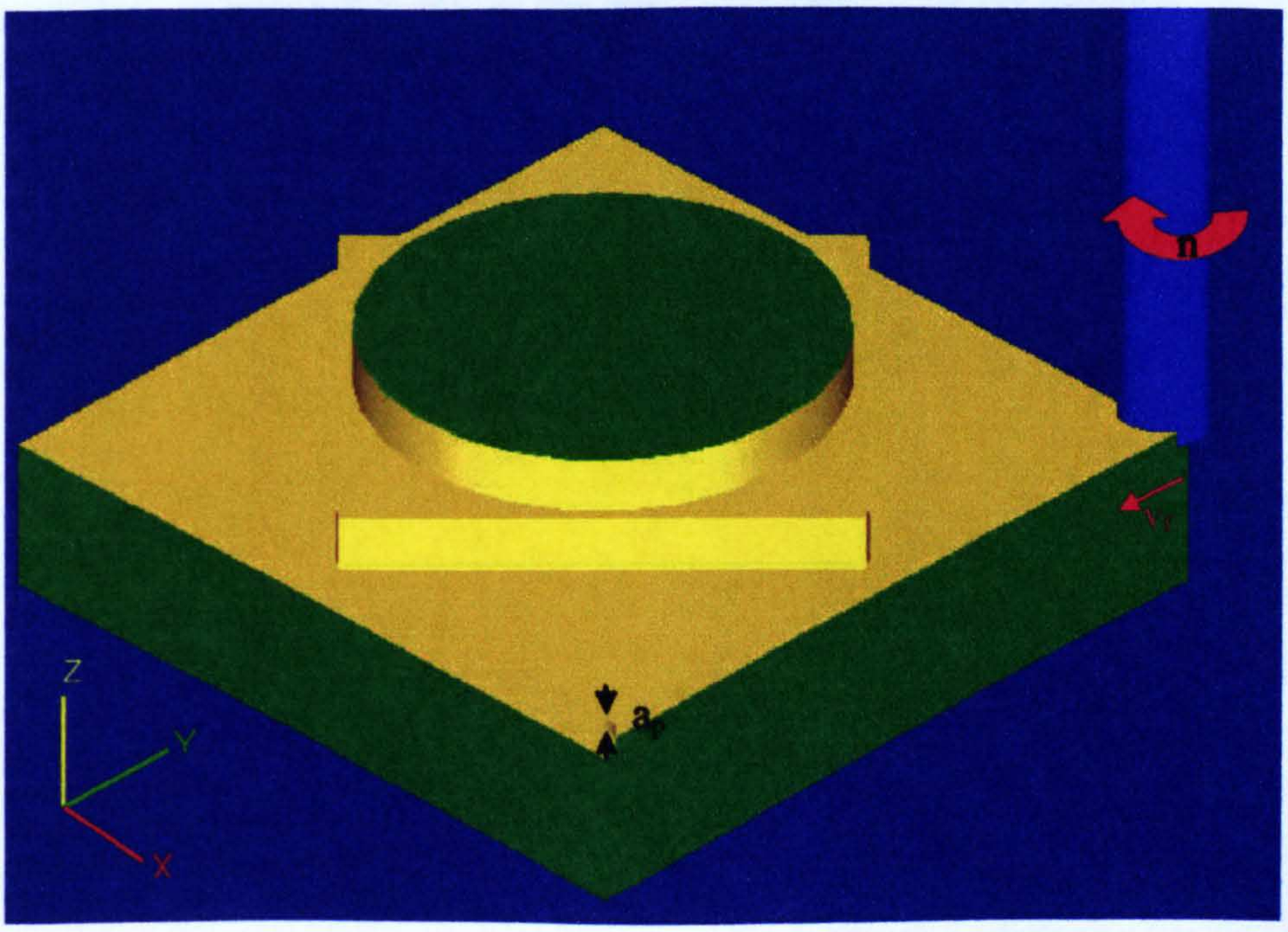

Figure 6.8 Layout of the outer square machining operation

In this study, the 'adapted-standard' micro-testpiece was generated in two different materials which were the AISI 1040 and TiAl6V4. The milling process of the micro-testpiece was based on the recommended machining parameters from the tools manufacturers and also as suggested in previous study related to micro-milling [39, 131, 134, 149, 179]. The cutting tool used was Ø=0.6mm end mill (R216.32-00630-AE06G 1620 Coromill Plura) from Sandvik Coromant.

Table 6.3 Machining parameters in generating micro-testpiece

Parameters	Material	
	AISI 1040	TiAl6V4
n (min^{-1})	50000	48000
f_z (mm)	0.011	0.010
a_p (mm)	0.03	0.03
a_e (mm)	0.03	0.03
V_f (mm/min)	1100	960
V_c (m/min)	94	90

6.3.1.2. Results and discussion

In Figure 6.9, optical images of the machined micro-testpieces ((a) – AISI 1040 and (b) – TiAl6V4) at x50 magnification from a Keyence VHX-Optical Digital Microscope are shown. From here, by observing the "as-machined" surfaces, it shows that no major defects (e.g. scratches) were found while the geometry looked clearly defined. In-depth analysis to investigate the significant features stated in ***Chapter 3*** such as circularity with the inner circle, linearity or straightness of the outer square, perpendicularity at the corners, angular accuracy and parallelism with the opposite sides of a square the machined

micro-testpieces were further evaluated under a CMM - The Zeiss F25 and Keyence VHX-Optical Digital Microscope.

Surface quality analysis was carried out using a Taylor Hobson Talysurf CLI 1000. The mechanism of analysing geometrical accuracy and surface roughness has been outlined in ***Chapter 3*** and results will be discussed in the following paragraphs.

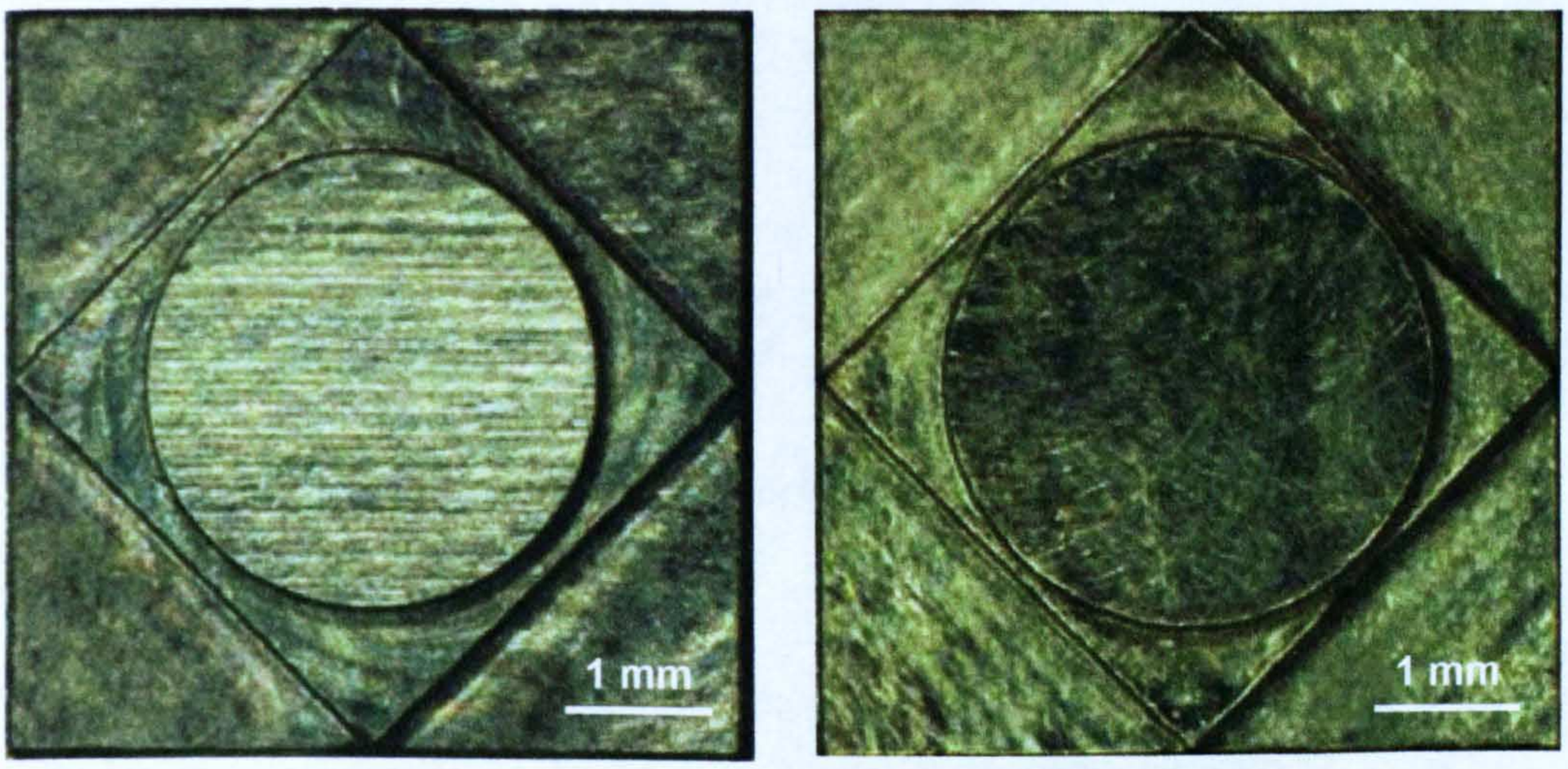

(a) AISI 1040 (b) TiAl6V4

Figure 6.9 Machined micro-testpieces

Surface quality results

The surface roughness of the machined micro-testpieces was measured over a sampling length of 0.8mm and a cut-off length of 0.04mm. The parameters used to evaluate the surface roughness were the arithmetic average roughness (R_a) and also the average maximum height of the analysed profile (R_z). Figure 6.10 illustrates the obtained R_a and R_z from the measurements made on both samples (AISI 1040 and TiAl6V4).

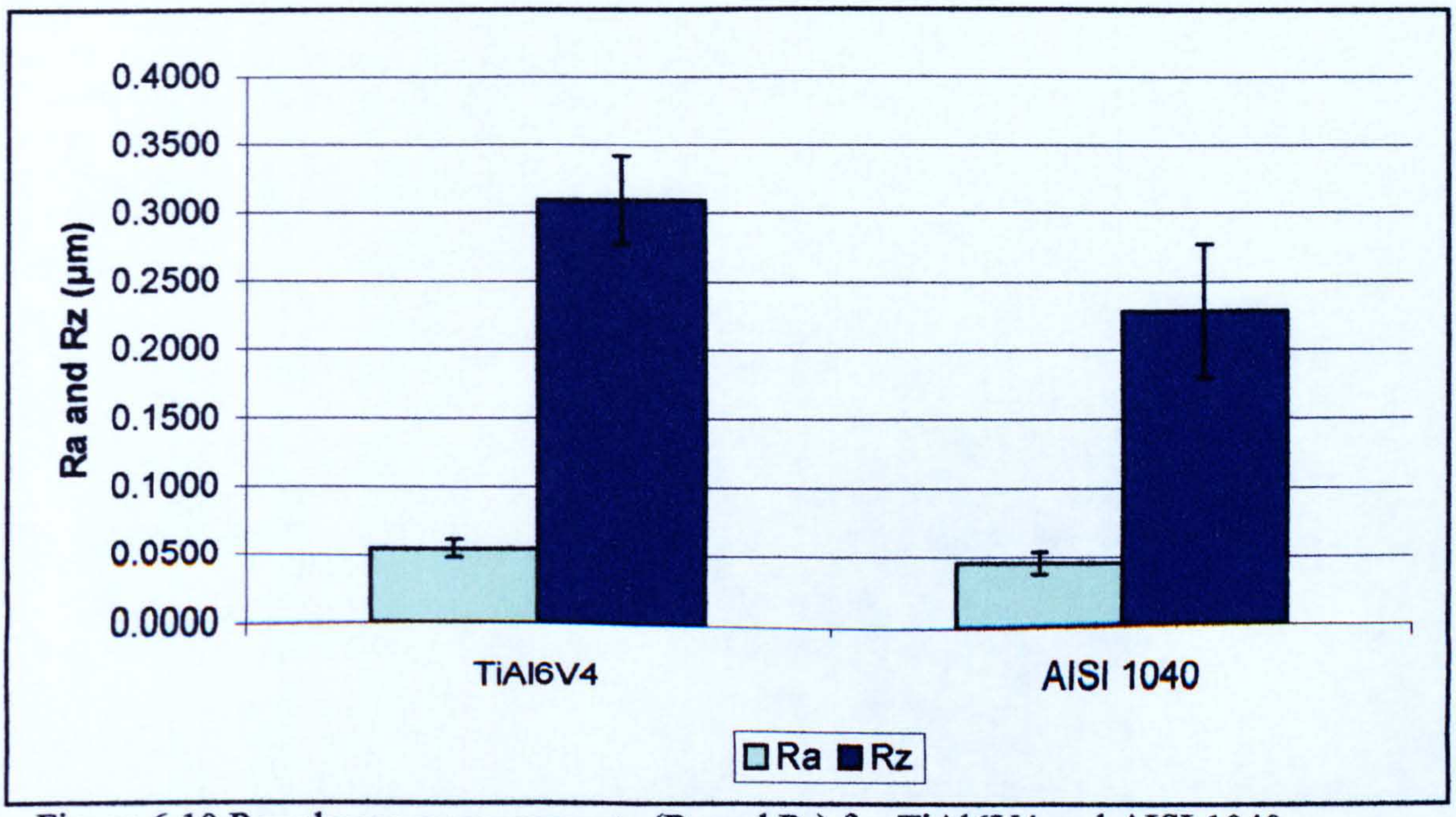

Figure 6.10 Roughness measurements (R_a and R_z) for TiAl6V4 and AISI 1040

Although it was not the scope of this work to obtain optimised cutting parameters for surface roughness, the measured R_a values varied between 0.04-0.07µm with higher values related to the surfaces generated towards the end of tool path (length cut of 129mm, machining time: approximately 42 min). By comparing the results above with the previous study in producing micro-parts, it can be concluded that the MMT is capable to produce an acceptable value of R_a and R_z based on the recommended machining parameters from the tool manufacturers on a micro-level machining. This observation is referring to work by Wuele [149] that has achieved 0.5µm for R_z while Dimov et. al. [34] has managed to produce R_a between 0.13 and 0.44 µm and Vogler [36] with R_a between 0.10 and 0.25µm. These comparable results show that the use of the custom-made MMT does not hinder the micro-milling process to produce a good and satisfactory surface quality.

Geometrical accuracy results

For the verification of the geometrical criteria mentioned in ***Chapter 3***, a Coordinate Measuring Machine (CMM) - Zeiss F25 with a 0.3mm probe was used to analyse the AISI 1040 sample. The results (expressed at 95% confidence interval) obtained from the subsequent highly accurate CMM evaluation can be summarised as in Table 6.4.

Table 6.4 CMM results for AISI 1040 micro-testpiece

Geometrical criteria	**Result**
Roundness of the cylinder centred in O	0.0052 mm
Straightness deviation of the sides of the squares (ABCD and EFGH)	<0.0001mm
Deviations from perpendicularity of the two adjacent sides of the squares (ABCD and EFGH)	<0.0040 degree
Angular deviations of the angles (45deg.) between the sides of squares ABCD and EFGH	<0.0010 degree
Flatness of the top of the cylinder centred in O	0.0012 mm

From these results, it can be noted that satisfactory geometrical accuracies of micro-components can be achieved using the particular MMT. Based on this, it was considered adequate to analyse the geometrical accuracy of the TiAl6V4 micro-testpiece using a Keyence VHX-Optical Digital Microscope. Table 6.5 shows the result of the measurement made based on the aspects discussed in ***Chapter 3*** such as $\emptyset_{Cylinder}$; $\angle A, \angle B, \angle C$ and $\angle D; \angle FEC$; $\|AB\|$, $\|AC\|$, $\|CD\|$ and $\|BD\|$. For each measurement, the average value was presented together with the calculated standard deviation (3σ - 99% of confidence interval).

Table 6.5 Results from the microscope analysis on TiAl6V4

Aspect	Result
$Ø_{Cylinder}$ (mm)	3.1047 ± 0.0062
$\angle FEC$ (degree)	45.0225 ± 0.5314
$\angle A$ (degree)	90.4433 ± 0.7677
$\angle B$ (degree)	89.9833 ± 0.6169
$\angle C$ (degree)	89.6267 ± 0.1644
$\angle D$ (degree)	90.0100 ± 0.3119
‖AB‖ (mm)	4.5068 ± 0.0095
‖CD‖ (mm)	4.4894 ± 0.0030
‖AC‖ (mm)	4.5221 ± 0.0064
‖BD‖(mm)	4.5154 ± 0.0217

Based on these results, it can be noted that the achieved dimensions deviated from their original by less than 5% which was likely caused by the tool wear. From here, once again, it can be concluded that acceptable geometrical accuracies of micro-parts can be achieved using the in-house developed MMT.

6.3.2. Machining micro-slots and thin wall

The main objective of this experiment was to study the capability of the MMT in producing micro-slots and thin walls in various materials using different size of cutting tools (Ø = 0.5mm, 0.6mm and 0.8mm). Furthermore, it also aimed to populate important information for the developed MicroMAS in terms of surface quality (MI_{Ra}) and tolerance (MI_{TOL}). Figure 3.13 shows the illustration of the proposed micro-slots, thin walls and surface profiling area (A_{Ra}), while Table 3.4 presents their dimensions.

6.3.2.1. Machining procedures and parameters

The experimental procedures in producing the thin walls and micro-slots are described as the following:

- In order to ensure that the top surface of the workpiece is flat, the workpiece was machined based on the layout of the facing operation shown in Figure 6.11(a). While Figure 6.11(b) presented the layout of the machining operation in ensuring that the surface of both sides where the micro-slots are being milled is perpendicular and flat.

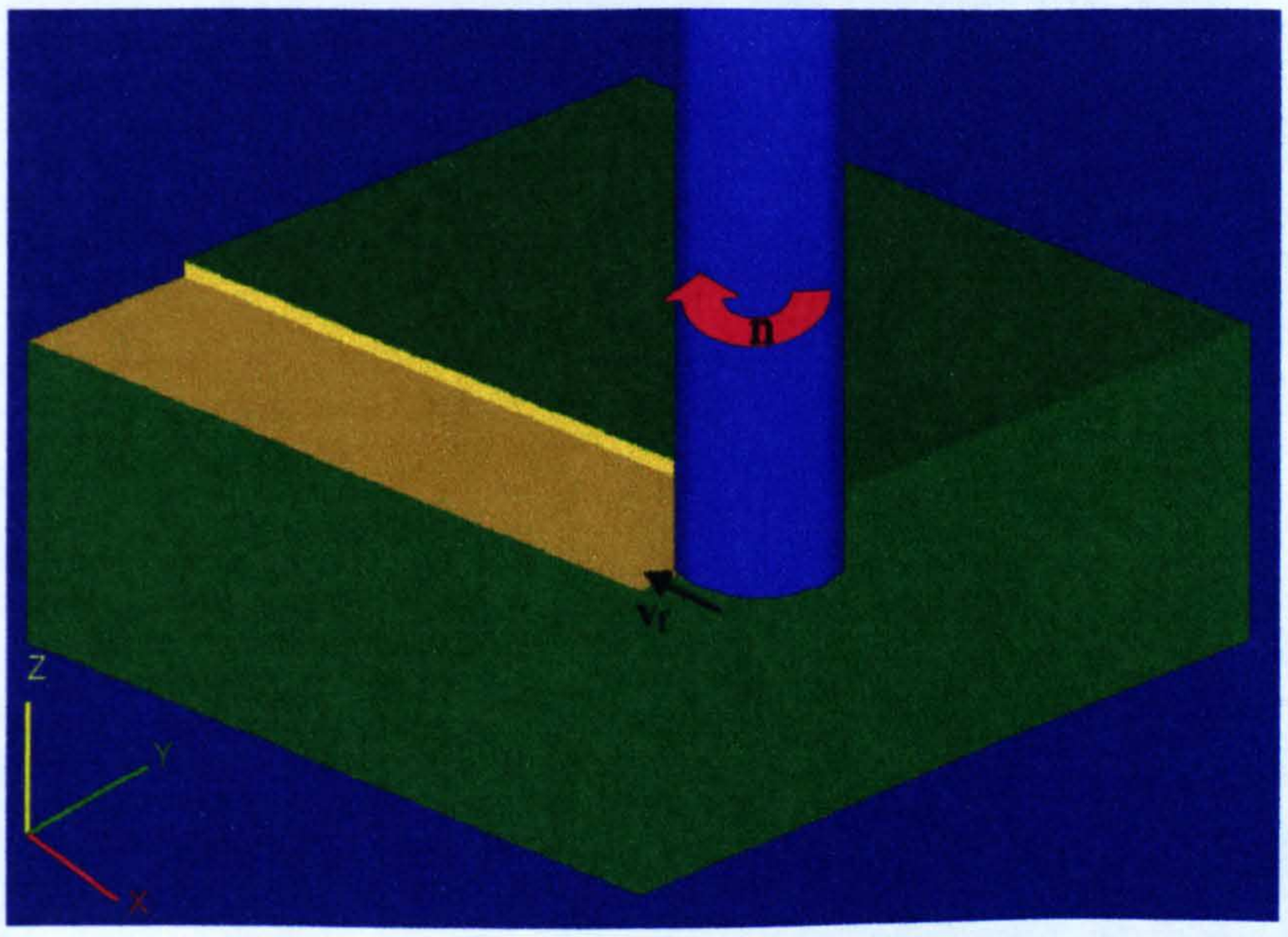

Figure 6.11(a) Top-flatness machining

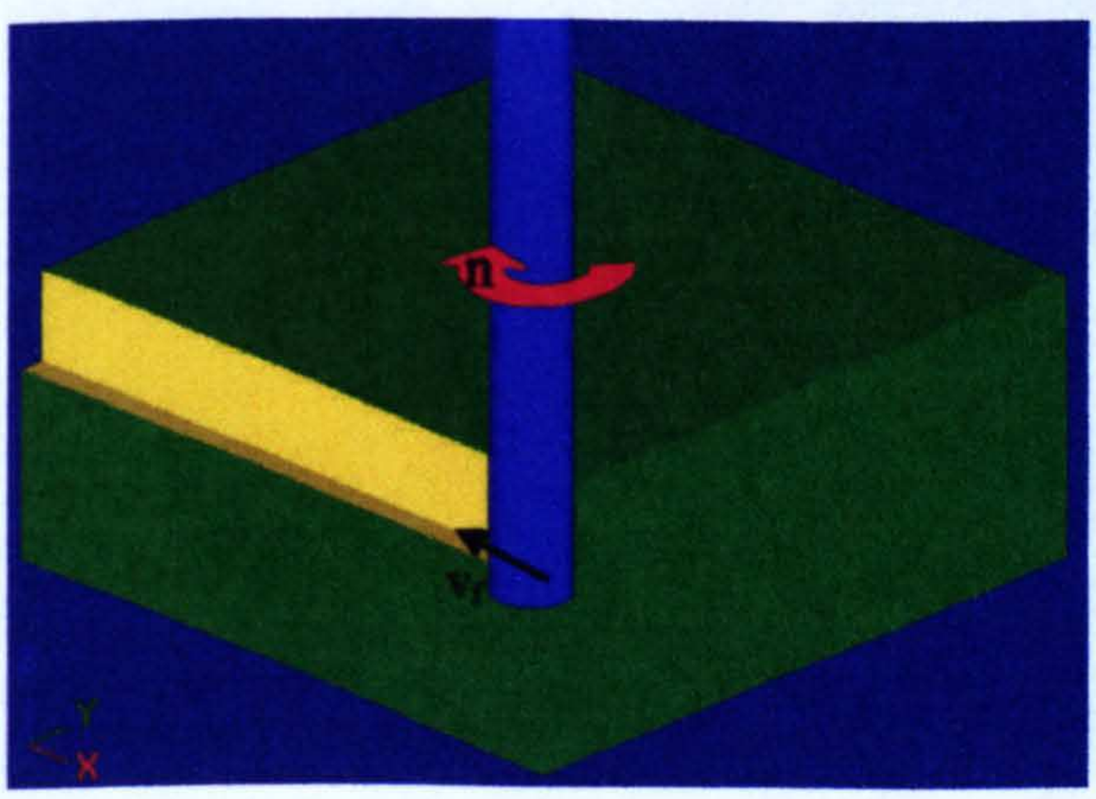

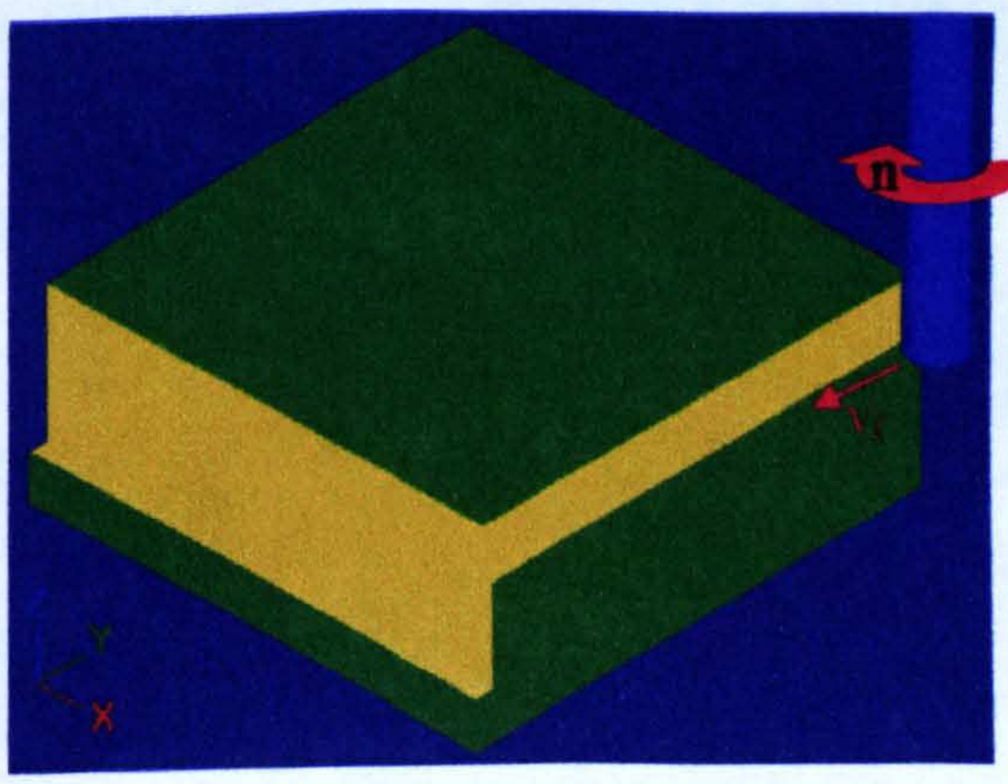

Figure 6.11(b) Side-flatness machining

- Next, the first slot was machined and followed by the second slot as presented in Figure 6.12(a) and Figure 6.12(b) respectively. The machining parameters used for generating micro-slots and thin walls are presented in Table 6.6. The cutting approach implemented in machining both slots is up-milling. The slots are being cut layer by layer based on the selected axial depth of cut value (a_p). For each layer, the number of cuts varied based on the size of the tool, the selected radial depth of cut value (a_e) and also the width of the slots. As an example, for tool with Ø=0.5mm and the slot's width=0.6mm, the generated number of cut is 5. Figure 6.13 shows the toolpath generated for the first slot based on the cutting approach discussed. Additionally, the suggested strategies in machining thin features made by Popov *et al.* [128] which proposed to machine from the least supported area towards the best supported thin features in a component.

- Finally, for the purpose of surface profiling analysis, the end part of the workpiece was surface-machined (Figure 6.12(c)). For this particular area (AR_a), the radial and axial depths of cut (a_e and a_p) were halved from the suggested machining parameters (as mentioned below) that have been used to machine the micro-slots.

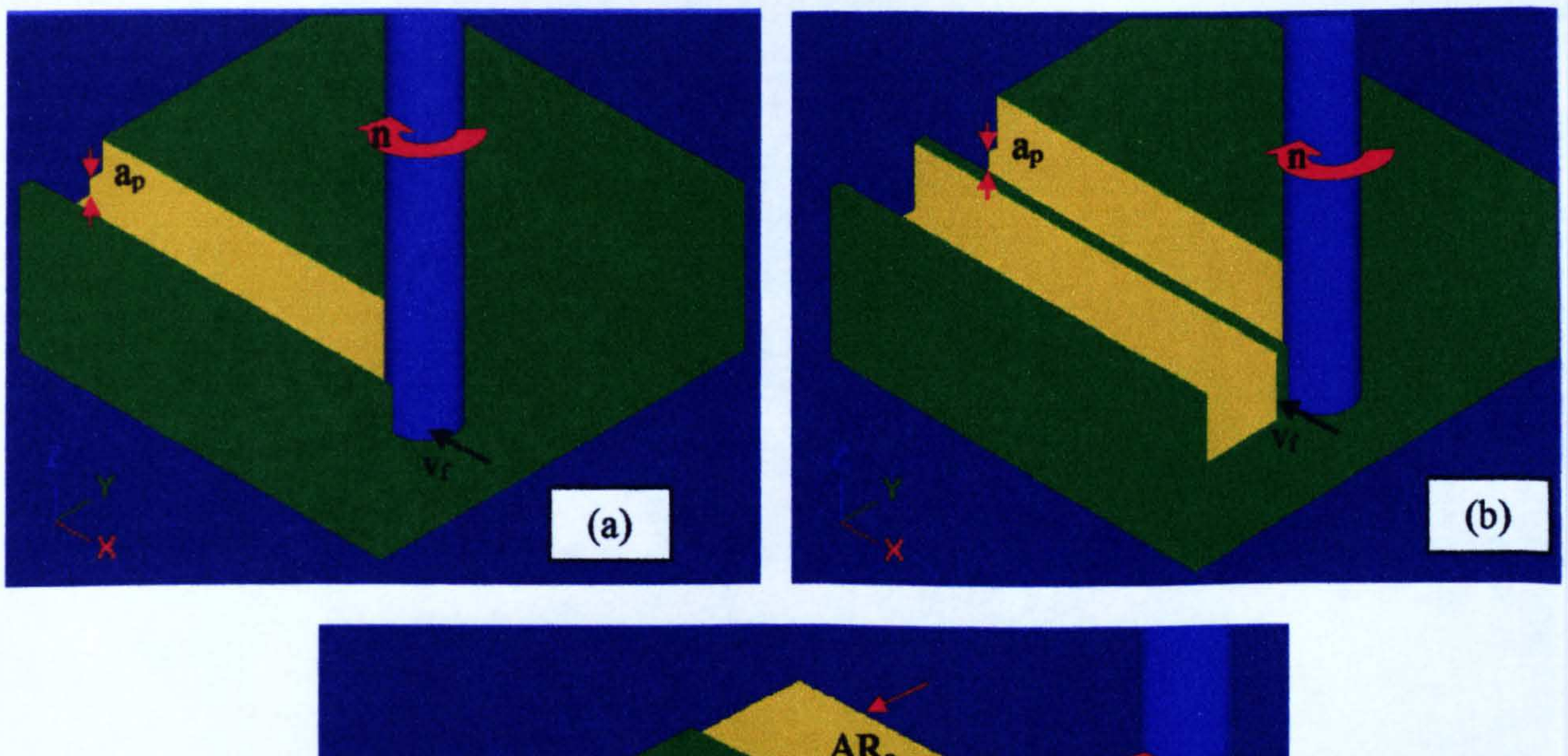

Figure 6.12 Experimental procedures in producing thin wall, slots and surface profile area (AR_a)

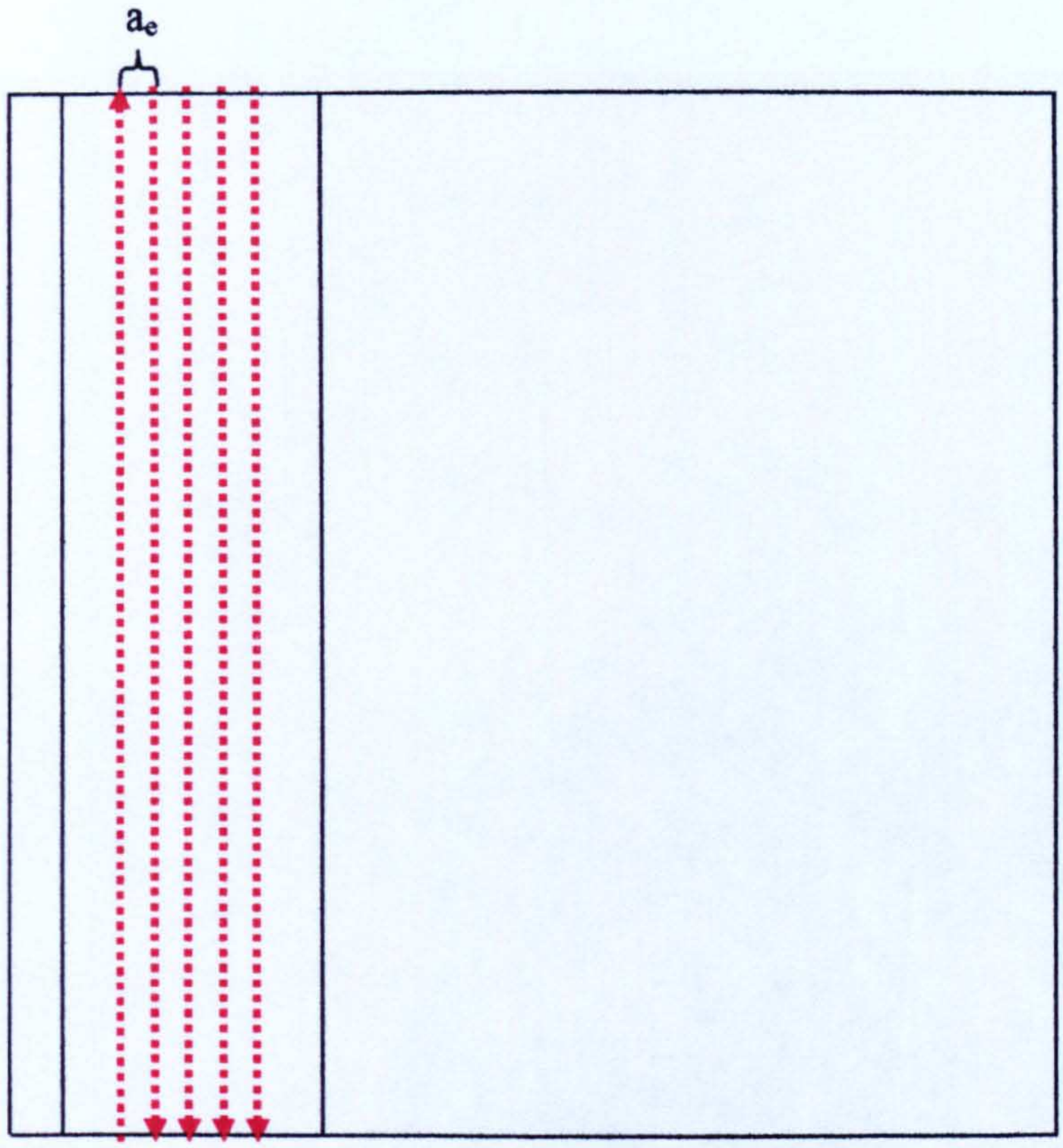

Figure 6.13 Cutting approach for Ø=0.5mm cutter

The above workpieces were machined in two different materials (316L and TiAl6V4) based on the recommended machining parameters from the tools manufacturers and also as suggested in previous related literature [128, 134, 158, 161, 178-180]. Table 6.6 shows the machining parameters employed in a wet condition environment (coolant: Hocut 3380) for both materials using micro-end mill cutters from Sandvik Coromant with Ø=0.5mm (R216.32-00530-AE05G 1620 Coromill Plura), Ø=0.6mm (R216.32-00630-AE06G 1620 Coromill Plura) and Ø=0.8mm (R216.32-00830-AE08G 1620 Coromill Plura).

Table 6.6 Machining parameters implemented in machining micro-slots and thin wall

Type of material	Tool Ø	n (min^{-1})	f_z (mm)	a_p (mm)	a_e (mm)	V_f (mm/ min)	V_c (m/ min)
316L	0.5	45000	0.006	0.025	0.025	540	70
	0.6	38000	0.006	0.030	0.030	456	
	0.8	28000	0.007	0.040	0.040	392	
TiAl6V4	0.5	38000	0.006	0.025	0.025	456	60
	0.6	32000	0.006	0.030	0.030	384	
	0.8	24000	0.007	0.040	0.040	336	

6.3.2.2. Results and discussion

Figure 6.14 shows the completed machined micro-slots and thin wall magnified under the optical microscope at magnification of x100 – x175 for 316L and TiAl6V4 in using different cutter size (ø= 0.5 – 0.8 mm).

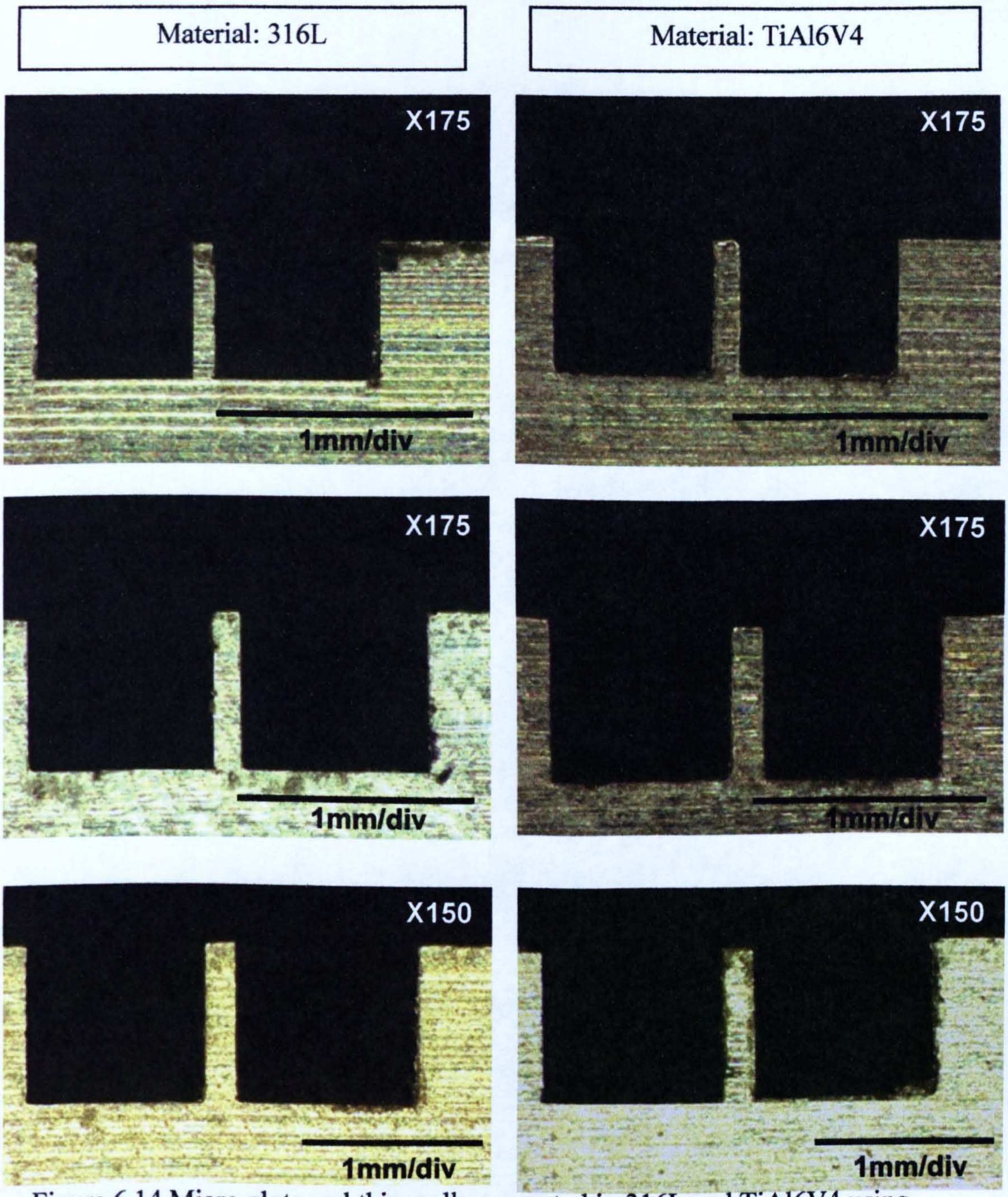

Figure 6.14 Micro-slots and thin walls generated in 316L and TiAl6V4 using Ø=0.5, 0.6 and 0.8 mm.

From the examination of the "as-machined" surfaces, it can be noted that the generated micro-slots and thin wall are flat and straight, the corners of the thin wall are sharp and there are no major defects at the surface profile area. This

indicates that the MMT basically can machine the proposed thin wall and micro-slots.

The surface roughness of the surface profiling area (A_{Ra}) was measured using a Talysurf CLI 1000 over a sampling length of 0.8mm and a cut-off length of 0.025mm. In order to assess the machined workpieces in details (e.g. width of the thin walls, perpendicularity at the corner for both sides of the thin wall's base), a Keyence VHX-Optical Digital Microscope was employed to analyse the geometrical accuracy.

Surface quality result

From the surface analysis being done, the results of the averaged surface roughness R_a and R_z are as shown in Table 6.7. Beside that, it also presents the maximum and minimum value of R_a and R_z based on the 10 measurements taken during the analysis.

Table 6.7 Surface quality result (R_a and R_z)

Type of material	Ø tool (mm)	R_a (µm)			R_z (µm)		
		Min	Max	Avg	Min	Max	Avg
316L	0.5	0.029	0.038	**0.033**	0.150	0.195	**0.171**
	0.6	0.014	0.022	**0.018**	0.087	0.136	**0.110**
	0.8	0.017	0.020	**0.019**	0.103	0.12	**0.110**
TiAl6V4	0.5	0.035	0.042	**0.039**	0.191	0.243	**0.222**
	0.6	0.040	0.057	**0.049**	0.227	0.317	**0.280**
	0.8	0.031	0.051	**0.039**	0.192	0.305	**0.232**

Legend: Max=Maximum, Min=Minimum, Avg=Average

Figure 6.15 presents the graph showing the R_a and R_z values for all the machined samples in this study. Each sample was given a unique identity to differentiate the material and its cutters size (e.g. Ti64-08 means the material is TiAl6V4 and the tool is Ø=0.8mm). The standard deviation values (3σ - 99% of confidence interval) are also included (as illustrated by the error bars in the graph).

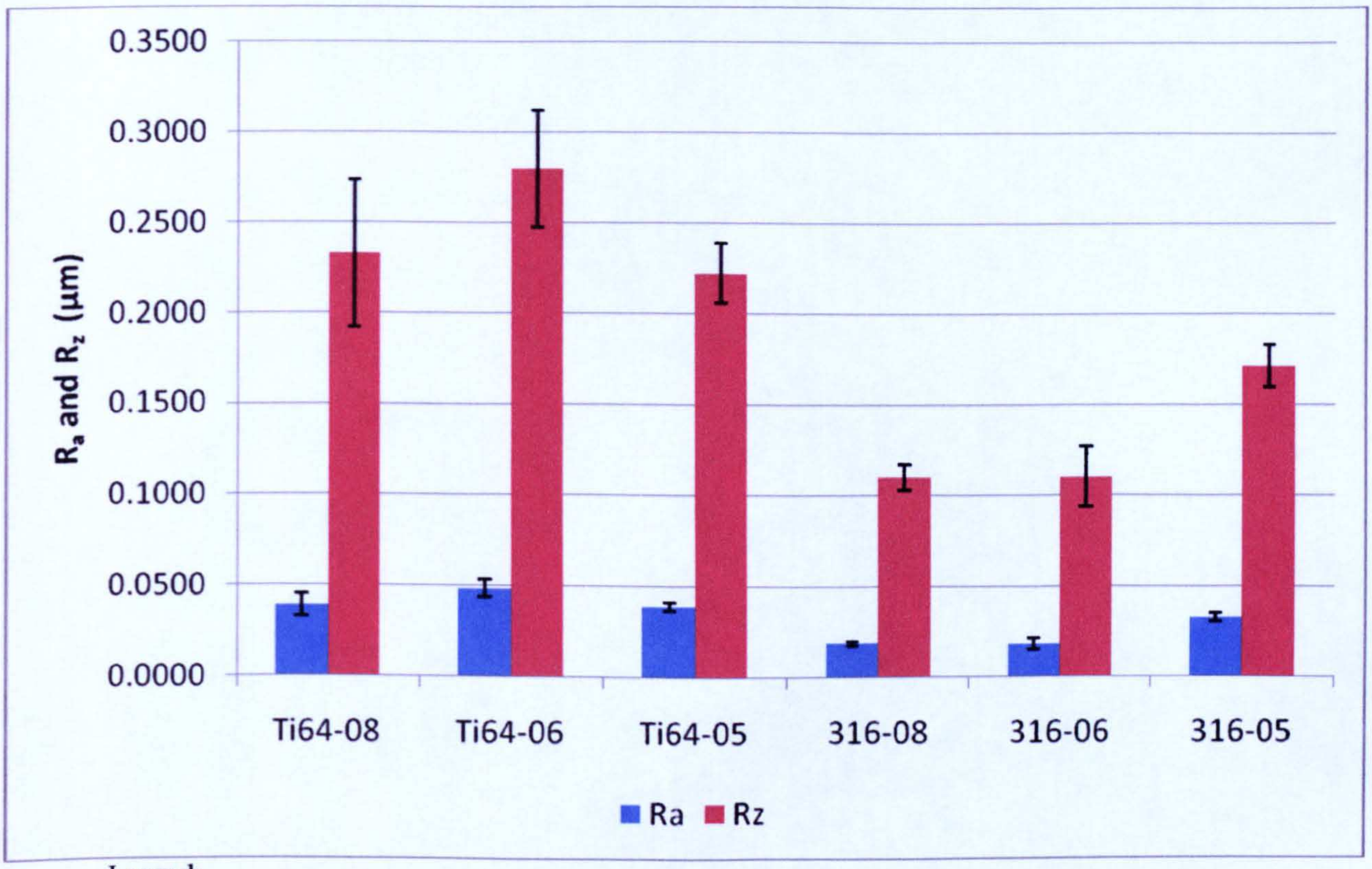

Legend:

Sample	Material	Tool Ø (mm)	Sample	Material	Tool Ø (mm)
Ti64-08	TiAl6V4	0.8	**316-08**	316L	0.8
Ti64-06		0.6	**316-06**		0.6
Ti64-05		0.5	**316-05**		0.5

Figure 6.15 Graph of the average value of R_a and R_z

The overall results of this study show that the achieved R_a in this experiment were between 0.02 and 0.06 µm with higher values associated to the surfaces

generated towards the end of the tool path (length cut: varied between 5.3 – 6.7m), while the obtained R_z were between 0.1 and 0.3 μm (machining time: approximately between 14 and 17 minutes varied for each workpiece). From Figure 6.15, it can be noted that the measured R_a for TiAl6V4 are higher than 316L, this is the direct consequences of the development of tool wear. For TiAl6V4, the obtained R_a was measured between 31% - 42% of its tool life while for 316L was between 14% and 19%. As an example, for tool Ø=0.5mm, the length of cut to machine the micro-slots, thin wall and surface profiling are was 6.7m, while the total length of cut of the tool for TiAl6V4 was 16m and 35 m for 316L. This means, the calculated tool life for machining the TiAl6V4 was 42% and for 316L, 19%. This explains the significant differences which were found in the obtained R_a between both materials.

Furthermore, by comparing these results (R_a and R_z) with those from the published literature in relation to the machining of micro-parts (e.g. thin feature) [34, 36, 149], the obtained R_a and R_z in this study can be considered as good and in an acceptable range. These comparable results show that the use of the custom-made MMT does not prevent the micro-milling process from generating a satisfactory surface quality after machining micro-slots and thin wall.

From this analysis, the obtained values of R_a were exploited in generating an index range for the MI_{Ra}. For this purpose, the average values of R_a were considered as the nominal values for the particular index range according to the type of workpiece material and also cutter size. As described in ***section 4.5***, the

selected nominal value will be considered as ***medium to manufacture*** level in the MicroMAS analysis with MI_{Ra} = 1.0. As an example, based on the above experimental results, Figure 6.16 presents the generated MI_{Ra} for 316L with the nominal value for tool with Ø=0.5mm being 0.033μm, Ø=0.6mm is 0.018μm and Ø=0.8mm, 0.019μm (as highlighted). The details of the generated index range for MI_{Ra} were discussed in Chapter 4.

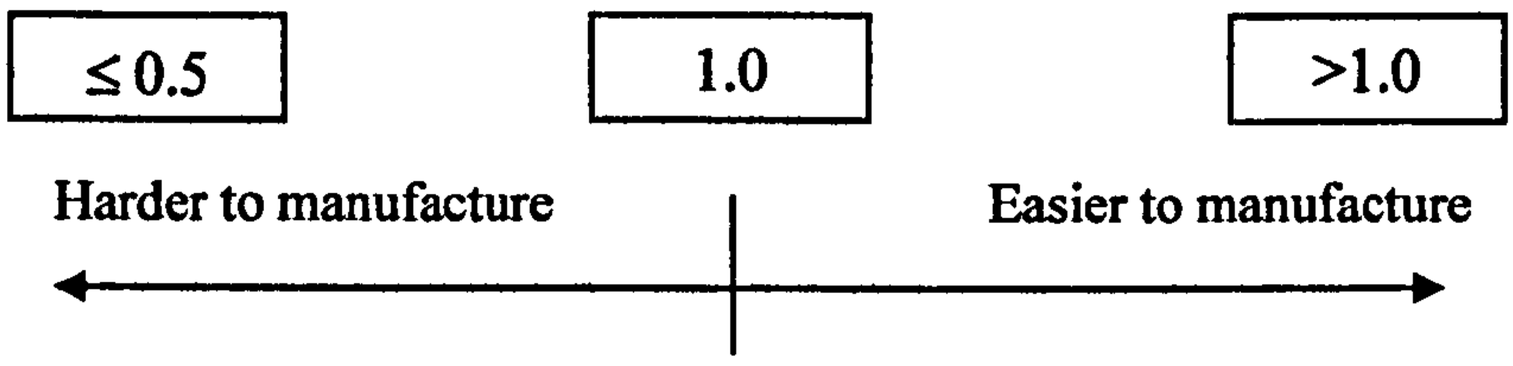

Tool Ø (mm)	R_a (in μm)		
0.5	0.016	0.033	0.043
0.6	0.008	0.018	0.028
0.8	0.009	0.019	0.029

Figure 6.16 Example of the generated MI_{Ra} range for 316L

Geometrical accuracy results

In order to further analyse the geometrical accuracy of the generated micro-slots and thin walls, the samples were being measured under an optical microscope for the width of slot 1, slot 2 and thin wall (W_1, W_2, W_{TW}), height of the thin wall (H_{TW}) and the angles at the base of thin walls (α_1, α_2). The standard deviation values (3σ - 99% of confidence interval) were also included. The analysis of the measurement results are divided into 3 sections: Table 6.8 for W_1 and W_2, Table 6.9 for W_{TW} and H_{TW} and finally Table 6.10 for α_1 and α_2.

Table 6.8 Measurements result for W_1 and W_2

Material	316			TiAl6V4		
Tool Ø (mm)	0.5	0.6	0.8	0.5	0.6	0.8
W_1						
Nominal dimension (mm)	0.600	0.720	0.960	0.600	0.720	0.960
Average (mm)	0.619	0.736	0.970	0.616	0.728	0.969
Std. Dev. (mm)	0.004	0.003	0.005	0.003	0.004	0.002
Deviation from nominal (mm)	0.019	0.016	0.010	0.016	0.008	0.009
% deviation relative to nominal	**3.13**	**2.17**	**0.99**	**2.70**	**1.10**	**0.92**
W_2						
Nominal dimension (mm)	0.600	0.720	0.960	0.600	0.720	0.960
Average (mm)	0.612	0.735	0.964	0.615	0.722	0.968
Std. Dev. (mm)	0.005	0.003	0.005	0.004	0.005	0.034
Deviation from nominal (mm)	0.012	0.015	0.004	0.015	0.002	0.008
% deviation relative to nominal	**1.97**	**2.06**	**0.43**	**2.45**	**0.26**	**0.80**

Based on the analysis from the tables, it can be concluded that the accuracies of the generated micro-slots were basically satisfactory in terms of their geometrical accuracy. From the results, the width attribute for both slots (W_1 and W_2) deviated less than 3.2% from the nominal value with the width of W_1 being slightly higher than W_2. This is the effect of the development of tool wear as the W_1 is machined first followed by W_2. The machining time for each slot is approximately between 2 and 4 min depending on the size of the slot (e.g. 0.60, 0.72, 0.96mm).

Table 6.9 Measurements results for W_{TW} and H_{TW}

Material	316			TiAl6V4		
Tool Ø (mm)	0.5	0.6	0.8	0.5	0.6	0.8
W_{TW}						
Nominal dimension (mm)	0.1000	0.120	0.160	0.100	0.120	0.160
Average (mm)	0.1003	0.1218	0.1604	0.1089	0.1285	0.1676
Std. Dev. (mm)	0.0027	0.0039	0.0020	0.0029	0.0030	0.0036
Deviation from nominal (mm)	0.0003	0.0018	0.0004	0.0089	0.0085	0.0076
% deviation relative to nominal	**0.3**	**1.5**	**0.25**	**8.9**	**7.08**	**4.75**
H_{TW}						
Nominal dimension (mm)	0.500	0.600	0.800	0.500	0.600	0.800
Average (mm)	0.495	0.592	0.793	0.498	0.593	0.796
Std. Dev. (mm)	0.004	0.003	0.005	0.003	0.003	0.003
Deviation from nominal (mm)	-0.005	-0.009	-0.007	-0.006	-0.008	-0.004
% deviation relative to nominal	**-1.08**	**-1.71**	**-1.35**	**-1.26**	**-1.51**	**-0.87**

From the analysis of Table 6.9 it could be noted that all W_{TW} are larger than the nominal dimension and there are considerable differences between the materials. The obtained W_{TW} for 316L are considered to be in a better conformity with the nominal value compared to TiAl6V4. This can be noted from the deviation stated in Table 6.10 where for 316L the percentage is less than 2% while it is between 4% and 9% for TiAl6V4. This result is attributed due to tool wear as it caused the sharp edge of the tool to become blunt. This leads to an increase of the cutting forces which create tool deflections and the geometric accuracy of the part deteriorates. Another possibility is the deviation of the tool diameter from the nominal value where the tolerance range for the

tool according to the manufacturer is 0; -0.04mm. However, there are no significant differences between the materials in the height aspect where H_{TW} for the thin wall are smaller than the nominal dimension by less than 2%.

Table 6.10 Measurement results for α_1 and α_2

Material	316					
Tool Ø (mm)	0.5		0.6		0.8	
Angles	α_1	α_2	α_1	A_2	α_1	α_2
Nominal dimension (°)	90.00	90.00	90.00	90.00	90.00	90.00
Average (mm)	90.48	90.75	90.16	90.77	90.70	90.83
Std. Dev. (mm)	0.346	0.141	0.156	0.163	0.085	0.071
Deviation from nominal	0.48	0.75	0.16	0.77	0.70	0.83
% deviation relative to nominal	**0.52**	**0.83**	**0.18**	**0.85**	**0.78**	**0.92**
TiAl6V4						
Angles	α_1	α_2	α_1	A_2	α_1	α_2
Nominal dimension (°)	90.00	90.00	90.00	90.00	90.00	90.00
Average (mm)	90.28	90.73	89.99	90.56	90.10	90.62
Std. Dev. (mm)	0.099	0.078	0.021	0.332	0.078	0.113
Deviation from nominal	0.28	0.73	0.01	0.56	0.10	0.62
% deviation relative to nominal	**0.31**	**0.81**	**0.01**	**0.62**	**0.11**	**0.69**

Based on results' analysis of α_1 and α_2 as shown in Table 6.10, it can be noted that the deviation from the perpendicularity for both angles are more than the nominal value by below 1%. It can be concluded that the generated thin wall did not show any sign of bending and has a satisfactory level of straightness. Finally, from the exploration on the geometrical accuracy of the machined

micro-slots and thin walls, it can be concluded that the MMT is capable to produce a high quality of such features (e.g. straight and geometrically accurate thin wall and micro-slots).

The results from the geometrical accuracy analysis above were extracted to generate the index for MI_{TOL} in MicroMAS. The values of the generated standard deviations were selected as the nominal values for MI_{TOL} which were divided according to the different feature size range. The determination of the feature size range was established on the variety of dimensions of the generated micro-slots and thin walls (e.g. W_1, W_2, W_{TW}). As an example, Figure 6.17 presents the generated MI_{TOL} for the MicroMAS which also consider the tolerance class between 2 and 6 from the International Tolerance Grade (ITG). The detail of the generated MI_{TOL} range was presented in ***Chapter 4***.

Feature size (mm)	≤ 0.5	1.0	>1.0
	Harder to manufacture ←		→ Easier to manufacture
	Tolerance value (mm)		
0.0 – 0.5	0.0012	0.0030	0.0060
0.5 – 1.0	0.0020	0.0046	0.0070
1.0 – 1.5	0.0024	0.0049	0.0078
1.5 – 2.0	0.0030	0.0062	0.0086
> 2.0	0.0034	0.0078	0.0092
Tolerance class	2	4	6

Figure 6.17 Example of the generated MI_{TOL}

6.3.3. Machining the 'micro-component demonstrator'

In order to further assess the capability of the MMT, a micro-component that comprised of various features/shapes such as through/blind cavities, slots and bosses was also machined (Figure 6.18). Besides assessing the capability of the MMT, this micro-component demonstrator was also employed as the example of a micro-part in illustrating the function of the Primitive Feature Analysis (PFA) technique (discussed in ***Chapter 4***) and also to simulate the flow of the developed MicroMAS (***Chapter 7***). In this study, TiAl6V4 was selected as the workpiece material to generate the micro-component demonstrator.

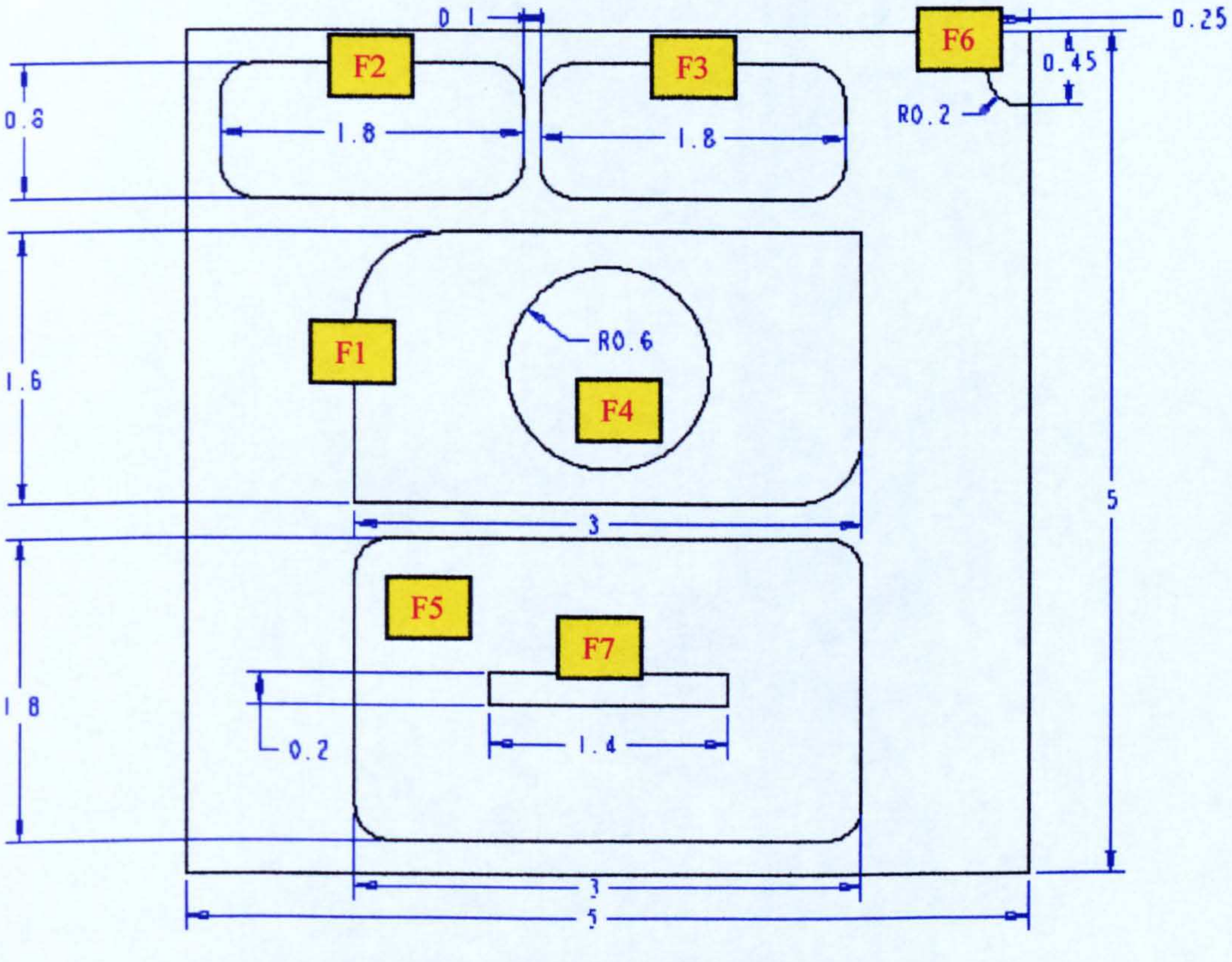

Figure 6.18 Micro-component demonstrator

6.3.3.1. Machining procedures and parameters

In order to generate this micro-component, the *contouring* and *pocketing* approaches provided in MasterCAM were selected. The procedure is described below:

- Prior to machining this micro-component, the top-flatness machining as mentioned in Figure 6.11(a) was implemented on the workpiece using the same machining strategy.
- Following this, the first feature (F1 in Figure 6.18) was machined using the machining layout as illustrated in Figure 6.19.

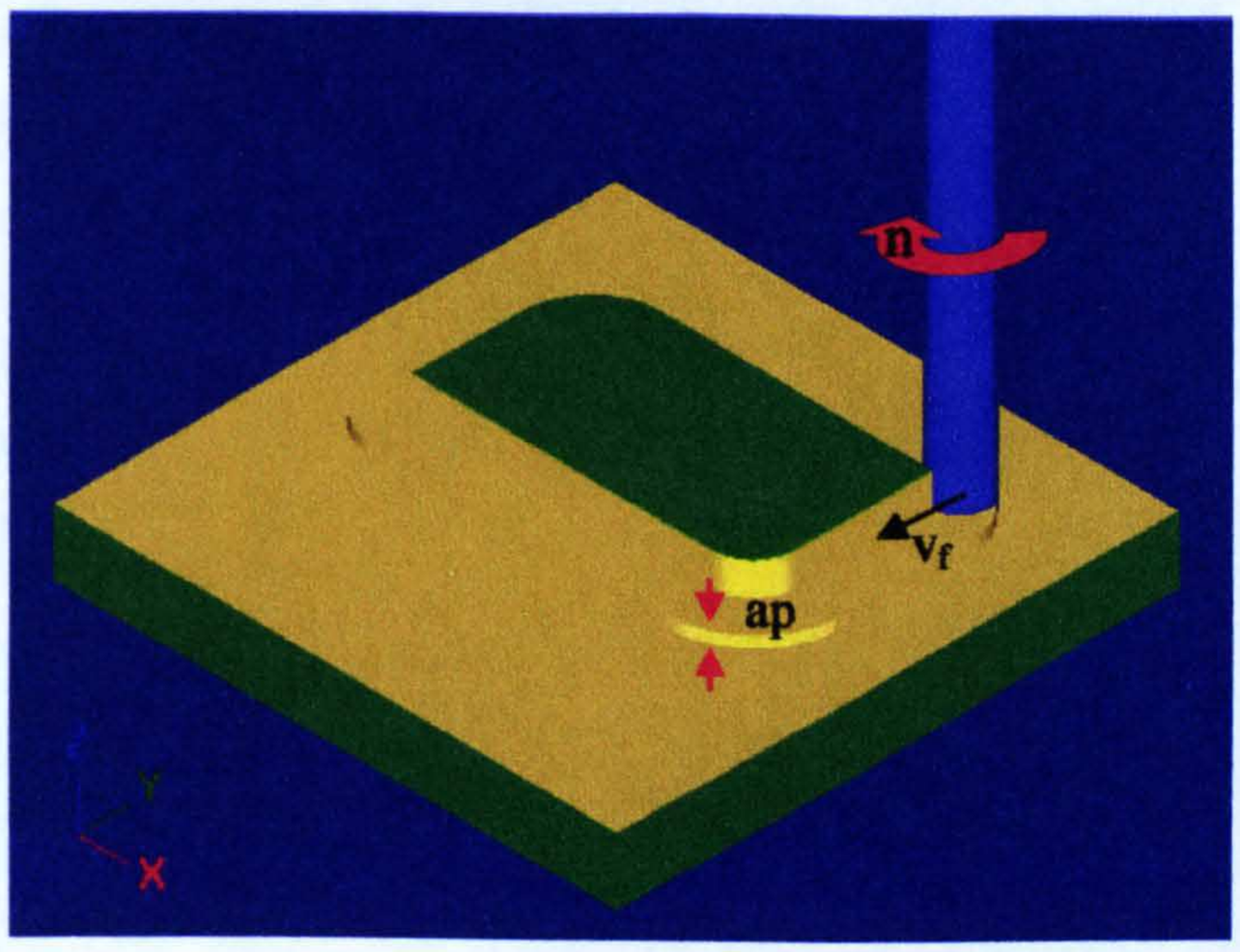

Figure 6.19 Machining F1

- Finally, by using the pocketing approach, Feature 2 to 6 (F2 – F6) were then machined using the approaches shown in Figure 6.20.

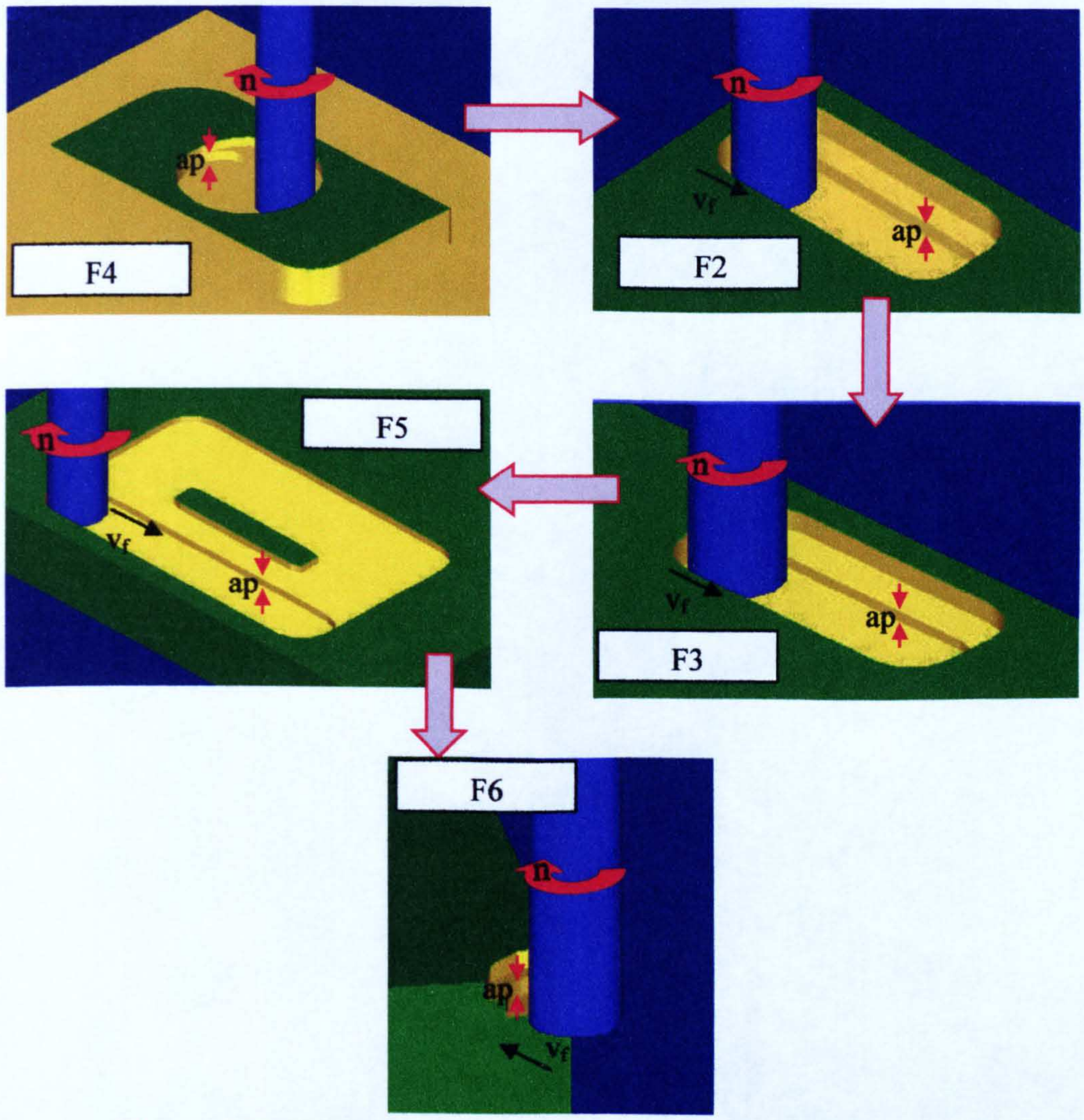

Figure 6.20 Machining strategies for Feature 2 – 6 (F2 – F6)

The workpiece shown in Figure 6.18 was machined based on the recommended machining parameters from the tool manufacturer and also as suggested in previous related literature [34, 128]. The cutter used was a micro-end mill from Sandvik Coromant Ø=0.5mm (R216.32-00530-AE05G 1620 Coromill Plura) using the cutting conditions: $n=38000min^{-1}$, $a_p=0.025mm$, $a_e=0.025mm$, $V_c=60m/min$, $f_z=0.006mm/tooth$, $V_f=456mm/min$, Hocut 3380 flood coolant supply.

6.3.3.2. Results and discussion

Figure 6.21 shows the machined micro-component magnified under an optical microscope at magnification of x50.

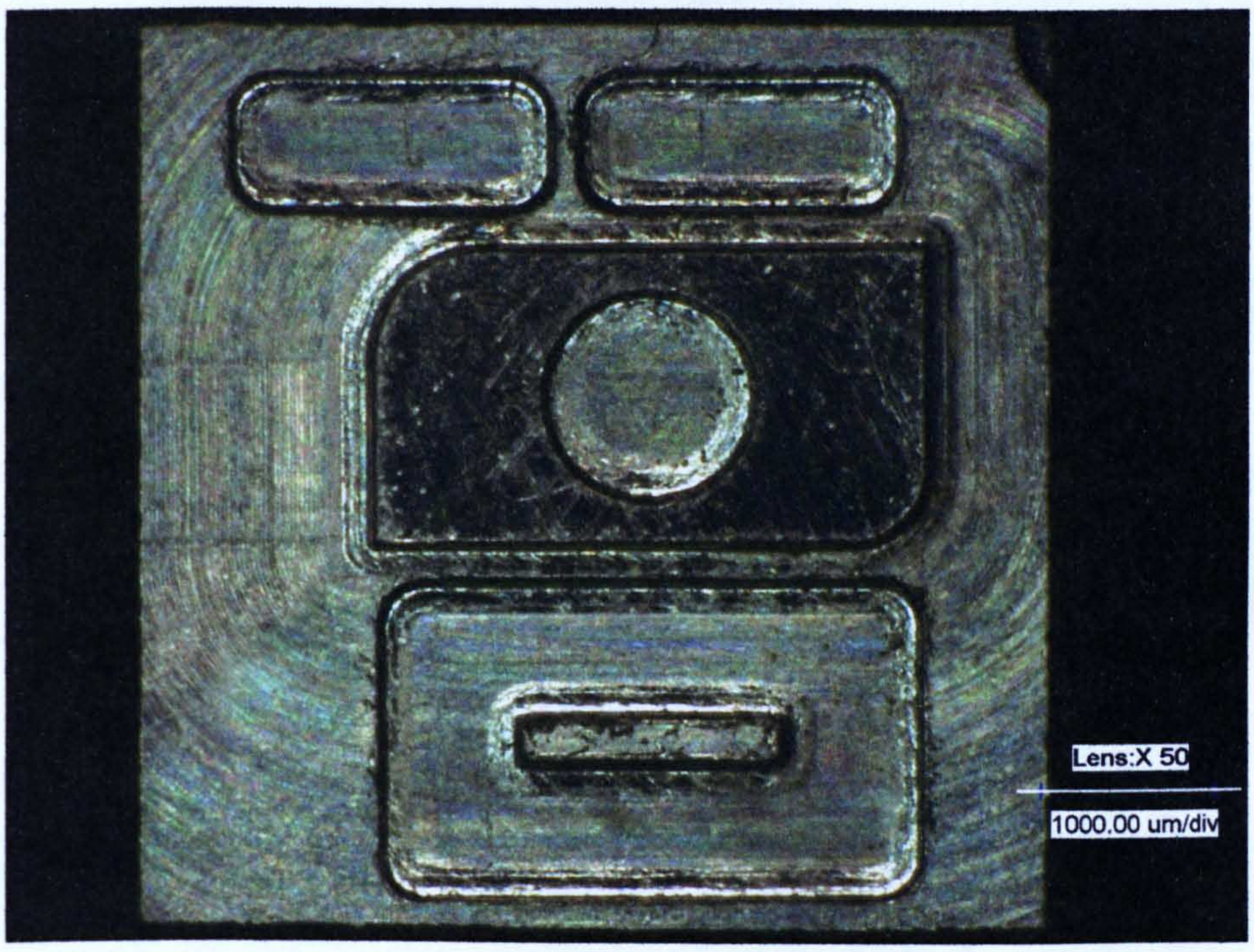

Figure 6.21 Machined micro-component

Referring to Figure 6.21, an inspection made of the "as-machined" surfaces indicated that the geometrical features of the micro-component were clearly defined and there were no obvious evidence of scratches or problems on its surfaces. The machining time for this micro-component was approximately 28 min. Analysis on its surface quality and geometrical accuracy will be discussed in the next paragraphs.

Surface quality results

The surface roughness of four different areas of the machined micro-part (F2, F3, F5, outer part of F1 – as highlighted in ***Figure 3.17***) were measured over a

sampling length between 0.5 and 0.8 mm and a cut-off length of 0.025 mm. Again the parameters used to evaluate the surface roughness were R_a and R_z, standard deviation values were included to 'verify' the obtained results. The average results of all measurements are presented in Table 6.11 for R_a and Table 6.12 for R_z.

Table 6.11 Roughness (R_a) result for micro-part

Area No.	R_a^{OutF1} (μm)	R_a^{F2} (μm)	R_a^{F3} (μm)	R_a^{F5} (μm)
1	0.046	0.049	0.062	0.064
2	0.048	0.050	0.043	0.057
3	0.051	0.052	0.059	0.059
Average	**0.048**	0.050	**0.054**	**0.060**
Std. dev.	**0.003**	0.002	**0.010**	**0.004**

Table 6.12 Roughness (R_z) result for micro-part

Area No.	R_z^{OutF1} (μm)	R_z^{F2} (μm)	R_z^{F3} (μm)	R_z^{F5} (μm)
1	0.222	0.207	0.287	0.323
2	0.241	0.361	0.307	0.274
3	0.251	0.297	0.285	0.269
Average	**0.237**	**0.288**	**0.293**	**0.303**
Std. dev.	**0.016**	**0.077**	**0.012**	**0.009**

The measured R_a values varied between 0.04μm and 0.06μm with higher values related to the surfaces generated towards the end of the toolpath due to the development of tool wear. It can be noted that the outer part of F1 produced the lowest R_a compared to other features as it has been machined first. The R_a value has increased gradually from feature to feature based on its machining sequences. While the lengths of cut for each feature are as follows: F1: 10.9m, F2: 0.23m, F3: 0.23m and F5: 1.18m with total length of cut to machine the micro-component is 12.87m. The length of cut suggested by the tool

manufacturer based on the proposed machining parameters was 16m. Based on this, the measured R_a for F1 was at 68% of the tool life, F2 at 70%, F3 at 71% and F5 at 80%. This also explains the gradually increase of R_a from the first machined feature to the end of the last feature.

Furthermore, by comparing this result (R_a and R_z) with previous literature in producing micro-component [36, 128, 149, 158], the obtained R_a and R_z in this study can be considered as good and in an adequate range. These comparable results show that the use of the custom-made MMT does not stop the micro-milling process in generating a satisfactory surface quality of a micro-component.

Geometrical accuracy results

In order to assess the geometrical accuracy of the machined micro-part, the dimensions of all features (as illustrated in ***Figure 3.16***) were measured using a Keyence VHX-Optical Digital Microscope. Table 6.13 presents the dimensions for all the features in the machined micro-part and again standard deviation values (σ - 99% of confidence interval) are included.

Table 6.13 Measurement results for micro-part

Feature		Nominal dimension (mm)	Average (mm)	Std. dev. (mm)	Deviation from nominal (mm)	% deviation relative to nominal
F1	W_{F1}	3.00	3.092	0.004	0.092	**3.07**
	L_{F1}	1.60	1.649	0.009	0.049	**3.08**
F2	W_{F2}	1.80	1.808	0.002	0.008	**0.45**
	L_{F2}	0.80	0.810	0.001	0.010	**1.19**
F3	W_{F3}	1.80	1.810	0.001	0.010	**0.53**
	L_{F3}	0.80	0.811	0.001	0.011	**1.36**
F4	R_{F4}	0.60	0.605	0.002	0.005	**0.77**
F5	W_{F5}	3.00	3.078	0.010	0.078	**2.60**
	L_{F5}	1.80	1.804	0.002	0.004	**0.20**
F6	W_{F6}	0.25	0.254	0.001	0.004	**1.68**
	L_{F6}	0.45	0.452	0.002	0.002	**0.42**
F7	W_{F7}	0.20	0.205	0.003	0.005	**2.70**
	L_{F7}	1.40	1.435	0.007	0.035	**2.49**
W_{TW}		0.10	0.104	0.004	0.004	**3.80**

From the analysis of the Table 6.13, it can be seen that all measured features are in good agreement with the nominal values, with the percentage of the deviation relative to nominal being less than 4%. In this particular condition, the deviations of the dimensions are believed to be attributed to the development of tool wear towards the end of the machining activity.

From the investigation on the geometrical accuracy of the machined micro-part, it can be concluded that the level of accurateness that can be achieved by the MMT is at a satisfactory level, where it can reach up to 96%.

6.4. Advantages of the MMT

Despite the problems and limitations that were discussed before, the custom-made MMT still offers several advantages as described below:

- *Ability to machine micro-products in full 3D features*

  One of the advantages of the MMT is the possibility to machine 3D micro-features; this has been demonstrated through experiments in machining the "adapted-standard" micro-testpieces, micro-slots and thin walls and also micro-component. Even though the machining parameters were not fully optimised, the MMT was shown to be capable to machine 3D features with a high level of surface quality and geometrical accuracy. This is based on the surface quality analysis and geometrical accuracy assessment towards the machined micro-features discussed above.

- *Facility of portable desktop machining*

  Referring to the descriptions in ***sections 6.2*** and ***6.3***, the developed MMT can be categorized as a portable desktop machine based on its size and components. This allows the MMT to be easy to move around and have more flexibility in factory/workshop layout because of its size. Furthermore, it gives the MMT the capability to be used in any locations (e.g. not necessarily in factory/workshop).

- *Customised set-ups at affordable costs using off-the-shelf components.*

  The MMT was constructed at a reasonable cost with commercially available parts such as positioning tables, motor and spindle units, machine base and machine frame. This can be done by choosing the "off-the-shelf" parts so there was no need for extra cost in customising or uniquely to design any of the machine components. The advantage of the custom-made machine tool was that the selected components consist of those that are really needed or essential to run the machine. As example, the overall cost

to developed this MMT is £15 000, while the cost for a precision machine tool can reached up to £500 000.

- *Save energy, weight, volume and manufacturing related cost*

  The size of the MMT which takes up less space than a big precision machine tool can contribute to economical space utilization, energy and also manufacturing cost saving (e.g. rental space for a factory) [146, 163].

6.5. Integration with MicroMAS

Emphasis was given towards the MMT as it is the domain implementation of the developed MicroMAS which was the main subject of this study. Additionally to make this study more appealing, the discussed MMT is a custom-made machine tool that have a variety of challenges (e.g. the workpiece and tool set-up, consequences of integrating several "off-the-shelf" components) and also it does not have any standard or guidelines to run it. In this chapter, detailed explanations on the condition and capability of the MMT including the related experiments were discussed thoroughly.

The experiments were carried out to emulate the real condition of the MMT in the MicroMAS. Figure 6.22 presents the integration between the micro-machining experiments in the MMT and the developed MicroMAS.

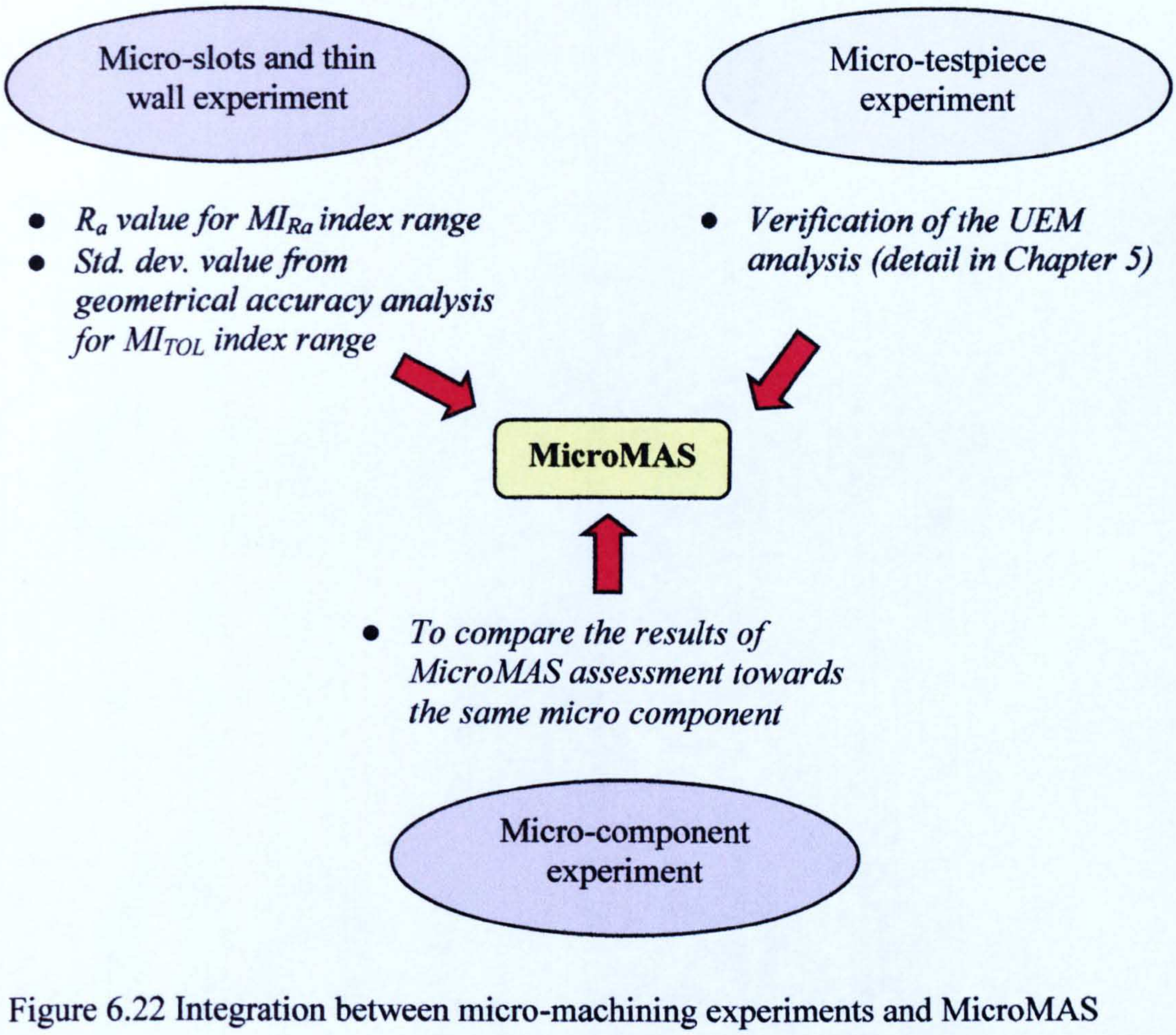

Figure 6.22 Integration between micro-machining experiments and MicroMAS

Based on Figure 6.22, each of the experimental results contributed directly or indirectly towards the developed MicroMAS as follows:

- The generation of index ranges for MI_{Ra} and MI_{TOL} were taken from the results of surface quality and geometrical accuracy of the micro-slots and thin walls experiment. For MI_{Ra}, the range was developed according to the type of material associated to the cutter size with the average values of R_a regarded as the nominal value for that particular index range. While for MI_{TOL}, the calculated standard deviations from the geometrical accuracy analysis were employed in generating the index range which was divided according to various feature sizes. This was discussed in ***Chapter 4***.

- The results from the micro-testpiece experiment (AISI 1040) were used to verify the UEM analysis and implemented the MIs analysis (MI_{UEM}). The CMM results from the geometrical accuracy analysis of the AISI 1040 were then partially compared with those obtained from the uncertainty model (analysed in GUM Workbench). This was discussed in ***Chapter 5***.
- Furthermore, the machined micro-component was also exploited as an example in simulating the flow of the MicroMAS. Thus the results from this work can be used to partly verify the function of MicroMAS (e.g. generated surface quality, part accuracy with the level of manufacturability).

6.6. Summary

This chapter has introduced and discussed the machining experiments carried out using the MMT. The development of the MMT has contributed significantly towards this study as it is the main domain or scope of the developed MicroMAS for micro-milling application. It presented problems and limitations faced when developing and exploiting MMT which has been observed through various machining testing and trials. The chapter also considered the solutions provided for those limitations in order to ensure the successful performance of the MMT. It also took into account the machining experiments done to assess the capability of the MMT which provided results and inputs to be included into the MicroMAS database and which also assisting in validating the result of the uncertainty model analysis.

Based on the results from the machining experiments, it has been proved that the MMT is capable in generating micro-components at acceptable accuracies/repeatabilities. Although it was not the scope of this study to seek optimised cutting parameters that result in fine surface roughness, the measured R_a and R_z and also the geometrical values achieved were acceptable giving a respectable range of precision. This provides an indication that the custom-built MMT has been developed to a satisfactory level of precision to enable micro-machining of surfaces with acceptable accuracies.

Additionally, the results from these experiments were successfully included into MicroMAS. This was completed by the generation of index ranges for MI_{TOL} and MI_{Ra}, verification of UEM results through the machined micro-testpiece (where UEM is also implemented in MicroMAS). Finally the results from the generated micro-component demonstrator can be partly compared with the simulation in analysing the sequence of the MicroMAS.

CHAPTER 7: IMPLEMENTATION OF MICRO-MANUFACTURABILITY ANALYSIS SYSTEM (MICROMAS)

7.1. Introduction

The development of the MicroMAS was the main objective of this study, to develop a manufacturability analysis system for micro-machining environment. This system, for the time being, has been explicitly developed to address a custom-made 4-axis Miniature Machine Tool (MMT) which requires a system that can support a robust and efficient generation of micro-part. In this chapter, an in-depth description of the developed system is presented. Firstly, an overview of the system development is briefly explained, following this, the execution of the MicroMAS is presented. Based on the Primitive Feature Analysis (PFA) phases (as discussed in ***Chapter 4***), the implementation of the MicroMAS was divided into four stages as follows:

i. Initial Assessment (IA)

ii. Single Feature Analysis (SFA)

iii. Coupled Feature Analysis (CFA)

iv. Outputs generation

Furthermore, in order to understand the algorithm of the system, a flowchart was employed to describe the execution of the data and the related inferences involved in the stages above. Additionally to observe the performance of the system in gathering important data from CAD model and also assessing its manufacturability aspects, a micro-component demonstrator was used to simulate the implementation of the MicroMAS (e.g. interfaces, pop-up form, user-system interaction, outputs window). Finally, this chapter considers the

advantages and possible limitations of this developed manufacturability analysis system.

7.2. MicroMAS development – an overview

As discussed in ***Chapter 3 (Figure 3.1)***, the development of the system is based on the three-step, unidirectional flowchart methodology that includes 3 modules: data input, manufacturability assessment, output reporting. The MicroMAS, developed in the Visual Basic.NET (VB) environment has employed the Primitive Feature Analysis (PFA) technique in gathering data from CAD model and assessing its manufacturability.

Figure 7.1 illustrates the overall relationships between various aspects (e.g. input, manufacturability assessment, output, database) in the MicroMAS. The data input into the system is done through the combination of two methods: *user-system interaction* and *a priori database*. In the *user-system interaction,* users are prompted to provide the requested data through the interfaces such as the characteristics of the primitive features (e.g. length, width, height, diameter), quality measures (e.g. tolerance and surface roughness value) and weight factor that reflects the importance of the manufacturability indexes (MI). While for the *priori database*, users are asked to select the data listed by the system such as the type of PF and its orientation, material and tool diameter.

Basically, MicroMAS is proposed to be utilized at the early design stage where user can assess the possibility of machining the CAD model using the MMT

through the manufacturability aspects incorporated in the system. The manufacturability aspects involved are dimensions, surface roughness, tolerance, primitive features and their interactions, material, uncertainty impact on machining the PF and also the condition of the MMT. The manufacturability assessment is made based on the Ruled-based System (RBS) through IF-THEN clauses that controls the analysis of MicroMAS and represents the system knowledge base via logical combinations. In this study, the related rules and conditions associated to micro-milling and all primitive features elements are saved in the form of IF-THEN clauses. All the rules and conditions stored in the database are interactively searched based on IF-THEN clauses in order to determine which rules satisfy the requirements expressed via inputs.

Related manufacturing information (e.g. materials, range of valid part dimension, geometrical interactions) and rules are embedded in the database to be used as a guide for assessing the manufacturability of the proposed design. The database was developed using Microsoft Access and linked to the VB. In order to reflect the actual condition of the MMT, results from micro-machining experiments and UEM analysis were input into the MicroMAS through the database (as discussed in ***Chapter 5*** and ***Chapter 6***).

The results from the manufacturability assessment are reported to users in various types such as result form and pop-up window. The results provided are the generated MIs and also redesign suggestions.

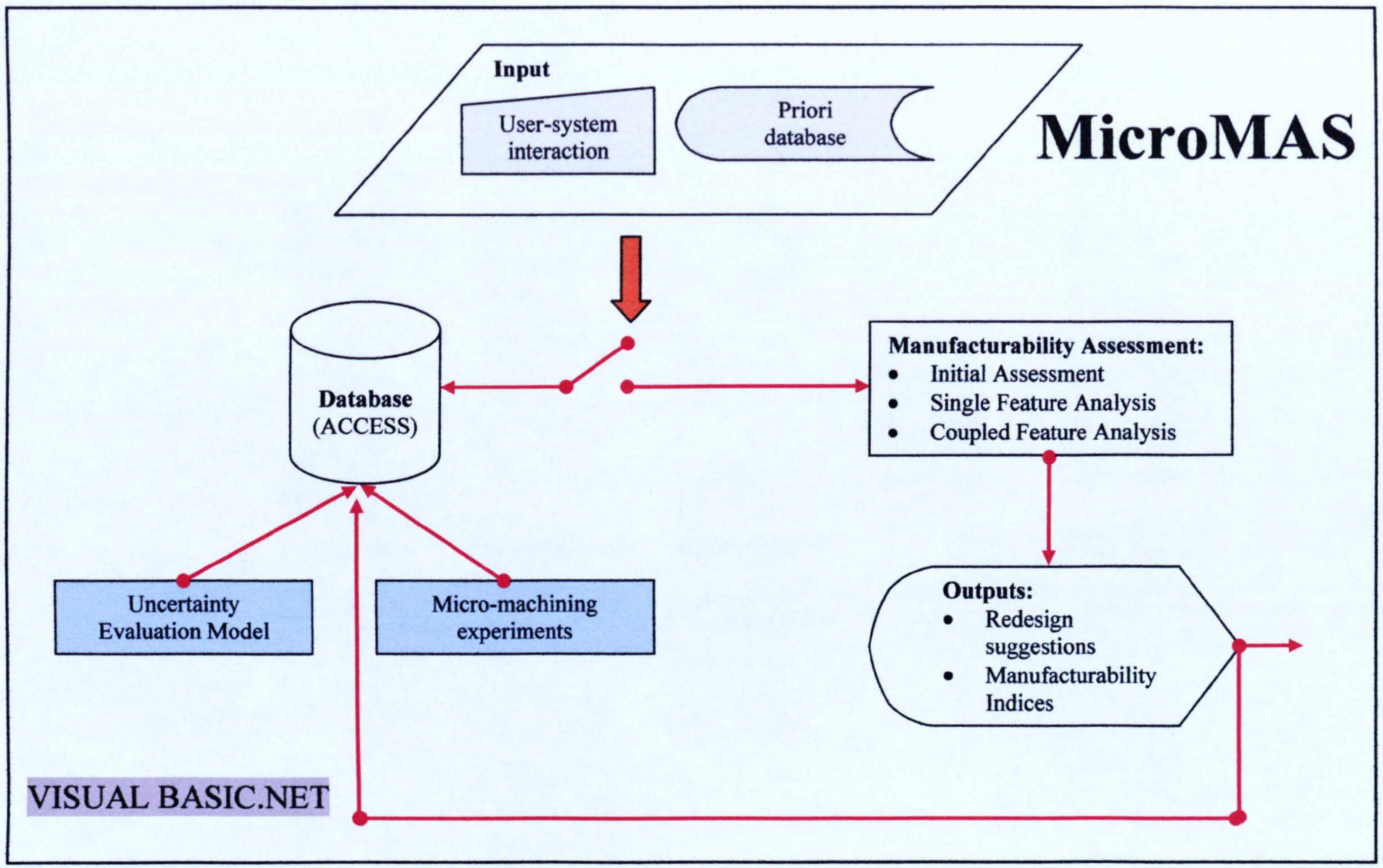

Figure 7.1 Relationships in MicroMAS

7.3. MicroMAS data flow description

In order to understand the execution of MicroMAS, Figure 7.2 describes the overall implementation of the system. Based on the three phases on the PFA technique development, the system expanded the phases to four sequential stages: (i) Initial Assessment (IA), (ii) Single Feature Analysis (SFA) (iii) Coupled Feature Analysis (CFA), (iv) Output generation. Table 7.1 summarises the objectives and expected outputs of the stages in MicroMAS.

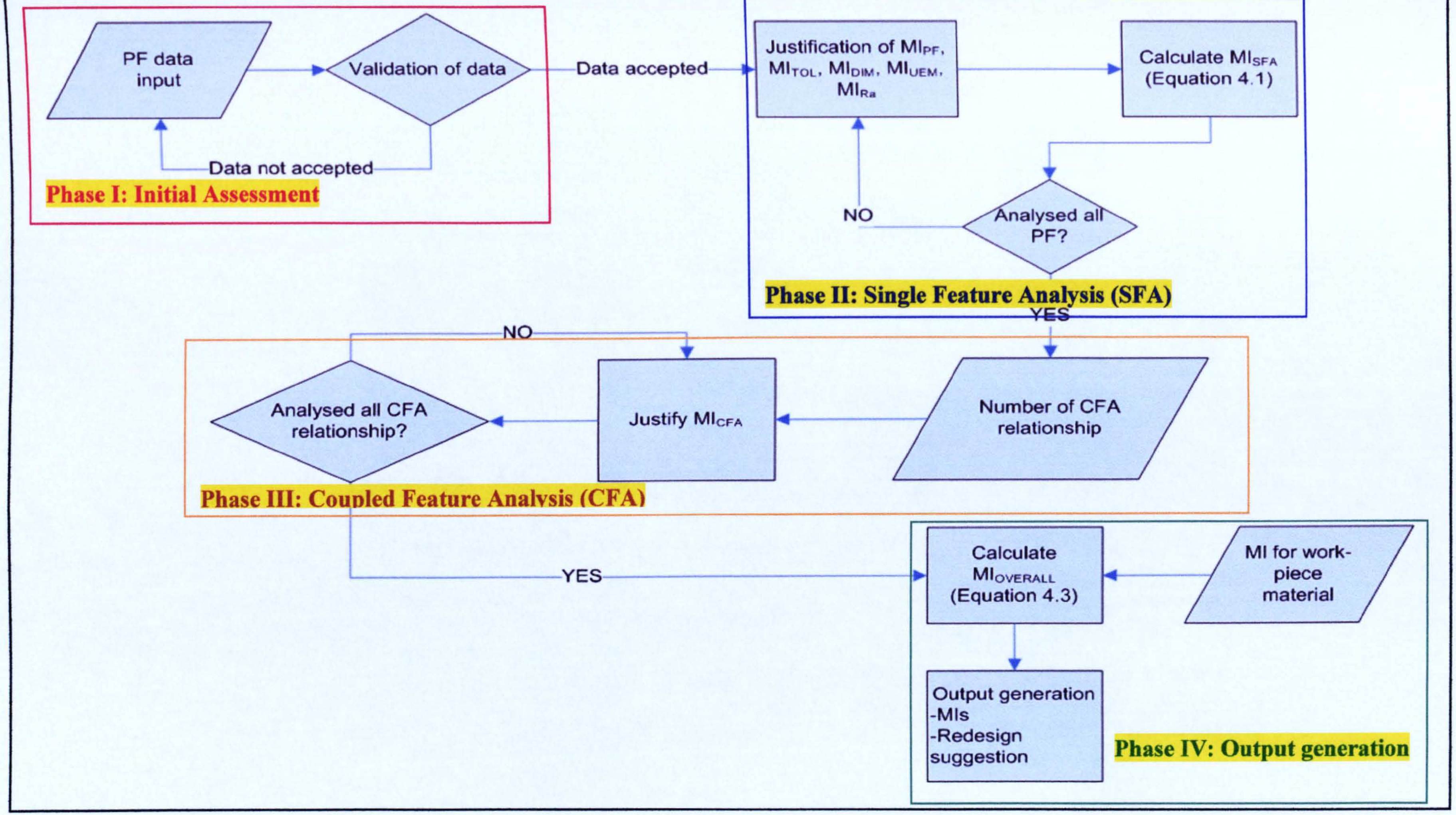

Figure 7.2 Overall system executions

Table 7.1 Summary of MicroMAS's stages

Stage	Objective	Expected Output
Initial Assessment (IA)	- Identify numbers of PFs - Verify dimensions of the part/features	Progress to the next phase. Possible of error notification.
SFA	- Assess each PF - Verify stiffness ratio (R_{ST}) - Calculate MI_{SFA}: $$MI_{SFA} = \frac{\sum K_i MI_i}{5},$$ i= PF, Ra, TOL, DIM,UEM (Equation 4.1)	MI_{SFA}. Stiffness ratio (R_{ST}).
CFA	- Assess the relationships between the PFs and calculate MI_{CFA}	MI_{CFA}.
Output	- Calculate $MI_{OVERALL}$: $$MI_{OVERALL} = \frac{MI_{MAT} + \sum_{n=1}^{n+1} MI_{CFA}}{n},$$ n=number of PFs (Equation 4.3)	$MI_{OVERALL}$. Redesign suggestions.

Legend:

SFA	Single Feature Analysis
CFA	Coupled Feature Analysis
MI_{SFA}	Manufacturability Index for single feature analysis phase
MI_{TOL}	Manufacturability Index for tolerance
MI_{Ra}	Manufacturability Index for surface roughness
MI_{DIM}	Manufacturability Index for tool dimension
MI_{UEM}	Manufacturability Index for uncertainty effect in machining the PF
MI_{PF}	Manufacturability Index for primitive feature
MI_{CFA}	Manufacturability Index for coupled feature analysis phase
$MI_{OVERALL}$	Manufacturability Index for overall micro-part

7.3.1. Initial assessment (IA)

As discussed in ***Chapter 4***, the main objective of this stage was to gather data from the proposed CAD model (micro-component) and furthermore to validate the collected data with the acceptable ranges stored in the database. Figure 7.3 (a) and (b) illustrate the flowchart of this stage where it starts with the users uniquely label the micro-component, then identifies the number of Primitive Features (PFs) contained in the proposed CAD model and selects the suitable type of workpiece material. Next, the users uniquely label each identified PF. The type of PF is then selected by the users (e.g. Box, Cylinder, Cone or Sphere) and the PF dimensions can be selected.

Following the data validation, the orientation of the PF is selected and if it is a cavity, the type of it (e.g. through or blind holes) is determined. Subsequently, the shape of the PF is decided based on the side angle value supplied by the users. Finally, the users choose the type of end corner, tool diameter, related tolerance and surface roughness value and also the uncertainty effect in machining the PF. All the data are saved in the database and once this inference is completed, the next stage is the SFA phase. This inference is repeated until the details of all PFs have been provided into the system.

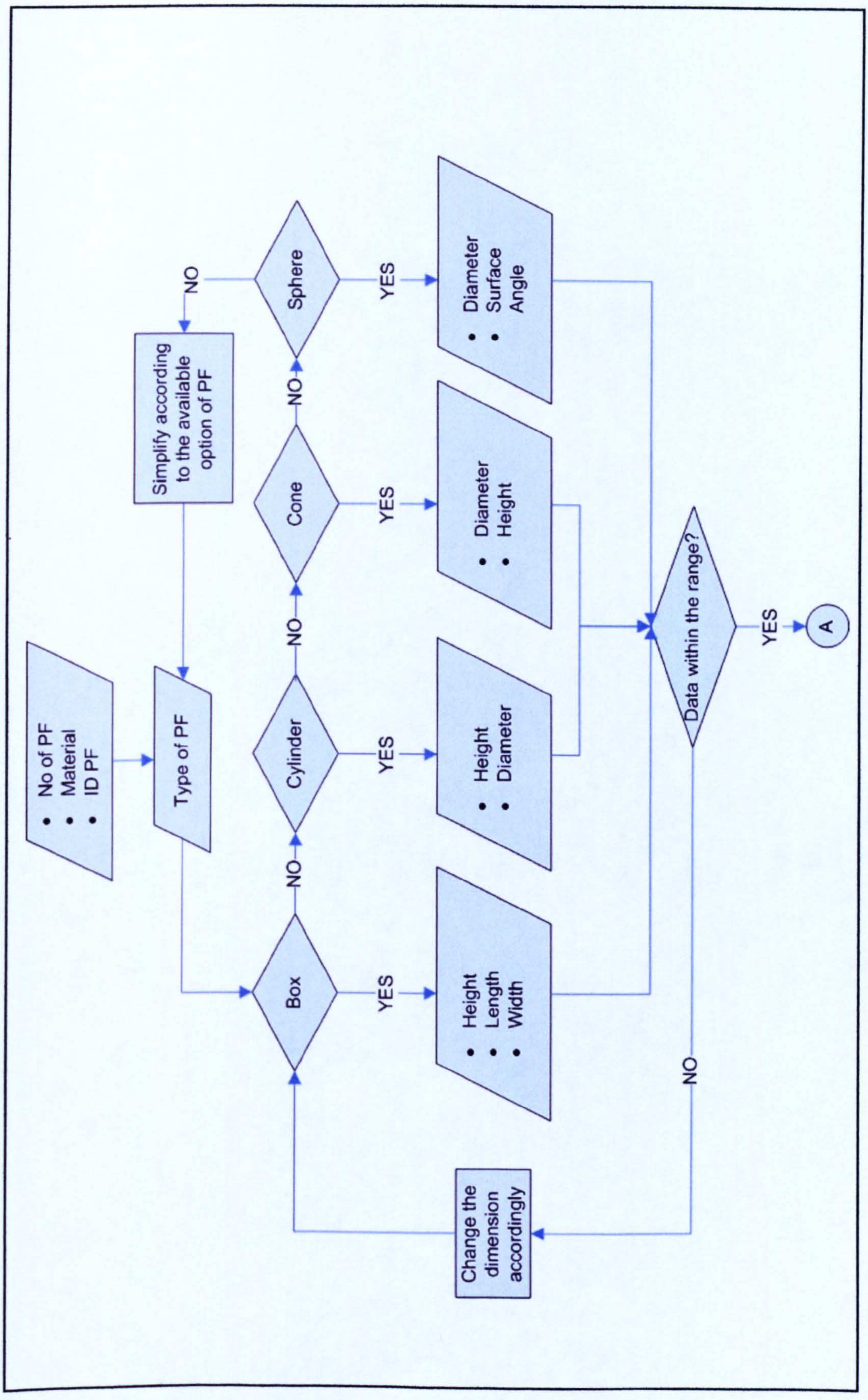

Figure 7.3 (a) Initial Assessment stage

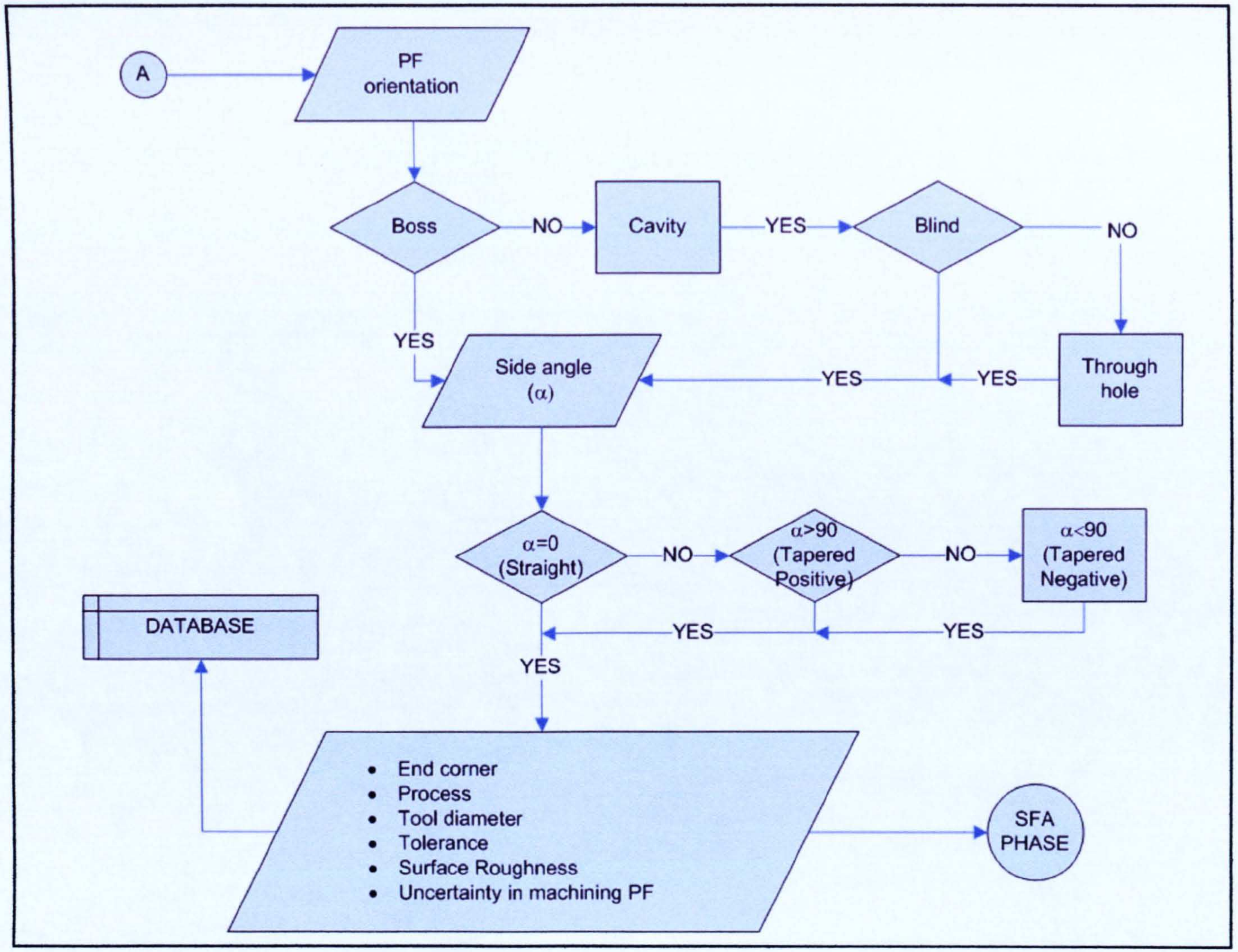

Figure 7.3 (b) Initial Assessment stage

7.3.2. Single feature analysis (SFA)

The main goals of this stage are to assess the MIs for each PF and to calculate the MI_{SFA}. Figure 7.4 (a) presents the flow of the data and inferences involved in assessing the PF in the aspect of tolerance, surface roughness, uncertainty effect in machining it and selected tool dimension. While Figure 7.4 (b) shows the execution of determining the MI_{SFA}. The loop in calculating the MI_{SFA} is controlled by the number of PF determined by the users in IA phase.

First, the users have to determine the weight factor (K_i) for each related MIs (MI_{PF}, MI_{TOL}, MI_{Ra}, MI_{DIM}, MI_{UEM}). Next, the justification for each MI is being done, the mechanism of determining the MIs have been discussed in ***Chapter 4***. Following this, the MI_{SFA} is calculated based on Equation 4.1 mentioned in Table 7.1. This procedure is repeated until the MIs and MI_{SFA} for all PFs have been determined. The results of MIs and MI_{SFA} are then saved in the database for future analysis.

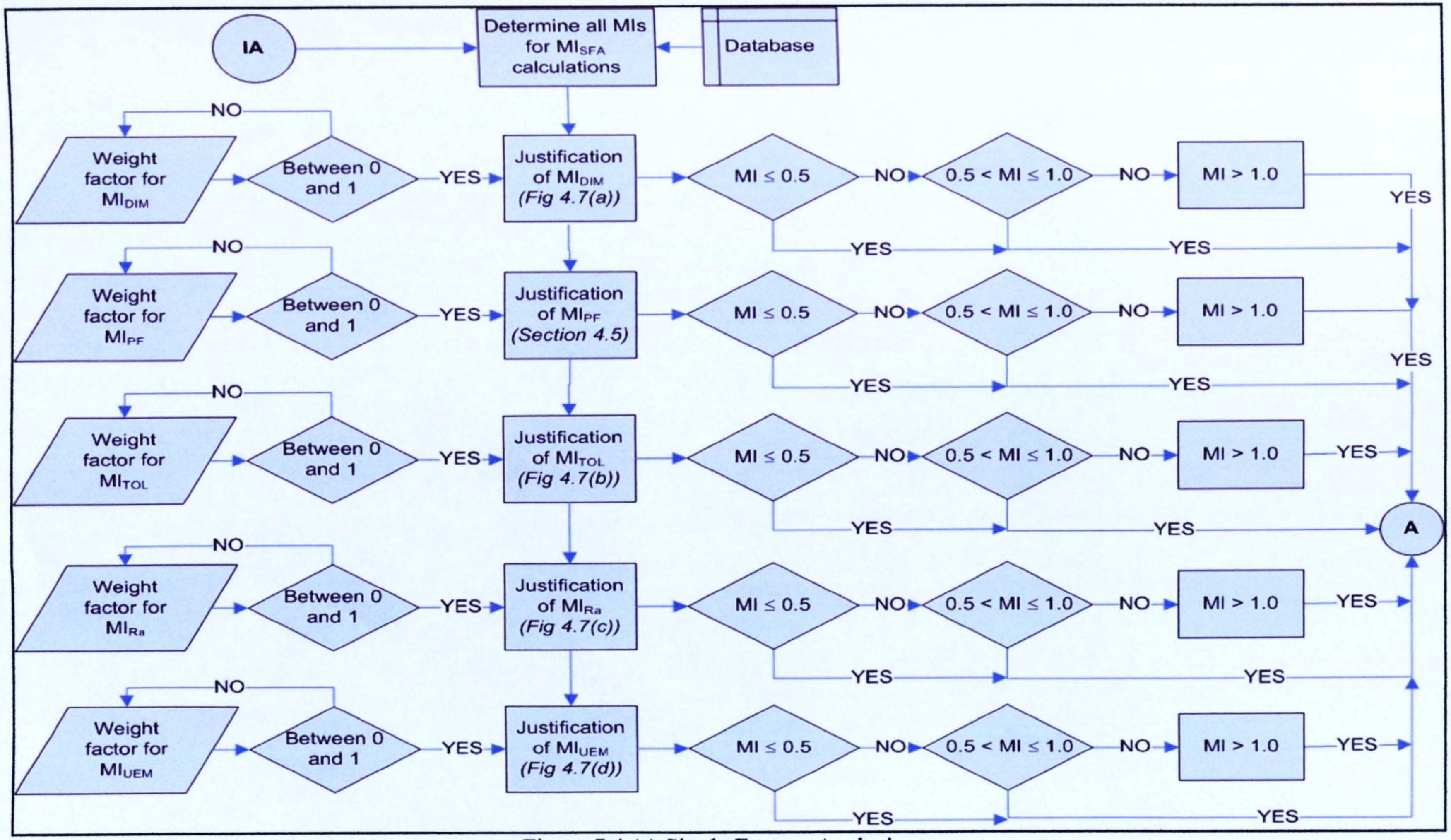

Figure 7.4 (a) Single Feature Analysis stage

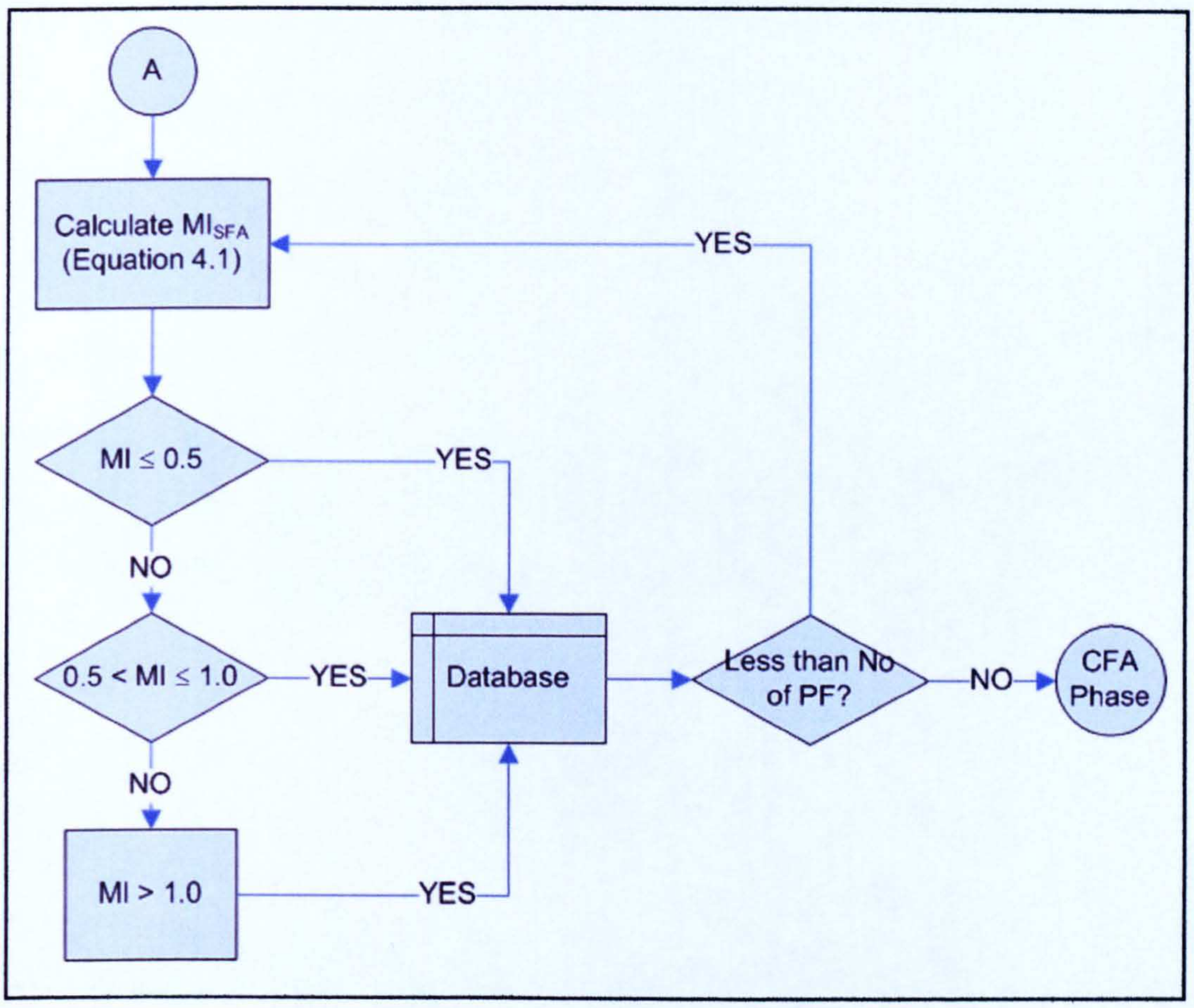

Figure 7.4 (b) Single Feature Analysis stage

7.3.3. Coupled feature analysis (CFA)

As mentioned in ***Chapter 4***, the objective of this stage is to determine the level of relationship among PFs by taking into consideration the distance and the type of interaction between them. Figure 7.5 shows the succession of the related inferences and data in CFA stage. In order to control the loop of CFA analysis, users provide the number of CFA relationship which represents the quantity of coupled primitive features in the analysed micro-component.

The calculation of MI_{CFA} is subjected to: (i) comparison between the relative distance (RD) and the minimum acceptable distance (MD) of the PFs and (ii) the type of the interactions (e.g. adjacent, attached or independent) between them; this is done by multiplying the related MI_{SFA} with the pre-defined coefficients (K_{RD}) as presented in ***Table 4.2*** (***Chapter 4***). Then, the level of manufacturability for each PF is justified based on the calculated MI_{CFA}. The results from CFA stage are stored in the database for analysis in the next step.

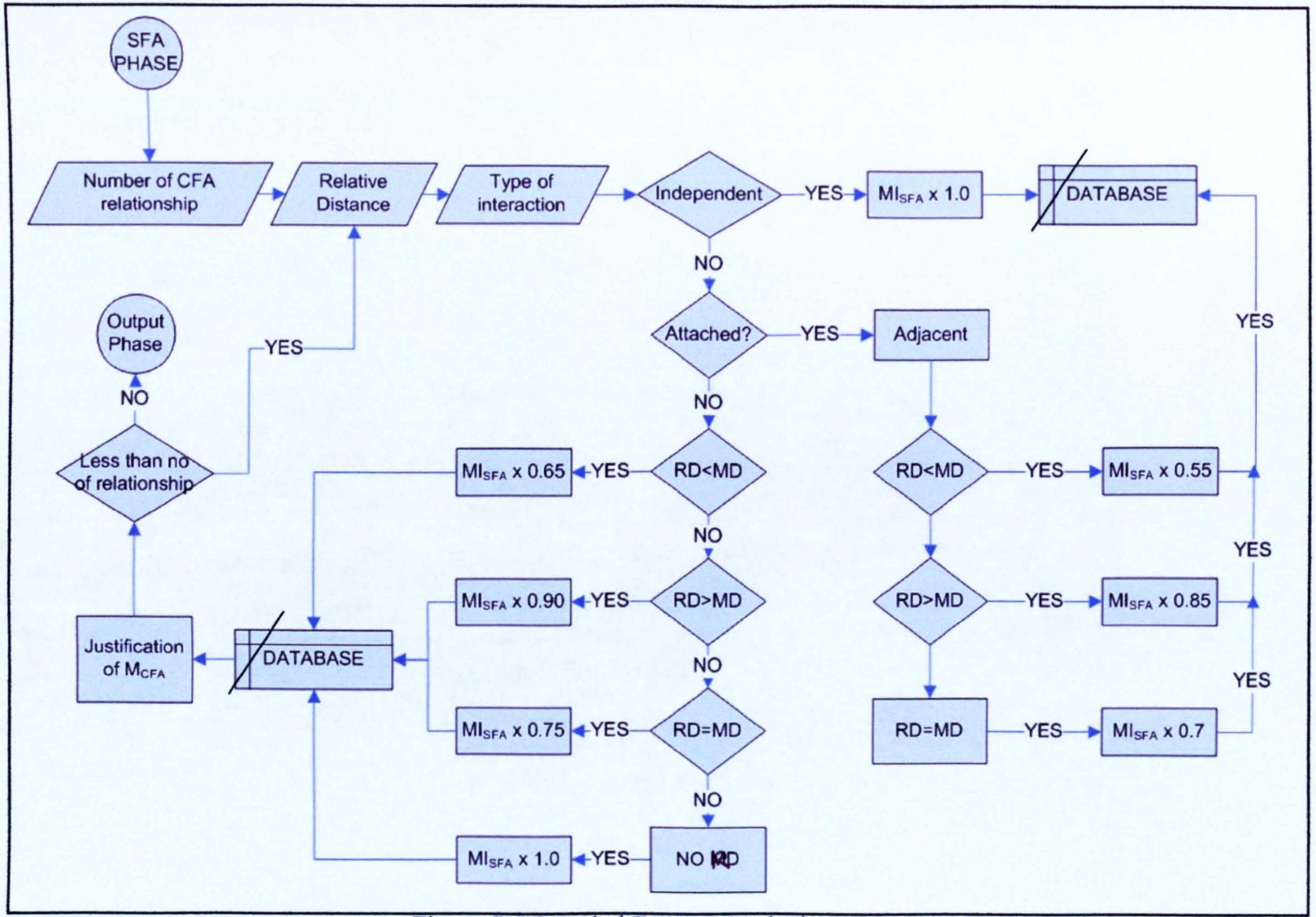

Figure 7.5 Coupled Feature Analysis stage

7.3.4. Output generation

In the final stage of the MicroMAS (Figure 7.6), the overall MI is evaluated based on the ***Equation 4.3*** declared in Table 7.1. This is done by taking into consideration the calculated MI_{CFA} and also the machinability index of the workpiece material (MI_{MAT}) as referred to in the literature [183-184].

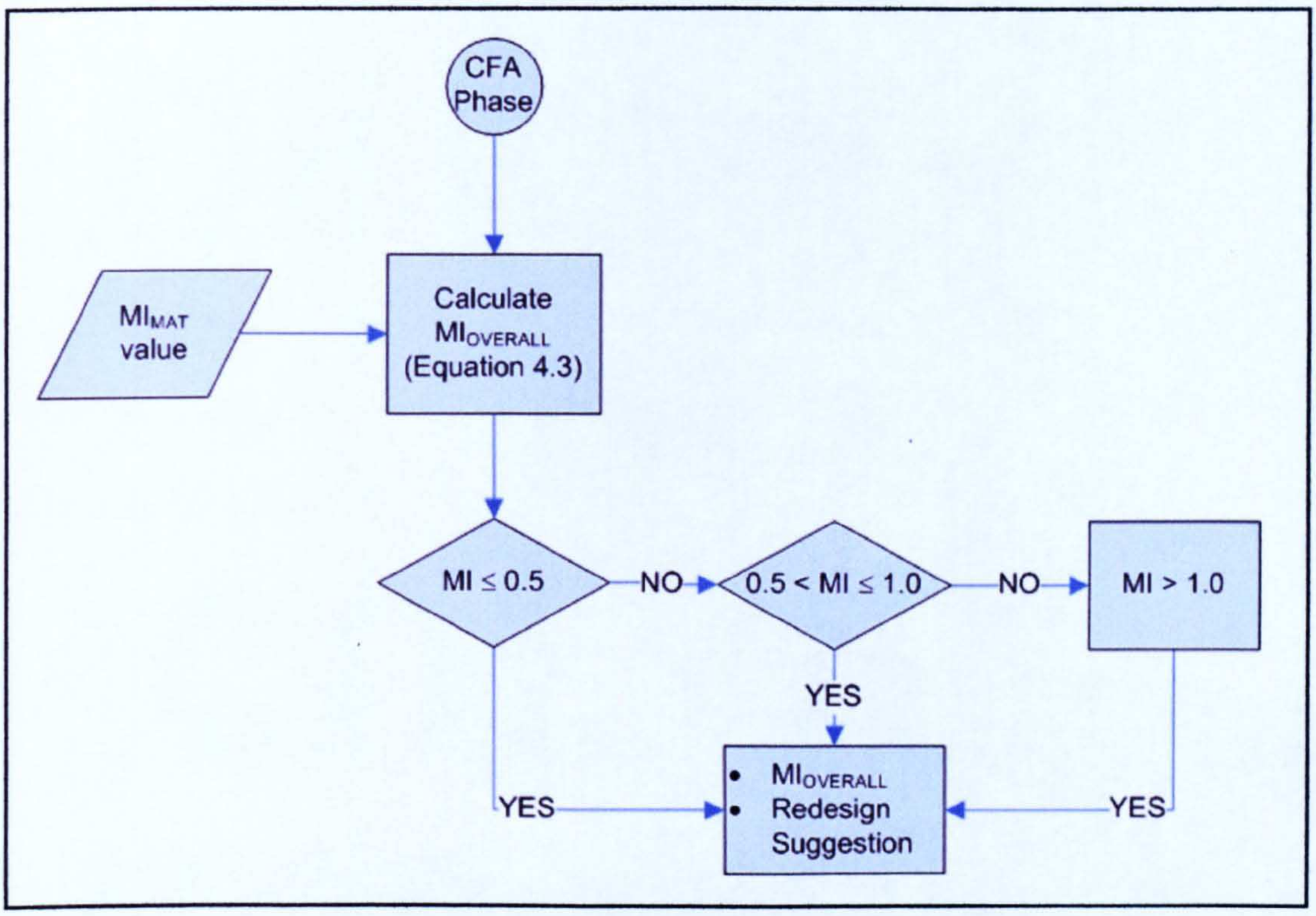

Figure 7.6 Output generations stage

Then, the level of manufacturability for the calculated $MI_{OVERALL}$ is justified. In order to upgrade the manufacturability level of the proposed design, the system gives suggestions about changing manufacturability aspects of the part/PFs as follows:

- Modify the PFs with low MI_{SFA} by redefining the value of surface roughness, tolerance and uncertainty effect in machining the feature.
- Suggestion on PF with low MI_{CFA} to reconsider (if possible) the relative distance between the PFs.

- Recommendations on changing the selected material to one with lower hardness that allows easier machining.
- Redefine the importance of the weight factors (K_i) of each MI involved in calculating the MI_{SFA}.

7.4. System implementation and simulation

In order to visualise the MicroMAS execution, the system is demonstrated in the next paragraphs by employing the machined micro-component demonstrator (Figure 7.7) as the example of the proposed CAD model. This section also described the flow of the activities that involved the user in using the MicroMAS. Figure 7.7 also presents the identified PFs which are numerically labelled (1 to 8).

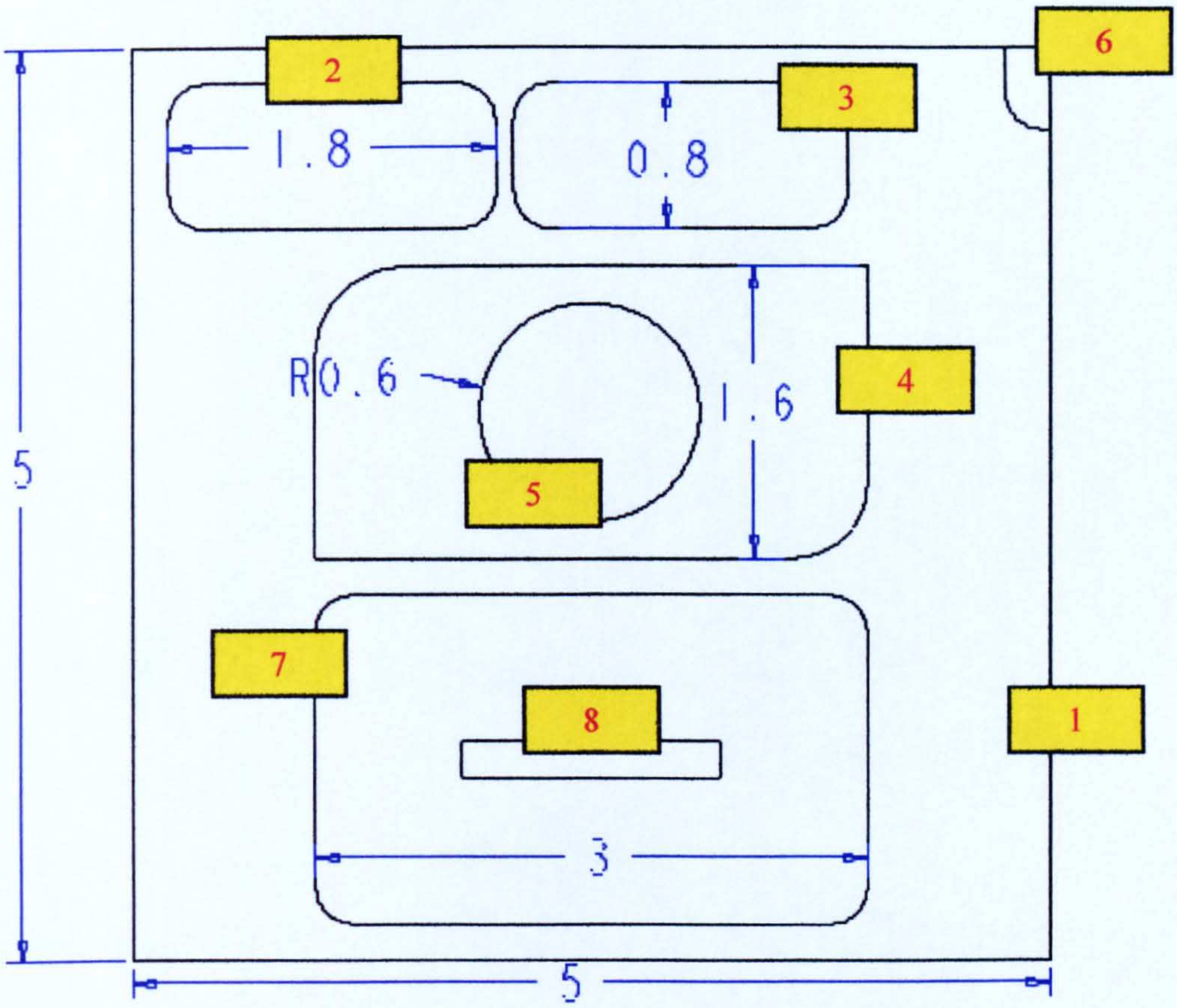

Figure 7.7 Top view of the proposed micro-component (in mm)

Figure 7.8 shows the introduction interface of the system, where to start the system the *Single Feature Analysis* item menu is selected. As a guideline for using the overall system, the *Guidelines* item menu can be chosen, nevertheless a brief instruction is provided in each stage/interface.

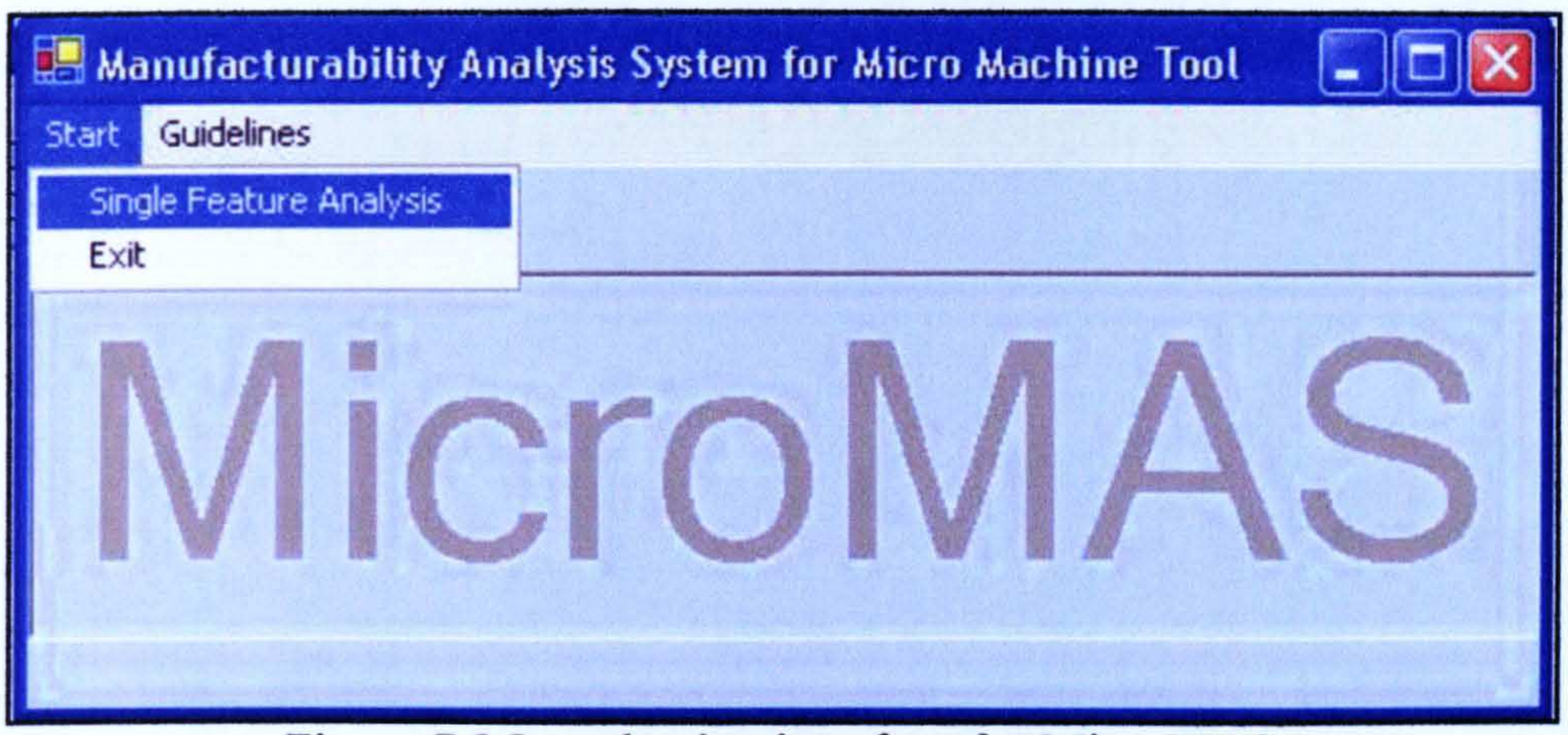

Figure 7.8 Introduction interface for MicroMAS

7.4.1. Input and single feature analysis interfaces

Figure 7.9 demonstrates the main interface where the input from the users is collected. A guideline for entering and using this interface is provided by selecting the button 'TO DO'. A pop-up window (Figure 7.10) showing the guidance to fill in the form and assess the preliminary result of the input is also presented. Figure 7.9 shows the data input for PF_8 of the micro-component. Fundamentally, there are five important steps involved in the input mechanism and SFA analysis as pictured in Figure 7.9.

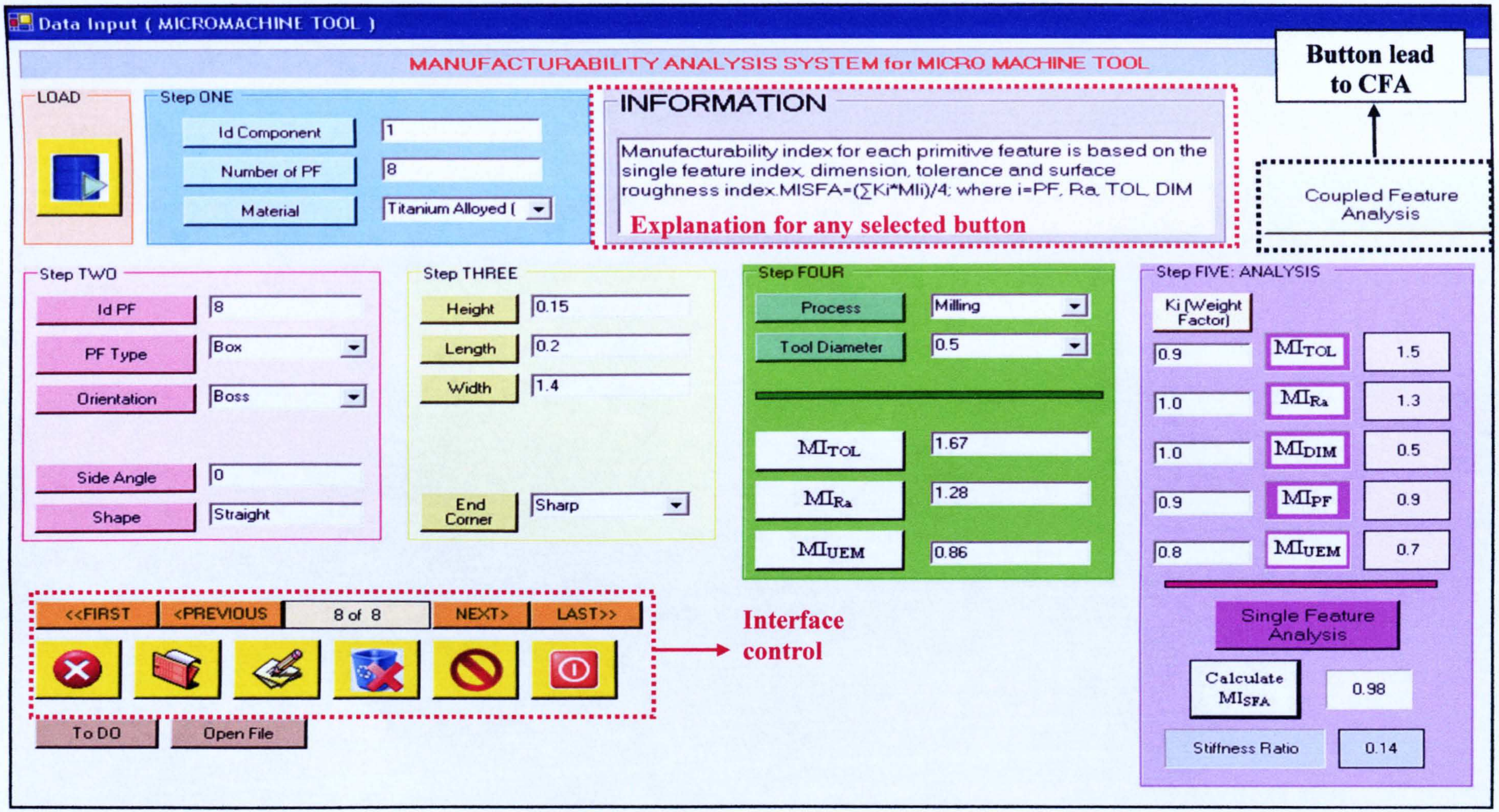

Figure 7.9 Interface for input mechanism and SFA analysis

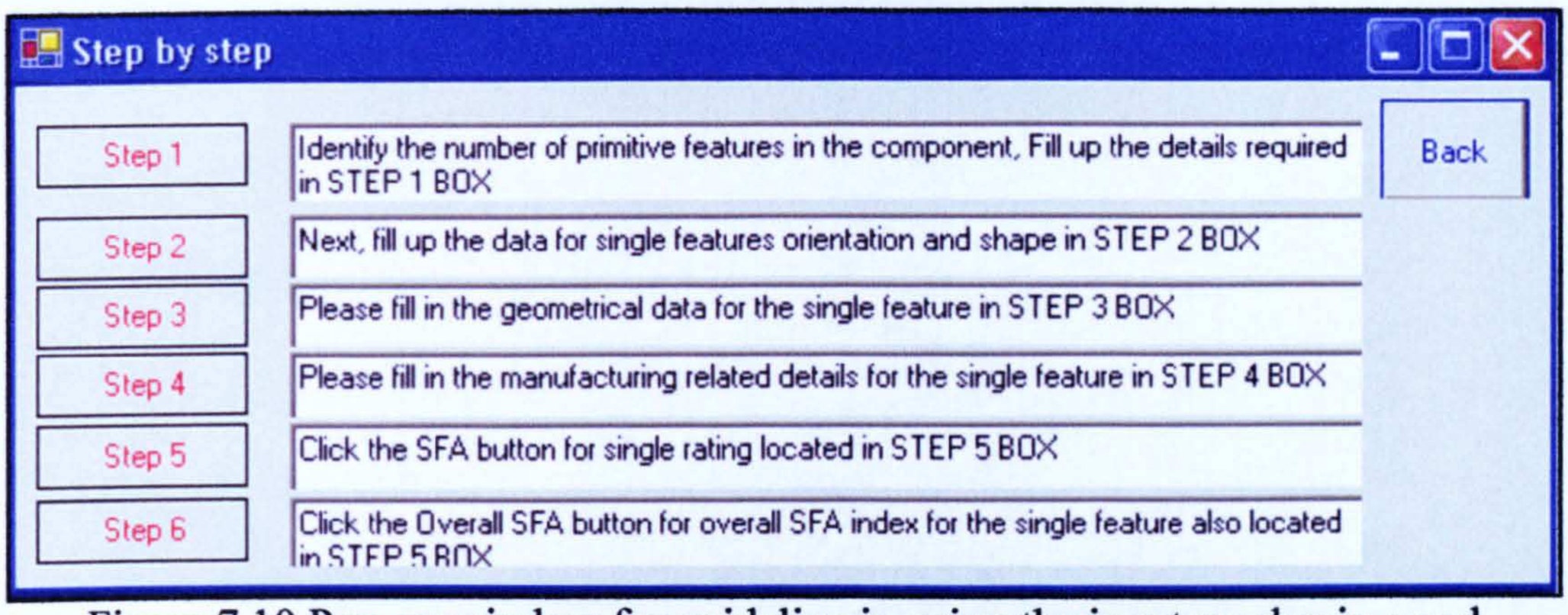

Figure 7.10 Pop-up window for guideline in using the input mechanism and SFA analysis interface

Step1. In the first step, the users input the unique identifier of the micro-component, followed by the number of the PFs contained in the proposed design. Then, the suitable material is selected from the list of available materials stored such as AISI 1040 – Mild Steel, 316L - Stainless Steel, and TiAl6V4 – Titanium Alloy. Figure 7.11 shows ***Step1*** interface that is being extracted from the main window form of the system.

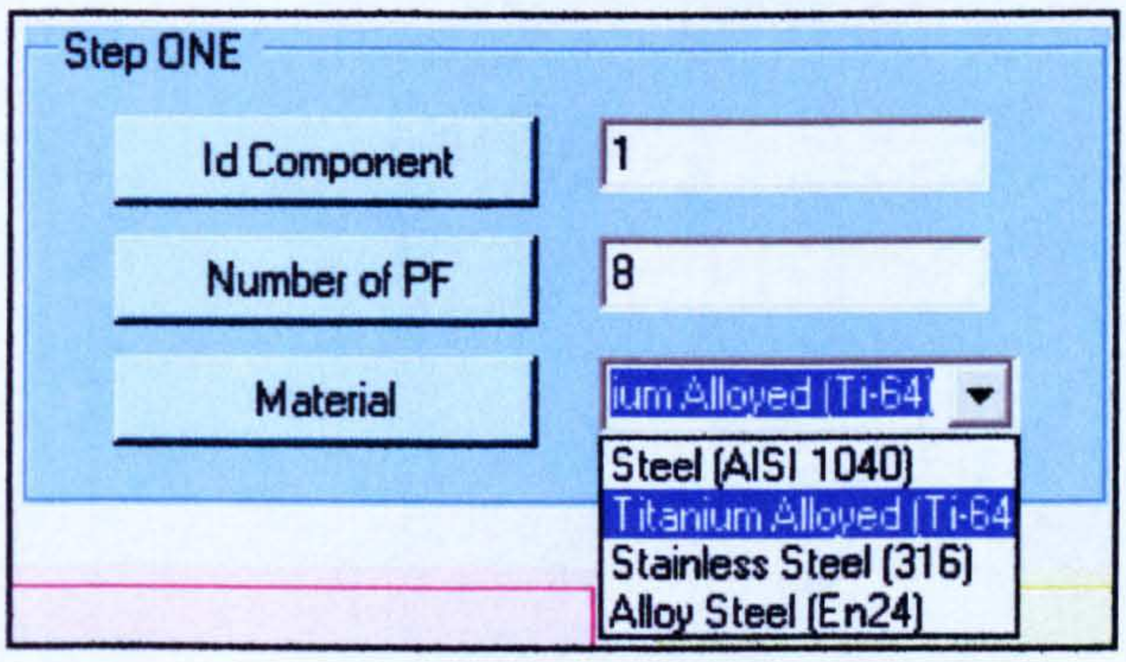

Figure 7.11 Step 1

Steps 2 to Step 5 are repeated until details of all PFs have been input into the system and the result of MI_{SFA} of each PF can be reviewed in Step 5.

Step2. Figure 7.12 shows the interface for ***Step 2***, where the users uniquely label each identified PF (e.g. 1, 2, 3). Here the data needed are the type of the PF (e.g. box, cylinder, cone), orientation (cavity or boss) and side angle. The shape of the PF (e.g. straight, tapered negative, tapered positive) is automatically determined by the system based on the provided value of the side angle. This second step reflects the required data for the SFA phase as discussed in ***Table 4.1*** and ***Figure 4.2, Chapter 4***.

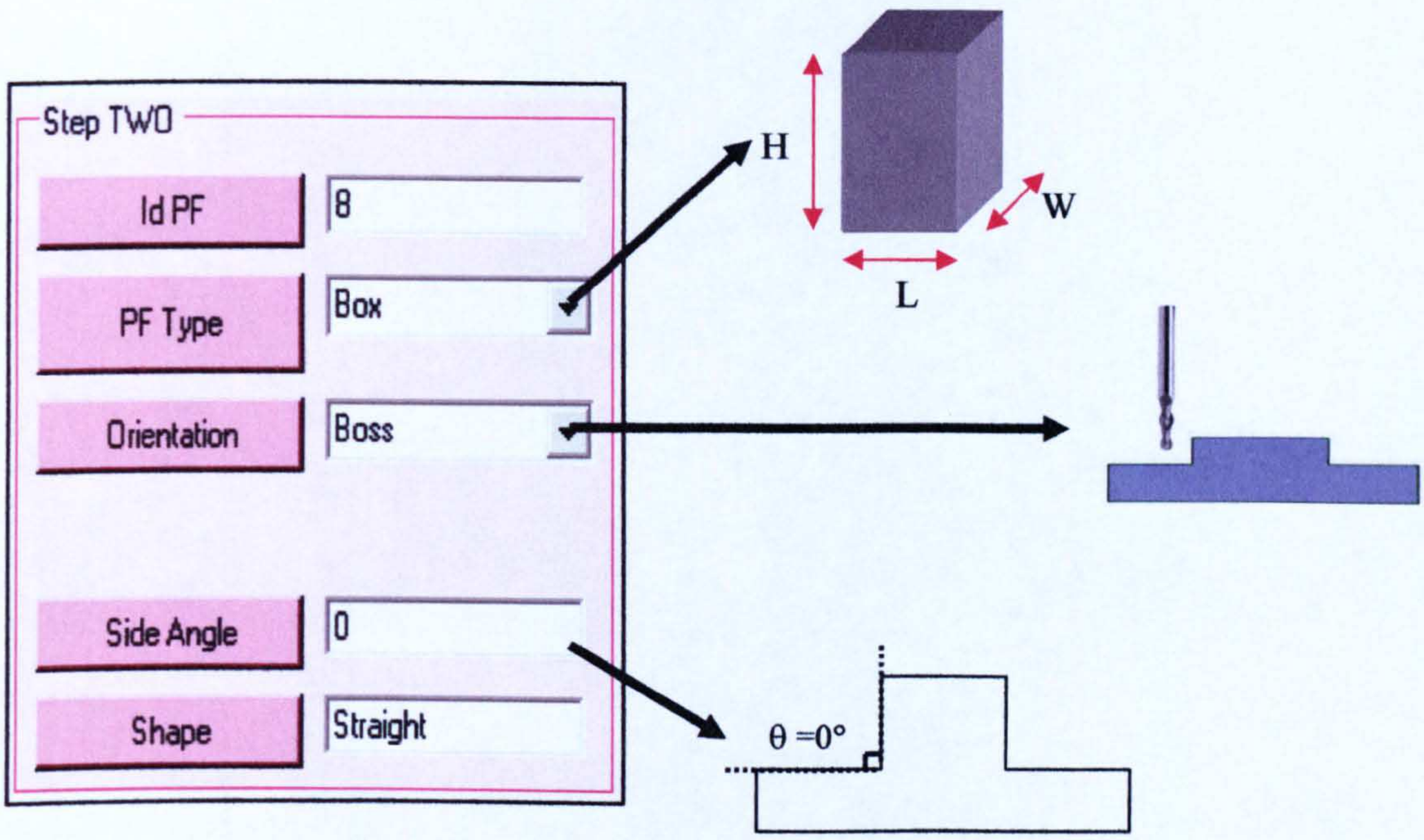

Figure 7.12 Step 2

Step3. Geometrical data of each identified PF are required in this step. The data depends on the type of PFs classified in ***Step 2*** as each PF requires different geometrical data. Figure 7.13 presents the extracted interface for users to input the required geometrical data. In order to help the users to input the relevant data according to the type of PF, the necessary geometrical characteristics are suggested by the system. This is also shows in Figure 7.13 where two different set of geometrical characteristics are being required from the users, where (a) is for Box while (b) is for Cylinder.

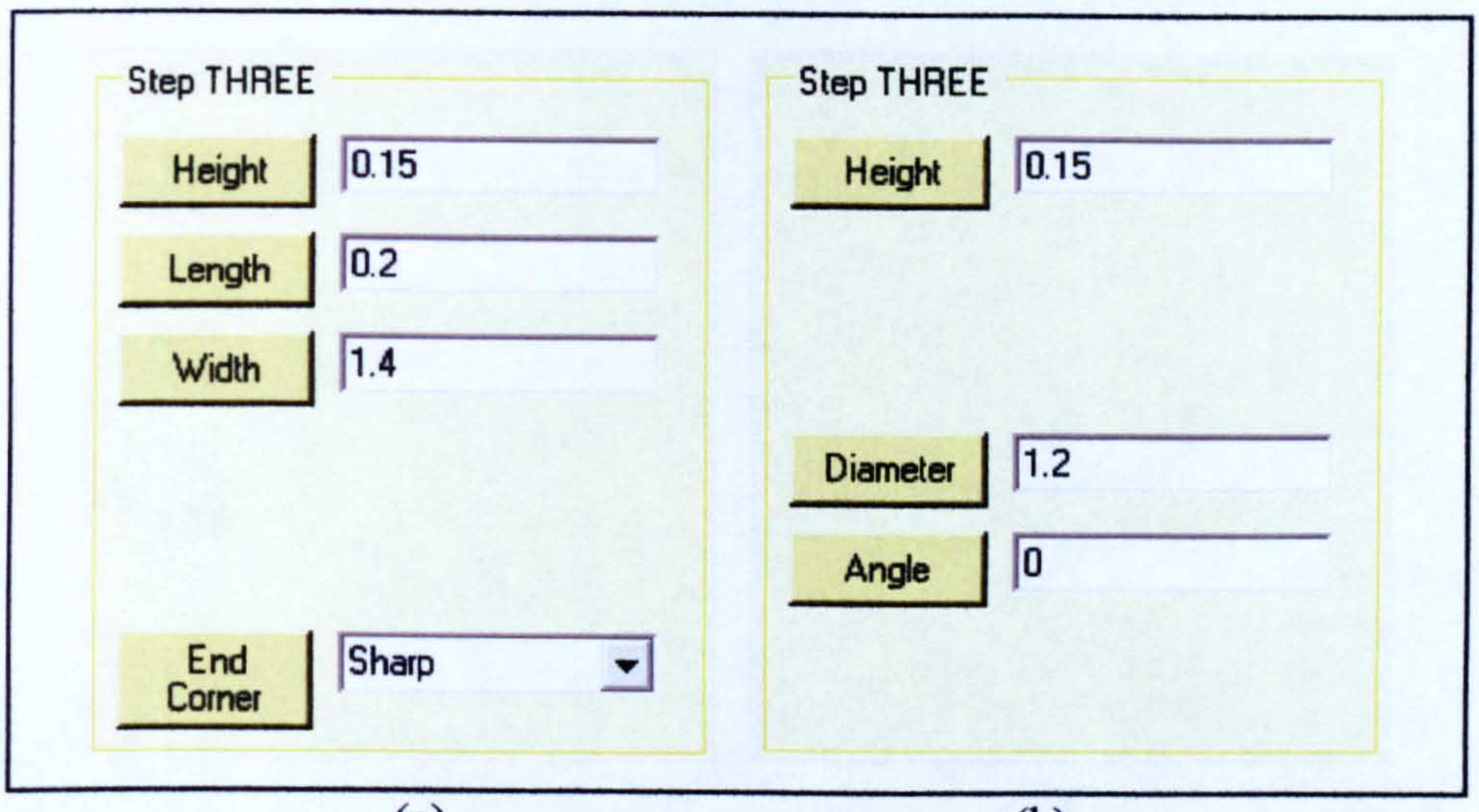

(a) (b)

Figure 7.13 Step 3

In validating the provided data for the PF's dimension, a highlighted warning scheme as shown in Figure 7.14 is being imposed by the system to notify the users if any of the input is out of the determined acceptable range stored in the database.

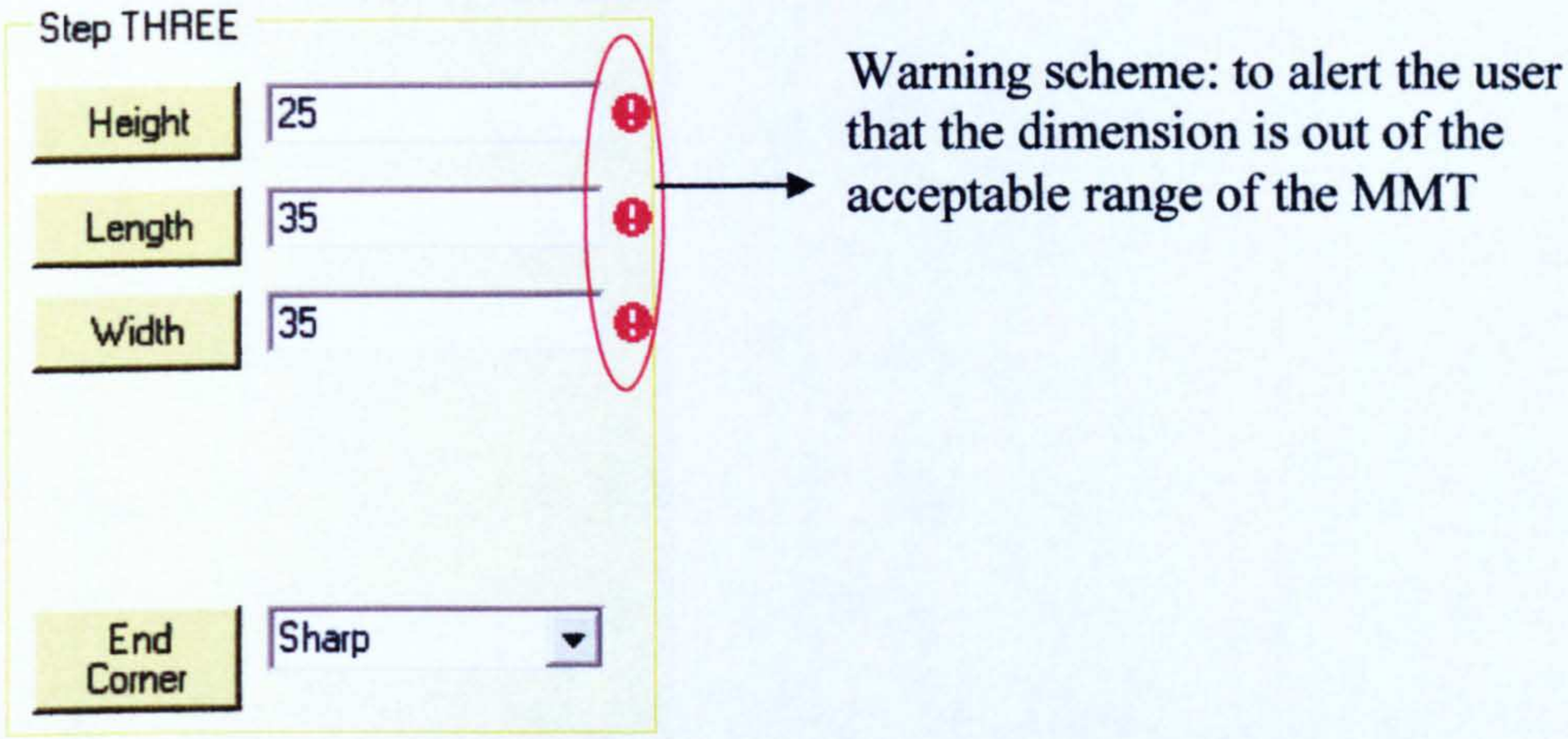

Figure 7.14 Warning scheme for data validation

Step 4. Manufacturing related details such as the process involved (micro-milling), diameter of the tools and part quality measures (tolerance, surface finish and uncertainty in generating the PF) are required at this step as pictured in Figure 7.15.

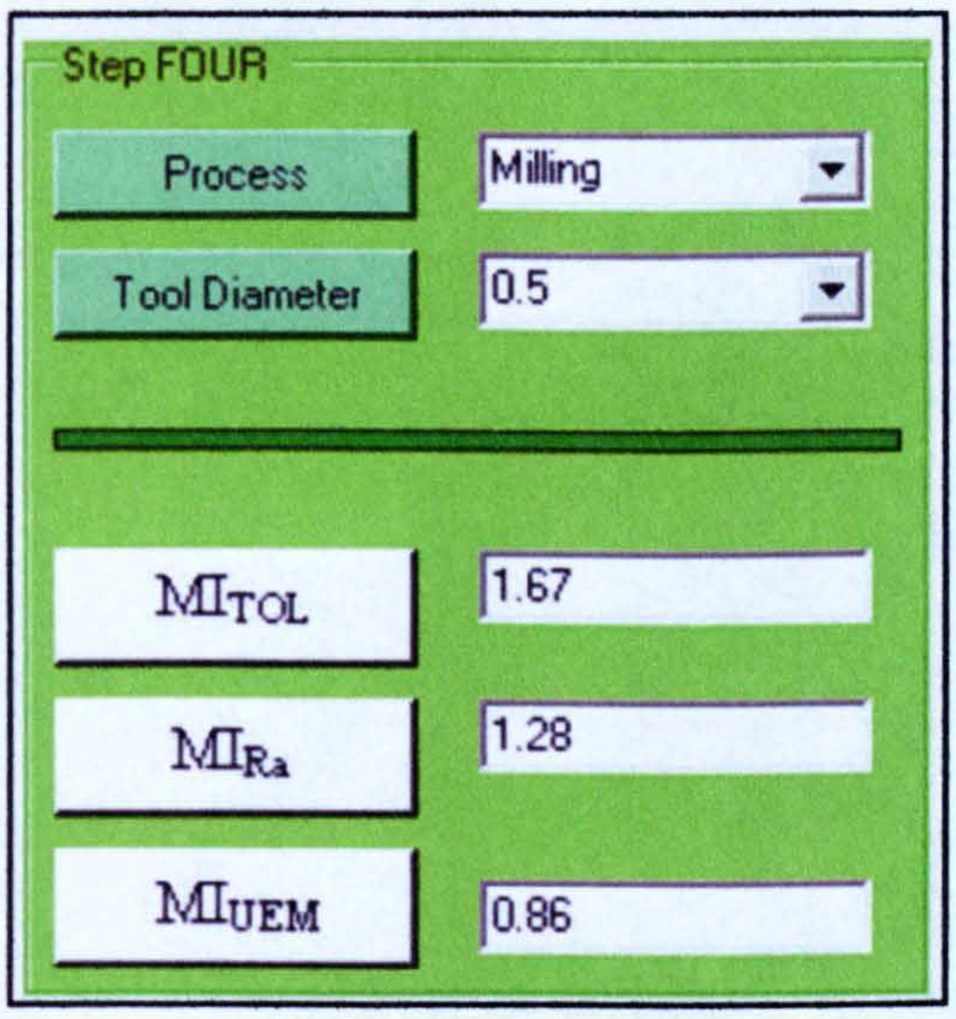

Figure 7.15 Step 4

For the part quality measures, in order to assist the users in determining the suitable and appropriate MI_{Ra}, MI_{TOL} and MI_{UEM}, each button provides a related guideline. As example, Figure 7.16 presents the pop-up guideline for

MI_{TOL}, where the track bars or sliders (as pointed in the figure) guides the users with tolerance value for *harder*, *medium* and *easy to manufacture*. Among the information provided in this pop-up window are the values of the tolerances for each level of manufacturability based on the feature size and its references to the International Tolerance Grade (ITG). Next, users input the tolerance value according to the feature size and by selecting the *Calculate* MI_{TOL} button, the MI_{TOL} value is generated. This value is passed back to the main interface window in Figure 7.15. The above discussed mechanism is again repeated for determining MI_{Ra} and MI_{UEM}. The MI_{Ra}, MI_{TOL} and MI_{UEM} are determined based on the related input in each guideline window and the indices scheme described in ***Chapter 4.***

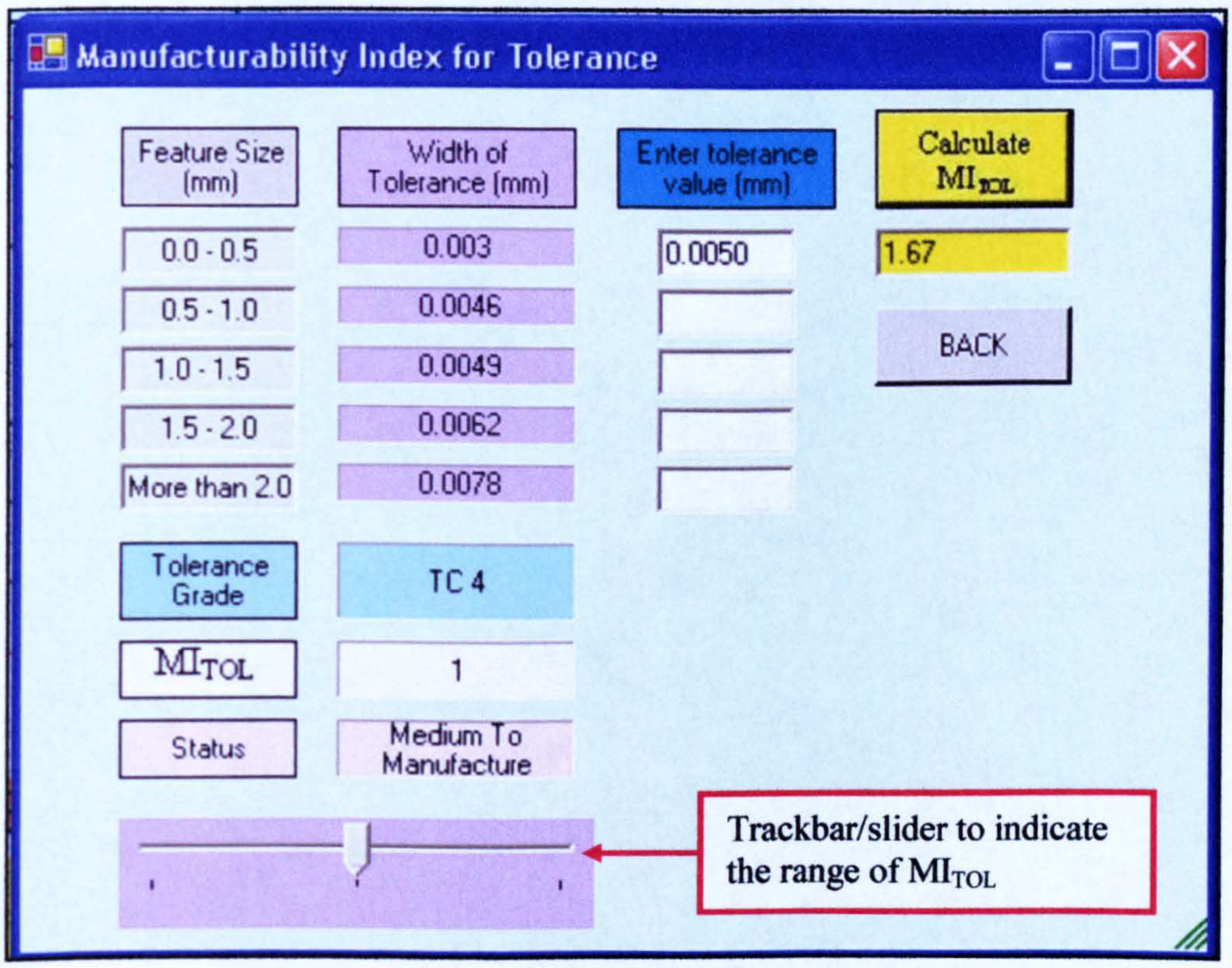

Figure 7.16 Determining the MI_{TOL}

Step 5. This step provides the generated final results of MI_{PF}, MI_{Ra}, MI_{TOL}, MI_{DIM}, MI_{UEM} and Stiffness Ratio (R_{St}). Firstly, weight factor ($0 < K_i \leq 1$) is

assigned to each index based on the users decision in determining which key characteristic are more important when considering the manufacturability of the PF. As example in Figure 7.17, the users choose the impact for tolerance and PF analysis is at 10% (K_i = 0.9) respectively, while the uncertainty in form manufacturing contributes 20% (K_i =0.8) impact in the manufacturability for the particular PF. Meanwhile, the users decided that surface roughness and tool dimension did not have any weightage of influence in the manufacturability of the PF, so value 1.0 is allocated.

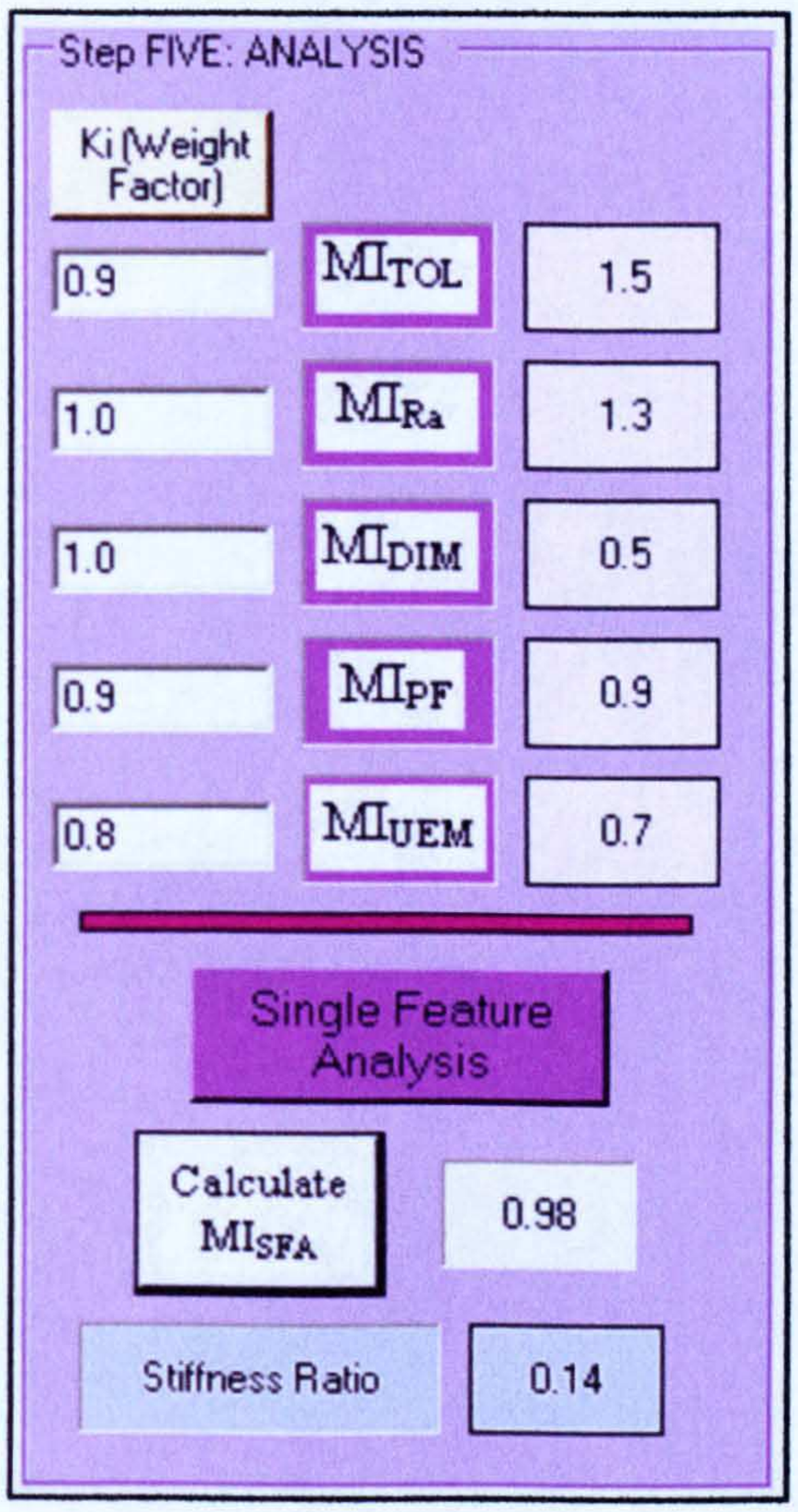

Figure 7.17 Step 5

Next, the *Single Feature Analysis* button is chosen to generate the new MIs after the K_i is being considered for each determined MIs from Step 4. Then, the *Calculate* MI_{SFA} button is selected to generate the MI_{SFA} subjected to Equation

4.1 and also the R_{St} value and analysis. A pop-up (Figure 7.18) provides the result of MI_{SFA} and its level of manufacturability and also the result of R_{St} and determines whether it is within the preset acceptable ranges.

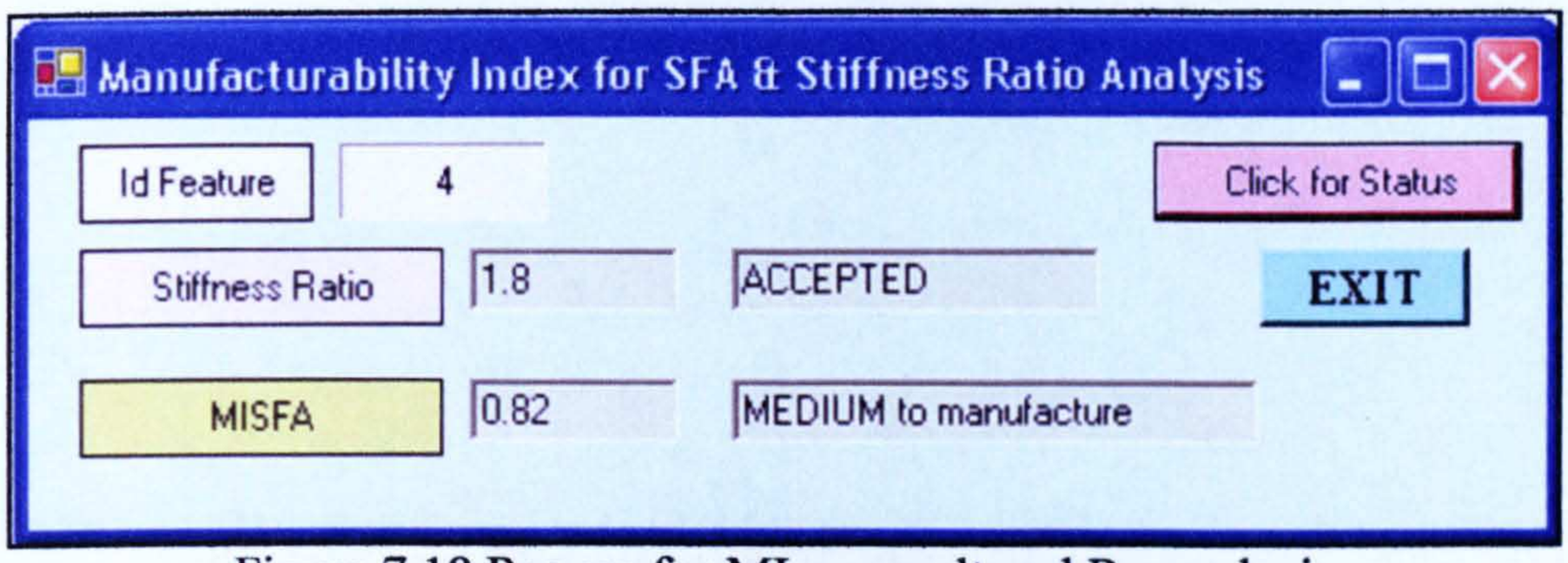

Figure 7.18 Pop-up for MI_{SFA} result and R_{St} analysis

7.4.2. Coupled feature analysis interfaces

Once the data input form reaches the maximum number of PFs contained in the analysed component, a CFA button appears in the main interface (as shown in Figure 7.9) confirming the completion of the ***Input and Single Feature Analysis*** stage. A new interface referring to CFA phase appears (see Figure 7.19), where the users have to input the number of the coupled features occurred in the component (Figure 7.19 (a)). Then, based on this number, the related input textboxes are generated by the system as shown in Figure 7.19 (b). Following this, for each coupled PFs, the users have to input the relative distance (RD) and the type of interactions between them. In assisting the users to determine the type of interactions, a graphical guideline is provided as illustrated in Figure 7.20.

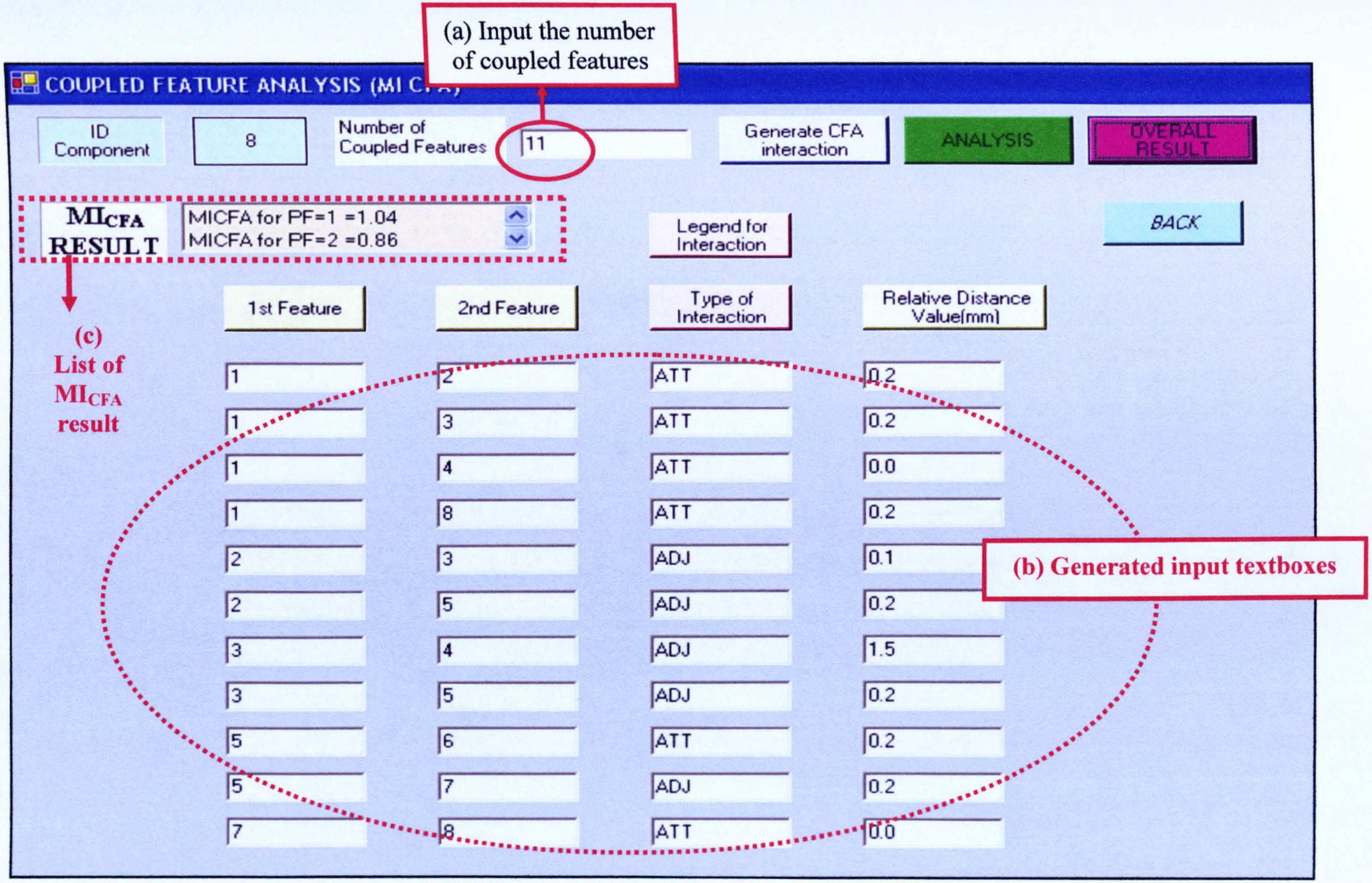

Figure 7.19 Interface for CFA stage

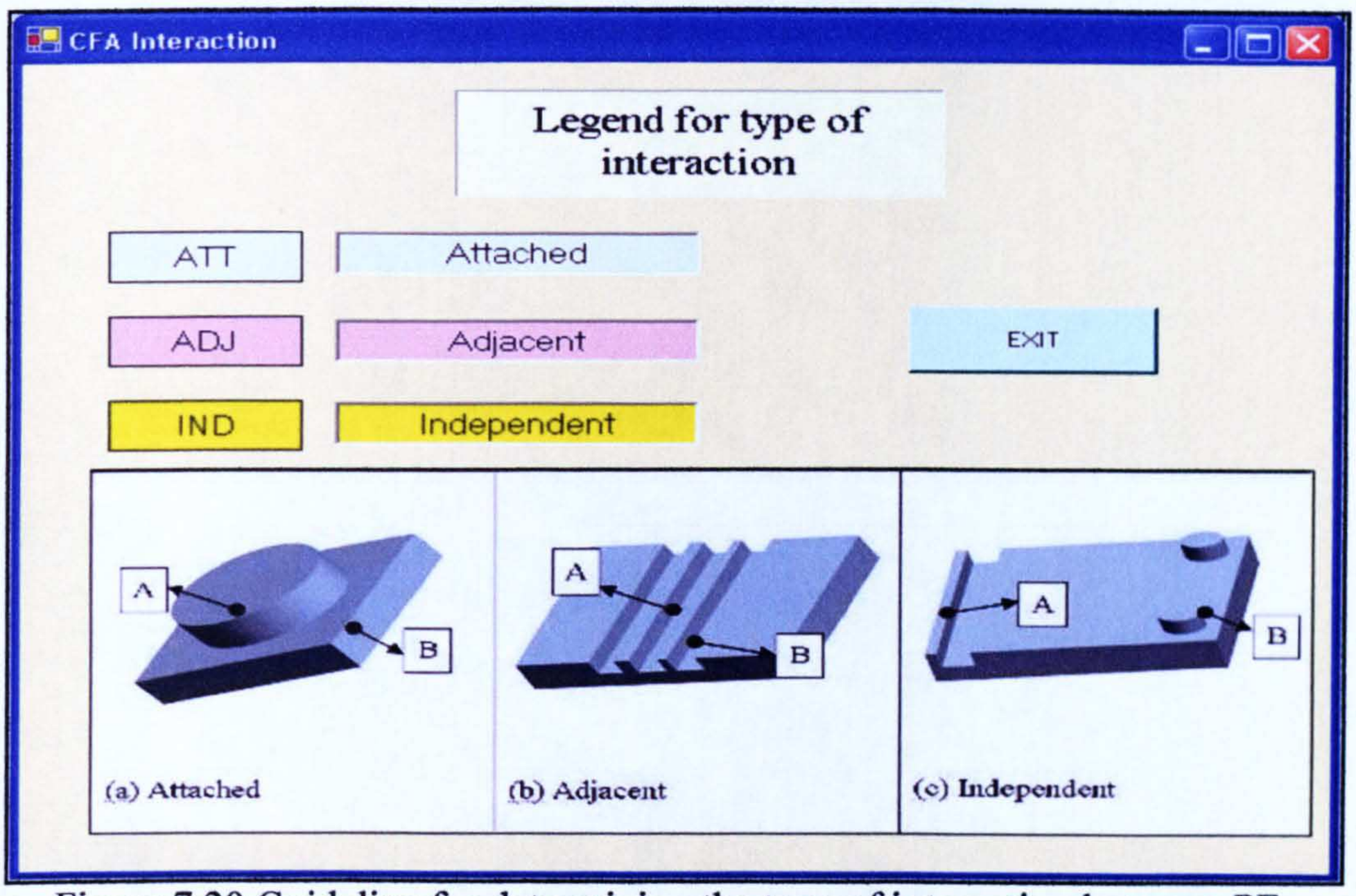

Figure 7.20 Guideline for determining the type of interaction between PFs

Once all the related information (PFs number, type of interaction and RDs) have been supplied, the *ANALYSIS* button is selected and the MI_{CFA} for each PF is calculated based on the scheme discussed in ***Chapter 4***. The result of MI_{CFA} is displayed in the dedicated *list box* as highlighted in Figure 7.19 (c). Following this, the *OVERALL RESULT* button is chosen to proceed to the final stage which is the outputs generation of the system.

7.4.3. Outputs generation interface

The overall output of MicroMAS is shown in Figure 7.21 containing: MI_{SFA} and MI_{CFA} for each PF and $MI_{OVERALL}$ of the analysed component.

RESULT

Number of PF: 8

Generate the boxes | List all MISFA and MICFA | BACK

Features Number	MISFA	MICFA	SUGGESTION (c)
1	1.04	1.04	EASY to manufacture. Any changes to quality measures aspects such as tolerance, surface roughness uncertainty in machining the PF and
2	1.02	0.92	MEDIUM to manufacture. To increase the MI value, redefine the importance of Ki(weight factor) in MISFA, check and revise (if needed)
3	0.96	0.62	MEDIUM to manufacture. To increase the MI value, redefine the importance of Ki(weight factor) in MISFA, check and revise (if needed)
4	1.12	0.53	MEDIUM to manufacture. To increase the MI value, redefine the importance of Ki(weight factor) in MISFA, check and revise (if needed)
5	1.04	0.57	MEDIUM to manufacture. To increase the MI value, redefine the importance of Ki(weight factor) in MISFA, check and revise (if needed)
6	1.04	0.80	MEDIUM to manufacture. To increase the MI value, redefine the importance of Ki(weight factor) in MISFA, check and revise (if needed)
7	1.08	0.60	MEDIUM to manufacture. To increase the MI value, redefine the importance of Ki(weight factor) in MISFA, check and revise (if needed)
8	1.04	0.52	MEDIUM to manufacture. To increase the MI value, redefine the importance of Ki(weight factor) in MISFA, check and revise (if needed)

(a) (b)

MI for OVERALL

MATERIAL: Titanium Alloyed (Ti64) / Soft Steel (AISI 1040) | MI_{MAT}: 1.05

CALCULATE $MI_{OVERALL}$: 0.83

Component is categorized as MEDIUM to manufacture. From SFA, PF=3 has the least Manufacturability Index (MI) for SFA: 0.96. Modification of the quality measures aspects and Ki(weight factor for each MI) for this PF is suggested to achieve a higher value of MI.

Figure 7.21 Overall result interface of MAS

Principally there are four steps involved in generating the final results of this system which are:

- Listing all the PFs contained in the analysed component (Figure 7.21(a)).
- Generating the calculated results of MI_{SFA} and MI_{CFA} from previous interfaces (Figure 7.21(b)).
- Based on the MI_{CFA} result, the system determines the level of manufacturability for each PF and moreover, suggestions are provided to increase the MI_{CFA} or MI_{SFA} such as redefining the importance of K_i in MI_{SFA}, checking and revising the PF's dimensions, quality measures inputs (e.g. selected surface roughness, tolerance value) and related relative distances between PFs (Figure 7.21(c)).
- The MI_{MAT} is determined based on the selected material and finally, the $MI_{OVERALL}$ is calculated employing Equation 4.3 which is stated in Table 7.1. Then, the system determines the level of manufacturability of the overall component. The system also highlights the PFs with least value of MI_{SFA} and MI_{CFA}. If a higher value of $MI_{OVERALL}$ is needed, then the system gives suggestions about changing manufacturability aspects of the component e.g. workpiece material of the component, modification of PFs with low MIs (Figure 7.22).

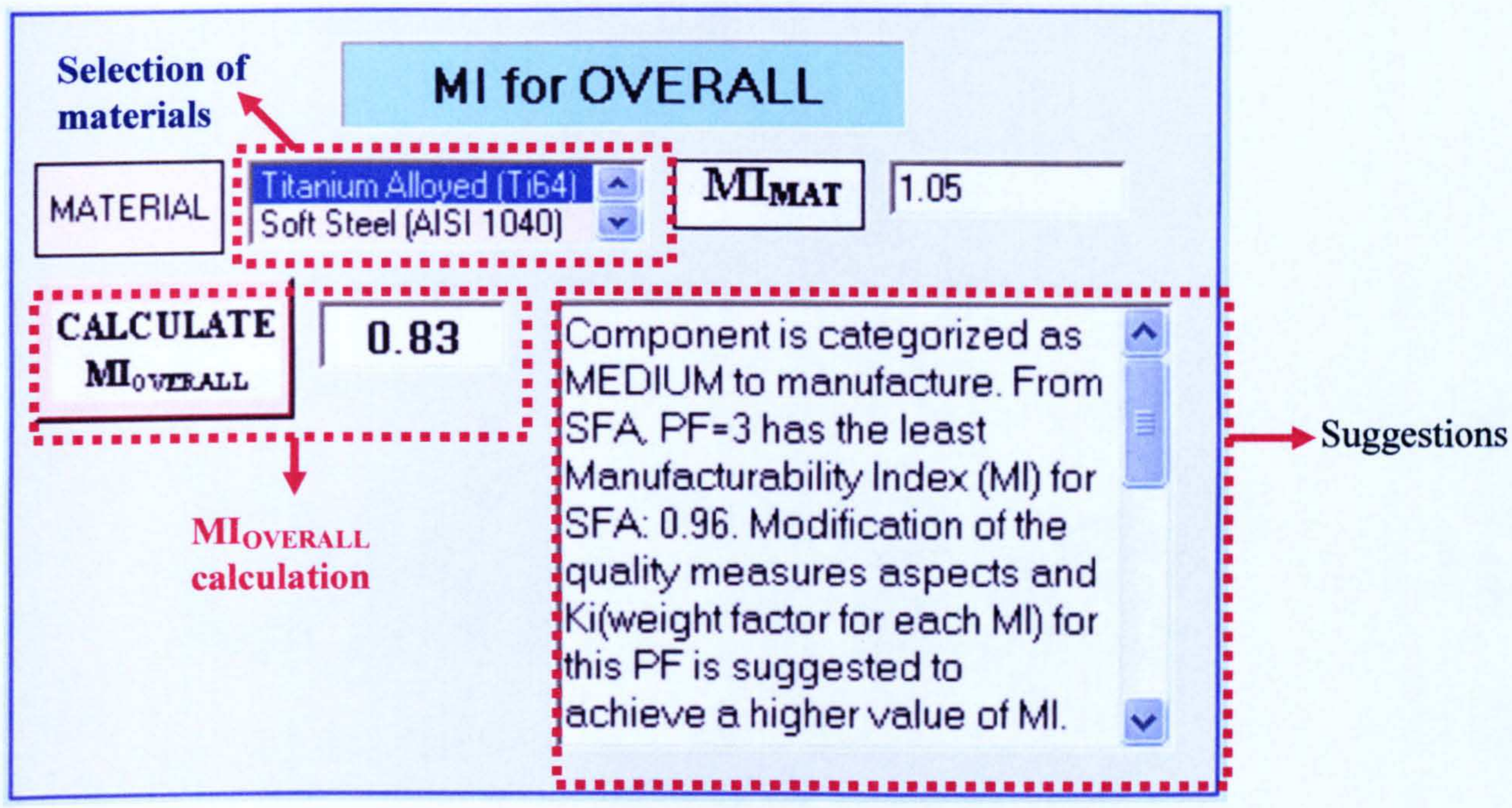

Figure 7.22 $MI_{OVERALL}$ result and suggestions

Based on the analysis towards the proposed components, the system indicates the level of manufacturability for the whole component, e.g. ***Medium*** with $MI_{OVERALL}$ = 0.83 for the analysed micro-part demonstrator. PF_3 is identified as the PF with the least value of MI_{SFA} (0.96), the suggestion provided for this condition is to revise the weight factor (K_i) and also to redefine the selected tolerance, surface roughness and uncertainty effect in machining the PF_3. While PF_7 is recognised as the PF with the least value of MI_{CFA} (0.60), this is believed due to its interactions with other PFs. For this situation, in order to increase the MI_{CFA} value, the system suggested to redefine (if possible) the related relative distances involving PF_7.

Additionally, for the overall suggestion, the system proposed to select material with higher value of MI_{MAT} and also to modify various aspects (e.g. tolerance,

surface roughness) of any PF with low value of MI_{SFA} and/or MI_{CFA} that decrease the value of $MI_{OVERALL}$.

7.5. Advantages and limitations

The implementation of PFA technique in MicroMAS has its own advantages and limitations. The main advantages of MicroMAS are listed below:

- Owing to the overall PF approach and innovative methods of combining data input mechanisms, MicroMAS offers high flexibility for users to extract essential data from the analysed design. Furthermore, the users have full control in defining the analysed design in such a way that is independent on the CAD systems.
- MicroMAS takes into consideration some quality measures (e.g. tolerance, roughness) that can affect the functionality of the analysed micro-component. Most of the current MAS focused solely in analysing manufacturability aspects while neglecting other important aspects such as part functionality.
- The level of manufacturability of the analysed micro-component is presented via a set of comprehensive and sequential aggregate indexes (MIs) which provide clear and meaningful result for the users. This enables the breakdown of the overall manufacturability index into its sub-components to allow the identification of changes needed in the design and/or the specifications of part quality measures; this will allow efficient manufacture of the analysed component.
- MicroMAS was developed using VB which provides a robust and dynamic window-based application where any changes in the

programming code can be easily done. MicroMAS also offers an open-environment system that is dynamic and adaptable to any changes in the future.

- The implementation of RBS and IF-THEN clauses in assessing manufacturability provide a thorough analysis through all the determined rules and conditions.

- As proposed, MicroMAS was suggested to be implemented at the early design stage in order to assist a user of the MMT in machining a CAD model of a micro-product. Based on the generated MIs and the proposed redesign suggestions, it provides ideas to the user on the relative ease of machining the component and also provides information to allow changing the design to meet the requirement of the MMT.

Although MicroMAS has achieved its objectives, it still has limitations as highlighted below:

- Even though it offers flexibility in defining the proposed design, the inference depends on users "translation" towards the design and thus some level of fuzziness might be introduced at the input stage. However, this gives an option for users to decide the most suitable ways to machine the proposed design on the MMT as various MI results can be generated owing to different interpretation of the design.

- Currently, the 'decomposing' of the micro-part in the Initial Assessment phase is based on a limited number of primitive features. Even though it was believed that at this stage, most of the micro-features machined through the micro-milling in the MMT can be interpreted using this

approach, more PF can be easily added as the MicroMAS is an open-system that allows flexibility in inserting any new changes.

- The assessment is based on information structured in a database that needs to be updated from time to time. However, this is a common limitation for all developed system.
- MicroMAS offers manufacturability assessment based only on micro-milling process. However, as the MicroMAS is an open system, other micro-manufacturing process can implement the foundation of this system development to fabricate its own MAS.
- The applicability of MicroMAS can be extended to other micro-machining process owned by the MMT such as micro-drilling/grinding. In order to implement MicroMAS for micro-drilling/grinding, among the aspects that are required to be analysed are:
  - PF interactions due to drilling/grinding process
  - Quality measures (e.g. tolerance, surface roughness, tool impact)
  - The MMT capabilities (e.g. drilling holes) in running both process
  - Modification and adjustment towards the MIs and K_{RD} scheme according to the process requirement
  - Consideration of features sequences related to the specification of the process (micro-milling/drilling/grinding)
- The outputs produced in MicroMAS are limited only to aggregate indexes (MIs) and redesign suggestions. However, the MicroMAS's

framework provides an easy-approach in further adding more relevant outputs.

7.6. Conclusions

From the discussion, it was shown that MicroMAS is capable of: (i) executing the PFA technique in data input mechanism and manufacturability assessment; (ii) analysing the micro-component design based on PFs contained in it; (iii) analysing the manufacturability aspects of the micro-component. Moreover, the calculated MI is also able to indicate the level of manufacturability for each PF (e.g. MI_{PF}, MI_{SFA}, MI_{CFA}) and its overall component ($MI_{OVERALL}$). The conclusions from the development of MicroMAS can be summarized as follows:

- The backbone for Primitive Feature Analysis (PFA) technique is the Primitive Feature (PF) concept (discussed in detail in ***Chapter 4***) which is combined with the positive (bosses) and negative (pockets) convention to define the component in details and produced meaningful interpretations.
- PFA technique consists of two crucial phases which are SFA and CFA in defining the micro-components and analysing its manufacturability. SFA was used for collecting essential data from the CAD model that are further populated with part quality measures, proved to be efficient in providing "necessary and sufficient" input data to MicroMAS. Furthermore, SFA provides an efficient way (MI_{SFA}) to evaluate the manufacturability of each PF of the analysed part. Since the analysed part has many PFs, MicroMAS provides a systematic way to check

interactions between them and to assess the manufacturability (MI_{CFA}) of coupled features. This enables the manufacturability analysis of the part as a result of multi-feature interactions and not as an outcome of a single entity (rigid) assessment commonly used in the most reported work.

- A new sequential MI scheme was demonstrated to indicate the level of manufacturability for each PF and also for the overall micro-component. Based on the generated indexes convention, the level of manufacturability for each PF (***Equation 4.1***) is determined based on several aspects such as PF (e.g. orientation, shape, type), quality measures (e.g. dimensional tolerance, surface roughness), tools diameter and process. $MI_{OVERALL}$ which indicates the overall manufacturability (***Equation 4.3***) of the component is calculated based on the aspects analysed above, the interactions occurred between PFs and also the selected workpiece material. Besides the MI scheme provided to the users, the system feedback takes the form of: suggestions to change manufacturability aspects of the part/PFs, e.g. dimensions, surface roughness, tolerances, workpiece material of PFs/part.
- Rule-based System (RBS) approach proved an efficient method in determining the output measures on the assessments of the manufacturability aspects based on the IF-THEN clauses.

Even though, the execution of PFA technique in MicroMAS that addressed the needs of the MMT is gradually reaching its maturity, the system is capable to analyse manufacturing aspects at an early stage of product development life cycles.

CHAPTER 8: DISCUSSION, CONCLUSIONS AND FUTURE WORK

8.1. Introduction

Manufacturability Analysis Systems (MASs) have been developed to enable the evaluation of easy to manufacture parts during the design stage. The main objective of this study was to develop a MAS for micro-milling domain. Also, to provide a system for a 4-axis Miniature Machine Tool which could assist user in generating micro-components.

The main focus of Chapter 8 is to provide a summary of the research and analysis conducted in the previous chapters. This chapter includes discussion on system development, experimental, numerical and analytical studies carried out. The main conclusions arising from this study combining the findings and contributions related to the aims and objectives for this research are also presented. Finally, recommendations on possible future work and further develop of the knowledge and understanding gained from this study is provided.

8.2. Discussion

The study carried out in this thesis is based on developing a MAS for micro-machining domain. Even though micro-machining is becoming more popular for generating small and high accuracy parts [25, 34-35], there is no clear indication that systems to assist with manufacturability assessment of these parts have been developed. MASs have been proved to work for various

manufacturing processes and it can be noted that such systems mainly addressed macro-manufacturing processes such as milling and drilling [5], turning [9], grinding [12] and injection moulding [16], while very little was found in the literature that addressed the MAS applicability in micro-manufacturing processes as discussed in ***Chapter 2***.

In line with the intention to develop a MAS for micro-machining environment, the custom-made 4-axis Miniature Machine Tool (MMT), was chosen to be the scope of the system development as at the same time the MMT require a system to support a robust and efficient generation of micro-part. As described in ***Chapter 3*** and ***Chapter 6***, the MMT is a custom-made machine tool so there are no standards, guidelines or any manual to refer to in operating the MMT. This demonstrated the requirement of the MMT that a system was needed to assist the user in producing micro-part via the MMT.

MicroMAS was developed to support the MMT in terms of assessing the micro-manufacturability aspects (e.g. materials used, dimensions of micro-component, surface roughness and tolerance) of a proposed CAD model. A Primitive Feature Analysis technique (PFA) has been introduced and developed in this study for the purpose of gathering essential data from the proposed CAD models and to further analyse their manufacturability. The framework and mechanism were described and discussed in ***section 4.4***, while the simulation of a PFA algorithm on a CAD model was presented in ***section 4.5***. This has demonstrated the ability of the technique to gather data and to

further analyse its manufacturability. In ***section 4.6*** and ***Chapter 7***, the implementation of PFA technique in MicroMAS has been described.

In order to embed real conditions of the MMT in the system, details from the various micro-machining experiments done on the MMT as discussed in ***Chapter 6*** and also the results from the Uncertainty Evaluation Model for the MMT (presented in ***Chapter 5***) were written into the system. The integration of information from the results of machining experiments as well as the UEM analysis into the MicroMAS made the system rich with knowledge offering users more representative information which generated more significant manufacturability indexes. Table 8.1 lists the summary of objectives and contributions of each key attribute involved in this study.

Table 8.1 A mapping of the objectives and contributions of key attributes in this study

Attribute	Objective	Contribution
MicroMAS	• To assess manufacturability aspects of micro-components to be machined via the MMT	• Provide a MAS for micro-machining domain • Assist the user in using the MMT in machining micro-part.
Primitive Feature Analysis	• To collect/gather information from the CAD model of the analysed micro-component • To analyse the manufacturability assessment based on primitive feature on three phases: primitive feature identification; Single Feature Analysis, Coupled Feature Analysis.	• Give opportunity in simplifying the way in 'translating' the CAD model into MAS • Provide new approach in assessing the manufacturability aspects.
Manufacturability Indices	• To provide scheme to rate the level of manufacturability from the analysis of PFA for MicroMAS	• Provide quantitative indication to user on the level of manufacturability.
Micro-machining experiments	• To analyse the surface roughness and tolerance of the machined micro-part via MMT • To assess the capability of the MMT in terms of machining 3D micro-parts, surface quality and geometrical accuracy.	• Offer related data (surface roughness and tolerance) to the system so that MicroMAS own the real condition of the MMT • Show the capability of the MMT
Uncertainty Evaluation Model	• To analyse the errors stemming from the construction of MMT that affect the geometrical accuracy of the machined micro-parts • To supply information of uncertainty value of form manufacturing effect into the system	• Provide a method/model that can predict the errors of in-house/custom-made machine tool • Judgement on the uncertainty of the MMT construction towards the geometrical accuracy.

8.3. Conclusions

The development of MicroMAS displayed a novel approach in terms of implementing manufacturability assessment for Micro-Engineering Technologies (MET) process (micro-milling). There has been very little work in looking at the MAS development for this type of machining process. The results from the manufacturability assessment in MicroMAS has been successfully achieved through a manufacturability index which indicates the relative ease of machining a CAD model and provides a list of related suggestions (e.g. changes of quality measures, recommendation of material with lower hardness). In the following, the key findings and concluding remarks of this study are presented:

- **PFA technique is introduced and employed to gather data from a CAD model and to analyse their manufacturability aspects**

Primitive Feature Analysis technique has been introduced to be the method in gathering data from the analysed micro-component CAD model while enabling the assessment of their manufacturability aspects. The technique enables method of gathering data from a CAD model using a simplify primitive feature concept. In order to define the analysed micro-components and produce meaningful interpretations, the PFA technique relies on algebraic (boss – positive, cavity – negative) PFs such as box, cylinder and cones contained in the proposed CAD model and the interactions between them. The PFA technique consists of three crucial phases which are: primitive feature identification, Single Feature Analysis (SFA) and Coupled Feature Analysis (CFA).

In the first phase, all the PFs contained in the analysed micro-components can be recognised together with their essential geometrical characteristics and data which are required as illustrated in ***Chapter 4***. For the *SFA phase*, it was discovered that the level of manufacturability of each defined PF can be determined based on its orientation, shape, end-corner specification and part quality measures (e.g. tolerance, surface roughness). Furthermore, SFA has also demonstrated an efficient way to evaluate the manufacturability of each PF of the analysed part through the determination of the MI_{SFA}.

Next, the *Coupled Feature Analysis (CFA)* can determine the level of relationship among PFs by taking into consideration the relative distance and the type of interactions (e.g. attached, adjacent and independent) between them. This enables the manufacturability analysis of the part as a result of multi-feature interactions and not as an outcome of a single entity (rigid) assessment commonly used in the most reported work in previously developed MAS. CFA also allows MicroMAS to provide a systematic way to check interactions between the PFs and to assess the manufacturability of coupled features through the calculation of MI_{CFA}.

As a conclusion, the PFA technique has demonstrated a simple approach in collecting relevant data from a CAD model of a micro-component and for analysis of manufacturability aspects (e.g. workpiece material, tolerance, surface roughness, machine tool capability, the contained PFs).

- **Manufacturability index(s) are used to express the level of manufacturability of the analysed CAD model**

  A sequential aggregate indexes scheme that was based on a rating convention has been effectively implemented in indicating the level of manufacturability of the analysed CAD model based on the PFA technique phases. Manufacturability Indexes (MIs) reflect the relative ease of machining the analysed micro-component based on various aspects such as the characteristics of the PF and their interactions, tolerance, surface roughness, machinability of the workpiece materials and tool dimensions. The implementation of MIs has demonstrated the ability to provide a fundamental indication to a user on the level of manufacturability in generating the micro-component by using the MMT. In-depth studies of the generated Manufacturability Indexes (MIs) which were used to indicate the level of manufacturability were discussed in ***section 4.3*** and ***4.5***. Moreover, a rating convention has been established to represent all the MIs (***Equation 4.2***) in determining their level of manufacturability. Furthermore, based on the determined level of manufacturability, suggestions have been proposed to a user to help enhance this level.

- **The combination of *user-system interaction* and *a priori database* as a new approach in input mechanism for MicroMAS**

  In order for the PFA technique to gather the related CAD data, *user-system interaction* and *a priori database* methods were combined and utilized as the input mechanism for the MicroMAS. This combination was discovered to provide more interactive, direct and flexible input session compared to

the feature extraction system. It was also proved that this combination is able to support the data gathering method that has been introduced in PFA technique. Furthermore, accurate and relevant data were also effectively supplied to the system.

- **Uncertainty Evaluation Model can be utilized to identify the variables that affect the geometrical accuracy of the machined micro-part**

The developed UEM has proven to be a satisfactory method to identify the errors stemming from the construction of the MMT that affect the geometrical accuracy of the machined micro-part. The evaluation of these errors allows key understanding on the origin of the errors on the machined micro-part have been discussed in ***sections 5.3*** and ***5.4***. However, the developed model does not include any error associated with machining process (e.g. tool deflection, tool wear, vibration, burr formation) as it exclusively focuses on errors originating from the construction of the MMT.

In this study, four sources of main errors have been identified which are: errors due to tool path generation stemming from the MMT construction, errors related to evaluation of workpiece reference point, errors related to temperature variations and errors originating from positioning inaccuracies of each table. These identified errors that were formulated based on the spiral milling movement, ISO guidelines and results from CMM evaluations have been successfully analysed through GUM Workbench.

From the analysis made, it was discovered that the errors stemming from the α (angle between tool and side of xz plane) and γ (angle between tool and z axis) indicated the main sources of errors of the MMT construction. Even though from the analysis, it shows that the positioning errors of the tools stemming from the inaccuracies in constructing the X, Y and Z planes were identified as the main uncertainty from the MMT construction but the calculated uncertainty value are of low values so still keeps the accuracies of the micro-parts at an acceptable level.

Moreover, in order for the MicroMAS to mirror the real condition of the MMT, the impact of UEM analysis is taken into consideration in calculating the Manufacturability Index for Single Feature Analysis (MI_{SFA}). The Manufacturability Index for Uncertainty Evaluation Model (MI_{UEM}) was being considered in the MI_{SFA} formula for each identified primitive feature (PF). With this scheme, it was found out that the manufacturability analysis in MicroMAS was more significant as it portrayed the current condition of the MMT. Furthermore, the development of UEM has also demonstrated a systematic method/procedure allowing errors stemming from its construction for any similar in-house developed MMT to be analysed.

- **The impact of integrating the results from UEM and micro-machining experiments within MicroMAS**

  Taking into consideration the main scope/domain for the MicroMAS implementation, it was necessary for the system to be integrated with

information related to the MMT such as machine capability, surface roughness and tolerance. Moreover, the study provided the opportunity for the system to mirror the real condition of the MMT so that realistic analysis of manufacturability could be made. The integration of results from the UEM analysis and also micro-machining experiments have been disclosed in ***section 5.7*** and ***6.5*** respectively.

By integrating results from the UEM analysis and also the machining experiments completed within the MMT into the MicroMAS, it has successfully provided the system with the real condition of the MMT. This integration was found to enhance the ability in the decision making process (e.g. determining the manufacturability indexes). As stated previously, from the UEM analysis the uncertainty effect in machining each primitive feature which could influence the accuracy of the form/shapes of the machined micro-features has also been taken into consideration.

From the machining experiments, the obtained results of surface roughness and geometrical accuracy have been successfully utilized to generate the Manufacturability Index for Surface Roughness (MI_{Ra}) and Manufacturability Index for Tolerance (MI_{TOL}). Besides providing the relevant information for the MicroMAS, the machining experiments were also employed for assessing the capability of the MMT in generating micro-parts. It can be concluded that despite being an in-house developed machine tool, it was found that the MMT was able to generate critical micro-structures such as thin walls and also micro-component with

acceptable surface quality and high satisfactory level of geometrical accuracy.

- Although it was not within the scope of this study to seek to optimise cutting parameters that result in fine surface roughness, the measured R_a and R_z values achieved were found to be acceptable and the geometrical accuracy values were also in a respectable range of precision. Measurements made on surface roughness of the machined micro-part discussed in ***sections 6.3.1.2, 6.3.2.2*** and ***6.3.3.2*** have confirmed the capability of the MMT in producing good and satisfactory surface quality (R_a= 0.02 – 0.07 μm). Furthermore, from the same sections, the analysis made on the geometrical accuracy of the machined micro-part also shows that acceptable geometrical accuracy of micro-part can be accomplished by using the MMT. The surface quality and geometrical accuracy were analysed and correlated with a variety of suggested machining parameters in generating micro-component in various materials.

This gives an indication that the custom-built MMT has been developed to a satisfactory level of precision to enable micro-machining of surfaces with acceptable accuracies.

8.4. Contributions of this research study

This study brings a new dimension in the MAS field as apparently for the first time it is being developed for a micro-processing method, i.e. micro-milling, as its scope of implementation. As detailed in ***Chapter 7***, by combining various

approaches/tools in developing the MicroMAS (e.g. VB, RBS, IF-THEN, database, UEM and micro-machining results), it has been proven that the manufacturability aspects of the micro-parts can be analysed in an interactive way between a user and the system. Furthermore, this system also assists a user in generating micro-components that will be machined using the MMT through manufacturability evaluation of a proposed CAD model. Among the key contributions of this study are as the following:

- This study introduces a new technique (Primitive Feature Analysis) in collecting important information from a CAD model of the analysed micro-component and further to asses their manufacturability. The technique that was based on primitive feature concept has been successfully employed in the developed system (MicroMAS). The novelty of the approach has been presented to the academic community [190].
- In developing the MicroMAS, a new framework has been presented which consists of the implementation of the PFA technique, the combination of *user-system interaction* and *collecting of manufacturing information* for input mechanism and also the integration between the system, UEM analysis and micro-machining experiments. Apparently, for the first time, the results from the UEM analysis have been integrated into a MAS development which allowed the real condition of the MMT to be emulated into the system. This new framework has also been presented to the academic community [190].
- A new sequential ***Manufacturability Indices*** scheme has been established to indicate the level of manufacturability for each PF and also for the analysis of micro-component. Based on the generated indexes convention

as discussed in ***Chapter 4***, the level of manufacturability for each PF (MI_{SFA}) was determined based on several aspects such as PF (e.g. orientation, shape, type); dimensional tolerance, surface roughness, uncertainty analysis on machining the PF, tools diameters and selected workpiece material. MI_{CFA} was determined on the relative distance and also the interactions which occurred between the PFs. $MI_{OVERALL}$ which indicates the overall manufacturability of the micro-component was calculated based on the aspects analysed above and also the selected workpiece materials. These indexes were presented by a rating convention that is divided into three levels: **Harder** to manufacture, **Medium** to manufacture and **Easier** to manufacture. This new rating convention has also been discussed and presented to the academic community [190].

- Apparently, for the first time, uncertainty evaluation analysis has been developed for identifying and analysing the variables that affect the geometrical accuracy of the machined micro-part originating from the construction of the MMT. More importantly, this study provides the opportunity to understand the source of errors on a machined micro-part via an MMT, either from the machining process or from the machine itself. The results from the uncertainty analysis that found the source of errors from the MMT construction have been presented to the academic community [191].
- The crucial contribution of this study is it proposed a methodology to evaluate the uncertainties of any similar in-house developed machine tools through the model which can identify the main sources of errors that affect the quality of the machined part. Once the model has been developed, the

geometrical errors in any situation can be evaluated when other (more) complex surfaces are generated. This methodology or approach in analysing uncertainties of a custom-made MMT has been presented to the academic community [191].

- In assessing the capability of the MMT, various micro-machining experiments based on machining parameters suggested by tool manufactures have been executed. Such as machining the "adapted standard testpiece", generating micro-slots and thin walls and also producing micro-components that consist of various features. These experiments can be distinguished as an initial effort into developing a new verification procedure for the performance of the machine tools when performing micro-machining. The results from these experiments have been presented to the academic community [191].

8.5. Future Work

Even though the aims and objectives of the current study have been achieved, the thesis has raised some gaps which can be further explored. Possible future works can be grouped into different categories, as follows:

- Based on critical analysis towards MicroMAS, the following areas of interest are identified for further research:
  - MicroMAS is proposed to produce more combinations of outputs which is believed will increase its effectiveness, such as estimations of production cost and time as well as process sequencing. Various combinations of output can increase the effectiveness of MAS as it provides 'enriched' knowledge/ recommendations that can assist the

end-user system in making more comprehensive technical decisions regarding the machining of proposed designs. Apart from this, the capability of assessing more robust manufacturability indices/ratings should be pursued. It is believed that more combinations of related elements would lead to a greater degree of accuracy on the generated manufacturability indices. It is also recommended to consider other manufacturing-related aspects such as ease of fixturing and process capability.

- At the moment, the system comprises only a limited number of primitive features. This is because it was believed that at this stage; the micro-features generated via micro-milling can be decomposed using this options of PFs. However, more PFs can be added in the future to build the capability of the MicroMAS.
- For its data input mechanism, it is interesting to explore the possibility of adapting the existing automatic data extraction tool into the MicroMAS. This approach can be combined with the PFA technique in assessing the manufacturability aspects.
- It is suggested to implement the PFA technique for developing MAS for other micro-machining processes.

- Further investigation based on the uncertainty evaluation is required to understand other possible errors that affect the geometrical accuracy of the machined micro-part generated through the MMT. This may provide further understanding on how other errors besides stemming from the construction of an MMT can affect the final quality of machined micro-part.

- Further work is required to define the methods to evaluate the uncertainty of more complex features and to translate them into uncertainty models. This will provide a better understanding on the capabilities of a MMT in generating various micro-parts. The related information can be injected into the MicroMAS and should provide better results in determining the level of manufacturability of a particular micro-part.

- As the Nottingham MMT is also claimed to be capable to perform micro-drilling and micro-grinding, these processes should be considered to be applicable for the MicroMAS so that it enhances the flexibility of the system. Moreover, it also provides an opportunity for the manufacturability aspects to be analysed based on a variety of manufacturing processes that allows considering the successions or interactions of the process.

REFERENCES

1. Gupta, S.K., Regli, W.C., Das, D. and Nau, S., *Automated manufacturability analysis: A survey.* Research in Engineering Design, 1997. 9(3): p. 168-190.
2. Boothroyd, G., Dewhurst, P. and Knight, W., *Product Design for Manufacture and Assembly.* 1994, New York: Marcel Dekker Inc.
3. Rao, S.S., Nahm, A., Shi, Z., Deng, X. and Syamil, A., *Artificial Intelligence and Expert System Applications in New Product Development - A Survey.* Journal of Intelligent Manufacturing, 1999. **10**(3-4): p. 231-244.
4. Krishnan, S., *Design for Manufacture: An Integrated System for Injection Moulding and Milling.* 1997, University of Maryland College Park.
5. Venkatachalam, A.R., Mellichamp, J.M. and Miller D.M., *A Knowledge-based Approach to design for Manufacturability.* Journal of Intelligent Manufacturing, 1993. **4**(5): p. 355-366.
6. Yuyin, S., Bopeng, Z., Fuzhi, C. and Qingguo, M. . *A Knowledge-based Design for Manufacture System. IEEE International Conference on Systems, Man and Cybernetics 1996.* 1996. Beijing, China.
7. Gebresenbet, T., Jain, P.K., and Jain, S.C., *Preliminary Manufacturability Analysis Using feature-function - Resource Considerations for Cylindrical Machined Parts.* International Journal of Computer Integrated Manufacturing, 2002. **15**(4): p. 361-378.
8. Jacquel, D., Salmon, J., *Design for Manufacturability: A Feature-Based Agent-Driven Approach.* Proceedings of the Institution of Mechanical Engineers, Part B: Journal of Engineering Manufacture, 2000. **214**(10): p. 865-879.
9. Arezoo, B., Ridgway, K. and Al-Ahmari, A.M.A., *Selection of Cutting Tools and Conditions of Machining Operations using an Expert System.* Computers in Industry, 2000. **42**(1): p. 43-58.
10. Jiang, B.C., Hsu, C.H., *Development of a Fuzzy Decision Model for Manufacturability Evaluation.* Journal of Intelligent Manufacturing, 2003. **14**(2): p. 169-181.
11. Ong, S.K., Sun, M.J. and Nee, A.Y.C., *A Fuzzy Set AHP-based DFM Tool for Rotational Parts.* Journal of Material Processing Technology, 2003. **138**(1-3): p. 223-230.
12. Jacob, D.V., Ramana, K.V. and Rao, P.V.M., *Automated Manufacturability Assessment of Rotational Parts by Grinding.* International Journal of Production Research, 2004. **42**(3): p. 505-519.
13. Chen, Y.M., Miller, R.A., Sevenler, K., *Knowledge-based Manufacturability Assessment: An Object-oriented Approach.* Journal of Intelligent Manufacturing, 1995. 6(5): p. 321-337.
14. Feng, R., *STL Toolkit: A Manufacturability Evaluation Environment.* 1998, The Ohio State University.
15. Chen, Y.M., Wen, C.C. and Ho, C.T. , *Extraction of Geometric Characteristics for Manufacturability Analysis.* Robotics and Computer Integrated Manufacturing, 2003. **19**(4): p. 371-385.
16. Marquez, M., White, A., and Gill, R., *A Hybrid Neural Network-feature-based Manufacturability Analysis of Mould Reinforced Plastic*

Parts. Proceedings of the Institution of Mechanical Engineers, Part B: Journal of Engineering Manufacture, 2001. **215**(8): p. 1065-1079.
17. Giannakakis, T., Vosniakos, G.C., *Sheet Metal Cutting and Piercing Operations Planning and Tools Configuration by an Expert System.* International Journal of Advanced Manufacturing Technology, 2008. **36**(7 - 8): p. 658 - 670.
18. Ramana, K.V., Rao, P.V.M., *Automated Manufacturability Evaluation System for Sheet Metal Components in Mass Production.* International Journal of Production Research, 2005. **43**(18): p. 3889-3913.
19. Sasaki, Y., Sonda, M., and Ito, K., *Development of a Computer-aided Process Planning System Based on a Knowledge Base.* Journal of Marine Science and Technology, 2003. 7(4): p. 175-179.
20. Chen, C.H., Occena, L.G., and Fok, S.C., *CONDENSE:A Concurrent Design Evaluation System for Product Design.* International Journal of Production Research, 2001. **39**(3): p. 413-433.
21. Kumar, S., Singh, R. and Sekhon G.S., *CCKBS: A Component Check Knowledge-based System for Assessing Manufacturability of Sheet Metal Parts.* Journal of Material Processing Technology, 2006. **172**(1): p. 64-69.
22. Giachetti, R.E., Alvi, M.I., *An Object-oriented Information Model for Manufacturability Analysis of Printed Circuit Board Fabrication.* Computers in Industry, 2001. **45**(2): p. 177-196.
23. Cherian, R.P., Midha, P.S., Smith, L.N., and Pipe, A.G., *Knowledge based and Adaptive Computational Techniques for Concurrent Design for Powder Metallurgy Parts.* Advances in Engineering Software, 2001. **32**(6): p. 455-465.
24. Smith, L.N., Midha P.S., *A Knowledge Based System for Optimum and Concurrent Design, and Manufacture by Powder Metallurgy Technology.* International Journal of Production Research, 1999. **37**(1): p. 125 - 137.
25. Alting, L., Kimura, F., Hansen, H.N., and Bissacco, G., *Micro Engineering.* Annals of CIRP 52, 2003. **2**: p. 635-658.
26. Chae, J., Park, S.S. and Freiheit, T., *Investigation of micro-cutting operations.* International Journal of Machine Tools and Manufacture, 2006. **46**(3 - 4): p. 313 - 332.
27. Dornfeld, D., Min, S., Takeuchi, Y., *Recent Advances in Mechanical Micromachining.* Annals of CIRP - Manufacturing Technology, 2006. **55**(2): p. 745 - 768.
28. Jun, M.B.G., Liu, X., DeVor, R.E., Kapoor, S.G., *Investigation of the Dynamics of Microend Milling-Part I: Model Development.* Journal of Manufacturing Science and Engineering, 2006. **128**(4): p. 893 - 900.
29. Rahman, M., Kumar, A.S., Prakash, J.R.S., *Micro Milling of Pure Copper.* Journal of Materials Processing Technology, 2001. **116**(1): p. 39 - 43.
30. Filiz, S., Conley, C.M., Wasserman, M.B., Ozdoganlar, O.B., *An Experimental Investigation of Micro-machinability of Copper 101 using Tungsten Carbide Micro-endmills.* International Journal of Machine Tools and Manufacture, 2007. **47**(7 - 8): p. 1088 - 1100.
31. Wang, W., Kweon, S.H., Yang, S.H., *A Study on Roughness of the Micro-End-Milled Surface Produced by a Miniatured Machine Tool.*

Journal of Materials Processing Technology, 2005. **162 - 163**: p. 702 - 708.
32. Zaman, M.T., Kumar, A.S., Rahman, M., Sreeram, S., *A Three-Dimensional Analytical Cutting Force Model for Micro End Milling Operation.* International Journal of Machine Tools and Manufacture, 2006. **46**(3 - 4): p. 353 - 366.
33. Alberz, A., Marz, J., *Restriction of production engineering on microspecific product development.* Microsystem Technologies, 2004. **10**(3): p. 205-210.
34. Dimov, S., Pham, D.T., Ivano, A., Popov, K., and Fansen, K., *Micromilling strategies: Optimization issues.* Proceedings of the I MECH E Part B Journal of Engineering Manufacture, 2004. **218**(7): p. 731-736.
35. Masuzawa, T., *State of the art of micromachining.* CIRP Annals - Manufacturing Engineering, 2000. **49**(2): p. 473-488.
36. Vogler, M., Liu,X., DeVor, R.E., Kapoor, S.G. *Miniaturized machine tools for CNC-based micro/meso-scale machining of 3D features. Third International Workshop on Microfactories*. 2002.
37. Mahalik, N.P., *Micromanufacturing and Nanotechnology*. 2006, Berlin: Springer-Verlag Berlin Heidelberg.
38. Bozdana, T.A., Axinte, D.A., *Design and demonstration of a 4-axis miniature machine tool to enable freeform micro-machining (Demo-μmach)*. 2006, University of Nottingham. p. 1 - 39.
39. Bissacco, G., Hansen, H.N., De Chiffre, L., *Micromilling of hardened tool steel for mould making applications.* Journal of Material Processing Technology, 2005. **167**(2 - 3): p. 201 - 207.
40. Bao, W.Y., Tansel, I.N., *Modelling Micro-End Milling Operations. Part II: Tool Run-Out.* International Journal of Machine Tools and Manufacture, 2000. **40**(15): p. 2175 - 2192.
41. Vogler, M.P., Kapoor, S.G., DeVor, R.E., *On the Modellng and Analysis of Machining Performance in Micro-Endmilling, Part II:Cutting Force Prediction.* Journal of Manufacturing Science and Engineering, 2004. **126**(4): p. 695 - 705.
42. Dhanorker, A., Ozel, T. *An Experimental and Modeling Study on Meso/micro End Milling Process. 2006 ASME International Conference on Manufacturing Science and Engineering.* 2006. Michigan.
43. Ducobu, F., Filippi, E., Rivière-Lorphèvre, E. *Chip formation and minimum chip hickness in micro-milling. 12th CIRP Conference on Modelling of Machining Operations*. 2009. Spain.
44. Kawahara N., S.T., Hirano T., Ishikawa Y., Kitahara T., Ooyama N., Ataka T., *Microfactories; new applications of micromachine technology to the manufacture of small products.* Microsystem Technologies, 1997. 3(2): p. 37 - 41.
45. Hansen, H.N., Eriksson, T., Arentoft, M., Paldan, N. *Design rules for microfactory solutions. 5th International Workshop on Microfactories.* 2006. France.
46. Rao, S.K., *The Development of Fuzzy Cognitive Map for Manufacturability Analysis Based on Part Features*. 1994, Texas A&M University-Kingsville.

47. Gupta, S.K., Nau D.S., *Systematic approach to analysing the manufacturability of machined parts.* Computer-Aided Design, 1995. **27**(5): p. 322-345.
48. Pham, D.T., Dimov, S.S., *An Approach to Concurrent Engineering.* Proceeding of Institutional of Mechanical Engineers, 1998. **212**(B): p. 13 – 27.
49. Lee, R.S., Chen, Y.M. and Lee, C.Z., *Development of a Concurrent Mold Design System: A Knowledge-based Approach.* Computer Integrated Manufacturing Systems, 1997. **10**(4): p. 287-307.
50. Dissinger, T.E., Magrab, E.B., *Geometric Reasoning for Manufacturability Evaluation-Application to Powder Metallurgy.* Computer-Aided Design, 1996. **26**(10): p. 783-794.
51. Horvath, L., Rudas, I.J., Machado, J.A.T. and Hancke, G.P. . *Application of Part Manufacturing Process Model in Virtual Manufacturing. 1999 IEEE International Symposium on Industrial Electronics (ISIE '99).* 1999.
52. Howard, L., Lewis, H., *Support Tool for Material and Process Combinations During Early Design.* International Journal of Production Research, 2006. **44**(17): p. 3379-3390.
53. Lu, S.C., *Volume-based Geometric Reasoning and Visualization to Support Manufacturability Evaluation in Die Casting.* 1996, The Ohio State University.
54. Tharakan, P.V., Zhao, Z., and Shah, J. *Manufacturability Evaluation Shell: A Reconfigurable Environment for Technical and Economic Manufacturability Evaluation. Design Engineering Technical Conferences and Computers in Information in Engineering Conference (DETC'03).* 2003. Chicago: ASME.
55. Giachetti, R.E., *Integrating Hypermedia Design Concepts with A Systems Analysis and Design Methodology to Develop Manufacturing Web Applications.* International Journal of Computer Integrated Manufacturing, 2005. **18**(4): p. 329-340.
56. Myint, S., Tabucanon, M.T., *The framework for an expert system to generate alternative products in concurrent engineering design.* Computers in Industry, 1998. **37**(2): p. 125 - 134.
57. Zha, X.F., Du, H., *Manufacturing Process and Material Selection in Concurrent Collaborative Design of MEMS Devices.* Journal of Micromechanics and Microengineering, 2003. **13**(5): p. 509-522.
58. Hayes, C.C., *Plan-based Manufacturability Analysis and Generation of Shape-changing Redesign Suggestions.* Journal of Intelligent Manufacturing, 1996. **7**(2): p. 121-132.
59. Korosec, M., Balic, J. and Kopac, J., *Neural Network based Manufacturability Evaluation of Free Form Machining.* International Journal of Machine Tools and Manufacture, 2005. **45**(1): p. 13-20.
60. Nasr, E.A., Kamrani, A.K., *Computer-Based Design and Manufacturing: An Information-based Approach.* 2007, New York, USA: Springer Science+Business Media, LLC.
61. Brissaud, D., Tichkiewitch, S. , *Innovation and Manufacturability Analysis in an Integrated Design Context.* Computers in Industry 2000. **43**(2): p. 111-121.

62. Chan, D.S.K., *Expert System for Product Manufacturability and Cost Evaluation.* Materials and Manufacturing Processes, 2003. **18**(2): p. 313-322.
63. Ramana, K.V., Singh, M., Gupta, A., Dey, R., Kapoor, A. and Rao, P.V.M., *A Manufacturability Advisor for Spun and Roll formed Sheet Metal Components.* International Journal of Advanced Manufacturing Technology, 2006. **28**(3-4): p. 249-254.
64. Scherer, K.P., Buchberger, P., Eggert, H., Stiller, P. and Stucky, P., *Knowledge based Support for Manufacturing of Microstructures.* Microsystem Technologies, 1996. **2**(4): p. 167-170.
65. Kusiak, A., Chen, M., *Expert Systems for Planning and Scheduling Manufacturing Systems.* European Journal of Operational Research, 1988. **34**(2): p. 113-130.
66. Amalnik, M.S., McGeough, J.A., *Intelligent Concurrent Manufacturability Evaluation Design for Electrochemical Machining.* Journal of Material Processing Technology, 1996. **61**(1-2): p. 130 -139.
67. Amalnik, M.S., El-Hofy, H.A. and McGeough, J.A., *An Intelligent Knowledge-based System for Wire-Electro-Erosion Dissolution in a Concurrent Engineering Environment.* Journal of Material Processing Technology, 1998. **79**(1-3): p. 155-162.
68. Gupta, S.K., Nau, D.S. and Regli, W.C. , 1998.*IMACS: A case study in real-world planning*,IEEE Intelligent Systems.**13**(3)p.49-60
69. Ong, S.K., Chew, L.C., *Evaluating the Manufacturability of Machined Parts and Their Setup Plans* International Journal of Production Research, 2000. **38**(11): p. 2397-2415.
70. Saaty, T.L., Vargas, L.G. , *Models, Methods, Concepts & Applications of the Analytic Hierarchy Process*. 2001: Springer.
71. Ong, S.K., Nee, A.Y.C., *An Intelligent Fuzzy Set-up Planner for Manufacturability and Fixturability Evaluations.* International Journal of Production Research, 1996. **34**(3): p. 665-686.
72. Ravinwongse, R., *An Intelligent Design Tool for Manufacturability Evaluation of Injection Molded Parts*. 1997, University of Missouri-Rolla.
73. Jia, H.Z., Ong, S.K., Fuh, J.Y.H., Zhang, Y.F., and Nee, A.Y.C. , *An Adaptive and Upgradeable Agent-based System for Coordinated Product Development and Manufacture.* Robotics and Computer-Integrated Manufacturing 2004. **20**(2): p. 79-90.
74. Gu, Z., Zhang, Y.F., and Nee, A.Y.C, *Identification of Important Features for Machining Operations Sequence Generation.* International Journal of Production Research, 1997. **35**(8): p. 2285 - 2307.
75. Medani, O., *Distributed early manufacturability assessment using STEP AP224 and XML*. 2005, University of Nottingham.
76. Medani, O., Ratchev, S.M. , *A STEP AP224 Agent-based Early Manufacturability Assessment Using XML.* International Journal of Advanced Manufacturing Technology 2006. **27**(9-10): p. 854-864.
77. Shiau, J.Y., Ratchev, S.M., and Valtchanov, G. *Distributed Collaborative Design and Manufacturability Assessment for Extended Enterprise in XML-based Agent System. 9th IEEE International Workshops on Enabling Technologies: Infrastructure for Collaborative Enterprises (WET ICE 2000)* 2000. Gaithersburg,MD.

78. Shiau, J.Y., *Web-enabled environment for manufacturability assessment*. 2001, University of Nottingham.
79. Hopgood, A.A., *Knowledge-based System for Engineers and Scientists*. . 1993: CRC Press, Inc.
80. Gurney, K., *An Introduction to Neural Networks*. 1997: Taylor and Francis.
81. Krishnan, K.K., *Design for Manufacturability Methodology and Data Representation Framework for Machined Components*. 1994, Virginia Polytechnic Institute and State University.
82. Sanchez, J.M., Priest, J.W. and Soto, R., *Intelligent Reasoning Assistant for Incorporating Manufacturability Issues into the Design Process*. Expert Systems with Applications, 1997. **12**(1): p. 81-88.
83. Gupta, S.K., Arni, R., and Chen, Y. . *Web-based Manufacturability Analysis*. 2003 16 January 2007]; Available from: http://www.glue.umd.edu/~skgupta/.
84. Yannoulakis, N.J., *A manufacturability evaluation and improvement system*. 1991, The Pennsylvania State University.
85. Yang, W., Ding, H. and Xiong, Y., *Manufacturability Analysis for a Sculptured Surface Using Visibility Cone Computation*. International Journal of Advanced Manufacturing Technology, 1999. **15**(5): p. 317-321.
86. Yang, W., Ding, H. and Xiong, Y. *Manufacturability Analysis for 5-Axis Sculptured Surface Machining. 1999 IEEE International Conference on Robotics and Automation*. 1999. Michigan: IEEE Robotics and Automation Society
87. Kalpakjian, S., Schmid, S.R., *Manufacturing Engineering and Technology (4th Edition)*. 2000: Prentice Hall.
88. Tomovic, M., *Geometric Constraint Toolbox for Foundry Tooling*. 2006: Purdue University.
89. Li, J., Gao, S., and Liu, Y., *Solid-based CAPP for surface micromachined MEMS devices*. Computer-Aided Design, 2007. **39**(3): p. 190 - 201.
90. *International Vocabulary of Basic and General Terms in Metrology (2nd Edition)*. 1993, ISO Geneva, Switzerland.
91. Taylor, B.N., Kuyatt, C.E., *Guidelines for Evaluating and Expressing the Uncertainty of NIST Measurement Results*, in *NIST Technical Note 1297 1994 Edition*. 1994, NIST.
92. Desenfant, M., Priel, M., *Road Map for Measurement Uncertainty Evaluation*. Measurement, 2006. **39**(9): p. 841 - 848.
93. Ridler, N., Lee, B., Martens, J., Wong, K., 2007.*Measurement Uncertainty, Traceability and the GUM*,IEEE Microwave Magazine.8(4)p.44 - 53
94. Kaarls, R. *Measurement Uncertainty in Calibration. Eurolab Workshop and Seminar on Measurement Uncertainty in Testing*. 1992. Barcelona.
95. *Guide to The Expression of Uncertainty in Measurement*. 1993.
96. von Martens, H.-J., *Evaluation of Uncertainty in Measurements - Problems and Tools*. Optics and Lasers in Engineering, 2002. **38**(3): p. 185 - 206.
97. Kessel, W., *Measurement Uncertainty According to ISO/BIPM-GUM*. Thermochimica Acta, 2002. **382**(1-2): p. 1 - 16.

98. Kirkup, L., Frenkel, R.B., *An Introduction to Uncertainty Measurement*. 2006, New York: Cambridge University Press.
99. Axinte, D.A., Belluco, W., De Chiffre, L., *Evaluation of cutting force uncertainty components in turning.* International Journal of Machine Tools and Manufacture, 2000. 41(5): p. 719 - 730.
100. Mohamed, M.I., Aggag, G.A., *Uncertainty evaluation of shore hardness testers.* Measurement, 2003. 33(3): p. 251 - 257.
101. Su, P.-G., Wu, R.-J, *Uncertainty of Humidity Sensors Testing by Means of Divided-flow Generator.* Measurement, 2004. 36(1): p. 21 - 27.
102. Choi, J.O., Hwang, E., So, H-Y., Kim, B., *An Uncertainty Evaluation for Multiple Measurements by GUM.* Accreditation and Quality Assurance: Journal for Quality, Comparability and Reliability in Chemical Measurement, 2003. 8(5): p. 13-15.
103. Choi, J.O., Kim, B., Hwang, E., So, H-Y., , *An Uncertainty Evaluation for Multiple Measurements by GUM, II.* Accreditation and Quality Assurance: Journal for Quality, Comparability and Reliability in Chemical Measurement, 2003. 8(5): p. 205 - 207.
104. Cox, M.G., Harris, P.M., *Measurement Uncertainty and Traceability.* Measurement Science and Technology, 2006. 17(3): p. 533-540.
105. Castro, H.F.F., *Uncertainty Analysis of a Laser Calibration System for Evaluating the Positioning Accuracy of a Numerically Controlled Axis of Coordinate Measuring Machines and Machine Tools.* Precision Engineering, 2008. 32(2): p. 106 - 113.
106. Axinte, D.A., Belluco, W., De Chiffre, L., *Reliable tool life measurements in turning - An application to cutting fluid efficieny evaluation.* International Journal of Machine Tools and Manufacture, 2001. 41(7): p. 1003 - 1014.
107. Stare, E., Beges, G., Drnovsek, J., *Evaluation of the Measurement Uncertainty when Measuring the Resistance of Solid Isolating Materials to Tracking.* Measurement Science and Technology, 2006. 17(7): p. 1801 - 1808.
108. Chen, C., *Evaluation of Measurement Uncertainty for Thermometers with Calibration Equations.* Accreditation and Quality Assurance: Journal for Quality, Comparability and Reliability in Chemical Measurement, 2006. 11(1 - 2): p. 75 - 82.
109. Park, C.J., Kang, K.H., Song, K.C., *Uncertainty evaluation of the thermal expansion of simulated fuel.* Thermochimica acta, 2006. 447(2): p. 197 - 201.
110. Costa-Felix, R.P.B., *Type B Uncertainty in Sound Power Measurmenets using Comparison Method.* Measurement, 2006. 39(2): p. 169 - 175.
111. Hoa, P.L.P., Gerlach, G., Suchaneck, G., *Uncertainty in Measurement of Semiconductor of Piezoresistive Sensors.* Microsystem Technologies, 2003. 9(3): p. 210 - 214.
112. Pauwels, J., van der Veen, A., Lamberty, A., Schimmel, A., *Evaluation of Uncertainty of Reference Materials.* Accreditation and Quality Assurance: Journal for Quality, Comparability and Reliability in Chemical Measurement, 2000. 5(3): p. 95 - 99.
113. Vozar, L., Hohenauer, W., *Uncertainty of Thermal Diffusivity Measurements Using the Laser Flash Method.* International Journal of Thermophysics, 2005. 26(6): p. 1899 - 1915.

114. Jack Feng, C.-X., Saal, A.L., Salsbury, J.G., Ness, A.R., Lin, G.C.S., *Design and Analysis of Experiments in CMM Measurement Uncertainty Study.* Precision Engineering, 2007. **31**(2): p. 94 - 101.
115. Tosello, G., Hansen, H.N., Gasparin, S., *Applications of Dimensional Micro Metrology to the Product and Process Quality Control in Manufacturing of Precision Polymer Micro Components.* CIRP Annals - Manufacturing Engineering 2009. **58**(1): p. 467 - 472.
116. Xu, C., *A Practical Model for Uncertainty Evaluation in Force Measurements* Measurement Science and Technology, 1998. 9(11): p. 1831 - 1836.
117. Misumi, I., Gonda, S., Kurosawa, T., Azuma, Y., Fujimoto, T., Kojima, I., Sakurai, T., Ohmi, T., Takamasu, K., *Reliability of Parameters of Associated Base Straight Line in Step Height Samples: Uncertainty Evaluation in Step Height Measurements Using Nanometrological AFM.* Precision Engineering, 2006. **30**(1): p. 13 - 22.
118. Uriarte, L., Herrero, A., Zatarin, M., Santiso, G., Lopez de Lacalle, L.N., Lamikiz, A., Albizuri, J., *Error Budget and Stiffness Chain Assessment in a Micromilling Machine Equipped with Tools Less than 0.3mm in Diameter.* Precision Engineering, 2007. **31**(1): p. 1 - 12.
119. Wirandi, J., Lauber, A., *Uncertainty and Traceable Calibration - How Modern Measurement Concepts Improve Product Quality in Process Industry.* Measurement, 2006. **39**(7): p. 612 - 620.
120. Lobato, H., Ferri, C., Faraway, J., Orchard, N., *Uncertainty Due to Experimental Conditions in Co-ordinate Measuring Machines.* Proceedings of the Institution of Mechanical Engineers, Part B: Journal of Engineering Manufacture, 2009. **223**(5): p. 499 - 509.
121. Losinger, W.C., *A Review of the GUM Workbench.* The American Statistician, 2004. **58**(2): p. 165 - 167.
122. Jurado, J.M., Alcazar, A., *A Software Package Comparison for Uncertainty Measurement Estimation According to GUM.* Accreditation and Quality Assurance: Journal for Quality, Comparability and Reliability in Chemical Measurement, 2005. **10**: p. 373 - 381.
123. *Metrodata - GUM Workbench.* 2007 [cited 2007 20/2/2007]; Available from: http://www.metrodata.de.
124. Brinksmeier, E., Gläbe, R., Riemer, O., Twardy, S. , *Potentials of Precision Machining Processes for the Manufacture of Micro Forming Molds* Microsystem Technologies, 2008. **14**(12): p. 1983 - 1987.
125. Gowri, S., Kumar, P.R., Vijayaraj, R., Balan, A.S.S., *Micromachining: Technology for the Future.* International Journal of Materials and Structural Integrity, 2007. **1**(1 - 3): p. 161 - 179.
126. Friedrich, C.R., Coane, P.J., Vasile, M.J., *Micromilling Development and Applications for Microfabrications.* Microelectronic Engineering, 1997. **35**(1 - 4): p. 367 - 372.
127. Bissacco, G., *Surface generation and optimization in micromilling.* 2004, Technical University of Denmark.
128. Popov, K., Dimov, S.S., Pham, D.T., Ivanov, A., *Micromilling strategies for machining thin features.* Proceedings of the Institution of Mechanical Engineers, Part C: Journal of Mechanical Engineering Science, 2006. **220**(11): p. 1677-1684.

129. Uriarte, L., Herrero, A., Ivanov, A., Oosterling, H., Stammler, L., Tang, P.T., Allen, D., *Micromilling Development and Applications for Microfabrications.* Proceeding of Institutional of Mechanical Engineers, Part C: Journal of Mechanical Engineering Science, 2006. **220**(11): p. 1665 - 1676.
130. Liu, X., DeVor, R.E., Kapoor, S.G. and Ehmann, K.F., *The Mechanics of Machining at the Microscale: Assessment of the Current State of the Science.* Journal of Manufacturing Science and Engineering, 2004. **126**: p. 666 - 678.
131. Aramcharoen, A., and Mativengaa, P.T., *Size effect and tool geometry in micromilling of tool steel.* Precision Engineering, 2009. **33**(4): p. 402 - 407.
132. Schmidt, J., Spath, D., Elsner, J., Huntrup, V., Tritschler, H., *Requirements of an Industrially Applicable Microcutting Process for Steel Micro-Structures.* Microsystem Technologies, 2002. 8(6): p. 402 - 408.
133. Weck, M., Fischer, S., Vos, M., *Fabrication of Microcomponents using Ultraprecision Machine Tools.* Nanotechnology, 1996. 8(3): p. 145 - 148.
134. Gietzelt, T., Eichhorn, L., and Schubert., K, *Manufacturing of microstructures with high aspect ratio by micromachining* Microsystem Technologies, 2008. **14**(9 - 11): p. 1525 - 1529.
135. Uriarte, L., Herrero, A., Ivanov, A., Oosterling, H., Stammler, L., Tang, P.T., Allen, D., *Comparison between microfabrication technique for metal tooling.* Proceeding of Institutional of Mechanical Engineers, Part C: Journal of Mechanical Engineering Science, 2006. **220**(11): p. 1665 - 1676.
136. Schmidt, J., Tritschler, H., *Micro Cutting of Steel.* Microsystem Technologies, 2004. **10**(3): p. 167 - 174.
137. Lanza, G., Fleischer, J., Kotschenreuther, J., Peters, J., Schlipf, M., *Statistical Modelling of Process Parameters in Micro Cutting.* Proceeding of Institutional of Mechanical Engineers, Part B: Journal of Engineering Manufacture, 2008. **222**(1): p. 15 - 22.
138. Aramcharoen, A., and Mativengaa, P.T., Yang, S., Cooke, K.E., Teer, D.G., *Evaluation and Selection of Hard Coatings for Micro Milling of Hardened Tool Steel.* International Journal of Machine Tools and Manufacture, 2008. **48**(14): p. 1578 - 1584.
139. Bissacco, G., Hansen, H.N., De Chiffre, L. , *Size effects on surface generation in micro milling of hardened tool steel.* Annals of CIRP - Manufacturing Technology, 2006. **55**(1): p. 593 - 596.
140. Lee, K., Dornfeld, D.A., *A Study of Surface Roughness in Micro-end Milling Process.* 2004, Laboratory for Manufacturing Automation. Consortium on Deburring and Edge Finishing, University of California Berkley.
141. Takacs, M., Vero, B., Meszaros, I., *Micromilling of Metallic Materials.* Journal of Materials Processing Technology, 2003. **138**(1 - 3): p. 152 - 153.
142. Denkena, B., Hoffmeister, H.-W., reichstein, M., Illenseer, S., and Hlavac, M., *Micro-machining processes for microsystem technology.* Microsystem Technologies, 2006. **12**(7): p. 659 - 664.

143. Uhlmann, E., Piltz, S., Schauer, K., *Micro Milling of Sintered Tungsten–copper Composite Materials.* Journal of Materials Processing Technology, 2005. **167**(2 - 3): p. 402 - 407.
144. Keppeler, C.R., *Micromilling for Mold Fabrication.* 2003, Precision Manufacturing Group, Laboratory for Manufacturing and Sustainability, University of Berkeley.
145. Kurita, T., Watanabe, S., Hattori, M. *Development of hybrid micro machine tool. Second International Symposium Open Environment conscious Desing and Inverse Manufacturing.* 2001.
146. Okazaki, Y., Mori, T., and Morita, N. . *Desktop NC milling machine with 200k rpm spindle. ASPE Annual Meeting.* 2001.
147. Bang, Y.B., Lee, K.M., Oh, S., *5-axis Micro Milling Machine for Machining Micro Parts.* International Journal of Advanced Manufacturing Technology, 2004. **25**(9 - 10): p. 888 - 894.
148. Min, S., Sangermann, H., Mertens, C., Dornfeld, D. , *A study on Initial Contact Detection for Precision Micro-Mold and Surface Generation of Vertical Side Walls in Micromachining.* CIRP Annals - Manufacturing Technology, 2008. **57**(1): p. 109 - 112.
149. Weule, H., Hüntrup, V., Tritschler, H., *Micro-Cutting of Steel to Meet New Requirements in Miniaturization* CIRP Annals - Manufacturing Technology, 2001. **50**(1): p. 61 - 64.
150. Fang, F.Z., Wu, H., Liu, X.D., Liu, Y.C., Ng, S.T., *Tool Geometry Study in Micromachining.* Journal of Micromechanics and Microengineering, 2003. **13**(5): p. 726 - 731.
151. Hupert, M.L., Guy, W.J., Llopis, S.D., Shadpour, H., Rani, S., Nikitopoulos, D.E., Soper, S.A. , *Evaluation of Micromilled Metal Mold Masters for the Replication of Microchip Electrophoresis Devices.* Microfluidics and Nanofluidics, 2007. **3**(1): p. 1 - 11.
152. Schaller, T., Bohn, L., Mayer, J., Schubert, K., *Microstructure grooves with a Width of Less than 50μm Cut with Ground Hard Metal Micro End Mills* Precision Engineering, 1999. **23**(4): p. 229 - 235.
153. Rodriguez, P., Perez, H., Labarga, J.E., Vizan A., *Research on Tool Life in Micro End Milling as Related to Workpiece Quality Criteria*, in *2008 ASME Early Career Technical Conference*. 2008: Miami, Florida, USA. p. 1.1 - 1.5.
154. Wang, B., Liang, Y.C., Zhao, Y., Dong, S. , *Measurement of the Residual Stress in the Micro Milled Thin Walled Structures.* Journal of Physics: Conference Series, 2006. **48**: p. 1127 - 1130.
155. Okazaki, Y., Mishima, N., and Ashida, K., *Microfactory - Concept, History and Developments.* Journal of Manufacturing Science and Engineering, 2004. **126**(4): p. 837-844.
156. Rooks, B., *The Shrinking Sizes in Micro Manufacturing.* Assembly Automation, 2004. **24**(4): p. 352 - 356.
157. Frazier, A.B., Warrington, R.O., Friedrich, C., *The Miniaturization Technologies: Past, Present, and Future.* IEEE Transactions on Industrial Electronics, 1995. **42**(5): p. 423 - 430.
158. Popov, K.B., Dimov, S.S., Pham, D.T., Minev, R.M., Rosochowski, A., Olejnik, L., *Micromilling: material microstructure effects.* Proceedings of the Institution of Mechanical Engineers, Part B: Journal of Engineering Manufacture, 2006. **220**(11): p. 1807 - 1813.

159. Mian, A.J., Driver, N., Mativenga, P.T., *Micromachining of coarse-grained multi-phase material.* Proceeding of Institutional of Mechanical Engineers, Part B: Journal of Engineering Manufacture, 2009. **223**(4): p. 377 - 385.
160. Litwinski, K.M., Min, S., Lee, D.E., Dornfeld, D., Lee, N., *Scalability of Tool Path Planning to Micro Machining.* 2006, Laboratory for Manufacturing and Sustainability, University of Berkeley.
161. Shi, J., Mi, J., Wang, J., Chen, K., Wang, W. and Cai, G., *Investigation on the Key Technologies of Micro Machine Tool and Prototype Development* Lecture Notes in Computer Science. Vol. Volume 5315/2008. 2008: Springer Berlin / Heidelberg.
162. Uriarte, L., Azcarate, S., Herrero, A., Lopez De Lacalle, L.N., Lamikiz, A., *Mechanistic modelling of the micro end milling operation.* Proceedings of the Institution of Mechanical Engineers-Part B (Journal of engineering manufacture), 2008. **222**(1): p. 23 - 33.
163. Kussul, E., Baidyk, T., Ruiz-Huerta, L., Caballero-Ruiz, A., Velasco, G., Kasatkina, L., *Development of micromachine tool prototypes for microfactories.* Journal of Micromechanics and Microengineering, 2002. **12**(6): p. 795-812.
164. Asad, A.B.M.A., Takeshi, M., Rahman, M., Lim, H.S. and Wong, Y.S, *Tool-based micro-machining.* Journal of Materials Processing Technology, 2007. **192 - 193**: p. 204 - 211.
165. Azizur R.M., R., M., Senthil Kumar, A. and Lim, H.S., *CNC microturning: an application to miniaturization.* International Journal of Machine Tools and Manufacture, 2005. **45**: p. 631 - 639.
166. Ashida, K., Mishima, N., Maekawa, H., Tanikawa, T., Kaneko, K., Tanaka, M. *Development of desktop machining microfactory-trial production of miniature machine products. Proceedings of the 2000 Japan-USA Flexible Automation Conference.* 2000. Michigan.
167. Iijima, D., Ito, S., Hayashi, A., Aoyama, H., Yamanaka, M. *Micro turning system: A super small CNC precision lathe for microfactories. Third International Workshops on Microfactories.* 2002.
168. Ho Bae, Y., Jo Ko, T., Mook Chung, B., Sool Kim, H. . *Micro machining with micro turning lathe. ASPE 16th Annual Meeting.* 2001.
169. Kitahara, T., Ashida, K., Tanaka, M., Ishikawa, Y., Oyama, N. and Nakazawa, Y. *Microfactory and Microlathe. Proc. of International Workshop on Microfactories.* 1988.
170. Hirano, T., Furuta,K. *Micromachine technology trends in microfactory. International Workshop on Microfactory.* 2002. Minneapolis.
171. Mishima, N., *Development of a Micro Manufacturing System and its Efficiency Evaluation Method*, in *International Conference on Automation Science and Engineering*. 2006, IEEE: Shanghai, China.
172. Subrahmaniam, R., Ehmann, K.F. *Development of a Meso-Scale Machine Tool (MMT) for Micro-Machining. Proceeding of the Japan-USA Symposium on Flexible Automation.* 2002. Hiroshima, Japan.
173. Slocum, A.H., *Precision Machine Design.* 1992: Society of Manufacturing Engineers.
174. Anonymous. *Hocut 3380 -High lubricity chlorine and sulphur free soluble oil.* 2009 [cited 2009 10/02/2009]; Available from: http://www.goldcrestoil.co.uk/images/stories/13050_Hocut_3280.pdf.

175. *316L stainless steel micro spray valve for precise aseptic and sterile fluid applications*. 2008, EFD Inc.
176. *ISO 10791 - 7: 1998 Test conditions for machining centres - Part7: Accuracy of a finished test piece*. 1998.
177. Anonymous. *Taylsurf CLI: High-resolution 3D Surface Profiling systems*. 2008 [cited 2008 02/05/2008]; Available from: http://taylorhobsonmedia.sitedesign.net/uploads/images/talysurf-cli-systems.pdf.
178. Rajurkar, K., Madou, M., *International Assessment of Research and Development in Micromanufacturing*. 2007: Baltimore. p. 39 - 64
179. Sreeram, S., Kumar, A.S., Rahman, M., Zaman, M.T., *Optimization of cutting parameters in micro end milling operations in dry cutting condition using genetic algorithms* International Journal of Advanced Manufacturing Technology, 2006. 30(11 - 12): p. 1030 - 1039.
180. Uriarte, L., Eguia, J. and Egana, F., *Micromilling Machines, Machine Tools for High Performance Machining*, L.N. Lopez de Lacalle, Lamikiz, A., Editor. 2009, Springer London: London. p. 369 - 396.
181. Jalukse, L., Koort, E., Traks, J., Leito, I. , *GUM Workbench as Measurement Modelling and Uncertainty Estimation Software: Experience at University of Tartu.* Accreditation and Quality Assurance: Journal for Quality, Comparability and Reliability in Chemical Measurement, 2003. 8(11): p. 520 - 522.
182. Tlusty, J., Smith, S. and Winfough, W.R., *Techniques for the Use of Long Slender End Mills in High-speed Milling* CIRP Annals - Manufacturing Engineering, 1996. 45(1): p. 393 - 396.
183. Anon. *Machinability Comparison Chart - Technical Resources for Manufacturing Professionals*. 2006 9 October, 2006]; Available from: http://www.carbidedepot.com/formulas-machinability.htm.
184. Bralla, J.G., *Handbook of Product Design for Manufacturing*. 1986, USA: Mc Graw Hill
185. Drake, P.J., *Dimensioning and Tolerancing Handbook*. 1999, New York: Mc Graw Hill.
186. Rothbart, H.A., *Mechanical Design Handbook*. 1985, New York: Mc Graw Hill
187. *ISO 230-3:2001 – Test code for machine tools – Part 3: Determination of thermal effects during CMM measurement*. 2001.
188. *ISO 230-2:2006 – Test code for machine tools – Part 2: Determination of accuracy and repeatability of positioning numerically controlled axes* 2006.
189. Limvachirakom, V., *Influence of Crystallographic Orientation of Diamond Tools on The Performance of High Speed Milling of A Ti Superalloy*. 2008, University of Nottingham: Nottingham.
190. Shukor, S.A., Axinte, D.A., *An approach of using primitive feature analysis in manufacturability analysis systems for micro-milling/drilling.* International Journal of Computer Integrated Manufacturing, 2009. 22(8): p. 727 - 744.
191. Axinte, D.A., Shukor, S.A., Bozdana, A.T., *An analysis of the functional capability of an in-house developed miniature 4-axis machine tool.* International Journal of Machine Tools and Manufacture, 2009.

APPENDIX 3.1
Specifications of flat end mill cutter with 0.5 and 0.8mm from Sandvik Coromant.

1. 0.5mm Flat end mill cutter

Flat End Cutters	
R216.32-00530-AE05G	
Z_n	2
D_c *(mm)*	0.5
l_2 *(mm)*	54
a_p *(mm)*	0.5
D_4 *(mm)*	0.46
dm_m *(mm)*	6

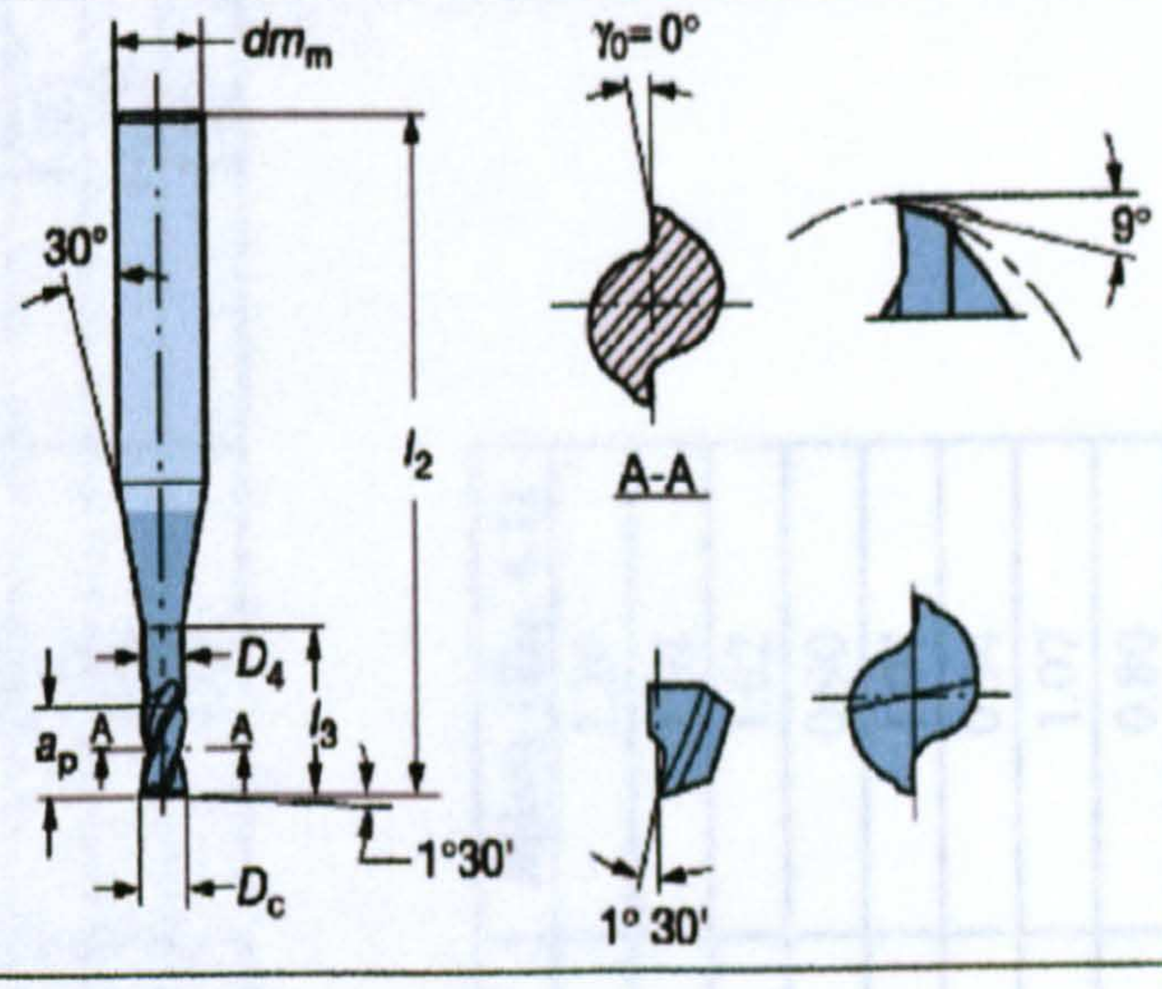

2. 0.8mm Flat end mill cutter

Flat End Cutters	
R216.32-00830-AE08G	
Z_n	2
D_c *(mm)*	0.8
l_2 *(mm)*	54
a_p *(mm)*	0.8
D_4 *(mm)*	0.76
dm_m *(mm)*	6

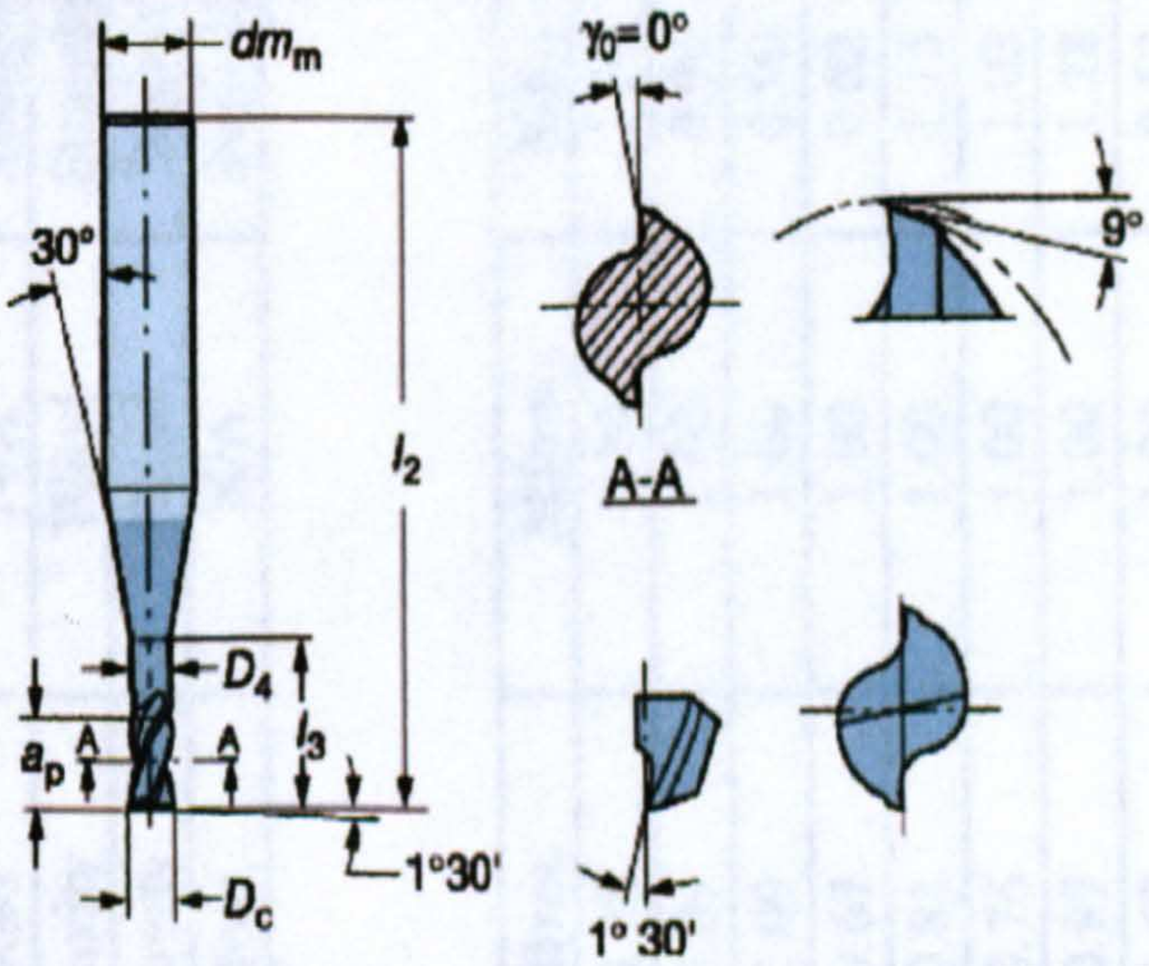

APPENDIX 4.1: Overall analysis of the micro component

Results from Single Feature Analysis

PF No	Type of PF	PF Orientation	Type of Cavity	PF shape	End-corner	MI_{PF}	Stiffness Ratio (RSt)
1	Box	Boss	N/A	Straight	Sharp	1.0	3.33
2	Box	Cavity	Blind	Straight	Radiused	1.0	5.33
3	Box	Cavity	Blind	Straight	Radiused	1.0	5.33
4	Box	Cavity	Blind	Straight	Radiused	1.0	1.25
5	Box	Boss	N/A	Straight	Radiused	1.5	10.67
6	Cylinder	Cavity	Blind	Straight	None	1.0	8.00
7	Box	Cavity	Blind	Straight	Radiused	1.0	12.00
8	Box	Boss	N/A	Straight	Sharp	1.0	1.33

Summary of MI_{SFA} results

PF No	MI_{PF}	MI_{TOL}	MI_{DIM}	MI_{Ra}	MI_{UEM}	MI_{SFA} (Eq. 4.1)
1	1.00	1.28	1.00	1.54	1.20	1.20
2	1.00	1.09	1.00	0.90	1.10	1.02
3	1.00	1.09	1.00	0.90	1.10	1.02
4	1.00	0.67	1.00	0.62	1.20	0.90
5	1.50	0.81	1.00	1.15	0.90	1.07
6	1.00	0.76	1.00	1.03	0.90	0.94
7	1.00	0.97	1.00	1.28	1.10	1.07
8	1.00	0.67	1.00	0.52	0.80	0.80

MI$_{CFA}$ results

1st PF	2nd PF	Interactions analysis	Distance (mm)	PF	1st MI	K$_{RD}$	2nd MI
PF_1	PF_2	Attached	0.20	PF_2	1.02	0.90	0.92
PF_1	PF_3	Attached	0.20	PF_3	1.02	0.90	0.92
PF_1	PF_4	Attached	0.00	PF_4	0.90	0.75	0.68
PF_1	PF_7	Attached	0.20	PF_7	1.07	0.90	0.96
PF_2	PF_3	Adjacent	0.10	PF_2	0.92	0.85	0.78
				PF_3	0.92	0.85	0.78
PF_2	PF_5	Adjacent	0.20	PF_2	0.78	0.85	0.66
				PF_5	1.07	0.85	0.91
PF_3	PF_4	Adjacent	0.20	PF_3	0.78	0.85	0.66
				PF_4	0.68	0.85	0.58
PF_3	PF_5	Adjacent	0.85	PF_3	0.66	0.85	0.56
				PF_5	0.91	0.85	0.77
PF_5	PF_6	Attached	0.20	PF_5	0.77	0.90	0.69
				PF_6	0.94	0.90	0.85
PF_5	PF_7	Adjacent	0.20	PF_5	0.69	0.85	0.59
				PF_7	0.96	0.85	0.82
PF_7	PF_8	Attached	0.00	PF_7	0.82	0.75	0.62
				PF_8	0.8	0.75	0.60

PF	FINAL MI$_{CFA}$	PF	FINAL MI$_{CFA}$
PF_1	1.20	PF_5	0.59
PF_2	0.66	PF_6	0.85
PF_3	0.56	PF_7	0.62
PF_4	0.58	PF_8	0.60

APPENDIX 4.2: MIPF ANALYSIS

Type of PF	PF orientation	Type of Cavity	PF shape	End-corner	MIPF
Box	Boss	N/A	Straight	Radiused	1.5
		N/A	Negative-tapered	Radiused	0.5
		N/A	Positive-tapered	Radiused	1.0
	Cavity	Through hole	Straight	Radiused	1.5
		Blind	Straight	Radiused	1.0
		Through hole	Negative-tapered	Radiused	0.5
		Blind	Negative-tapered	Radiused	0.5
		Through hole	Positive-tapered	Radiused	1.0
		Blind	Positive-tapered	Radiused	1.0
	Boss	N/A	Straight	Sharp	1.0
		N/A	Negative-tapered	Sharp	0.5
		N/A	Positive-tapered	Sharp	0.5
	Cavity	Through hole	Straight	Sharp	1.0
		Blind	Straight	Sharp	0.5
		Through hole	Negative-tapered	Sharp	0.5
		Blind	Negative-tapered	Sharp	0.5
		Through hole	Positive-tapered	Sharp	0.5
		Blind	Positive-tapered	Sharp	0.5
	Boss	N/A	Straight	Fillet	1.5
		N/A	Negative-tapered	Fillet	0.5
		N/A	Positive-tapered	Fillet	1.0
	Cavity	Through hole	Straight	Fillet	1.5
		Blind	Straight	Fillet	1.0
		Through hole	Negative-tapered	Fillet	0.5
		Blind	Negative-tapered	Fillet	0.5
		Through hole	Positive-tapered	Fillet	1.0
		Blind	Positive-tapered	Fillet	1.0
Cylinder	Boss	N/A	Straight	N/A	1.5
		N/A	Negative-tapered	N/A	0.5
		N/A	Positive-tapered	N/A	1.0
	Cavity	Through hole	Straight	N/A	1.5
		Blind	Straight	N/A	1.0
		Through hole	Negative-tapered	N/A	0.5
		Blind	Negative-tapered	N/A	0.5
		Through hole	Positive-tapered	N/A	1.0
		Blind	Positive-tapered	N/A	1.0
Cone	Boss	N/A	Straight	N/A	1.0
	Cavity	N/A	Straight	N/A	0.5
Sphere	Boss	N/A	Straight	N/A	0.5
	Cavity	N/A	Straight	N/A	1.0

APPENDIX 5.1: Uncertainty evaluation model

Model equation:

$R=\sqrt{X^2+Y^2}$;

$X=a\cdot(\cos(\omega\cdot(t\cdot 0.0377)))+\Delta X_1+\Delta X_2+\Delta X_3+\Delta X_4$;

$\Delta X_1=L\cdot(\sqrt{\cos(\alpha)^2-\cos(\gamma)^2})$;

$Y=a\cdot(\sin(\omega\cdot(t\cdot 0.0377)))+\Delta Y_1+\Delta Y_2+\Delta Y_3+\Delta Y_4$;

$\Delta Y_1=\Delta Y_0+L\cdot\sin(\alpha)$;

List of quantities:

Quantity	Unit	Definition
R	mm	the radius of a circle
X	mm	the x value
Y	mm	the y value
a	mm	radius
ω	rad/sec	angular velocity
t	sec	time
ΔX_1	mm	Uncertainty due to X,Y,U planes deviation for X
ΔX_2	mm	Uncertainty due to original position deviation of table movement for X
ΔX_3	mm	Uncertainty due to temperature deviation for X
ΔX_4	mm	Uncertainty due to worktable accuracy for X
L	mm	Tool length
α	rad	Angle between Tool (Z) and side of U table
γ	rad	Angle between Tool (Z) and top of U table
ΔY_1	mm	Uncertainty due to X, Y and U planes deviation for Y
ΔY_2	mm	Uncertainty due to original position deviation for Y
ΔY_3	mm	Uncertainty due to temperature deviation for Y
ΔY_4	mm	Uncertainty due to worktable accuracy for Y
ΔY_0	mm	value of shifted planes

R: Result

X: Interim result

Y: Interim result

a: Constant
Value: 1.5 mm

ω: Type B rectangular distribution
Value: 5.5554 rad/sec
Half-width of distribution: 0.0002 rad/sec

t: Constant
Value: 11 sec

ΔX_1: Interim result

ΔX_2: Type A
Method of observation: Direct
Number of observation: 12

No.	Observation
1	0.0001
2	0.00009
3	0.00008
4	0.00007
5	0.00011
6	0.00012
7	0.0001
8	0.00008
9	0.00011
10	0.00007
11	0.00006
12	0.00008

Arithmetic mean: $89.17 \cdot 10^{-6}$ mm
Standard deviation: $18.8 \cdot 10^{-6}$ mm
Standard uncertainty: $5.43 \cdot 10^{-6}$ mm
Degrees of freedom: 11

ΔX_3: Type B rectangular distribution
Value: 0.0002 mm
Half-width of distribution: $1 \cdot 10^{-5}$ mm

ΔX_4: Type B rectangular distribution
Value: 0.0003 mm
Half-width of distribution: $1.5 \cdot 10^{-5}$ mm

L: Type B rectangular distribution
Value: 4.85 mm
Half-width of distribution: 0.0002 mm

α:

Type A summarized
Value: 0.0004986904339099 52 rad
Standard uncertainty: 0.0001340555071392 45 rad
Degrees of freedom: 7

γ:

Type A summarized
Value: 0.0011401759779215 1 rad
Standard uncertainty: 0.0003826797420383 6 rad
Degrees of freedom: 7

ΔY_1:

Interim result

ΔY_2:

Type A
Method of observation: Direct
Number of observation: 12

No.	Observation
1	0.00009
2	0.0001
3	0.00012
4	0.00011
5	0.00008
6	0.00007
7	0.00006
8	0.00009
9	0.00008
10	0.00013
11	0.00009
12	0.00007

Arithmetic mean: $90.83 \cdot 10^{-6}$ mm
Standard deviation: $21.1 \cdot 10^{-6}$ mm
Standard uncertainty: $6.09 \cdot 10^{-6}$ mm
Degrees of freedom: 11

ΔY_3:

Type B rectangular distribution
Value: 0.0002 mm
Half-width of distribution: $1 \cdot 10^{-5}$ mm

ΔY_4:

Type B rectangular distribution
Value: 0.0003 mm
Half-width of distribution: $1.5 \cdot 10^{-5}$ mm

ΔY_0:

Type B rectangular distribution
Value: 0.0007 mm
Half-width of distribution: 0.000002 mm

Uncertainty budget:

Quantity	Value	Standard uncertainty	Degrees of freedom	Sensitivity coefficient	Uncertainty contribution	Corr.-coeff.	Index
X	-0.99812 mm	$2.13 \cdot 10^{-3}$ mm					
Y	1.118437 mm	$652 \cdot 10^{-6}$ mm					
a	1.5 mm						
ω	5.555400 rad/sec	$115 \cdot 10^{-6}$ rad/sec	∞	$-2.75 \cdot 10^{-3}$	$-317 \cdot 10^{-9}$ mm	0.00	0.000
t	11.0 sec						
ΔX_1	$4.97 \cdot 10^{-3}$ mm	$2.13 \cdot 10^{-3}$ mm					
ΔX_2	$89.17 \cdot 10^{-6}$ mm	$5.43 \cdot 10^{-6}$ mm	11	-0.666	$-3.62 \cdot 10^{-6}$ mm	0.00	0.000
ΔX_3	$200.00 \cdot 10^{-6}$ mm	$5.77 \cdot 10^{-6}$ mm	∞	-0.666	$-3.84 \cdot 10^{-6}$ mm	0.00	0.000
ΔX_4	$300.00 \cdot 10^{-6}$ mm	$8.66 \cdot 10^{-6}$ mm	∞	-0.666	$-5.77 \cdot 10^{-6}$ mm	0.00	0.000
L	4.850000 mm	$115 \cdot 10^{-6}$ mm	∞	$-311 \cdot 10^{-6}$	$-35.9 \cdot 10^{-9}$ mm	0.00	0.000
α	$499 \cdot 10^{-6}$ rad	$134 \cdot 10^{-6}$ rad	7	not valid	$698 \cdot 10^{-6}$ mm	0.45	0.198
γ	$1.140 \cdot 10^{-3}$ rad	$383 \cdot 10^{-6}$ rad	7	-3.67	$-1.40 \cdot 10^{-3}$ mm	-0.90	0.802
ΔY_1	$3.119 \cdot 10^{-3}$ mm	$650 \cdot 10^{-6}$ mm					
ΔY_2	$90.83 \cdot 10^{-6}$ mm	$6.09 \cdot 10^{-6}$ mm	11	0.746	$4.54 \cdot 10^{-6}$ mm	0.00	0.000
ΔY_3	$200.00 \cdot 10^{-6}$ mm	$5.77 \cdot 10^{-6}$ mm	∞	0.746	$4.31 \cdot 10^{-6}$ mm	0.00	0.000
ΔY_4	$300.00 \cdot 10^{-6}$ mm	$8.66 \cdot 10^{-6}$ mm	∞	0.746	$6.46 \cdot 10^{-6}$ mm	0.00	0.000
ΔY_0	$700.00 \cdot 10^{-6}$ mm	$1.15 \cdot 10^{-6}$ mm	∞	0.746	$862 \cdot 10^{-9}$ mm	0.00	0.000
R	1.49905 mm	$1.57 \cdot 10^{-3}$ mm	10				

Result: Quantity: R
Value: 1.4990 mm
Expanded Uncertainty: $\pm 3.6 \cdot 10^{-3}$ mm
Coverage Factor: 2.3
Coverage probability: 95.45%

Appendix 5.2: Results of uncertainty evaluation for X, Y and Z

No	time (t)	r	Expanded Uncertainty	Coverage factor	X	Std. Uncertainty X	Y	Std. Uncertainty Y
1	0.0377	1.5062	0.005000	2.4	1.472780	0.002130	0.31557600	0.000650
2	0.0754	1.5066	0.004700	2.4	1.375880	0.002130	0.61381200	0.000650
3	0.1131	1.5067	0.004200	2.4	1.219090	0.002130	0.88538400	0.000650
4	0.1508	1.5065	0.003500	2.4	1.009260	0.002130	1.11842300	0.000651
5	0.1885	1.5060	0.002700	2.4	0.755570	0.002130	1.30274400	0.000650
6	0.2262	1.5053	0.001800	2.2	0.469100	0.002130	1.43029200	0.000650
7	0.2639	1.5043	0.001500	2.4	0.162360	0.002130	1.49549100	0.000650
8	0.3016	1.5031	0.001700	2.4	-0.151220	0.002130	1.49549300	0.000650
9	0.3393	1.5018	0.002100	2.2	-0.457950	0.002130	1.43029800	0.000651
10	0.3770	1.5004	0.002800	2.2	-0.744430	0.002130	1.30275500	0.000651
11	0.4147	1.4990	0.003600	2.3	-0.998120	0.002130	1.11843700	0.000652
12	0.4524	1.4977	0.004300	2.4	-1.207950	0.002130	0.88540100	0.000653
13	0.4901	1.4964	0.004700	2.4	-1.364750	0.002130	0.61383100	0.000655
14	0.5278	1.4953	0.005100	2.4	-1.461660	0.002130	0.31559600	0.000656
15	0.5655	1.4944	0.005200	2.4	-1.494440	0.002130	0.00373000	0.000658
16	0.6032	1.4938	0.005000	2.4	-1.461660	0.002130	-0.30813600	0.000658
17	0.6409	1.4934	0.004700	2.4	-1.364770	0.002130	-0.60637400	0.000658
18	0.6786	1.4933	0.004200	2.4	-1.207980	0.002130	-0.87794800	0.000657
19	0.7163	1.4935	0.003500	2.4	-0.998150	0.002130	-1.11099000	0.000656
20	0.7540	1.4940	0.002600	2.3	-0.744460	0.002130	-1.29531500	0.000654
21	0.7917	1.4948	0.001800	2.2	-0.457990	0.002130	-1.42286600	0.000652
22	0.8294	1.4957	0.001500	2.4	-0.151260	0.002140	-1.48807000	0.000650
23	0.8671	1.4969	0.001700	2.4	0.162320	0.002140	-1.48807700	0.000650
24	0.9048	1.4982	0.002200	2.2	0.469060	0.002140	-1.42288600	0.000652
25	0.9425	1.4996	0.002900	2.2	0.755530	0.002140	-1.29534600	0.000655
26	0.9802	1.5010	0.003600	2.3	1.009230	0.002130	-1.11103200	0.000660
27	1.0179	1.5023	0.004300	2.4	1.219070	0.002130	-0.87799900	0.000660
28	1.0556	1.5036	0.004800	2.4	1.375860	0.002130	-0.60643100	0.000671
29	1.0933	1.5047	0.005100	2.4	1.472780	0.002130	-0.30819800	0.000676
30	1.1310	1.5056	0.005200	2.4	1.505560	0.002130	0.00366800	0.000679

α	Std. uncertainty	Uncertainty Contribution	Index	γ	Std. uncertainty	Uncertainty Contribution	Index
0.00049900	0.00013400	0.00017600	0.00700000	0.00114000	0.00038300	0.00206000	0.99300000
0.00049900	0.00013400	0.00002700	0.00000000	0.00114000	0.00038300	0.00192000	1.00000000
0.00049900	0.00013400	0.00012300	0.00500000	0.00114000	0.00038300	0.00170000	0.99500000
0.00049900	0.00013400	0.00026900	0.03500000	0.00114000	0.00038300	0.00141000	0.96500000
0.00049900	0.00013400	0.00040200	0.12600000	0.00114000	0.00038300	0.00106000	0.87300000
0.00049900	0.00013400	0.00051800	0.38400000	0.00114000	0.00038300	0.00065600	0.61600000
0.00049900	0.00013400	0.00061200	0.87800000	0.00114000	0.00038300	0.00022700	0.12100000
0.00049900	0.00013400	0.00067900	0.91100000	0.00114000	0.00038300	0.00021200	0.08900000
0.00049900	0.00013400	0.00071700	0.55400000	0.00114000	0.00038300	0.00064200	0.44600000
0.00049900	0.00013400	0.00072300	0.32400000	0.00114000	0.00038300	0.00105000	0.67600000
0.00049900	0.00013400	0.00069800	0.19800000	0.00114000	0.00038300	0.00140000	0.80200000
0.00049900	0.00013400	0.00064200	0.12500000	0.00114000	0.00038300	0.00170000	0.87500000
0.00049900	0.00013400	0.00055800	0.07800000	0.00114000	0.00038300	0.00192000	0.92200000
0.00049900	0.00013400	0.00045000	0.04600000	0.00114000	0.00038300	0.00206000	0.95400000
0.00049900	0.00013400	0.00032100	0.02300000	0.00114000	0.00038300	0.00211000	0.97700000
0.00049900	0.00013400	0.00017900	0.00700000	0.00114000	0.00038300	0.00206000	0.99300000
0.00049900	0.00013400	0.00002810	0.00000000	0.00114000	0.00038300	0.00193000	1.00000000
0.00049900	0.00013400	0.00012400	0.00500000	0.00114000	0.00038300	0.00170000	0.99500000
0.00049900	0.00013400	0.00027000	0.03500000	0.00114000	0.00038300	0.00141000	0.96400000
0.00049900	0.00013400	0.00040400	0.12900000	0.00114000	0.00038300	0.00105000	0.87100000
0.00049900	0.00013400	0.00052100	0.39400000	0.00114000	0.00038300	0.00064600	0.60600000
0.00049900	0.00013400	0.00061400	0.89200000	0.00114000	0.00038300	0.00021300	0.10700000
0.00049900	0.00013400	0.00068100	0.89900000	0.00114000	0.00038300	0.00022800	0.10100000
0.00049900	0.00013400	0.00071800	0.54200000	0.00114000	0.00038300	0.00065900	0.45800000
0.00049900	0.00013400	0.00072300	0.31700000	0.00114000	0.00038300	0.00106000	0.68300000
0.00049900	0.00013400	0.00069600	0.19500000	0.00114000	0.00038300	0.00142000	0.80500000
0.00049900	0.00013400	0.00063900	0.12300000	0.00114000	0.00038300	0.00171000	0.87700000
0.00049900	0.00013400	0.00055500	0.07600000	0.00114000	0.00038300	0.00193000	0.92300000
0.00049900	0.00013400	0.00044600	0.04500000	0.00114000	0.00038300	0.00206000	0.95500000
0.00049900	0.00013400	0.00031800	0.02200000	0.00114000	0.00038300	0.00211000	0.97800000

Δx_2	Std. uncertainty	Uncertainty Contribution	Index	Δx_3	Std. uncertainty	Uncertainty Contribution	Index
0.00008917	0.00000577	0.00000531	0.00000000	0.00000200	0.00000577	0.00000565	0.00060000
0.00008917	0.00000543	0.00000496	0.00000000	0.00000200	0.00000577	0.00000527	0.00000000
0.00008917	0.00000543	0.00000439	0.00000000	0.00000200	0.00000577	0.00000467	0.00000000
0.00008917	0.00000543	0.00000364	0.00000000	0.00000200	0.00000577	0.00000387	0.00000000
0.00008917	0.00000543	0.00000272	0.00000000	0.00000200	0.00000577	0.00000290	0.00000000
0.00008917	0.00000543	0.00000169	0.00000000	0.00000200	0.00000577	0.00000180	0.00000000
0.00008917	0.00000543	0.00000059	0.00000000	0.00000200	0.00000577	0.00000062	0.00000000
0.00008917	0.00000543	0.00000055	0.00000000	0.00000200	0.00000577	0.00000058	0.00000000
0.00008917	0.00000543	0.00000166	0.00000000	0.00000200	0.00000577	0.00000176	0.00000000
0.00008917	0.00000543	0.00000269	0.00000000	0.00000200	0.00000577	0.00000286	0.00000000
0.00008917	0.00000543	0.00000362	0.00000000	0.00000200	0.00000577	0.00000384	0.00000000
0.00008917	0.00000543	0.00000438	0.00000000	0.00000200	0.00000577	0.00000466	0.00000000
0.00008917	0.00000543	0.00000495	0.00000000	0.00000200	0.00000577	0.00000527	0.00000000
0.00008917	0.00000543	0.00000531	0.00000000	0.00000200	0.00000577	0.00000564	0.00000000
0.00008917	0.00000543	0.00000543	0.00000000	0.00000200	0.00000577	0.00000577	0.00000000
0.00008917	0.00000543	0.00000531	0.00000000	0.00000200	0.00000577	0.00000565	0.00000000
0.00008917	0.00000543	0.00000496	0.00000000	0.00000200	0.00000577	0.00000528	0.00000000
0.00008917	0.00000543	0.00000439	0.00000000	0.00000200	0.00000577	0.00000467	0.00000000
0.00008917	0.00000543	0.00000363	0.00000000	0.00000200	0.00000577	0.00000386	0.00000000
0.00008917	0.00000543	0.00000271	0.00000000	0.00000200	0.00000577	0.00000288	0.00000000
0.00008917	0.00000543	0.00000166	0.00000000	0.00000200	0.00000577	0.00000177	0.00000000
0.00008917	0.00000543	0.00000055	0.00000000	0.00000200	0.00000577	0.00000058	0.00000000
0.00008917	0.00000543	0.00000059	0.00000000	0.00000200	0.00000577	0.00000063	0.00000000
0.00008917	0.00000543	0.00000170	0.00000000	0.00000200	0.00000577	0.00000181	0.00000000
0.00008917	0.00000543	0.00000274	0.00000000	0.00000200	0.00000577	0.00000291	0.00000000
0.00008917	0.00000543	0.00000365	0.00000000	0.00000200	0.00000577	0.00000388	0.00000000
0.00008917	0.00000543	0.00000441	0.00000000	0.00000200	0.00000577	0.00000468	0.00000000
0.00008917	0.00000543	0.00000497	0.00000000	0.00000200	0.00000577	0.00000528	0.00000000
0.00008917	0.00000543	0.00000531	0.00000000	0.00000200	0.00000577	0.00000565	0.00000000
0.00008917	0.00000543	0.00000543	0.00000000	0.00000200	0.00000577	0.00000577	0.00000000

Δx_4	Std. uncertainty	Uncertainty Contribution	Index	Δy_2	Std. uncertainty	Uncertainty Contribution	Index
0.00030000	0.00000866	0.00000847	0.00000000	0.00009083	0.00000609	0.00000128	0.00000000
0.00030000	0.00000866	0.00000791	0.00000000	0.00009083	0.00000609	0.00000248	0.00000000
0.00030000	0.00000866	0.00000701	0.00000000	0.00009083	0.00000609	0.00000358	0.00000000
0.00030000	0.00000866	0.00000580	0.00000000	0.00009083	0.00000609	0.00000452	0.00000000
0.00030000	0.00000866	0.00000434	0.00000000	0.00009083	0.00000609	0.00000527	0.00000000
0.00030000	0.00000866	0.00000270	0.00000000	0.00009083	0.00000609	0.00000578	0.00000000
0.00030000	0.00000866	0.00000094	0.00000000	0.00009083	0.00000609	0.00000605	0.00000000
0.00030000	0.00000866	0.00000087	0.00000000	0.00009083	0.00000609	0.00000606	0.00000000
0.00030000	0.00000866	0.00000264	0.00000000	0.00009083	0.00000609	0.00000580	0.00000000
0.00030000	0.00000866	0.00000430	0.00000000	0.00009083	0.00000609	0.00000529	0.00000000
0.00030000	0.00000866	0.00000577	0.00000000	0.00009083	0.00000609	0.00000454	0.00000000
0.00030000	0.00000866	0.00000698	0.00000000	0.00009083	0.00000609	0.00000360	0.00000000
0.00030000	0.00000866	0.00000790	0.00000000	0.00009083	0.00000609	0.00000250	0.00000000
0.00030000	0.00000866	0.00000847	0.00000000	0.00009083	0.00000609	0.00000128	0.00000000
0.00030000	0.00000866	0.00000866	0.00000000	0.00009083	0.00000609	0.00000002	0.00000000
0.00030000	0.00000866	0.00000847	0.00000000	0.00009083	0.00000609	0.00000126	0.00000000
0.00030000	0.00000866	0.00000791	0.00000000	0.00009083	0.00000609	0.00000247	0.00000000
0.00030000	0.00000866	0.00000701	0.00000000	0.00009083	0.00000609	0.00000358	0.00000000
0.00030000	0.00000866	0.00000579	0.00000000	0.00009083	0.00000609	0.00000453	0.00000000
0.00030000	0.00000866	0.00000432	0.00000000	0.00009083	0.00000609	0.00000528	0.00000000
0.00030000	0.00000866	0.00000265	0.00000000	0.00009083	0.00000609	0.00000579	0.00000000
0.00030000	0.00000866	0.00000088	0.00000000	0.00009083	0.00000609	0.00000606	0.00000000
0.00030000	0.00000866	0.00000094	0.00000000	0.00009083	0.00000609	0.00000605	0.00000000
0.00030000	0.00000866	0.00000271	0.00000000	0.00009083	0.00000609	0.00000578	0.00000000
0.00030000	0.00000866	0.00000439	0.00000000	0.00009083	0.00000609	0.00000526	0.00000000
0.00030000	0.00000866	0.00000582	0.00000000	0.00009083	0.00000609	0.00000451	0.00000000
0.00030000	0.00000866	0.00000703	0.00000000	0.00009083	0.00000609	0.00000356	0.00000000
0.00030000	0.00000866	0.00000792	0.00000000	0.00009083	0.00000609	0.00000246	0.00000000
0.00030000	0.00000866	0.00000848	0.00000000	0.00009083	0.00000609	0.00000125	0.00000000
0.00030000	0.00000866	0.00000866	0.00000000	0.00009083	0.00000609	0.00000001	0.00000000

Δy_3	Std. uncertainty	Uncertainty Contribution	Index	Δy_4	Std. uncertainty	Uncertainty Contribution	Index
0.00020000	0.00000577	0.00000121	0.00000000	0.00030000	0.00000866	0.00000181	0.00000000
0.00020000	0.00000577	0.00000235	0.00000000	0.00030000	0.00000866	0.00000353	0.00000000
0.00020000	0.00000577	0.00000339	0.00000000	0.00030000	0.00000866	0.00000509	0.00000000
0.00020000	0.00000577	0.00000429	0.00000000	0.00030000	0.00000866	0.00000643	0.00000000
0.00020000	0.00000577	0.00000499	0.00000000	0.00030000	0.00000866	0.00000749	0.00000000
0.00020000	0.00000577	0.00000549	0.00000000	0.00030000	0.00000866	0.00000823	0.00000000
0.00020000	0.00000577	0.00000574	0.00000000	0.00030000	0.00000866	0.00000861	0.00000000
0.00020000	0.00000577	0.00000574	0.00000000	0.00030000	0.00000866	0.00000862	0.00000000
0.00020000	0.00000577	0.00000550	0.00000000	0.00030000	0.00000866	0.00000825	0.00000000
0.00020000	0.00000577	0.00000501	0.00000000	0.00030000	0.00000866	0.00000752	0.00000000
0.00020000	0.00000577	0.00000431	0.00000000	0.00030000	0.00000866	0.00000646	0.00000000
0.00020000	0.00000577	0.00000341	0.00000000	0.00030000	0.00000866	0.00000512	0.00000000
0.00020000	0.00000577	0.00000237	0.00000000	0.00030000	0.00000866	0.00000355	0.00000000
0.00020000	0.00000577	0.00000122	0.00000000	0.00030000	0.00000866	0.00000183	0.00000000
0.00020000	0.00000577	0.00000001	0.00000000	0.00030000	0.00000866	0.00000002	0.00000000
0.00020000	0.00000577	0.00000119	0.00000000	0.00030000	0.00000866	0.00000179	0.00000000
0.00020000	0.00000577	0.00000234	0.00000000	0.00030000	0.00000866	0.00000352	0.00000000
0.00020000	0.00000577	0.00000339	0.00000000	0.00030000	0.00000866	0.00000509	0.00000000
0.00020000	0.00000577	0.00000429	0.00000000	0.00030000	0.00000866	0.00000644	0.00000000
0.00020000	0.00000577	0.00000501	0.00000000	0.00030000	0.00000866	0.00000751	0.00000000
0.00020000	0.00000577	0.00000550	0.00000000	0.00030000	0.00000866	0.00000824	0.00000000
0.00020000	0.00000577	0.00000574	0.00000000	0.00030000	0.00000866	0.00000862	0.00000000
0.00020000	0.00000577	0.00000574	0.00000000	0.00030000	0.00000866	0.00000861	0.00000000
0.00020000	0.00000577	0.00000548	0.00000000	0.00030000	0.00000866	0.00000822	0.00000000
0.00020000	0.00000577	0.00000499	0.00000000	0.00030000	0.00000866	0.00000748	0.00000000
0.00020000	0.00000577	0.00000427	0.00000000	0.00030000	0.00000866	0.00000641	0.00000000
0.00020000	0.00000577	0.00000337	0.00000000	0.00030000	0.00000866	0.00000506	0.00000000
0.00020000	0.00000577	0.00000233	0.00000000	0.00030000	0.00000866	0.00000349	0.00000000
0.00020000	0.00000577	0.00000118	0.00000000	0.00030000	0.00000866	0.00000177	0.00000000
0.00020000	0.00000577	0.00000001	0.00000000	0.00030000	0.00000866	0.00000002	0.00000000

Uncertainty contribution	Index	Δz_3	Std. uncertainty	Uncertainty contribution	Index	Δz_4	Std uncertainty	Uncertainty contribution	Index
0.00000597	0.0100	0.0002	0.00005770	0.00005770	0.9660	0.0003	0.00000866	0.00000866	0.0220
0.00000597	0.0100	0.0002	0.00005770	0.00005770	0.9650	0.0003	0.00000866	0.00000866	0.0220
0.00000597	0.0100	0.0002	0.00005770	0.00005770	0.9620	0.0003	0.00000866	0.00000866	0.0220
0.00000597	0.0100	0.0002	0.00005770	0.00005770	0.9590	0.0003	0.00000866	0.00000866	0.0220
0.00000597	0.0100	0.0002	0.00005770	0.00005770	0.9550	0.0003	0.00000866	0.00000866	0.0210
0.00000597	0.0100	0.0002	0.00005770	0.00005770	0.9500	0.0003	0.00000866	0.00000866	0.0210
0.00000597	0.0100	0.0002	0.00005770	0.00005770	0.9440	0.0003	0.00000866	0.00000866	0.0210
0.00000597	0.0100	0.0002	0.00005770	0.00005770	0.9370	0.0003	0.00000866	0.00000866	0.0210
0.00000597	0.0100	0.0002	0.00005770	0.00005770	0.9290	0.0003	0.00000866	0.00000866	0.0210
0.00000597	0.0100	0.0002	0.00005770	0.00005770	0.9210	0.0003	0.00000866	0.00000866	0.0210
0.00000597	0.0100	0.0002	0.00005770	0.00005770	0.9120	0.0003	0.00000866	0.00000866	0.0210
0.00000597	0.0100	0.0002	0.00005770	0.00005770	0.9020	0.0003	0.00000866	0.00000866	0.0200
0.00000597	0.0100	0.0002	0.00005770	0.00005770	0.8920	0.0003	0.00000866	0.00000866	0.0200
0.00000597	0.0090	0.0002	0.00005770	0.00005770	0.8810	0.0003	0.00000866	0.00000866	0.0200
0.00000597	0.0090	0.0002	0.00005770	0.00005770	0.8700	0.0003	0.00000866	0.00000866	0.0200
0.00000597	0.0090	0.0002	0.00005770	0.00005770	0.8580	0.0003	0.00000866	0.00000866	0.0190
0.00000597	0.0090	0.0002	0.00005770	0.00005770	0.8460	0.0003	0.00000866	0.00000866	0.0190
0.00000597	0.0090	0.0002	0.00005770	0.00005770	0.8330	0.0003	0.00000866	0.00000866	0.0190
0.00000597	0.0090	0.0002	0.00005770	0.00005770	0.8200	0.0003	0.00000866	0.00000866	0.0180
0.00000597	0.0090	0.0002	0.00005770	0.00005770	0.8070	0.0003	0.00000866	0.00000866	0.0180
0.00000597	0.0080	0.0002	0.00005770	0.00005770	0.7940	0.0003	0.00000866	0.00000866	0.0180
0.00000597	0.0080	0.0002	0.00005770	0.00005770	0.7800	0.0003	0.00000866	0.00000866	0.0180
0.00000597	0.0080	0.0002	0.00005770	0.00005770	0.7660	0.0003	0.00000866	0.00000866	0.0170
0.00000597	0.0080	0.0002	0.00005770	0.00005770	0.7520	0.0003	0.00000866	0.00000866	0.0170
0.00000597	0.0080	0.0002	0.00005770	0.00005770	0.7380	0.0003	0.00000866	0.00000866	0.0170
0.00000597	0.0080	0.0002	0.00005770	0.00005770	0.7240	0.0003	0.00000866	0.00000866	0.0160
0.00000597	0.0080	0.0002	0.00005770	0.00005770	0.7100	0.0003	0.00000866	0.00000866	0.0160
0.00000597	0.0070	0.0002	0.00005770	0.00005770	0.6970	0.0003	0.00000866	0.00000866	0.0160
0.00000597	0.0070	0.0002	0.00005770	0.00005770	0.6830	0.0003	0.00000866	0.00000866	0.0150
0.00000597	0.0070	0.0002	0.00005770	0.00005770	0.6690	0.0003	0.00000866	0.00000866	0.0150

Uncertainty contribution	Index	Δz_3	Std. uncertainty	Uncertainty contribution	Index	Δz_4	Std uncertainty	Uncertainty contribution	Index
0.00000597	0.0100	0.0002	0.00005770	0.00005770	0.9660	0.0003	0.00000866	0.00000866	0.0220
0.00000597	0.0100	0.0002	0.00005770	0.00005770	0.9650	0.0003	0.00000866	0.00000866	0.0220
0.00000597	0.0100	0.0002	0.00005770	0.00005770	0.9620	0.0003	0.00000866	0.00000866	0.0220
0.00000597	0.0100	0.0002	0.00005770	0.00005770	0.9590	0.0003	0.00000866	0.00000866	0.0220
0.00000597	0.0100	0.0002	0.00005770	0.00005770	0.9550	0.0003	0.00000866	0.00000866	0.0210
0.00000597	0.0100	0.0002	0.00005770	0.00005770	0.9500	0.0003	0.00000866	0.00000866	0.0210
0.00000597	0.0100	0.0002	0.00005770	0.00005770	0.9440	0.0003	0.00000866	0.00000866	0.0210
0.00000597	0.0100	0.0002	0.00005770	0.00005770	0.9370	0.0003	0.00000866	0.00000866	0.0210
0.00000597	0.0100	0.0002	0.00005770	0.00005770	0.9290	0.0003	0.00000866	0.00000866	0.0210
0.00000597	0.0100	0.0002	0.00005770	0.00005770	0.9210	0.0003	0.00000866	0.00000866	0.0210
0.00000597	0.0100	0.0002	0.00005770	0.00005770	0.9120	0.0003	0.00000866	0.00000866	0.0210
0.00000597	0.0100	0.0002	0.00005770	0.00005770	0.9020	0.0003	0.00000866	0.00000866	0.0200
0.00000597	0.0100	0.0002	0.00005770	0.00005770	0.8920	0.0003	0.00000866	0.00000866	0.0200
0.00000597	0.0100	0.0002	0.00005770	0.00005770	0.8920	0.0003	0.00000866	0.00000866	0.0200
0.00000597	0.0090	0.0002	0.00005770	0.00005770	0.8810	0.0003	0.00000866	0.00000866	0.0200
0.00000597	0.0090	0.0002	0.00005770	0.00005770	0.8700	0.0003	0.00000866	0.00000866	0.0200
0.00000597	0.0090	0.0002	0.00005770	0.00005770	0.8580	0.0003	0.00000866	0.00000866	0.0190
0.00000597	0.0090	0.0002	0.00005770	0.00005770	0.8460	0.0003	0.00000866	0.00000866	0.0190
0.00000597	0.0090	0.0002	0.00005770	0.00005770	0.8330	0.0003	0.00000866	0.00000866	0.0190
0.00000597	0.0090	0.0002	0.00005770	0.00005770	0.8200	0.0003	0.00000866	0.00000866	0.0180
0.00000597	0.0090	0.0002	0.00005770	0.00005770	0.8070	0.0003	0.00000866	0.00000866	0.0180
0.00000597	0.0080	0.0002	0.00005770	0.00005770	0.7940	0.0003	0.00000866	0.00000866	0.0180
0.00000597	0.0080	0.0002	0.00005770	0.00005770	0.7800	0.0003	0.00000866	0.00000866	0.0180
0.00000597	0.0080	0.0002	0.00005770	0.00005770	0.7660	0.0003	0.00000866	0.00000866	0.0170
0.00000597	0.0080	0.0002	0.00005770	0.00005770	0.7520	0.0003	0.00000866	0.00000866	0.0170
0.00000597	0.0080	0.0002	0.00005770	0.00005770	0.7380	0.0003	0.00000866	0.00000866	0.0170
0.00000597	0.0080	0.0002	0.00005770	0.00005770	0.7240	0.0003	0.00000866	0.00000866	0.0160
0.00000597	0.0080	0.0002	0.00005770	0.00005770	0.7100	0.0003	0.00000866	0.00000866	0.0160
0.00000597	0.0070	0.0002	0.00005770	0.00005770	0.6970	0.0003	0.00000866	0.00000866	0.0160
0.00000597	0.0070	0.0002	0.00005770	0.00005770	0.6830	0.0003	0.00000866	0.00000866	0.0150
0.00000597	0.0070	0.0002	0.00005770	0.00005770	0.6690	0.0003	0.00000866	0.00000866	0.0150

Appendix 6.1 Multimetre set-up